Studies in Systems, Decision and Control 95

Andrey E. Gorodetskiy
Vugar G. Kurbanov *Editors*

Smart Electromechanical Systems: The Central Nervous System

Springer

Studies in Systems, Decision and Control

Volume 95

Series editor

Janusz Kacprzyk, Polish Academy of Sciences, Warsaw, Poland
e-mail: kacprzyk@ibspan.waw.pl

About this Series

The series "Studies in Systems, Decision and Control" (SSDC) covers both new developments and advances, as well as the state of the art, in the various areas of broadly perceived systems, decision making and control- quickly, up to date and with a high quality. The intent is to cover the theory, applications, and perspectives on the state of the art and future developments relevant to systems, decision making, control, complex processes and related areas, as embedded in the fields of engineering, computer science, physics, economics, social and life sciences, as well as the paradigms and methodologies behind them. The series contains monographs, textbooks, lecture notes and edited volumes in systems, decision making and control spanning the areas of Cyber-Physical Systems, Autonomous Systems, Sensor Networks, Control Systems, Energy Systems, Automotive Systems, Biological Systems, Vehicular Networking and Connected Vehicles, Aerospace Systems, Automation, Manufacturing, Smart Grids, Nonlinear Systems, Power Systems, Robotics, Social Systems, Economic Systems and other. Of particular value to both the contributors and the readership are the short publication timeframe and the world-wide distribution and exposure which enable both a wide and rapid dissemination of research output.

More information about this series at http://www.springer.com/series/13304

Andrey E. Gorodetskiy · Vugar G. Kurbanov
Editors

Smart Electromechanical Systems: The Central Nervous System

Springer

Editors
Andrey E. Gorodetskiy
Institute of Problems in Mechanical Engineering
Russian Academy of Sciences
Saint Petersburg
Russia

Vugar G. Kurbanov
Institute of Problems in Mechanical Engineering
Russian Academy of Sciences
Saint Petersburg
Russia

ISSN 2198-4182 ISSN 2198-4190 (electronic)
Studies in Systems, Decision and Control
ISBN 978-3-319-53326-1 ISBN 978-3-319-53327-8 (eBook)
DOI 10.1007/978-3-319-53327-8

Library of Congress Control Number: 2017930190

Printed on acid-free paper

This Springer imprint is published by Springer Nature
The registered company is Springer International Publishing AG
The registered company address is: Gewerbestrasse 11, 6330 Cham, Switzerland

Preface

Smart electromechanical systems (SEMS) are used in cyber-physical systems (CPhS). Cyber-physical systems have the ability to integrate computing, communication, and storage of information, monitoring, and control of the physical world objects. The main tasks in the field of theory and practice CPhS are to ensure the efficiency, reliability, and safety of functioning in real time. It is important to bear in mind that the behavior of the system is based on the information received from the central nervous system (CNS) about the environment and the state of the system.

The purpose of the publication was to introduce the latest achievements of scientists of the Russian Academy of Sciences in the theory and practice of SEMS CNS and development of methods for their design and simulation based on the principles of bionics, adaptability, intelligence, and parallelism in information processing and computation.

The topics of primary interest include but are not limited to the following:

- Methods and principles of construction CNS;
- Sensory system (receipt, transfer, and pretreatment measurement information);
- Fuzzification and identification of measurement information;
- Modeling and decision making;
- Formation of control actions and working bodies.

This book is intended for students, scientists, and engineers specializing in the field of smart electromechanical systems and robotics and includes many scientific domains such as receipt, transfer, and pretreatment measurement information, decision-making theory, control theory, and working bodies of robots that imitate the complexity and adaptability of biologic systems.

We are grateful to many people for the support received during the writing of this book. A list of their names cannot be represented here, but to all of them we are deeply grateful.

Saint Petersburg, Russia
November 2016

Andrey E. Gorodetskiy
Vugar G. Kurbanov

Contents

Part I
Methods of Designing

Challenges Related to Development of Central Nervous System of a Robot on the Bases of SEMS Modules

Andrey E. Gorodetskiy, I.L. Tarasova and Vugar G. Kurbanov

Abstract *Purpose* when modern problems of robotics are being settled, the bionic approach, when robots imitate complexity and adaptability of biological systems, is becoming more and more widespread. Smart Electromechanical Systems (SEMS) are used in cyberphysical systems. These systems integrate many functions, namely computing, control, communication and storage of information, monitoring and control over both their parameters and ones of the environment. It is important to bear in mind that the behavior of the system is based on information obtained from the Central Nervous System of a Robot (CNSR) about the state of environment and conditions of system. The purpose of the publication is to describe approaches to the solution of the problem of development of the central nervous system of robots constructed on the basis of SEMS modules. *Results* the concept of development of the central nervous system of a robot on the basis of SEMS modules is suggested. *Practical importance* the principles of development of the central nervous system suggested in the article can be used for modeling and decision-making in control systems of smart robots.

Keywords Electromechanical systems · Sense organs of a human · Central nervous system of a human · Central nervous system of a robot · Measurement · Calculation · Management · Transfer of operating signals · Working bodies

A.E. Gorodetskiy (✉) · I.L. Tarasova · V.G. Kurbanov
Institute of Problems of Mechanical Engineering,
Russian Academy of Sciences, St. Petersburg, Russia
e-mail: g27764@yandex.ru

I.L. Tarasova
e-mail: g17265@yandex.ru

V.G. Kurbanov
e-mail: vugar_borchali@yahoo.com

A.E. Gorodetskiy and V.G. Kurbanov (eds.), *Smart Electromechanical Systems: The Central Nervous System*, Studies in Systems, Decision and Control 95,
DOI 10.1007/978-3-319-53327-8_1

1 Introduction

The proper functioning of any control system (CS), it must receive information about the environment and the "behavior" of the robot. Without them, she would not be able to take decisions expected of it, i.e., define the objectives and functioning reach these goals. Such a behavior of the robot is called feasible or purposeful [1]. Therefore robot software "senses" and their improvement is very important and urgent task.

Currently, "senses" of the robot are various sensors (displacement, velocity, acceleration, forces, tactile sensors, etc.), forming a sensor robot system, which collects two types needed for CS information: on their own robot state and the state of object manipulation environment [2]. However, for what would the robots can independently, without needing human intervention, formulate objectives and to successfully carry them out, they should be provided not only more sophisticated sensors sensations, but also have the ability to understand the feelings the language, that is, have a sense of the type of "your own–someone else" "dangerous–safely", "favorite–unloved", "pleasant–unpleasant" and others.

Some of these sensors senses may be analogs human senses, such as hearing, vision, tactile sensitivity. But not necessarily limited to the human senses. The robot can be made to receive the radio waves, ultrasonic oscillations, ultraviolet light or electrical signals simply by connecting it to "central nervous system" should be sensors that provide convenient electrical output signal [3].

Should be used and in some cases already in use bionic approaches in the creation of the senses and the "central nervous system" of robots (CNSR). Different countries have developed different types of devices using this approach. We study various devices for pattern recognition, artificial eyes for reading of letters and numbers, artificial ears for speech perception, various kinds of tactile sensors and other analogs of the senses [4]. It is hoped that some of these studies will facilitate the solution to the problem of communication between humans, computers, and other devices. Of course, any of the devices are now being developed will be useful later for use in robots.

There are bodies of animals feelings that we still have not learned to play. The most difficult ones are gustatory and olfactory. Fortunately, until they are of special importance. There is no doubt that if it became necessary, he would have started the study of possible ways of playing. It would be nice if the robot senses authorities have all the properties of the sense organs of humans and animals. To solve the problems it is first necessary to study linguistics and formalize the sense of language, namely, alphabets and rules of construction of the signs of the letters (words) of the signs—proposals, as well as rules for understanding the meaning of sentences, the formation of new proposals and transmit them to others.

2 The Bodies of the Human Senses

Preparation and primary analysis of information from the outside world and from other organs of the body, i.e. from the external environment and internal environment of the body is provided by the senses—a specialized peripheral anatomical and physiological systems. It is believed that a person has 5 main senses: sight, hearing, smell, taste and touch. Recently, it is added on to another and sixth: Equilibrium [5]. Apparently, little studied and practical man lost seventh sense organ is Telepathy, or thought transference at a distance by means of electromagnetic waves of the radio. Moreover, 90% of the information people receive visually—through sight; 9% of the information people have hearing (auditory); only 1% through other senses.

The vision (visio, visus)—a physiological process of perception of size, shape and color of objects, as well as their relative position and distance between them; a source of vision is the light emitted or reflected from objects in the external world. The function of vision carried out thanks to a complex system of different interconnected structures—visual analyzer, consisting of peripheral (retina, optic nerve, optic tract) and a central department, which brings together the subcortical and stem centers (lateral geniculate body, the cushion of the thalamus, the upper hills of the midbrain roof) as well as the visual cortex of the cerebral hemispheres. The human eye perceives only light waves of a certain length—about 380–770 nm. Light rays from treated subjects tested through the optical system of the eye (cornea, lens and vitreous body) and fall on the retina. In the retina, the light-sensitive cells are concentrated—the photoreceptors (rods and cones). Light falling on the photoreceptor, causes rearrangement contained therein visual pigments (in particular, the most studied of them rhodopsin), and this, in turn,—the occurrence of nerve impulses, which are transmitted in the following description of retinal neurons and in the optic nerve. According to the optic nerve and optic tract followed by nerve impulses arrive in the lateral geniculate body—subcortical centers of view, and from there to the cortical center of vision, located in the occipital lobes of the brain, which is the formation of the visual image [6].

Alphabet language of vizion (light sensations) are the colors. Accepted provide the seven colors of the rainbow: red, orange, yellow, green, blue, indigo and violet. Thus each color has its own frequency of electromagnetic oscillations. Rules for the structure of the letters (colors) signs (images) from—suggestions (paintings) signs have long been studied and applied in painting [7]. However, a sufficiently complete and formalized description of linguistics sensations of light, suitable for giving these abilities of robots does not yet exist.

Hearing (auditus)—a feature that allows the perception of human and animal sounds. The mechanism of the auditory sensation is caused by the activity of the auditory analyzer. The peripheral portion of the analyzer includes an outer, middle and inner ear. Concha converts the acoustic signal coming from the outside, reflecting and directing the ear canal sound waves. The external auditory canal, acts as a resonator, change the properties of the acoustic signal—increases the intensity

of the tones the frequency of 2–3 kHz. The most significant conversion of sound occurs in the middle ear. Here, due to the difference in the area of the eardrum and the stapes base, as well as through the lever mechanism of the auditory ossicles and the tympanic cavity muscles significantly increases the intensity of the sound conducted by reducing its amplitude. Middle ear system provides transition vibrations of the eardrum to the inner ear fluids—perilymph and endolymph. At the same time leveled to some extent (depending on the frequency of the sound), the acoustic impedance of the air in which the sound wave propagates, and the inner ear fluids. Converted waves are perceived by the cochlea, which ranges receptor cells, located on the basilar plate (membrane) in different areas, rather strictly corresponding to the frequency of the exciting sound wave it. The resulting excitation in certain groups of receptor cells distributed along the fibers of the auditory nerve in the nucleus of the brain stem, subcortical centers located in the midbrain, reaching the auditory cortex area, localized in the temporal lobes, where he formed an auditory sensation. At the same time as a result of crossing pathways from the audio signal and the right and left ear of the falls at the same time to both hemispheres of the brain. Auditory pathway has five synapses, each of which is encoded by a nerve impulse differently. Coding mechanism is so far not fully disclosed, which significantly limits the possibility of practical audiology [6]. It was believed that the human ear perceives sounds frequency from 16–20 to 15–20 kHz. Subsequently, it was established that the human bone in terms of sound perception characteristic having a higher (200 kHz) frequency, i.e. ultrasound. At the same time with an increase in frequency of ultrasound sensitivity to reduced. The fact that the auditory perception of the ultrasound is placed in the current views of the hearing evolution, because this feature is inherent in any and all types of mammals. Measurement sensitivity to ultrasound is important to assess human hearing status, widening and deepening opportunity audiometry.

Sounds—a harmonic oscillations whose frequencies are treated as integers, and cause a person a pleasant sensation (consonance). Close, but different frequency vibrations cause discomfort (dissonance). Sound vibrations with a continuous spectrum of frequencies perceived by the person as noise. Alphabet hearing the language (sound sensations) are the notes. They are seven: “C”, “D”, “E”, “F”, “G”, “A”, “B”. Rules for the structure of the letters (notes) marks (tunes), signs of—suggestions (music) has long been studied and applied in music [8]. However, a sufficiently complete and formalized description of linguistics sensations of light, suitable for giving these abilities of robots does not yet exist.

The sense of smell—a sense of smell, the ability to detect the smell of substances dispersed in the air (or dissolved in water—for animals living in it). Unified theory of the origin of smell is not. Nominated stereochemical hypothesis (J. Eymur, 1964) [9], according to which the interaction between the molecules of odorous substances with the membrane of the olfactory cells at the same time depends on the spatial shape of the molecule and on the presence of certain functional groups. It is assumed that the olfactory pigment molecule can easily pass into an excited state by the action of the vibrating molecules of odorous substances. Olfactory receptors are excited substances with a molecular weight of 17

(ammonia) 300 (alkaloids). According to this theory, there are 7 primary odors (seven letters of the alphabet sense of smell)—camphor, floral, musk, mint, ether, pungent and putrid. The remaining odors (e.g., garlic) are complex, consisting of several primary. Camphor odor molecules must be approximately spherical shape with a diameter of 0.7 nm, with floral—disc-shaped with a handle, etc. We calculated the approximate dimensions of the receptor "holes", or nests, on the membrane of the olfactory cells, which should include the molecules of odorous substances.

In the formation of the olfactory sensations involved and other mucous membrane receptors of the mouth: Tactile, temperature, pain. Irritants only olfactory receptors, called olfactory (vanillin, benzol, xylene), unlike the mixed irritating also other receptors (ammonia, chloroform). The spectrum of odors perceived by man is very wide; undertaken many attempts to systematize them. German psychologist H. Henning (1924) identified 6 major odor (fruity, floral, resinous, spicy, putrid, burnt), which reflects the relationship between the so-called prism odors. Later it was shown inaccuracy Henning classification, and is now used by the scheme of the 4 basic smells (fragrant, sour, burnt, putrid), whose intensity is usually measured by the conventional 9-point scale.

Until now sufficiently complete and formalized description of the olfactory sensations linguistics suitable for giving these abilities of robots does not exist [10].

Taste—a type of feeling, formed by the action of different substances mainly on the taste buds. Senses of taste and sense of smell allows us to distinguish between undesirable for the reception and even deadly food from the delicious and nutritious. Smell allows animals to recognize the proximity of other animals, or even certain animals among many others. Finally, both closely related to feelings of emotional and behavioral primitive functions of the nervous system.

Taste is mostly a function of the taste buds of the mouth, but each of their life experience knows that a great contribution in the sense of taste and smell makes. In addition, food texture, perceived via the mouth tactile receptors in the presence of food substances that stimulate pain closure such as peppers significantly alter taste perception. The importance of taste is that it allows a person to choose the food in accordance with the desires and often due to metabolic needs of the body tissues with respect to certain substances.

Not all specific chemicals excite different taste receptors, are known. Psychophysiological and neurophysiological studies have identified at least 13 possible or probable chemical receptors in taste cells. Among them, sodium 2 receptor, 2 potassium, chlorine 1, 1 adenosine, inosine 1, 2 receptor for sweet, bitter for 2 receptor, glutamate receptor 1 and 1 receptor for hydrogen ions. For practical analysis of flavor potential of these receptors are grouped into five main categories, called primary flavors (taste the letters of the alphabet): sour, salty, sweet, bitter and umami.

A person can feel the hundreds of different flavors. It is believed that all of them are combinations of the primary taste sensations (taste alphabet) as well as all the colors that we see are combinations of the primary colors (light alphabet). Until

now sufficiently complete and formalized description of linguistic taste, suitable for giving these abilities of robots does not exist [11].

Touch—a complex sensation that occurs when irritation of the skin receptors, the external surfaces of the mucous membranes and the muscular-articular apparatus. The main place in the formation of the sense of touch belongs to the skin analyzer, which carries out the perception of external mechanical, thermal, chemical, and others skin irritations. The sense of touch, being the most ancient form of sensations is composed of tactile, temperature, pain and movement sensation. The main role belongs to the sense of touch tactile sensations—touch and pressure. Touch receptors in the skin are a tree-like branched free end of the nerve fibers, terminal branches of which penetrate between the connective and epithelial cells, obvivaya outer root sheath of hair. Oscillation long hair outer portion is transmitted to the root portion and causes the excitation of nerve fibers. By increasing the intensity of touch begins to feel a sense of pressure. This means that the affected muscle receptors, tendons and fascia. One nerve fibers branching may approach 300 cutaneous receptors. Touch is divided into active and passive Active touch appears (shown in the manipulation of the subject and his feeling in humans) to active actions of the body, contributing to a more complete perception of the subject Passive touch occurs when the simple action of the stimulus on the skin and is not accompanied by specific reactions of the organism, usually aimed at clarifying the nature of the action of the stimulus.

Equilibrium—a sense of orientation in space, which Rudolf Steiner did not hesitate to include in terms of feelings: "We are aware of the third sense if you think about what people distinguish between top and bottom If it ceases to distinguish it, then he faces a great danger, if he can not stand upright and tilted We can point to the body, which has a close relationship with this feeling, namely, the three semicircular canal in the ear. If the damage of the body man loses his sense of orientation" [12]. The body is a sense of balance in the ear (the analysis is in the cerebellum) [6]. In general, receptors are found in all parts of the body and internal organs Pain signals to transmit information about the state of health of an organ.

Telepathy—parapsychological phenomenon of transmission of thoughts and feelings at a distance and to provide, thus, impacts on living and non-living objects, without the use of any technical means. Telepathy—the most common psychic phenomena. It has repeatedly been tested almost every one of us The most striking example—telepathic connection between mother and child: a mother loving her child immediately feels the danger to the child at any distance Equally obvious telepathic connection between loving people who feel the slightest nuances of the state of mind of each other.

When telepathic communication logical beginning of human consciousness practically involved—working mostly intuition This manifests complete configuration at each other participants of such a connection. However, to put a telepathic experiment is extremely difficult to rigorous scientific framework. In the world a variety of experiments to establish telepathic communications were delivered in situations where other communication channels were unavailable or undesirable. As a result, the fundamental possibility of telepathic communication has been

experimentally proved. This was clearly confirmed that such a link exists outside the sphere of influence of all known fields—electromagnetic, gravitational etc.

3 The Central Nervous System of the Human Senses

The sense organs perceive only the information, then this information must be transformed into nerve impulses and act in the brain to analyze and develop a response. This scheme similar to the following: RECEPTOR → NERVOUS ZONE → CIRCUIT CRUST → IMPULSE → RESPONSE. Signals from outside the treated area of the cerebral cortex, which are the core of the central nervous system senses (CNSHS) person. Each sense organ corresponds to certain areas of the cerebral cortex (see Fig. 1).

At the same time the human senses is much weaker than that of animals. Man worse sees, hears a sound in a narrower range, distinguishes less odor, but it is important to understand that the formation of certain organs occurs under the terms of the environment, it is an adaptation to the environment. However, despite the weaker senses, people communicate better with each other and have a more appropriate behavior thanks to a more developed central nervous system with the linguistic abilities. It is also important that when a person denies one of the senses, the others start to work harder [7]. According to James "conceptual" operation—this is not a mere contemplation of the world, but in a highly selective process in which the body receives instructions on how to operate it in respect of the world, to meet their needs and interests [8].

Another important property of human perception of the world is the existence of ties between the perceived information from different senses. In particular, it has long been known that there is a close relationship of sound and color [10]. In

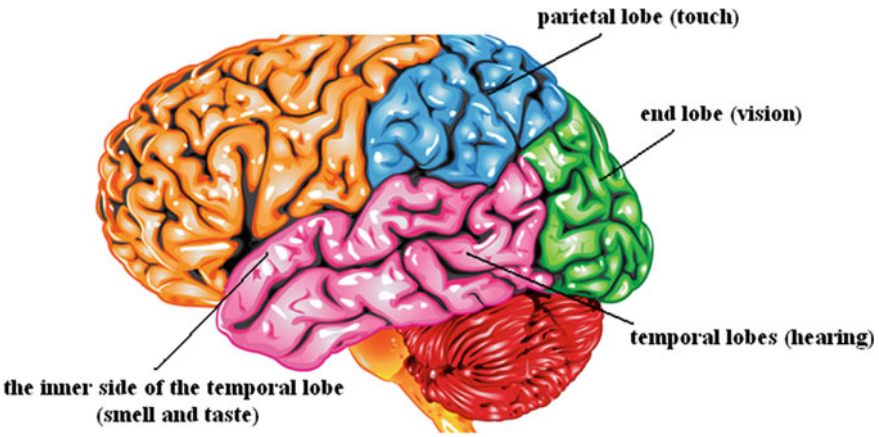

Fig. 1 Certain areas of the cerebral cortex

particular, the ability to "hear" colors or "see" the music called seventh sense—**synesthesis** [11]. People have the ability to perceive the world in a lot of senses, considered to be unique. But no more. There is nothing supernatural in nature synesthesia not. It is given to all human beings. After input from all the senses are mixed in infant brain. But at the age of about six months they are separated: the sounds—"right" visual information—"left". Scientifically—the process of the withering away of neurons, synaptic creating bridges [13]. In synesthesiks bridges remain intact, and feelings—not separated. As if superposed. Moreover, the so-called psychics, listening to music, sometimes felt in the mouth all sorts of tastes: sweet, bitter, salty, sour. I check out this professor of psychology and neuroscience, University of California Vilayanur S. Ramachandran, who has developed a special test. On the computer screen appear black two and located in random order five. Average person is very difficult to distinguish one from the other. A synesthesiks easy to see that form a triangle of two. After all, they are colored to him. Using these tests, Ramachandran and his colleagues found: synesthesia far more common than previously thought. About one hundred adults [13].

Synesthesia had many famous people. For example, the French poet Arthur Rimbaud associated the vowel sounds with certain colors. Color musical notes saw the composer Alexander Scriabin. Abstract artist Wassily Kandinsky, on the contrary, I heard the sound of colors. By synesthesiks include Leo Tolstoy, Maxim Gorky, Marina Tsvetaeva, Konstantin Balmont, Boris Pasternak, Andrei Voznesensky [14].

Suffice it to sound mathematical models of human functioning CNS not yet developed that prevents the establishment of full-fledged CNS robots.

4 Tasks of Construction of the Central Nervous System Robots

Solving the problem of creating a "central nervous system" senses of robots comes down, first of all, to research and develop chains of type about the following scheme: Receptors (sensors, gauges and other measuring robot system) → NERVOUS CIRCUIT (information signal receiving channel and primary processing) → ZONE BARK (combining signals, pattern recognition, classification, decision) → PULSE (information control signaling channel, conversion and formation of the control action) → RESPONSE (moving, stretching and other actions of the robot working bodies) (see Fig. 2); it is divided into two related tasks. The first is to create a more sophisticated sensors and systems engineering sensations. The second—the creation of software robots provide the ability to understand the language of feelings and create behavioral processes on the basis of the analysis of sensations, i.e., robots provide the possibility of reflective reasoning essentially approximating the latest sign systems to those enjoyed in their daily practice, man.

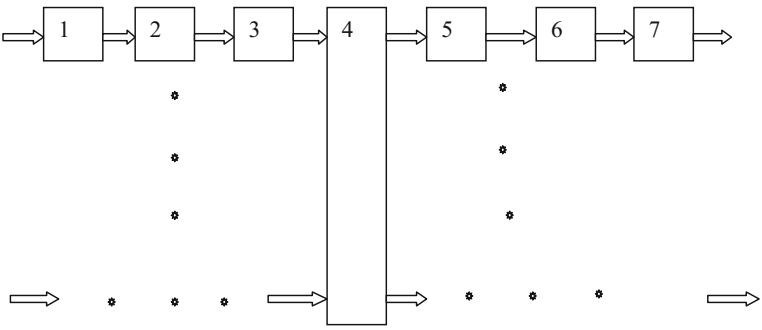

Fig. 2 *1*—Measuring system (sensors), *2*—measuring the signal transmission channel, *3*—block pre-processing of the measurement signals, *4*—fuzzification block, pattern recognition and decision making, *5*—channel transmission of control signals, *6*—forming unit control actions, *7*—working bodies robot

There is quite a lot of development of measuring systems and sensors that simulate the vision (block 1). This is a different vision system, CCD, opto-electronic and television measuring system, size, brightness, etc. Parameters [15]. The same can be said about the systems that simulate the ear [16]. There is some progress in the field of measuring systems and sensors that simulate the sense of touch [17]. Little studied and practically poorly used are measurement systems that simulate the sense of smell and taste [18]. Almost no development concerning the research and creation of technical systems that simulate the sense of balance and telepathy [18]. Consequently, the decision of the task is not yet complete in many respects.

Methods and means of transmission and conversion of signals to isolate the information parameters from the mixture SNR is well studied and has a large number of different hardware transmit and transmit-filter (blocks 2, 3, 5) signals [19]. As is well researched and developed the technical means of formation of control actions (block 6) [20].

Known methods of data fuzzification (signals), inference and logical interval, logic and probabilistic and logical and linguistic methods of pattern recognition and decision making (block 6) [21, 22]. However, the task of creating mathematical and software tools to ensure the robots the ability of reflective reasoning essentially approximating sign systems last to those enjoyed in their daily practice, people are still at a very early stage, limited modeling behavioral processes on the basis of sensations analysis [23].

Thus, the available technical solutions at this stage, make it possible to proceed to the creation of simplified prototypes CNS robots. One of the most promising options mathematical implementation block 4 may be implement logical-mathematical form on the basis of behavioral analysis processes sensations of touch signals from the robot system. In this first and very important for the further operation is logical constructions fuzzification data received through the touch information channels from the various sensors. To do this, the sensors can be

combined in groups, forming the following bodies of the robot senses like a man: vision as a set of **X**; hearing as set **Y**; a plurality of smell **Z**; taste as a plurality of **U**; the sense of touch in the form of a plurality of **V**; a plurality balance **W** and a plurality telepathy **Q**.

$$\boldsymbol{X_i} \subset \boldsymbol{X}, \quad \boldsymbol{Y}_i \subset \boldsymbol{Y}, \quad \boldsymbol{Z_i} \subset \boldsymbol{Z}, \quad \boldsymbol{U_i} \subset \boldsymbol{U}, \quad \boldsymbol{V_i} \subset \boldsymbol{V}, \quad \boldsymbol{W_i} \subset \boldsymbol{W}, \quad \boldsymbol{Q_i} \subset \boldsymbol{Q}.$$

A set of these subsets depends on a set of sensors forming the senses of a particular robot. For example, to view a subset of the following can be entered: X_1—Contour image, X_2—the size of the image, X_3—the brightness of the image, X_4—color image, X_5—the distance to the object, X_6—approach speeds, X_7—removal rate.

For the hearing following subsets can be entered: Y_1—volume, Y_2—the tone, Y_3—interval, Y_4—approach speeds, Y_5—removal rate, Y_6—direction.

For the following subsets of smell can be entered: Z_1—type of smell, Z_2—the intensity of the odor, Z_3—the direction of the smell, Z_4—approach speeds, Z_5—removal rate.

For the following subsets can be introduced to the taste: U_1—type of taste, U_2—the power of taste, U_3—direction.

To touch these subsets can be entered: V_1—the evenness of the surface, V_2—dry surface, V_3—surface temperature.

Sense of balance is usually provided by robots gyroscopes. In this case, the following subsets can be entered: W_1—deviation "up–down", W_2 of—deviation "forward–backward", W_3—deviation "left–right", W_4—speed deviation "up–down", W_5—speed deviation "forward–backward", W_6—speed deviation "left–right".

Telepathy robots, in contrast to the human, it is explicable phenomenon and receive messages using a wireless connection. Currently, the most widely used for this purpose «Wi–Fi». Most simply a subset of the set Q_i forming telepathy Q form in advance at the stage of designing a robot designed to perform various technological operations. In this case, these instructions are subsets or types of reactions ($qij \in Q_i$), are stored in the robot's memory and retrieved therefrom inference engine [24, 25]. The choice of instructions carried out by checking the feasibility of certain rules of the data subset ($x_{ij} \in X_i$; $y_{ij} \in Y_i$; $z_{ij} \in Z_i$; $u_{ij} \in U_i$; $v_{ij} \in V_i$; $w_{ij} \in W_i$). Such rules usually have the form:

$$\textit{If } x_{ij} = 1 \wedge y_{ij} = 1 \wedge z_i = 1 \wedge u_{ij} = 1 \wedge v_{ij} = 1 \wedge w_{ij} = 1, \textit{ then } q_{ij} = 1 \qquad (1)$$

With a large number of logical variables, such rules can be just as much. Then, a sequential scan of the rules in order to identify their feasibility will take a long time. In this case, it is desirable to utilize parallel computing. For this purpose, as shown in [25, 26], we can use the procedure algebraization logical expressions.

These logical type (x_{ij}; y_{ij}; z_{ij}; u_{ij}; v_{ij}; w_{ij}) are extracted from the data or signals from the sensors senses of robots by their fuzzification. For example, X_3 by fuzzification get the following logical variables: x_{31}—«very weak brightness»,

x_{32}—«weak brightness», x_{33}—«normal brightness», x_{34}—«strong brightness» and x_{35}—«very strong brightness». It is easy to notice that each boolean variable connected an inherent attribute. In the simplest example of such an attribute is the interval. In more complex cases, the attributes may be the probability $P\{x_{ij} = 1\}$ or membership functions $\mu(x_{ij})$. Therefore, the data from the sensor senses the robots are stored in memory in the form of logical-interval, logical and probabilistic or logical-linguistic variables [26]. Therefore, the inference engine will almost always receive not one solution, but several with varying degrees of certainty. For example:

If: $x_{ij} = 1$ with probability P_x and $y_{ij} = 1$ with probability P_y and $z_i = 1$ with probability P_z and $u_{ij} = 1$ with probability P_u and $v_{ij} = 1$ with probability P_v and $w_{ij} = 1$ with probability P_w, the $q_{ij} = 1$ P_q likely.

His will naturally lead to ambiguous behavior of the robot. A man in this situation it is advisable to behave purposefully or intuitively, based on our own experience, or genetically inherent behavioral patterns [27]. Task empowering robots skills purposeful behavior is still at a very early stage. Usually in such cases, the robot control system should start the search procedure for the optimal solution.

This will naturally lead to ambiguous behavior of the robot. A man in this situation it is advisable to behave purposefully or intuitively, based on our own experience, or genetically inherent behavioral patterns [27]. Task empowering robots skills purposeful behavior is still at a very early stage. Usually in such cases, the robot control system should start the search procedure for the optimal solution. This requires the use of known [28–35] algorithms for computing attributes such logical functions as intervals, probability and membership functions. After selecting the optimal solution in the block (4) runs defuzzification operation [36, 37], which means the procedure for the conversion of fuzzy values derived from fuzzy inference, in the clear. These quantities channel transmitting control signals (5) transmitted to the block (6) generating control actions. Typically, the optimal working bodies formed by the control laws in the block (6) and (7), which come to a control signal (voltage). Methods of search of optimal control actions studied adequately, for example, in [38]. However, there are some difficulties associated with their parallel structures [39] for intelligent robots, built on the basis of SEMS modules.

5 Conclusion

For what could be robots independently, without needing human intervention, formulate objectives and to successfully carry them out, they should be provided not only more sophisticated sensors sensations, but also have the ability to understand the language of feelings. should be used and in some cases already in use bionic approaches in the creation of the senses and the “central nervous system” of robots (CNSR).

To solve the problem of creating CNSR is necessary, first of all, to study and to formalize linguistics sense of language, namely, alphabets and rules of construction of the letters signs (words) of the signs—proposals, as well as rules for

understanding the meaning of sentences, the formation of new proposals and their transfer others. However, quite reasonable mathematical models of functioning of the central nervous system is not yet developed, which prevents the creation of full-fledged CNSR.

Meeting the challenge of creating mathematical and software tools to ensure the robots the ability of reflective reasoning essentially approximating the latest sign systems to those enjoyed in their daily practice, people are still at a very early stage, limited to behavioral modeling processes based on the analysis of sensations. Nevertheless, the available technical solutions at this stage, make it possible to proceed to the creation of simplified prototypes CNSR. One of the most promising options for its implementation can be mathematical logical-mathematical approach to the implementation of behavioral formation processes based on the analysis of sensation of sensory signals from the robot system.

Currently, the most thoroughly studied the problem of choosing the optimal solutions for the formation of behavioral processes in the conditions of incomplete certainty interval, probabilistic or linguistic type. However, intelligent robots, built on the basis of SEMS modules there are certain difficulties compute control actions since the adoption of decisions related to their parallel structures.

Acknowledgements This work was financially supported by Russian Foundation for Basic Research, Grant 16-29-04424

References

1. Dobrynin, D.A.: Intelligent robots yesterday, today, tomorrow. In: X natsional'naia konferentsiia po iskusstvennomu intellektu s mezhdunarodnym uchastiem KII-2006 (25–28 sentiabria 2006 g., Obninsk). X National Conference on Artificial Intelligence with international Participation. Conference Proceedings. V.2. M: FIZMATLIT. Obninsk, 25–28 Sept 2006 (in Russian)
2. Hahalin, G.K.: Applied ontology language hypergraphs. In: Trudy vtoroi Vserossiiskoi Konferentsii s mezhdunarodnym uchastiem "Znaniia-Ontologii-Teorii" (ZONT-09). Proceedings of the Second Russian Conference with International Participation "Knowledge-Ontologies-Theories", pp. 223–231. Novosibirsk, 20–22 Oct 2009 (in Russian)
3. Hahalin, G.K., Kurbatov, S.S., Naydenova, K.A.: The integration of intelligent systems analysis/synthesis of image and text: project outlines INTEGRO. In: Trudy Mezhdunarodnoi nauchno-tekhnicheskoi konferentsii "Otkrytye semanticheskie tekhnologii proektirovaniia intellektual'nykh sistem" OSTIS-2011. Proceedings of the International Scientific-Technical Conference "Open Semantic Technologies of Intelligent Systems" OSTIS-2011, pp. 302–318. Minsk, Belarus, 10–12, Feb 2011(in Russian)
4. Hahalin, G.K., Kurbatov, S.S., Litvinovich, A.V.: Synthesis of visual objects on natural-language description. In: Trudy vtoroi Mezhdunarodnoi nauchno-tekhnicheskoi konferentsii "Komp'iuternye nauki i tekhnologii" (KNiT-2011). Proceedings of the Second International Scientific and Technical Conference "Computer Science and Technology", pp. 595–600. Belgorod, 3–7 Oct 2011 (in Russian)
5. Fominih, I.B.: Adaptive systems and information model of emotions. In: Trudy Mezhdunarodnoi konferentsii Intellektual'noe upravlenie: novye intellektual'nye tekhnologii v zadachakh upravleniia (ICIT'99). In Proceedings of the International Conference Intelligent

Control: the New Intelligent Technology in Control Problems, ICIT'99. Pereslavl, 6–9 Dec 1999 (in Russian)
6. Vagin, V.N., Anishchenko, I.G.: The concept of the mark in science and art. In: Novosti iskusstvennogo intellekta. The News of Artificial Intelligence, vol. 3 (2006) (in Russian)
7. Voskresenskiy, A.L., Hahalin, G.K.: Context fragmentation in linguistic analysis. In: Desiataia natsional'naia konferentsiia po iskusstvennomu intellektu s mezhdunarodnym uchastiem KII-2006. Tenth National Conference on Artificial Intelligence with International Participation. Proceedings of the Conference. M. Fizmatlit, vol. 3, Obninsk, 25–28 Sept 2006 (in Russian)
8. Gorbushin, N.G.: Models of sense and consciousness in artificial intelligence. In: Desiataia natsional'naia konferentsiia po iskusstvennomu intellektu s mezhdunarodnym uchastiem KII-2006. Tenth National Conference on Artificial Intelligence with International Participation. Proceedings of the Conference. M. Fizmatlit, Obninsk, 25–28 Sept 2006 (in Russian)
9. Golovin, S.Y.: Slovar' prakticheskogo psikhologa [Dictionary Practical Psychologist]. Harvest, Minsk (1998) (in Russian)
10. Zinchenko. V.P.: In: Meshcheryakov, B.G (ed.) Bol'shoi psikhologicheskii slovar [A Significant Psychological Dictionary]. M. Prime Evroznak. Academy of Russian Sciences (2003) (in Russian)
11. Karpov, V.E.: Emotions robots. In: XII natsional'naia konferentsiia po iskusstvennomu intellektu s mezhdunarodnym uchastiem KII-2010. XII National Conference on Artificial Intelligence with International Participation. Conference Proceedings, vol. 3, pp. 354–368. Tver, M. Fizmatlitv, 20–24 Sept 2010
12. Steiner, R.: Antroposofiia. Fragment 1910 g [Anthroposophy. Detail 1910], 504 p. M. Titurel (2005) (in Russian)
13. Fominykh, I.B.: Emotions as a unit estimates the behavior of intelligent systems. In: Desiataia natsional'naia konferentsiia po iskusstvennomu intellektu s mezhdunarodnym uchastiem KII-2006. Tenth National Conference on Artificial Intelligence with International Participation. Proceedings of the Conference, vol. 3. M. Fizmatlit, Obninsk, 25–28 Sept 2006 (in Russian)
14. Afanasieff, V.V.: Sveto-zvukovoi muzykal'nyi stroi [Light-Sound Music System]. M. "Music" (2002) (in Russian)
15. Polivtsev, S.A., Khashan, T.S.: The study of geometric and acoustic properties of the sensors for the technical hearing system. Problemy bioniki. Problems Robots Bionics, vol. 6 (2003) (in Russian)
16. Ying, M. Bonifas, A.P., Lu, N., Su, Y., Li, R., Cheng, H., Ameen, A., Huang, Y., Rogers, J. A.: Silicon Nanomembranes for Fingertip Electronics. IOP Publishing Ltd. (2012)
17. Tactile organs. In: Entsiklopedicheskii slovar' Brokgauza i Efrona. Brockhaus and Efron Encyclopedic Dictionary, vol. 86 (vol. 82 and 4 additional), 1890–1907. St. Petersburg (in Russian)
18. Semashko, N.A.: Bol'shaia meditsinskaia entsiklopediia [Great Medical Encyclopedia]. OGIZ RSFSR, Moscow (1934) (in Russian)
19. In: Proceedings of the Institute of Mechanics, vol. 9, part II. Ural Scientific Center RAS (2012) (in Russian)
20. Rachkov, Y.M.: Tekhnicheskie sredstva avtomatizatsii [Technical Means of Automation]. Textbook, 2nd edn., 185 p. M. Mgiu (2009) (in Russian)
21. Gorodetskiy, A.E., Kurbanov, V.G., Tarasova, I.L.: Ergatic operating instructions manual methods of analysis and decision-making processes in injuries and accidents of power. Informatsionno-upravliaiushchie sistemy. Information and Control Systems, vol. 6, pp. 29–36 (2103) (in Russian)
22. Gorodetskiy, A.E., Dubarenco, V.V., Kurbanov V.G., Tarasova, I.L.: Logical and probabilistic modeling techniques poorly formalized processes and systems. Izvestiia IuFU. Tekhnicheskie nauki. Proceedings of the SFU, No. 6(131), pp. 255–257. Technical Science (2012) (in Russian)

23. Koss, V.A.: The model of natural intelligence and ways of achieving the objectives of artificial intelligence. Matematicheskie mashiny i sistemy. Mathematical Machines and Systems, vol. 1, Issue 4 (2006) (in Russian)
24. Gavrilova, T.A., Khoroshevskiy, V.F.: Bazy znanii intellektual'nykh sistem [Base Knowledge of Intelligent Systems]. Piter, St. Petersburg (2001) (in Russian)
25. Kulik, B.A., Kurbanov, V.G., Fridman A.Y.: Parallel processing of the data and knowledge of the methods of the algebra of tuples. In: Trudy SPRIIAN. Proceedings SPIIRAS, vol. 5(36), pp. 168–179 (2014). doi:10.15622/sp.36.10 (in Russian)
26. Gorodetsky, A.E., Tarasova, I.L.: In: Nechetkoe matematicheskoe modelirovanie plokho formalizuemykh protsessov i sistem [Fuzzy Mathematical Modeling Badly Formalized Processes and Systems], 306 p. SPb Publishing House of the Polytechnic, University Press (2010) (in Russian)
27. Gorodetskiy, A.E., Kurbanov, V.G., Tarasova, I.L.: Methods of synthesis of optimal intelligent control systems SEMS. In: Smart Electromechanical Systems, pp. 25–45. doi:10.1007/978-3-319-27547-5_4
28. Zadeh, L.A.: The concept of a linguistic variable and its application to approximate reasoning. Inf. Sci. **8**(3), 199–249 (1975)
29. Ahlefeld, H., Hertzberger, Y.: Vvedenise v interval'nye vychisleniia [Introduction to Interval Calculations], 360 p. M. Mir (1987) (in Russian)
30. Levin, V.I.: Interval'naia matematika i issledovanie sistem v usloviiakh neopredelennosti [Interval Mathematics and Research Systems in Conditions of Uncertainty]. Rochester Institute of Technology, Penza (1998) (in Russian)
31. Levin, V.I.: Interval continuous logic and its application in control problems. In: Izv. RAN. Teoriia i sistemy upravleniia. Theory and control Systems, vol. 1. Bulletin of the Russian Academy of Sciences (2002) (in Russian)
32. Levin, V.I.: Continuous logic and its application. In: Informatsionnye tekhnologii. Inf. Technol. **1**, 17–21 (1997) (in Russian)
33. Gorodetskiy, A.E., Dubarenko, V.V.: Combinatorial method of calculating the probabilities of complex logic functions. *Zhurnal vychislitel'noi matematiki i matematicheskoi fiziki*. J. Comput. Math. Math. Phys. **39**(7), 1246–1249 (1999) (in Russian)
34. Dubarenko, V.V., Kurbanov, V.G., Kuchmin, A.Y.: A method of calculating the probabilities of logic functions. *Informatsionno-upravliaiushchie sistemy*. Inf. Control Syst. **5**, 2–7 (1999) (in Russian)
35. Gitman, M.B.: Vvedenie v teoriiu nechetkikh mnozhestv i interval'nuiu matematiku: Ch1: Primenenie lingvisticheskoi peremennoi v sistemakh priniatiia reshenii [Introduction to the Theory of Fuzzy Sets and Interval Mathematics: Part 1: Application of the linguistic Variable in the Decision-Making Systems]. Perm State University Publishing House, Perm, vol. 45 p. (1998) (in Russian)
36. Komartsova, L.G., Maksimov A.V.: Neirokomp'iutery [Neurocomputers], 320 p. M. Publishing House of the Moscow State Technical University (2002) (in Russian)
37. In: Trusova, P.V. (ed.) Vvedenie v matematicheskoe modelirovanie [Introduction to Mathematical Modeling: Textbook], 440 p. M. Logos (2005) (in Russian)
38. Gorodetskiy, A.E., Dubarenko, V.V., Kurbanov, V.G.: Method of searching for optimal control actions on objects with dynamic adaptation to changes in the environment. In: 6-i Sankt-Peterburgskii simpozium po teorii adaptivnykh sistem (SPAS'99). 6th St. Petersburg Symposium on Adaptive Systems Theory (SPAS'99), pp. 228–232. St. Petersburg (1999) (in Russian)
39. Dobrynin, D.A., Karpov, V.E.: Modeling some forms of adaptive behavior of intelligent robots. Informatsionnye tekhnologii i vychislitel'nye sistemy. Inf. Technol. Comput. Syst. **2**, 45–56 (2006) (in Russian)

Unified Logical Analysis in Robots' CNS Based on N-Tuple Algebra

Boris A. Kulik and Alexander Ya. Fridman

Abstract *Objective* A robot's behavior in a complex environment is largely determined by the ability to perform complex logical analysis of the current situation. Such analysis uses both deductive and non-deductive methods (defeasible reasoning, hypothesis, abductive conclusion, and so on). The aim of this publication is to describe approaches to mathematical modeling of the unified logical analysis within the central nervous system of a robot taking into account peculiarities of human reasoning where imaginative schemas play a significant role. *Results* A mathematical model is proposed for a generalized logical analysis on the basis of *n*-tuple algebra. This model is distinguished with representation of inference as a cognitive image-schematic structure "container", which mathematically corresponds to the inclusion relation between structures of *n*-tuple algebra involved in reasoning. *Practical significance* The proposed methods and algorithms of generalized logical analysis can be used for formation of intelligent robot control systems.

Keywords Deductive and defeasible reasoning · Abductive conclusion · Central nervous system of a robot · Cognitive semantics · *N*-tuple algebra

1 Introduction

A generalized logical analysis means a combination of deductive and non-deductive techniques to analyze systems and reasoning, considered from some unified theoretical positions. Below, it is supposed that a model of logical human thinking is

B.A. Kulik (✉)
Institute of Problems in Mechanical Engineering,
Russian Academy of Sciences, St. Petersburg, Russia
e-mail: ba-kulik@yandex.ru

A.Ya. Fridman
Institute for Informatics and Mathematical Modelling,
Kola Science Centre of the Russian Academy of Sciences, Apatity, Russia
e-mail: fridman@iimm.ru

A.E. Gorodetskiy and V.G. Kurbanov (eds.), *Smart Electromechanical Systems: The Central Nervous System*, Studies in Systems, Decision and Control 95,
DOI 10.1007/978-3-319-53327-8_2

used for constructing a mathematical model for logical analysis in the central nervous system (CNS) of a robot.

Usually in the literature on artificial intelligence, non-deductive methods (defeasible reasoning, argumentation, hypothesis, abduction, etc.) are presented as something loosely related to deduction. As a rule, their theoretical foundation is based on special (non-classical) logics and a specifically introduced terminology [1–4], which sometimes makes it difficult to understand the essence of logical analysis and even narrows possibilities and areas of its applications. Closer ties can be determined between the objectives of deductive and non-deductive analysis by using some schemas of the cognitive approach [5]. One of them is the "container" schema that provides a good example of Euler/Venn diagrams. In mathematics, this schema corresponds to the inclusion relation upon sets. In this chapter, we consider a possibility to use such a schema for building not only a logical inference theory, but also some methods to analyze defeasible reasoning, including abduction.

Researches on cognitive semantics [6, 7] have shown that a person think with the help of imaginative schemas rather than according to the laws of formal logic. As a result, some of his obtained proofs become much shorter than those presented in the style of predicate logic. This is not surprising when you consider that "imaginative schemas" provide for some seemingly primitive, but at the same time sufficiently rigorous, methods to analyze reasoning. This refers to the "naive" set theory (called algebra of sets in modern interpretation) based on the inclusion relation. Started in the early XX century, the debate about foundations of mathematics has undermined the confidence of many mathematicians to this theory because some paradoxes were discovered in its basics. Though it became clear later that the paradoxes resulted not from objective reasons, but from errors of reasoning (in particular, from the ambiguity of understanding the membership relation in the formulation of Russell's paradox) [8], the credibility of algebra of sets was never fully restored.

Another argument against algebra of sets as an instrument of logical analysis was that its apparatus (in particular, Euler/Venn diagrams) was used mainly to analyze relatively simple reasoning such as syllogisms and propositional calculus problems [9, 10]. That is why opportunities to apply it for many of the more complex models and for artificial intelligence systems were not even discussed. This difficulty has been overcome with the development of n-tuple algebra (NTA). On the one hand, NTA is isomorphic to algebra of sets, but at the same time NTA is applicable for processing sophisticated structures. Moreover, NTA occurred to be a useful tool for modeling and analysis of defeasible reasoning that includes abduction as well [11].

NTA is an algebra of arbitrary n-ary relations based on properties of the Cartesian product of sets. Connections between NTA and logical calculi are reflected in the fact that NTA objects model truth scopes of logical formulas, NTA operations correspond to the logical connectives, and the inclusion relation upon NTA structures is fully consistent with respect to deducibility relation in logical calculi.

Traditionally, deductive analysis and the logical inference in particular is considered from the point of view of the theory of formal systems, where concluding a consequence or verifying its correctness is done by means of serial application of

certain inference rules to a set of logical formulas that play the role of premises (or axioms) for a reasoning system. NTA can implement deductive analysis not only by using the inference rules (including the resolution method), but also by checking correctness of the inclusion relation between NTA structures, which represent logical formulas. In some cases, this method not only allows to simplify the task of obtaining consequences with certain properties (for example, a consequence with a specific composition of meaningful variables), but also to find a closer connection between deductive and non-deductive methods of analysis. In particular, abductive conclusion can be obtained in NTA by running certain algorithms to adjust structures, in which the inclusion relation is violated. In NTA, generation and validation of hypotheses can also be implemented by checking inclusion relations or by constructing projections of NTA structures. These projections have the property to be a superset of the source structures.

NTA structures also comply well with the problem of logical-mathematical implementation of the behavioral processes formation based on analysis of sensations in a robots' CNS [12]. There it was proposed to integrate robots sensors into some groups forming the robots humanlike sense organs: sight, hearing, smell, taste, etc. in the form of sets $X, Y, Z, U, \ldots$ In each of the introduced sets, we can distinguish some subsets, which characterize the properties of an observed or studied object. Let they be $X_i \subset X, Y_i \subset Y, Z_i \subset Z, U_i \subset U, \ldots$ The totality of such subsets depends on the set of sensors employed in the senses of a particular robot. For instance, the following subsets can be assigned to its sight: X_1—the contour of image; X_2—the size of the image; X_3—the brightness of the image; X_4—the color of the image; X_5—the distance to the object. Also, some sets can represent the situations within which the robots will interact, as well as their possible responses or actions. Then the formalization task for building a CNS of robots' senses can be considered in terms of NTA, if we use the mentioned sets as attributes, and the interconnections among them will be displayed as relations [13].

In NTA, arbitrary n-ary relations can be expressed as four types of matrix-like structures called **NTA objects**. Every NTA object is immersed into a certain space of **attributes**. **Domain** is a set of values of an attribute.

Names of NTA objects contain an identifier followed by a sequence of attributes names in square brackets; these attributes determine the **relation diagram**, in which the NTA object is defined. For example, $R[XYZ]$ denotes an NTA object defined within the space of attributes X, Y, Z, and $R[XYZ] \subseteq X \times Y \times Z$.

2 Deductive Analysis from the Perspective of the Cognitive Schema "Container"

Deductive analysis (DA) includes solving the following two problems.

The first task of DA is validating a specific consequence B for some given premises A_i;

The second task of DA is deriving possible consequences from some given premises A_i with consideration of certain semantic constraints, for instance, presence of given variables or their combinations in a consequence, deriving a consequence with the minimal number of significant variables, etc.

In propositional and predicate calculi, the first task is mainly used, but the second task is no less important in terms of practical applications. They are solved by means of inference rules. Systems of these rules vary in different scientific schools, but anyway, it is difficult to predict the optimal procedure for applying these rules in advance. In many cases, non-optimal order of application of the rules can lead to an ample increase in algorithm execution time.

Solving such problems in NTA is not based on inference rules only, but also on certain types of algorithms that use some generalized operations and verify inclusions of sets into other ones [11, 13]. In many cases, these algorithms are more efficient than conventional algorithms based on the resolution method.

Formulas of classical logic, representing premises and consequences, are expressed as NTA objects, with which you can perform generalized operations and check generalized relations of equality and inclusion. Consider an example.

Example 1 Suppose a robot must find an object located in one of the three rooms, with one of the rooms it may not enter (there is a danger), and one empty room. The following conditions (premises) are given that can be used to solve the problem.

(1) the first room is not dangerous, the second room is not empty;
(2) the third room is not dangerous, the second room is not empty.

We also know that one of the rules is true, and the other rule is false. Is it possible to locate the desired object on the basis of these data?

Let A denotes the statement "this room contains the desired object", B is the phrase "the room is empty", and C means "there is a danger in the room". To model this problem by NTA, let us use names of rooms R_1, R_2, R_3 as attributes; each of the rooms may be in one of the three permitted situations from the set $\{A, B, C\}$. Then conditions can be expressed by C-n-tuples:

(1) $T_1[R_1R_2] = [\{A, B\}\{A, C\}]$;
(2) $T_2[R_2R_3] = [\{A, C\}\{A, B\}]$.

To solve the problem, it is necessary to consider two cases: (1) the first condition is true, and the second is false; (2) the first condition is false, and the second is true.

Let us consider the first case. If T_2 is false, then $\overline{T_2} =]\{B\}\{C\}[$ is true. The solution of the problem can be found by calculation the generalized intersection of true conditions:

$$T_1 \cap_{\mathrm{G}} \overline{T_2} = [\{A, B\}\,\{A, C\}] \cap_G]\{B\}\{C\}[$$

$$= [\{A, B\}\{A, C\}*] \cap \begin{bmatrix} *\{B\} & * \\ *\{A, C\} & \{C\} \end{bmatrix} = [\{A, B\}\{A, C\}\{C\}].$$

The resulting C-n-tuple contains 4 possible placement options (it becomes clear by calculating the Cartesian product $\{A, B\} \times \{A, C\} \times \{C\}$), but the conditions of the problem require for different situations in different rooms, so the only option (B, A, C) is correct. Thus, the desired object is located in the second room. Similar results were obtained when testing the second case.

The proposed transition to algebraic representations becomes clear when you consider that NTA objects model the truth domains of logical formulas. Suppose that some given premises A_i and an expected consequence C are possible to express as NTA structures. Then the validation algorithm for the consequence C from the given premises A_i has to calculate their generalized intersection and check the generalized inclusion [13]:

$$(A_1 \cap_G \ldots \cap_G A_n) \subseteq_G C \tag{1}$$

It was found that all the inference rules in mathematical logic and natural calculus after Gentzen comply with (1) after converting premises and conclusions into NTA structures. The validation algorithm based on the relation (1) is proved to be correct [13]. This relation implements a "container" schema and results in some statements unusual for the traditional theory of logical inference.

(1) There exists a **minimal consequence** for a given set of premises. It is equal to the generalized intersection of the premises: $A = A_1 \cap_G \ldots \cap_G A_n$. The concept of the minimal consequence allows to calculate the number of all possible consequences in systems with finite ranges of variables values [11]. It is equal to 2^N where $N = |U| - |A|, |U|$ is the number of elementary n-tuples in the universe, and $|A|$ is the number of elementary n-tuples in the minimal consequence. NTA provides a method to calculate quantitative characteristics of NTA objects.

(2) Any superset of a minimal consequence A (i.e. any relation $A \cap_G R$ where R is an arbitrary relation) is a consequence from the given system of premises. Thus, in many cases, **formal logical inference significantly increases the degree of uncertainty comparing to the statements contained in the minimal consequence**. As a result, if a minimal consequence contains a statement C that has no alternatives, it is possible to find such a statement R in another correct consequence that will contain an alternative to C. For example, if a minimal consequence A contains the statement "This obstacle is insurmountable by bypassing it from the left" and does not contain the alternative statement "This obstacle is surmountable by bypassing it from the left with difficulty", the statement "This obstacle is insurmountable by bypassing it from the left or surmountable with difficulty" will be a correct consequence from A according to the rules of logical calculi.

(3) The reasonability of increasing uncertainty in a consequence by addition arbitrary relations to A is justified only in cases where the given system of premises results in a formula with a reduced number of variables compared to the overall composition of the variables in the premises. It is proved in NTA

that this way we obtain an **inductive generalization of a minimal consequence** [11]. Thus, a consequence with a reduced variables composition is formed by adding some combination of values for "disappearing" variables, which were missed in a minimal consequence. The solution to this problem in NTA is obtained by using a simple algorithm to calculate projections of the resulted formula. Conventional inference engines propose no simple algorithms to solve this task. Such NTA algorithms can be used to solve the second problem of DA as well, namely to derive possible consequences with specific properties from a given set of premises A_i. Consider an example.

Example 2 Suppose that one of the two rooms contains an object that can be a danger to a robot or to be safe. It is necessary to find out whether the robot can enter at least one of these rooms, if the following is known: (1) if the first room is empty, the object is safe; (2) if the object is dangerous, the second room is empty; (3) if the first room is not empty, then the second room is empty. To solve the problem, you need to answer the question whether these conditions infer that the object is safe.

We introduce the notation as follows. Let x means "the first room is empty", y stands for "the second room is empty", z denotes "the object is safe". Then the premises A_1, A_2, A_3 can be expressed by the logical formulas:

$$A_1 : x \to z; \quad A_2 : \neg z \to \neg y; \quad A_3 : \neg x \to y.$$

The intended consequence of these premises should be z. To verify this by using NTA methods, we will consider attributes as variables X, Y, Z with two values: 1 (literal itself) or 0 (negation of a literal). After substituting, we obtain expressions for the premises and the consequence C:

$$A_1[XZ] =]\{0\}\ \{1\}[; A_2[YZ] =]\{0\}\ \{1\}[; A_3[XY]]\{1\}\ \{1\}[; C[Z] = [\{1\}].$$

Using the NTA methods, we calculate the minimal consequence:

$$A[XYZ] = A_1[XZ] \cap_G A_2[YZ] \cap_G A_3[XY] = \begin{bmatrix} \{1\} & * & \{1\} \\ \{0\} & \{1\} & \{1\} \end{bmatrix}.$$

By adding dummy attributes, $C[Z]$ is possible to rewrite as occurs when the relation

$$C[XYZ] = [\ *\ *\ \{1\}].$$

It is easy to verify that $A[XYZ] \subseteq C[XYZ]$, which proves the correctness of the consequence and, accordingly, the possibility for the robot to enter into any room.

The same answer can be obtained after solving this problem by the method of calculating projections of the minimal consequence. In this case, when the minimal

consequence $A[XYZ]$ is represented as a C-system, it is sufficient to eliminate attributes X and Y from the matrix representation in order to get the same result.

Let us consider the second task of DA. According to (1), a totality of consequences $\{C_j\}$ can be inferred from the premises A_i by using the following relationship: any NTA object C_j, which satisfies the relation $A \subseteq C_j$ where A is the minimal consequence of the premises A_i, is their correct consequence. It is clear that it makes no sense to infer all possible consequences from a given system of premises; besides, their number was proved to grow exponentially [11]. Only consequences having some pre-defined properties are of interest actually. In particular, the shortened variables composition as compared with the minimal consequence can be one of such properties. Example 2 illustrates this case.

For constructing such consequences, NTA proposes calculating projections of the minimal consequence. Let us consider this method in more detail. Suppose a minimal consequence A was obtained in the space of attributes $X_1, \ldots, X_n$. In NTA, any projection of an NTA object is proved to be its superset. Therefore, an arbitrary projection of the minimal consequence A is a correct consequence. Such projections are easy to calculate, if the NTA object is a C-n-tuple or a C-system [13]. Then it is enough to eliminate the corresponding attributes from this NTA object, i.e. to remove these attributes from the relation diagram and delete the columns with these attributes from the matrix representation.

In some cases, the minimal consequence is easier to obtain as a D-system [11]. To calculate its projection then, it is necessary to convert it to the C-system. There are NTA algorithms designed for such transformations. Their disadvantage is that they have exponential computational complexity in general. Although for systems of small dimension and some special cases investigated in [13], their complexity is relatively low.

Calculations of projections for a minimal consequence do not always lead to a positive result since many NTA objects have projections that do not contain useful information. These are projections represented by a complete set of all combinations of attributes. For the C-system $C[XYZ] = \begin{bmatrix} \{1\} & \{0\} & * \\ * & \{1\} & \{1\} \end{bmatrix}$ as an example, such projections are all projections with a single attribute. At the same time, all projections with two attributes do not include complete sets of elementary n-tuples and therefore they can be used as consequences. For instance, the projection $[XY]$ (first and second columns) does not contain a complete set of elementary n-tuples and corresponds to the logical formula $x \vee y$.

The literature on mathematical logic mainly uses the first problem of DA in examples of logical inference when it is needed to validate a given consequence, and such consequences usually contain a reduced composition of variables. However, there are no effective methods to obtain such consequences, since it is only possible for a matrix representation of logical formulas.

3 Analysis of Hypotheses and Abduction Based on Calculation of Projections

Abduction can be represented as a search of explanations for "unexpected" results, which traditionally should not take place in a given standard situation [14]. In a reasoning system, abduction can be considered as an explanation for appearance of not clearly formulated facts or arguments, which refute a formally correct consequence of a given premises system. Hypotheses are used as explanations, whereby the abduction is a variant of revised reasoning. In many publications, in [1–3] for instance, revised reasoning is associated with non-classical logics, in particular, with non-monotonic logic. Thus, modeling of revised reasoning allows violations of the laws of classical logic and, in particular, the laws of algebra of sets.

To model deductive and revised reasoning in NTA, we have proposed a general theoretical approach that, firstly, does not violate any laws of algebra of sets, and, secondly, uses relation (1) obtained in the framework of NTA. However, while in deductive analysis, the relation (1) serves a measure of formal correctness for a consequence, violations of (1) indicate a necessity to proceed to non-deductive analysis during analysis of hypotheses and revised reasoning. Moreover, NTA-characteristic matrix properties provide an effective search for necessary consequences or hypotheses with predetermined features in the course of applying both deductive and non-deductive methods of analysis.

Analysis of the arguments, on which many authors offer to abandon classical logic when modeling revised reasoning, has shown that so-called violations of the monotony of logical inference in practical reasoning result actually from violations of some implicitly given constraints [11]. In the theoretical foundations of NTA, such violations of constraints revealed by using certain methods are called **collisions** [13].

An example of a collision is as follows. Suppose, from certain given premises, we concluded two statements: (a) "all objects in this room are dangerous" and (b) "all objects in this room are not dangerous". There is no formal contradiction in them, since a formal negation of the first statement is the statement "some of objects in this room are not dangerous" rather than the statement (b). At the same time, the statements (a) and (b) infer that no objects exist in the room. From a formal point of view, this is not a contradiction, but a situation in which a (sometimes implicit) constraint is violated. In this case, the constraint is the existence of any objects in the room. Violation of this constraint results in a collision during reasoning. Let us consider some types of collisions.

The term "collision" was initially used by Kulik [8] for analysis of syllogistics-like reasoning, where two kinds of formal collisions were defined, namely.

a **paradox collision** arises if premises infer a statement like "No A are A" ($A \supset \overline{A}$), that is, the volume of the term A is empty;

a **cycle collision** occurs when the relation $A \subseteq B \subseteq \ldots \subseteq A$ can be deduced from a system of sets; this means that the terms contained in the cycle are equal.

The collisions listed above can be detected without taking the subject domain into account; this is why we named them **formal collisions**.

The third kind of collisions is not a formal one; it features a situation when some consequences do not match some indisputable facts or justified statements. We call this collision an **inadequacy collision**.

Unlike a logical contradiction which expresses an absolute degeneration of premises, collisions can have opposite interpretations in different cases. In other words, a collision, as opposed to a contradiction, is semantically dependable. For example, within one system, the equality $A = \varnothing$ means an absence of the object A that is necessary for existence of the system, and in another system this equality specifies a status of the object A. The first case requires changing the premises while the second case provides a new useful datum and amends our knowledge.

Let us adduce an example of collisions upon NTA structures.

Example 3 A closed box contains articles described by their shapes (a sphere or a cube), colors (white or red) and materials (plastic or wood) It is necessary to determine which types of objects can be in a box, if it is known: (1) all balls are red; (2) all the wooden objects are painted white; (3) all plastic items are not balls.

Let S stands for balls, W denotes white items, and P means plastic items. We write the conditions of the problem in the language of propositional calculus:

(1) $A_1 = S \to \bar{W}$;
(2) $A_2 = \bar{P} \to W$;
(3) $A_3 = P \to \bar{S}$.

Now we express premises in NTA terms, matching variables S, W, Z with attributes X_S, Y_W, Z_P respectively:

$$A_1[X_S Y_W] =]\{0\}\{0\}[;\ A_2[X_P\, Y_W] =]\{1\}\{1\}[;\ A_3[X_P Y_S] =]\{0\}\{0\}[$$

$$A[X_S Y_W Z_P] = A_1 \cap_G A_2 \cap_G A_3 = \left]\begin{matrix} \{0\} & \{0\} & \varnothing \\ \varnothing & \{1\} & \{1\} \\ \{0\} & \varnothing & \{0\} \end{matrix}\right[.$$

After converting A into the C-system we find: $A[X_S Y_W Z_P] = \begin{bmatrix} \{0\} & \{1\} & * \\ \{0\} & \{0\} & \{1\} \end{bmatrix}$.

The first column of the resulting C-system contains only a singleton component $\{0\}$. This is the sign of the paradox collision $S \supset \bar{S}$. Indeed, the expression $(S \supset \bar{S}) = \bar{S} \vee \bar{S} = \bar{S}$ corresponds to the C-n-tuple $R[X_S Y_W Z_P] = [\{0\}\ *\ *\ ]$ in NTA, and therefore, the collision $S \supset \bar{S}$ is a consequence of the initial system of premises.

Identification of the paradox collision in the analyzed reasoning system means that there are no balls in the box, and all of the items have a cube shape.

Collisions can model the following cases.

(1) When new knowledge is input, some different attributes become identical in composition of their elements, which contradicts to the semantics of the system.

(2) A discrepancy occurs between the obtained results and some restrictions that are hard to formalize and they are described in task settings. For instance, a modeled system can contain some limitations expressed as relations, which must not appear in consequences.

It is not easy to foresee all possible kinds of collisions; they can well be unique for some logical systems. We propose the following brief definition for the term "collision" in NTA.

Collisions are situations recognized as violations of some formally expressed rules and/or limitations, which control consistency and meaning content of a logical system. In many cases, the collisions detection means semantic incorrectness of reasoning.

The concept of collisions allows for a formal definition of hypotheses in NTA. Let us suppose that a system of premises expressed as NTA objects $A_1, \ldots, A_n$ is given and the NTA object $A = A_1 \cap_G \ldots \cap_G A_n$ is calculated.

A certain formula H is called a **hypothesis**, if $A \subseteq_G H$ is false. Otherwise, H is a consequence according to (1).

The hypothesis is **correct**, if:

(1) $A \setminus_G H \neq \varnothing$, i.e., the new system of premises is consistent;
(2) the object $H \cap_G A$ contains no collisions.

Processing of hypotheses is an intrinsic part of abduction. Let us now formally define abduction.

If B is an estimated consequence of the premises $A_1, \ldots, A_n$ and the statement $A \subseteq_G B$ is known to be false (once again, $A = A_1 \cap_G \ldots \cap_G A_n$), then a hypothesis H is an admissible **abductive conclusion** when the two following conditions are met:

(1) H is a correct hypothesis (i.e. $A \subseteq_G B$ is false) and $H \cap_G A$ is not empty;
(2) $(H \cup_G A) \subseteq_G B$, that is, adding H into the system of premises results in deducibility of the estimated consequence B.

Let us consider the condition

$$(H \cup_G A) \subseteq_G B \tag{2}$$

If the anticipated consequence B is known, then the need for a hypothesis arises, if $A \setminus B = R \neq \varnothing$, i.e. the formal condition for a consequence (namely, $A \subseteq_G B$) is not met. On the basis of these relations, we can construct the following algorithm.

3.1 Search Algorithm for Abductive Conclusions

Step 1 Calculate the "remainder" $R = A \setminus_G B$;
Step 2 Build an intermediate object R_i, for which $R \subseteq_G R_i$ is true;
Step 3 Calculate $H_i = \bar{R}_i$ (R_i can now be denoted by $\overline{H_i}$);

Step 4 Calculate $H_i \cap_G A$ and check it for presence of collisions; if they are detected, return to Step 2, otherwise *End*.

The Step 2 of this algorithm allows to obtain R_i by means of methods to calculate projections of the object R discussed in the previous section. Thus we can form hypotheses with predetermined properties, in particular, the hypothesis with a certain pre-defined composition of attributes.

Let us give an example.

Example 4 There are 3 rooms, the first and the third ones may be empty or contain some objects, the second room is not empty, but a dangerous object can be inside it. Then opening of this room leads to a big trouble. However, this room can contain an object that a robot needs in accordance with its job. It is also given that: (1) if the first room is not empty, then the second room contains a useful (desired) object, or the first room contains a dangerous object; (2) if the second room contains a dangerous object, the first room is empty and the third room is not empty; (3) if the third room is empty, then either the object in the second room is useful or the object in the first room is dangerous. Can we conclude that the robot can find the desired object in the second room?

To start solving, we express the given statements in the language of propositional calculus. Denotations are as follows: A is "the first room is empty", B means "the object in the second room is useful", C states that "the first room contains a dangerous object", and D stands for "the third room is empty". By transforming every premise and the question into DNFs, we obtain:

- for the first premise: $A \vee (B \wedge \neg C) \vee (\neg B \wedge C)$;
- for the second premise: $B \wedge (\neg A \wedge D)$;
- for the third premise: $\neg D \vee (B \wedge \neg C) \vee (\neg B \wedge C)$;
- for the question under investigation: B.

To present these formulas as NTA objects, let us use the universe $X_A \times X_B \times X_C \times X_D = \{0,1\}^4$ where $A = B = C = D = 1$ and $\neg A = \neg B = \neg C = \neg D = 0$. Then premises become C-systems:

$$P_1 = \begin{bmatrix} \{1\} & * & * & * \\ * & \{1\} & \{0\} & * \\ * & \{0\} & \{1\} & * \end{bmatrix}; \quad P_2 = \begin{bmatrix} * & \{1\} & * & * \\ \{0\} & * & * & \{1\} \end{bmatrix};$$

$$P_3 = \begin{bmatrix} * & * & * & \{0\} \\ * & \{1\} & \{0\} & * \\ * & \{0\} & \{1\} & * \end{bmatrix},$$

and the estimated consequence will look like the C-n-tuple $S[X_B] = [\{1\}]$.

Solution of the problem can be found by checking the relation $(P_1 \cap_G P_2 \cap_G P_3) \subseteq_G S[X_B]$. To do this, we calculate

$$P[X_A X_B X_C X_D] = P_1 \cap_G P_2 \cap_G P_3 = \begin{bmatrix} \{1\} & \{1\} & * & \{0\} \\ * & \{1\} & \{0\} & * \\ \{0\} & \{0\} & \{1\} & \{1\} \end{bmatrix}$$

For testing the inclusion, we add the missing attributes into S:

$$S[X_A X_B X_C X_D] = [*\{1\} * *].$$

Then testing shows that the third C-n-tuple of P is not included in S, so the estimated consequence (the object in the second room is useful) is not deducible yet. To confirm or deny correctness of this consequence, it is required to clarify certain circumstances. The search for such circumstances can be formulated as a search for an abductive conclusion.

Assume that the consequence S is correct. Then we need to find additional hypotheses suitable for addition to the given premises. Let us write intermediate results in the new notation.

Intersection of premises equals to $A[X_A X_B X_C X_D] = \begin{bmatrix} \{1\} & \{1\} & * & \{0\} \\ * & \{1\} & \{0\} & * \\ \{0\} & \{0\} & \{1\} & \{1\} \end{bmatrix}$, and the expected consequence is: $B[X_A X_B X_C X_D] = [*\{1\} * *]$.

Next, we use the algorithm.

$$R = A \backslash_G B = \begin{bmatrix} \{1\} & \{1\} & * & \{0\} \\ * & \{1\} & \{0\} & * \\ \{0\} & \{0\} & \{1\} & \{1\} \end{bmatrix} \cap_G [*\{0\} * *] = [\{0\}\{0\}\{1\}\{1\}].$$

You can select any projection of R as R_i. It is reasonable to check the third room, since it cannot contain a dangerous object. Then the projection will be $R[X_D]$ and we obtain $R_i = [\ * * * \{1\}]$. So, $H_i = \overline{R_i} = [\ * * * \{0\}]$.

Thus, we can conclude that the visit to the second room will be safe, if inspection of the third room shows it is not empty.

4 Conclusion

Proposed methods of constructing deductive and defeasible reasoning are based on cognitive semantics; they use an algebraic approach to logical inference as well as to generation and validation of hypotheses. Due to the matrix representation of logical structures, it becomes possible to form a set of admissible hypotheses considering some predefined properties. This approach is expected to increase the transparency of reasoning mechanism in the course of modeling of unified logical analysis within a robot's CNS together with providing flexibility in adjusting the reasoning system for solving various practical problems.

Acknowledgements The authors would like to thank the Russian Foundation for Basic Researches (grants 14-07-00257, 15-07-04760, 15-07-02757, 16-29-04424, and 16-29-12901) for partial funding of this research.

References

1. Vagin, V.N., Golovina, E.Y., Zagoryanskaya, A.A., Fomina, M.V.: Exact and Plausible Reasoning in Intelligent Systems. Fizmatlit, Moscow (2008). (in Russian)
2. Russel, S., Norvig, P.: Artificial intelligence: a modern approach, 2nd edn. Prentice Hall, Englewood Cliffs NJ (2003)
3. Thayse A., Gribomont P., Hulin G. et al.: Approche Logique de l'Intelligence Artificielle, vol. 2: De la Logique Modale à la Logique des Bases de Données. Paris: Dunod (1989)
4. Pollock, J.L.: Defeasible reasoning. Cogn. Sci. **11**, 481–518 (1987)
5. Lakoff, J.: Women, fire, and dangerous things: what categories reveal about the mind. University of Chicago Press, Chicago (1987)
6. Sowa, J.F.: Conceptual structures—information processing in mind and machines. Addison-Wesley Publ. Comp, Reading, MA (1984)
7. Kuznetsov, O.P.: Cognitive semantics and artificial intelligence. Sci. Tech. Info. Process. **40**(5), 269–276 (2013)
8. Kulik, B.: Logic of Natural Reasoning. Nevsky Dialekt, Saint Petersburg (2001). (in Russian)
9. Pospelov, D.A.: Modeling of reasoning. Experience in analysis of intelligent acts. Radio i Svyaz' Publ, Moscow (1989). (in Russian)
10. Kuzichev, A.S.: Venn diagrams. Nauka Publ, Moscow (1968). (in Russian)
11. Kulik, B.A., Zuenko, A.A., Friedman, A.Y.: Deductive and defeasible reasoning on the basis of a unified algebraic approach. Sci. Tech. Info. Process. **42**(6), 402–410 (2015)
12. Gorodetsky A.E., Kurbanov V.G., Tarasova I. L.: Challenges related to development of central nervous system of a robot on the bases of SEMS modules. (in this collection)
13. Kulik, B., Fridman, A., Zuenko, A.: Algebraic approach to logical inference implementation. Comput. Info. **31**(6), 1295–1328 (2013)
14. Kapitan, T.: Peirce and the structure of abductive inference. In: Houser, D., Roberts, D., Van Evra, J. (eds.) Studies in the logic of Charles Sanders Peirce, Nathan, pp. 477–496. Indiana University Press, Bloomington (1997)

SEMS-Based Control in Locally Organized Hierarchical Structures of Robots Collectives

Alexander Ya. Fridman

Abstract *Objective* Development of brainware to integrate interactions of hierarchical groups of robots, built on the basis of SEMS modules, with the purpose to support making objective compromise strategic and tactical decisions. *Results* Coordination and planning methods are proposed for hierarchical collectives of such robots within the frame of the situational approach. Sufficient conditions are obtained for coordinability of hierarchical dynamic systems with using local quality criteria gradients and ideas of local organization of reasonable behavior. For groups of robots built in the paradigm of Dynamic Intelligent Systems (DIS), a coordination principle is proposed based on the known principles of interactions prediction. On the basis of the notion of the effective N-attainability, a procedure is developed to directly synthesize plans to control such collectives. *Practical significance* The proposed methods of coordination and planning will allow efficient usage of available resources in order to provide acceptable results for all (or most) modules having purposeful behavior.

Keywords Smart electromechanical systems · Coordination and planning · Hierarchical collectives of intelligent robots · Situational approach

1 Introduction

In terms of information and control systems, smart electromechanical systems (SEMS) can be seen as a collective of "cognitive information management systems built into their environment" [1, 2], is a kind of cyber physical systems [3]). Apparently, similar devices need to have two-way communication with the outside world, but the main feature of their capabilities to solve complex problems lies in

A.Ya. Fridman (✉)
Institute for Informatics and Mathematical Modelling,
Kola Science Centre of RAS, Apatity, Russia
e-mail: fridman@iimm.ru

A.E. Gorodetskiy and V.G. Kurbanov (eds.), *Smart Electromechanical Systems: The Central Nervous System*, Studies in Systems, Decision and Control 95,
DOI 10.1007/978-3-319-53327-8_3

intelligent processing of the available information to make decisions about preferred actions in changing situations. Methods to intellectualize SEMS are still unsettled, they include evolutionary approach [4], self-learning [5] and other approaches that exist in the artificial intelligence. For the same purpose, we develop an algebraic approach [6, 7] in recent years. However, existing publications insufficiently illuminate the task of implementing the decisions made in groups of intellectualized devices. Many authors have noted the importance of this task. For example, the paper [4] states: "The emergence of horizontal linkages for cooperation and coordination between the individual cognitive units plays a key role in the formation of multilevel integrated structures with elements of group management strategies. This is due to inefficiency (and impossibility, in some cases) to solve complex problems by means of individual isolated subsystems. This integration serves as a necessary condition for hybridization and multidimensionality of intelligent systems, the characteristic attribute of which is the ability to assess, predict and control the collective behavior or group dynamics of cognitive systems at a metalevel". In [8] the solution of such problems rests with the Planning and Management System (PMS) intended to control purposeful behavior. However, no structure was proposed for such a system.

In the author's opinion, in order to achieve synergies between SEMS modules in all of the above-mentioned and other problems, we need a common methodological basis for providing the desired group behavior of robots teams. As each module has a purposeful behavior, no solution of this problem can be based on centralized control and requires for more flexible decentralized strategies. In this formulation, a robots team can be seen as a System of Systems (SoS) (e.g., see [9]), where coordination and planning tasks come to the fore, and a hierarchy of SoS subsystems is traditionally used to reduce complexity of the control problem (in this problem, each SEMS module is a subsystem of a SoS).

In accordance with the above rationale, a development of the situational approach [10] is further proposed to build a PMS brainware for hierarchical groups of SEMS modules. In this case, a significant part of the problem consists in a formalization of the term "situation" often used and rarely defined with sufficient correctness. This is done in the next section of this paper.

2 Basics of Situational Approach and Its Implementation for Hierarchical Systems

The situational approach has been applied in various problems, including the one considered in this paper, namely modeling and management of complex objects. The central concept here is the concept of *situation* as the temporal cutoff of a trajectory, along which characteristics of an object change in an abstract multidimensional space. Criteria to select this space have changed little compared with the requirements for such selection of the elements of the state vector in the classical

state space theory [11], developed for control of dynamic objects that allow their description in the form of differential and difference equations. Namely, the state space should include all time-varying characteristics of the object that significantly affect achievement of control or simulation goals. The procedure for constructing such state space, that is, separating the object of study itself from its environment, is usually taken outside the scope of the simulation process, since constructive techniques to choose elements of the state vector are not invented yet. The need to compare different trajectories (object scenarios) with each other, as well as restrictions on the part of the feasibility of data processing algorithms of the object, lead to the fact that state elements domains are in some way digitized on the basis of linear, nonlinear, or ordinal scales.

Specific definitions of the situation depend on the application domain and the used formalization method [12, 13]. In general, the complete situation is described in three main aspects. They include knowledge about the current structure of an object, the current state of its control system and the accepted control technology (strategies) [10]. Thus, each situation is described by a set of variables that characterize these aspects. The core of the classic situational control [10] is a semiotic (symbolic) model, which is built as a network, the nodes of which are internally consistent formal models, and transitions between nodes are defined by some rules to transform parameters of these formal models (so called correlating or logic-transformational rules (LTR). Building a semiotic model is done in terms of a certain language of situational control that is a fairly complex (in structure) subset of natural language. For example, in [10] it is assumed that creation of situational control requires for using a set of approximately 200 base relations divisible by 10–12 categories and linking together the basic concepts of the semiotic model. The number of such concepts is by an order of magnitude greater than the number of base relations and considerably depends on the specific subject area. Creation and development of situational control systems requires huge investment of resources to collect information about the controlled object, its operation and methods to control is, as well as to systematize this information in the framework of a semiotic model. That is why the authors of this method considered it appropriate to apply it only in cases where other formalization methods lead to the problem with too big (for practical implementation) dimension. Additional complexity arises form absence of constructive procedures to construct semiotic models.

Next, we investigate the possibility of adapting the situational approach for studying dynamics of hierarchical spatial objects based on a conceptual model, which forms the core of situational modeling system (SMS) [14]. To this end, let us consider the formalization of the situational control method in somewhat greater detail in accordance with [10].

Background information for creation a situational control system is grouped as follows:

Q_j, $j = 1, 2, \ldots$ is a set of current situations at the object (an analogue of values of the state vector);
U_k, $k = 1, 2, \ldots, N_U$ is a set of possible one-step impacts (controls);

S_i, $i = 1, 2, \ldots$ is a set of current complete situations, which include not only the present situation, but also information about the state of the control system and control strategies. Every complete situation converts the object from one current situation to another by implementing a certain one-step control from the set U:

$$S_i; Q_j \underset{U_k}{\longrightarrow} Q_i. \tag{1}$$

The classification problem for situations is in referring the current situation to one or more classes, corresponding to a single one-step control. If the result of classification is unique and the selected class of situations requires for some new impact on the object, the control related to this class is ejected to the object; otherwise selection of a control is made by extrapolating and comparing the effects of alternative actions.

In the situational modeling system [14], the control of an object is transformed into a choosing (at each step or cycle of simulation) one of the possible alternative structures of this object contained in a cohesive fragment of the SMS model. Every such structure uniquely identifies the current *complete situation* at the given initial conditions. Thus, the set of controls U in SMS contains alternative structures specified during constructing the model of the object under study by decomposition of its component parts and/or the links between them with the help of OR-relations. These alternatives are called *sufficient situations*. This way the SMS model observes one of the prerequisites for effective application of the situational approach: the number of possible control decisions has to be significantly less than the number of possible situations [10]. Then the task of analyzing the current situation in SMS turns to the task of assessing the previous control with the purpose to make a decision to alter (or not to alter) the structure of the object.

To use SMS, one shall represent a SoS as a hierarchy of *objects* (components of the object under investigation) reflecting their organizational relations. Every object implements its purposeful behavior by minimizing specific generalized expenditures based on the following criterion that can be assigned to any SMS element:

$$\Phi ::= \left(\frac{1}{m} \sum_{i=1}^{m} \left(\frac{a_i - a_{i0}}{\Delta a_i} \right)^2 \right)^{1/2} ::= \left(\frac{1}{m} \sum_{i=1}^{m} \delta a_i^2 \right)^{1/2}, \tag{2}$$

where: a_i are some of output resources of a model element; m is the number of such resources defining the number of classes in classification procedures; a_{i0} and $\Delta a_i > 0$ are adjusting parameters reflecting requirements of a super-object to the nominal value a_i of a resource and to its acceptable deviation from the nominal value; $\delta a_i ::= \frac{a_i - a_{i0}}{\Delta a_i}$ is the relative deviation of an actual value of a resource a_i from its nominal value a_{i0}.

If a_i are interpreted as scalar quality criteria for a SoS component that has rated values a_{i0}, then (2) corresponds to a general criterion with significance coefficients inversely proportional to permissible variations of the resources, and so the latter

statement does not contradict common sense. Namely, the smaller a Δa_i is, the bigger is the weight of the corresponding scalar criterion it the sum (2), the more important this criterion is supposed to be for the decision maker (DM) who controls this object. The criterion (2) provides a general estimation of any state or situation that occurred within a SoS since it equals unity when all output resources of a given SoS element have their margin values:

$$\Phi = 1, \text{ if } \quad |a_i - a_{i0}| = \Delta a_i, \quad \text{that is} \quad |\delta\, a_i| = 1,\ i = \overline{1, m} \tag{3}$$

and does not exceed unity if all resources are within the given boundaries.

Conditions (3) allow to easy locating the source of problems in a SoS. Its malfunctioning results from the poor performance of an element that is the lowest in the hierarchy of objects and has the value of its criterion (2) far above unity [14].

The specific value of the change of the criterion (2) at changing one of its arguments

$$\delta\, \Phi_i ::= \frac{\partial \Phi / \partial a_i}{\Delta a_i} = m\, \Phi\, \delta\, a_i, \tag{4}$$

reflects its relative flexibility to variations of this argument. Assuming that every resource is equally important for reaching a DM's goal (possible generalization is evident), it is reasonable to estimate the specific value of generalized expenses for a certain DM for reaching the goal per every argument as:

$$\eta_i ::= \frac{1}{m}\, \delta\, \Phi_i = \Phi\, \delta\, a_i \tag{5}$$

The generalized expenses η_i (5) do not exceed unity if all resources are within the boundaries. If this element consumes any (material) resources from other SMS elements, total expenses have to include expenses for getting the input resources. Then formula (5) transforms into the following one:

$$\eta_i ::= \Phi\, \delta\, a_i + \frac{1}{m} \sum_{j=1}^{n} \eta_j, \tag{6}$$

where η_j are expenses for producing input resources of the given model element calculated according to (5) or (6) as well.

The constructed SoS model provides comparative analysis of SoS alternative structures. It is aimed at decision making support by choosing one of the possible structures to realize the object under investigation. The modeling process steps as follows [14].

The atomic information in SMS is a *fact* giving any actual or desirable values of a certain resource. It can include, for instance, features of a product for sale or a utility to buy. A finite set of facts inputted by a user determines an *initial situation*. It is interpreted as a task to be achieved at a certain SoS structure.

So, as soon as a user has defined an initial situation by either choosing a list of resources or a map area of interest for her/him, the automatically found *decisive object* (DO) with its dominated connected fragment of the model will describe the *complete situation* for the given task. It means this fragment contains all information necessary to investigate the task, and the level of the decisive object in the object tree points at the organizational level of decision making. The complete situation possibly includes some structure alternatives due to comprising some objects with OR-decomposition or alternative sets of resources. Each of the alternatives is called a *sufficient situation*, it can be compared with other sufficient situations for the same DO in statics. To do so, SMS comprises a hierarchical system of criteria allowing to choose a sufficient situation or few situations preferable for optimizing this or that quality criterion for the decisive object. To learn probable consequences of the chosen alternatives, a DM may proceed with a simulation of every sufficient situation. Then the modeling system will generate an appropriate invoking of executors for elements of this situation and provide them with all necessary and properly updated information during the simulation. This way it is easy to investigate different scenarios of the future by modeling the whole SoS or its any part. A *scenario* is formed by a series of sufficient situations for the same decisive object. Scenario simulation is possible both with and without classification of situations.

Classification of situations occurring within a SoS is implemented according to the following definitions.

Definition 1 Two sufficient situations for the same DO belong to one class, if both of them have the minimal summand of the expenses (5) or (6) for the same output resource.

Definition 2 The optimal sufficient situation for the given class is the situation having the lowest value of the expenses (5) or (6).

To decide a proper structure of her/his subordinated part of a SoS, a DM seated in a DO can do the following steps at any modeling interval: ask SMS to classify the current situation for this DO according to Definition 1; decide the preferable class of situations for further functioning; receive from SMS the best structure for the chosen class according to Definition 2; change adjusting parameters a_{i0} and Δa_i for this DO in the way corresponding to this best situation.

Thus, the criterion (2) was initially intended for classification of situations and scenarios in SMS. However, it was ascertain to be useful for other modeling tasks as well, in particular, for coordination of SoS subsystems [14] considered below.

3 Coordination in SMS

As adjusting parameters a_{i0} and Δa_i (see (2)) directly reflect requirements of a DM to the nominal value of the quality criterion a_{i0} for an object and its allowable deviation Δa_i in the next step of modeling, (2) shows that it looks natural to

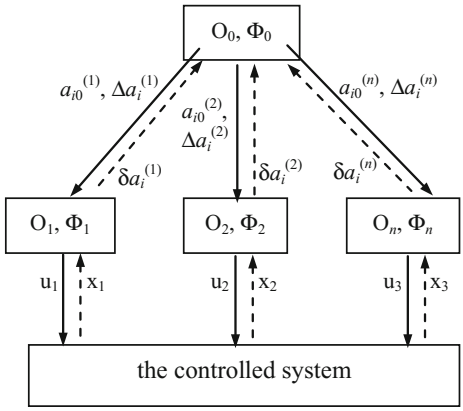

Fig. 1 The two-level system

coordinate SoS according to the principle of interaction prediction [15]. The DM sets the global task (i.e. the task for the whole system or its any connected subsystem) by selecting the dominant scalar criterion, which must make a minimum contribution to the generalized criterion (2), for the root object this DM is in charge of. Suppose, it is $a_{10}^{(0)}$.

As in [15] and without loss of generality, let us consider a two-level system (Fig. 1) where the top-level object (Coordinator) O_0 having a generalized quality criterion Φ_0 of the type (2), sends adjusting parameters to the subordinate objects (sub-objects) $O_1 - O_n$, which have similar quality criteria, and receives feedback signals as relative deviations of the actual values of the sub-objects' local quality criteria from their nominal values δa_i. Sub-objects interact via the controlled system and have no information on the states of other sub-objects, that is, the entire system is locally organized.

Assume for the moment that all the a_i are numeric variables. In the next section, this restriction will be removed.

In terms of system analysis, the proposed principle to coordinate this system corresponds to the external (objective) approach to assessing the effectiveness of subsystems within a metasystem. This principle states as follows: sub-objects tasks will be coordinated with respect to the Coordinator's task, if the sign of the gradient of the generalized Coordinator's criterion for its current dominant scalar criterion will coincide with signs of gradients of this generalized criterion for all current values of scalar criteria for sub-objects.

From (2) we obtain:

$$\frac{\partial \Phi_k}{\partial a_i^{(k)}} = \frac{2}{m_k} \frac{a_i^{(k)} - a_{i0}^{(k)}}{\Delta^2 a_i^{(k)}}, \tag{7}$$

which implies that the sign of the derivative can be changed as desired by selecting the value $a_{i0}^{(k)}$ greater than or less than $a_i^{(k)}$. On the other hand, if we assume actions

of all the sub-objects equally important to achieve the goal of the Coordinator (possibility of generalization is obvious), then:

$$\frac{\partial \Phi_0}{\partial a_i^{(k)}} = \sum_{j=1}^{m_0} \frac{\partial \Phi_0}{\partial a_j^{(0)}} \frac{\partial a_j^{(0)}}{\partial a_i^{(0)}} = \frac{2}{m_0} \sum_{j=1}^{m_0} \mu_j \frac{\partial a_j^{(0)}}{\partial a_i^{(0)}} \approx \frac{2}{nm_0} \sum_{j=1}^{m_0} \mu_j \frac{Inc[a_j^{(0)}]}{Inc[a_i^{(0)}]}, \tag{8}$$

where: $\mu_j = \frac{a_j^{(0)} - a_{j0}^{(0)}}{\Delta^2 a_j^{(0)}}$, and *Inc*[*] is a change (increment) of the parameter named within the parentheses for the latest time step.

The system is coordinated, if the Coordinator will select all $a_{i0}^{(k)}$ so that the signs of partial derivatives (7) (for $k = 0$ and $i = 1$) and (8) (for all k from 1 to n and all i for each sub-object) will coincide.

As mentioned above in the Introduction, obtained sufficient coordinability conditions resemble the ideas of ensuring stability of the local control in collectives of automata [16], which require for positive values of derivatives of a generalized criterion similar to (2) on the input parameters of the corresponding member of the collective.

The simulation results (e.g., [17]) have shown that the above-presented gradient method of coordination allows you to:

increase the stability of the system to external disturbances and to minimize the cross-effect of the lower level control elements;
more than twice the range of stability of the system to structural perturbations (compared to the pure local control).

Now we will show how to solve the problem of subsystems coordination, if it is impossible to determine a numerical metric analogous to (2) upon their state space. Below, this idea is exemplified with a collective of DIS (e.g., [18]).

4 Coordination in Collectives of DIS

DIS is described as a discrete dynamic system [18]

$$D = \langle X, N, \varphi, \psi \rangle, \tag{9}$$

where: X is a topological state space $x \in X$ with the proximity relation σ; N is the set of natural numbers, which mark discrete points of time; ϑ is the set of all subsets of X;

φ: $\vartheta \rightarrow \vartheta$ is a closure function with the following property:

$$\text{if } x \in \vartheta, \quad \text{then} \quad x \subseteq \varphi(x); \tag{10}$$

ψ: $\vartheta \times N \rightarrow \vartheta$ is a transition function with the following properties:

$$\begin{aligned} &\psi(x,0) = x \quad \text{for any} \quad x \in \varphi, \\ &\psi(\psi(x,t_1),t_2) = \psi(x,t_1+t_2). \end{aligned} \tag{11}$$

If a DIS is based on rules that contain sets of formulas of a language L, dynamics of this DIS in markovian case is described by the following equation:

$$x(t+1) = \varphi(\psi(\varphi(x(t) \cup u(t) \cup \delta(t))), \tag{12}$$

where: $u(t) \subseteq U(t) \subseteq U \subseteq L$ is a set of facts that are added to the state $x(t)$ (controls); $\delta(t) \subseteq \Delta(t) \subseteq \Delta \subseteq L$ is a set of facts that appear as a result of unpredictable changes in DIS's environment (disturbances).

The trajectory (12) is stable, if the function φ is monotonic and ψ is monotonic with respect to the state [18]. In what follows we assume that any referenced DIS meets these conditions.

In [18], the possibility is examined to control interactions within a team of "peer" DISs (the ones with identical knowledge bases). An example of such a group can serve vehicles involved in road traffic. We believe, it is of interest to investigate hierarchical systems, which include DISs as elements of different levels.

Again as in [15], we consider a two-level DISs system similar to Fig. 1, however, coordinating signals are denoted as γ_i and the feedback signals from the underlying DIS to the Coordinator are denoted as x_i. For simplicity, we assume all DISs in the lower level to be of the same type. Such a team may take part, for example, in the solution of any construction task by a collective of robots (O_i in Fig. 1, $i \in I = \{1, \ldots, n\}$), one of which serves as a job coordinator (O_0 in Fig. 1).

According to the principles of decentralized control, the purpose of coordinating signals γ_i, coming from the Coordinator to systems of the lower level, is a specification of such conditions for the tasks they have to manage that they would issue proper control signals u_i, which ensure fulfillment of both their own goals and the task of the whole system. Correspondingly, there exist two concepts of coordinability for the lower-level systems: coordinability with respect to the task of the Coordinator and coordinability in relation to the global task. There are several modes of coordination [15], the method of interaction prediction looks the most suitable for a collective of DISs. In implementing this method, the Coordinator informs the subordinate systems about its desired values of interactions among them and each of the lower-level systems is trying to reach the corresponding predetermined value, assuming that the other subsystems will operate properly as well.

4.1 Coordinability with Respect to the Coordinator's Task

When interpreting the method of interaction prediction for the two-level collective of DISs, we assume that at the beginning of every stage of the operation t_j, the

Coordinator informs systems O_i about their desired states $\underline{x}_i$ to be achieved at this stage. Thus, we should take $\gamma_i = \underline{x}_i$ in Fig. 1. As feedback signals from the lower-level DISs, the Coordinator uses their states x_i as the most comprehensive sets of local information. Then natural formulation for coordinability conditions with respect to the Coordinator's task requires that each subordinated DIS can achieve the desired state from its current state x_i. Obviously, this requires for existence of a plan to achieve $\underline{x}_i(t_j)$ from $x_i(t_j)$ [18], i.e. existence of a sequence of control impacts on the environment, which would allow to come closer to the desired state (in general, in the presence of disturbances). It is also clear that, generally speaking, every O_i may need different time to achieve a given state; therefore it is possible to propose two approaches to the organization of interactions among subsystems in time. Either the Coordinator shall generate the specified states, taking into account the potential to achieve them in a single cycle of the system, then you can synchronize the internal time of the DISs, or the DISs system shall have the event-driven planning adopted in the preparation of activity networks. Preference for one of the above approaches is determined by the specificity of the subject area. For simplicity, it is further assumed that the Coordinator's time and local times of all O_i are synchronized, and its increment is accepted as equal to 1. Thus, $t \in T = \{0, 1, 2, \ldots\}$.

Under coordination by the method of interaction prediction, disturbances will occur in a system O_i, if the states of the lower-level systems are different from the ones set by the Coordinator. More detail description of the disturbances is only possible after a more specific description of the problem to be solved by a collective of DISs and the environment; that is beyond the purpose of this paper. However, in view of (12), we can interpret a necessary coordinability condition with respect to the Coordinator's task as a requirement to move "as close as possible" to end states for all dominated DISs by the end of the current control step:

$$\begin{gathered} \forall \delta_i(t) \subseteq \Delta(t), \forall \underline{x}_i(t+1) \subseteq X, \forall i \in I \\ \exists u_i*(t) \subseteq U(t) : x_i*(t+1) \backslash \underline{x}_i(t+1) \\ \subseteq \underline{x}_i(t+1) \backslash \underline{x}_i(t+1), \end{gathered} \tag{13}$$

where: $x_i^*(t+1) = \varphi(\psi(\varphi(x_i(t) \cup u_i^*(t) \cup \delta_i(t)))$ is the best possible state for the DIS O_i by the end of a control step;

$x_i(t+1) = \varphi(\psi(\varphi(x_i(t) \cup u_i(t) \cup \delta_i(t)))$ is any other possible state for the DIS O_i by this instant.

In [18], it is shown that for stabilization of a trajectory of a DIS, i.e. for compensation of disturbances influence, it is enough to apply the following control:

$$u(x(t+1), t+1)) = \varphi(\psi(x(t+1)), t+1)) \backslash \varphi(\psi(\varphi(\psi(\varphi(x(t) \cup \delta(t)), t)), t+1)). \tag{14}$$

Considering (12), the relation (14) will look like:

$$u(x(t+1),t+1)) = \underline{\underline{x}}(t+2/t+1))\backslash x(t+2/t). \tag{15}$$

where: $\underline{\underline{x}}(t + 2/t + 1)$ is the prediction for the value of the state x at the instant t + 2 made at the time t + 1 in the absence of disturbances; $x(t + 2/t)$ is the prediction for the value of the state x at the instant t + 2 made at the time t considering disturbances, which existed at that point, and assuming absence of disturbances at the time t + 1.

Formulas (14), (15) allow to take into account unavoidable delay of control signals because of unpredictable disturbances from the environment [15].

Given (12) and (15), the necessary condition for coordinability with respect to the problem of the Coordinator (13) takes the form:

$$\begin{gathered}\forall \delta_i(t) \subseteq \Delta(t), \quad \forall \underline{x}_i(t+1) \subseteq X, \quad \forall i \subseteq I \\ \exists u_i * (t) \subseteq U(t) : \underline{\underline{x_i}} * (t+2/t+1))\backslash x_i(t+2/t) \subseteq \underline{\underline{x_i}}(t+2/t+1))\backslash x_i(t+2/t),\end{gathered} \tag{16}$$

4.2 Coordinability in Relation to the Global Task

Let us assume first that the two-level system of DIS is single-purpose, and this purpose is to achieve a given external state of the Coordinator $\underline{x}_0 \in X_0$. In the above-mentioned example with the construction, the purpose $\underline{x}_0$ can be formalized as a clear description of the expected results (e.g., a drawing of the building). Then the system will be coordinated in relation to the task of achieving $\underline{x}_0$, if the Coordinator will be able to find a set of predicted values $\underline{x}_i \subseteq X$, $\forall i \in I$ at the time t so that (after their issuance to the subordinated DISs and subsequent impact of these systems on the environment) the Coordinator's state will move closer to $\underline{x}_0$. To present this statement more formally, let us detail the task of the Coordinator.

For the Coordinator, disturbances are deviations of the current states of its subordinated DISs from their given values and control signals are expected states of the lower-level DISs. Accordingly, after receiving the feedback signals from the subordinated DISs (a one-step delay is assumed to exist for each DIS and for reaction of the environment), the Coordinator's state equation can be represented similar to (12):

$$x_0(t+4) = \varphi_0(\psi_0(\varphi_0(x_0(t) \cup u_0(t) \cup \delta_0(t))), \tag{17}$$

where: $\delta_0(t)$: $X_1 \times X_2 \times \ldots \times X_n \rightarrow \Delta_0$ is the functional mapping of the impact of deviations of the current states of subordinates DISs from their given values upon

the general state of the job; $u_0(t)$ is a general description of the predicted job's state for the next step.

Relation (17) shows that the Coordinator O_0 should solve two disparate tasks: first, to evaluate the current progress and to develop a strategy for further solving the problem on the basis of this assessment; second, to allocate tasks for the next step among the subordinated DISs. Therefore, the structure of the Coordinator should be presented in the form shown in Fig. 2.

Here: BOSS stands for the Block to Objectify the current State of solving the problem and to develop Strategies for further action; its state equation is described by the relation (16);

BAC_i denotes the Blocks to Correct Actions, which are responsible for mapping a generalized description of the job state predicted for the next step to the anticipated states of their subordinated DIS O_i.

Then, by analogy with (15), the formulated above coordinability statement for a collective of DISs in relation to the global task can be written in the form:

$$\begin{gathered} \forall t \in T, \quad \forall x_i(t) \subseteq X_i, \quad \forall i \subseteq I, \quad \forall \underline{x}_0 \subseteq X_0 \\ \exists x_i * (t+4) \subseteq X_i : x_0 * (t+4) \backslash \underline{x}_0 \subseteq x_0 * (t) \backslash \underline{x}_0. \end{gathered} \tag{18}$$

If you do not separate BACs within the Coordinator, it should receive disturbances as a vector with the following components:

$$\delta_{i0} = x_i(t+1) \backslash \underline{x}_i(t+1), i \subseteq I, \tag{19}$$

and O_0 will directly generate $\underline{x}_i$ as its output signals.

The possibility to construct DISs hierarchies for solving multi-purpose tasks is evident as well. Then, the goal state of the Coordinator ($\underline{x}_0$ in Fig. 2) will depend on time and should be selected within the system with the use of a preference relation on the set of goals [18]. Such problems can arise, for example, in problems of structure control for the virtual enterprises [19]. However, they require for a separate consideration.

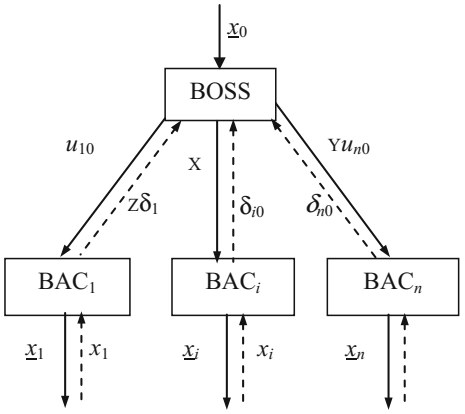

Fig. 2 The coordinator's structure

Since (see the beginning of this section) the existence of a plan to achieve the desired state is a necessary condition for coordinability of a system (similar to the controllability condition in the classical optimal control theory), we will now describe the possibility of developing such a plan for DIS and SCM.

5 Planning for DIS

DISs allow for knowledge representation both by rules and semantic networks [18]. Further on, we will consider the rule-based DISs. IN such a DIS, the knowledge base comprises a set of rules of the following format:

$$\Pi = \langle C, A, D \rangle, \tag{20}$$

where:

C	is a precondition (condition) of a rule;
A	is a set of facts added after application of the rule Π;
D	is a set of facts deleted after application of the rule Π
C, A и D	are sets of formulas of a certain language L.

Any rule must meet the relation

$$A \cap D = \varnothing. \tag{21}$$

Any rule belongs to only one of the two classes: RD or RS.

Every rule of the class RD contains an action applied to the external environment by an executive body or a procedure that computes and assigns to a variable certain values of some database attributes considering their values available in the current state. These actions result in changes of the DIS's database state. This group of rules describes changes of the system's state in time and is called "rules of (diachronic) transition".

Rules of the RS class are bind with no actions, they do not change the environment; rather, they change the knowledge of it. In other words, they represent the theory of the subject domain.

Then the DIS's knowledge base is

$$R = \langle \mathrm{RS}, \mathrm{RD} \rangle. \tag{22}$$

5.1 DISs Purposeful Behavior

As noted above, a DIS can be described by the relations (9)–(12), and to comply with the property (10), no RS-class rules are supposed to be capable of removing facts [18].

Then $\psi(\bullet, 1)$ is the transition function, and $\{\varphi(\psi(x, i)) \mid i \in N\}$ describes orbit or trajectory of the dynamic system.

Dynamics of a rule-based DIS (in the Markov case) is described by Eq. (12).

Let us consider the relationship of the knowledge base R architecture with properties of the model (9)–(12) [18].

Suppose, $L(R)$ is a set of formulas from the language L, which occur in the rules of R.

Definition 3 If X is set of DIS's states, then the pair of points (x_0, x_1) in the space $X \times X$ is called N-attainable one, if there exist control signals $U(j)$ $(j = 0, 1, \ldots, N-1)$, for which $x_1 \subseteq x\,(N)$ with the initial conditions $x(0) \subseteq x_0 \cup U(0)$, where $x(t)$, $t \in N$ are solutions of the DIS's state equation.

Definition 4 If a pair of points (x_0, x_1) is N-achievable and every fact of $x(N)$ does not occur in more than one rule within the corresponding trajectory, then the pair of points (x_0, x_1) is called effectively N-attainable.

Let $\tau \subset L(R)$ be a set of facts. If a sequence of rules $\Pi_1, \Pi_2, \ldots, \Pi_k$ from R is given, the set of facts $S(\Pi_1, \Pi_2, \ldots, \Pi_k)$ derived after application of τ rules from this sequence is defined by induction:

$$\begin{aligned} S(\Pi_1) &= \tau \backslash D_1 \cup A_1; \\ S(\Pi_1, \Pi_2, \ldots, \Pi_i) &= S(\Pi_1, \Pi_2, \ldots, \Pi_{i-1}) \backslash D(\Pi_i) \cup A(\Pi_i). \end{aligned} \tag{23}$$

Definition 5 A rule Π_i is called admissible one, if there is a control U_{i-1}, for which

$$C_i \subseteq (S(\Pi_1, \Pi_2, \ldots, \Pi_{i-1}) \cup U_{i-1}.) \tag{24}$$

Definition 6 The sequence of rules and controls $\Pi = <(\Pi_1, U_1), (\Pi_2, U_2), \ldots, (\Pi_k, U_k)>$ is called a plan to achieve the state ω from the current state ι, if:

(1) each rule from this sequence is admissible;
(2) $\omega \subseteq S(\Pi_1, \Pi_2, \ldots, \Pi_k)$.

Theorem For every pair of points $(x_0, x_1) \in X \times X$, the plan $\Pi = <(\Pi_1, U_1), (\Pi_2, U_2), \ldots, (\Pi_k, U_k)>$ exists, if and only if the pair (x_0, x_1) is N-attainable.

In [18], an algorithm is proposed to search for a sequence of admissible rules and their relevant controls that make up the plan to achieve the state ω from the current state ι. According to the principles of dynamic programming, this algorithm works "backward in time" from the target state. However, this approach is difficult to consider the rules of the RD class since they not always have an inverse operator. In connection with written above, we now propose a planning procedure that works in "live time" starting from the initial DIS's state.

5.2 Direct Planning for DISs

The above-cited theorem determines the necessary and sufficient conditions for existence of a plan to transfer a system from an initial state x_0 to the end state x_1. If we toughen conditions of this theorem and require for effective N-attainability of a pair of points (x_0, x_1) rather than their N-attainability (see Definition 4), we can obtain a direct planning algorithm similar to the ideas of derivative-based control implemented in the "classical" automatic control theory.

Let $x(t + 1)$ be a DIS's state vector obtained by solving the Eq. (12) at the step t + 1. Then $x(t + 1) \setminus x(t)$ are the new facts that have appeared on this stage of inference. If the DIS is on a trajectory, which has the property of the effective N-attainability, then the emerging facts should not repeat all along this trajectory. Consequently, the following relation is true:

$$\bigcap_{t=1}^{N-1} x(t+1)\backslash x(t) = \varnothing. \tag{25}$$

Then for synthesis a plan by direct inference, it is possible to calculate the intersection of already appeared new facts at each step k and choose the current control so as to:

$$\sum\nolimits_k \bigcap (x(k+1)\backslash x(k)) = \varnothing. \tag{26}$$

Hence, the procedure of the direct planning will look as follows:

(1) Let x_1 is a target state and x_0 is the initial state of a DIS.
(2) k: = 0, $\sum_k := \varnothing$.
(3) Let $x(k)$ be the current state. If $x_1 \subseteq x(k)$, then stop. Also, let Π^k: = $\{\Pi_1^k, \Pi_2^k, \ldots, \Pi_l^k\}$ be the set of admissible rules at the step k.
(4) Apply a rule from Π^k and check the condition (26). If it holds, then k: = k + 1 and go to step 3, otherwise select another (not applied yet) rule from Π^k and return to the beginning of step 4. If none of the admissible rules result in fulfilling the condition (26), then the step k is considered a failure; the rule led to it is marked as a dead-end; backtrack to the previous step of inference; k : = k − 1 and go to step 3.

It is possible to show that, if there exist an effective (in the sense of Definition 4) plan to achieve the state x_1 from the state x_0, then the described procedure will complete construction of this plan. The rate of planning will increase, if to view the entire set of admissible rules at step 4 and, if there are several rules that satisfy the condition (26), choose one of them, Π^{*k}, for which the relation is true:

$$x_1 \backslash x*(k) \subseteq x_1 \backslash x_i(k), \tag{27}$$

where $x^*(k)$ is the state after application the rule Π^{*k} and $x_i(k)$ are the states after application of any other rules meeting the condition (26).

6 Conclusion

Some change-based methods to coordinate interactions among components of a hierarchical object are developed. Coordination and direct planning algorithms are proposed for both numeric and non-numeric metrics upon the state spaces of these components.

Acknowledgements The author would like to thank the Russian Foundation for Basic Researches (grants 14-07-00257, 15-07-04760, 15-07-02757, 16-29-04424, and 16-29-12901) for partial funding of this research.

References

1. Lee, E.: Cyber physical systems: design challenges. University of California, Berkeley Technical Report No. UCB/EECS-2008-8. Retrieved 07 June 2008
2. NSF Cyber-Physical Systems Summit. Retrieved 01 Aug 2008
3. NSF Workshop On Cyber-Physical Systems. Retrieved 09 June 2008
4. Shkodyrev, V.P.: Technical systems control: from mechatronics to cyber-physical systems. In: Gorodetskiy, A.E. (ed.) Studies in Systems, Decision and Control, vol. 49, pp. 3–6. Smart Electromechanical Systems. Springer International Publishing, Switzerland (2016). 277 pp
5. Gorodetskiy, A.E.: Smart electromechanical systems modules. In: Gorodetskiy, A.E. (ed.) Studies in Systems, Decision and Control, vol. 49, pp. 7–15. Smart Electromechanical Systems. Springer International Publishing, Switzerland (2016). 277 pp
6. Kulik, B.A., Fridman, A.Ya.: Logical Analysis of data and knowledge with uncertainties in SEMS. In: Gorodetskiy, A.E. (ed.) Studies in Systems, Decision and Control, vol. 49, pp. 45–59. Smart Electromechanical Systems. Springer International Publishing, Switzerland (2016). 277 pp
7. Kulik, B., Fridman, A., Zuenko, A.: Logical inference and defeasible reasoning in N-tuple algebra. In: Naidenova, X., Ignatov, D. (eds.) Diagnostic test approaches to machine learning and commonsense reasoning systems, pp. 102–128. IGI Global, Hershey, PA (2013)
8. Agapov, V.A., Gorodetskij, A.E., Kuchmin, A.J., Selivanova, E.N.: Medical microrobot. Patent RU, no. 2469752 (2011)
9. Gorod, A., Fridman, A., Saucer, B.: A quantitative approach to analysis of a system of systems operational boundaries. In: Proceedings of International Congress on Ultra Modern Telecommunications and Control Systems (ICUMT-2010), pp. 655–661. Moscow, Russia, 18–20 Oct 2010
10. Pospelov, D.A.: Situational Control: Theory and Practice. Battelle Memorial Institute, Columbus, OH (1986)
11. Zadeh, L.A., Desoer C.A.: Linear System Theory. Krieger Pub. Co. (1979)
12. Rosario, N.M.: Hierarchical structure in financial markets. Eur. Phys. J. B **11**, 193–197 (1999)

13. Baroni, M., Dinu, G., Kruszewski, G.: Don't count, predict! a systematic comparison of context-counting vs. context-predicting semantic vectors. In: Proceedings of the 52nd Annual Meeting of the Association for Computational Linguistics, vol. 1, pp. 238–247 (2014)
14. Sokolov, B., Fridman, A.: Integrated situational modeling of industry-business processes for every stage of their life cycle. In: 4th International IEEE Conference "Intelligent Systems" (IS 2008), vol. 1, pp. (8-35)–(8-40). Varna, Bulgaria, 6–8 Sep 2008
15. Mesarovic, M.D., Macko, D., Takahara, Y.: Theory of Hierarchical Multilevel Systems. Academic Press, New York, London (1970)
16. Stefanuk, V.L.: Stability of local control in a system with contralinear interaction of subsystems. In: Proceedings of European Control Conference (ECC'93), vol. 1, pp. 117–119. Groningen (1993)
17. Fridman, A., Fridman, O.: Gradient coordination technique for controlling hierarchical and network systems. Syst. Res. Forum **4**(2), 121–136 (2010)
18. Osipov, G.: Attainable sets and knowledge base architecture in discrete dynamic knowledge-based systems. In: Proceedings of the Workshop "Applied Semiotics: Control Problems (ASC 2000)". ECAI2000. 14th European Conference of Artificial Intelligence, pp. 39–43. Berlin, 20–25 Aug 2000
19. Sokolov, B., Ivanov, D., Fridman, A.: Situational modelling for structural dynamics control of industry-business processes and supply chains. Intelligent Systems: From Theory to Practice, pp. 279–308. Springer-Verlag Berlin Heidelberg, London (2010)

Part II
Behavioral Decisions

Logical-Mathematical Model of Decision Making in Central Nervous System SEMS

Andrey E. Gorodetskiy, I.L. Tarasova and Vugar G. Kurbanov

Abstract *Purpose* Smart Electromechanical Systems (SEMS) are used in cyber-physical systems and, in particular, in intelligent robots. SEMS are able to integrate functions of calculation, management, communication, storage of information, monitoring, measurement and control of own parameters and parameters of the environment. It is important to consider that the behavior of a system is based on the information about the environment and conditions of the system obtained from the Central Nervous System of a Robot (CNSR). The purpose of the publication is to describe the approaches of adoption of behavioral decisions like a human on the basis of information obtained from CNSR that are constructed on the basis of SEMS modules. *Results* Deductive, inductive and abductive types of adoption of behavioral decisions in CNSR on the basis of SEMS modules are offered. *Practical importance* The principles and approaches to decision-making on the basis of information from CNSR suggested in the article can be used to set a strategy and tactics of control over intelligent robots.

Keywords Smart electromechanical systems · Sensory organs of a person · The central nervous system of a person · The central nervous system of a robot · Measurement · Calculation · Management · Deduction · Induction and abduction

A.E. Gorodetskiy (✉) · I.L. Tarasova · V.G. Kurbanov
Institute of Problems of Mechanical Engineering, Russian Academy of Sciences, Moscow, Russia
e-mail: g27764@yandex.ru

I.L. Tarasova
e-mail: g17265@yandex.ru

V.G. Kurbanov
e-mail: vugar_borchali@yahoo.com

A.E. Gorodetskiy and V.G. Kurbanov (eds.), *Smart Electromechanical Systems: The Central Nervous System*, Studies in Systems, Decision and Control 95,
DOI 10.1007/978-3-319-53327-8_4

1 Introduction

The operation of the automatic control system (ACS) of the robot based on the information from the sensory systems with respect to the environment and the state of the robot. Without this information, the ACS will not be able to take decisions expected of it, i.e., to set goals and achieve the functioning of these goals [1]. However, for that to robots that are created on the basis of SEMS modules could independently, without needing human intervention, formulate objectives and to successfully carry them out, they should be provided not only more sophisticated sensors senses (sensors), but also have the ability to understand the feelings language, i.e., have a sense of the type of "the–another", "dangerous–safely", "favorite–unloved", "pleasant–unpleasant" and others, formed as a result of solving systems of logic equations. If there is ability to create such a database in the central nervous system of the robot (CNSR) there is a possibility of independent decision-making with respect to purposeful behavior [2].

2 Fuzzification Data

The first and very important operation for further logical constructions in decision-making is the fuzzification of incoming data at the touch CNSR information channels from the various sensors. To do this, first of all, to combine sensors forming groups following bodies robot senses like a man: vision as a set of **X**; hearing as set **Y**; a plurality of smell **Z**; taste as a plurality of **U**; the sense of touch in the form of a plurality of **V**; a plurality balance **W** and a plurality telepathy **Q**.

$$\boldsymbol{X_i} \subset \boldsymbol{X}, \boldsymbol{Y_i} \subset \boldsymbol{Y}, \boldsymbol{Z_i} \subset \boldsymbol{Z}, \boldsymbol{U_i} \subset \boldsymbol{U}, \boldsymbol{V_i} \subset \boldsymbol{V}, \boldsymbol{W_i} \subset \boldsymbol{W}, \boldsymbol{Q_i} \subset \boldsymbol{Q}.$$

A set of these subsets depends on a set of sensors forming the senses of a particular robot. For example, to view a subset of the following can be entered: X_1—contour image, X_2—the size of the image, X_3—the brightness of the image, X_4—color image, X_5—the distance to the object, X_6—approach speeds, X_7—removal rate.

For the hearing following subsets can be entered: Y_1—volume, Y_2—the tone, Y_3—interval,; Y_4—approach speeds, Y_5—removal rate, Y_6—direction.

For the following subsets of smell can be entered: Z_1—type of smell, Z_2—the intensity of the odor, Z_3—the direction of the smell, Z_4—approach speeds, Z_5—removal rate.

For the following subsets can be introduced to the taste: U_1—type of taste, U_2—the power of taste, U_3—direction.

To touch these subsets can be entered: V_1—the evenness of the surface, V_2—dry surface, V_3—surface temperature.

Sense of balance is usually provided by robots gyroscopes. In this case, the following subsets can be entered: W_1—deviation "up–down", W_2 of—deviation "forward–backward", W_3—deviation "left–right", W_4—speed deviation "up–down", W_5—speed deviation "forward–backward", W_6—speed deviation "left–right".

Telepathy robots, in contrast to the human, it is explicable phenomenon and receive messages using a wireless connection. Currently, the most widely used for this purpose "Wi-Fi". Most simply a subset of the set Q_i forming telepathy Q form in advance at the stage of designing a robot designed to perform various technological operations. In this case, these instructions are subsets or types of reactions ($q_{ij} \in Q_i$), are stored in the robot's memory and retrieved therefrom inference engine [3]. The choice of instructions carried out by checking the feasibility of certain rules of the data subset ($x_{ij} \in X_i$; $y_{ij} \in Y_i$; $z_{ij} \in Z_i$; $u_{ij} \in U_i$; $v_{ij} \in V_i$; $w_{ij} \in W_i$). Such rules usually have the form:

$$\textit{If } x_{ij} = 1 \wedge y_{ij} = 1 \wedge z_i = 1 \wedge u_{ij} = 1 \wedge v_{ij} = 1 \wedge w_{ij} = 1, \quad \textit{then} \quad q_{ij} = 1 \tag{1}$$

With a large number of logical variables, such rules can be just as much. Then, a sequential scan of the rules in order to identify their feasibility will take a long time. In this case, it is desirable to utilize parallel computing. For this purpose, as shown in [4], we can use the procedure algebraization logical expressions, is as follows.

The rules of the form (1) are the implications in terms of the algebra of logic or Boolean algebra:

$$x_{ij} \wedge y_{ij} \wedge z_{ij} \wedge u_{ij} \wedge v_{ij} \wedge w_{ij} \rightarrow q_{ij} \tag{2}$$

Expressions of the form (2) can be transformed into a form of algebra Zhegalkin or equivalent algebraic equations on mod 2 [5].

$$s_{ij} \oplus s_{ij} * q_{ij} \oplus 1 = b_{ij}, \tag{3}$$

where: $\oplus$—plus sign mod 2, $*$—mark of multiplication mod 2, b_{ij}—0 or 1 (b_{ij} [0,1]) and $s_{ij} = x_{ij} * y_{ij} * z_{ij} * u_{ij} * v_{ij} * w_{ij}$.

Then the resulting system logic equations can be rewritten in matrix form by mod 2 [6]:

$$\mathbf{A} * \mathbf{F} = \mathbf{B}, \tag{4}$$

where: **B**—binary vector of dimension n, **F**—a fundamental vector of logic n the dimension of the system being built from combinations of logical variables x_{ij}, y_{ij}, z_{ij}, u_{ij}, v_{ij}, w_{ij}, q_{ij}, obtained in fuzzification of sensory data, and supplemented with 1 in place of the last element, A—rectangular binary matrix of dimension [n, m].

The procedure of obtaining the system of Eq. (4) can be easily formalized. To do this, you can first build a fundamental vector **F** system:

$$\mathbf{F^T} = |s_{11}, s_{12}, \ldots, s_{1n}, s_{21}, \ldots, s_{mn}, s_{11} * s_{12}, \ldots, s_{11} * s_{12} * \ldots * \times s_{mn}, s_{11} * q_{11}, \ldots, s_{11} * s_{12} * \ldots * s_{mn} * q_{11} * \ldots * q_{mn}, 1| \quad (5)$$

It uses the following algorithm for constructing:

- lists all logical variables sensor data,
- after which lists all combinations of two logical variables sensor data,
- then lists all combinations of three logical variables sensor data,
- then lists all combinations of four logical variables sensor data,
- and so on, and is placed in the end product of all logical variables sensor data.

Then build the fundamental matrix of system **A**:

$$A = \left| \begin{array}{c} 100\ldots0 \\ 010\ldots0 \\ \ldots..\ldots.. \\ \ldots..\ldots.. \\ 000\ldots1 \\ 110\ldots0 \\ 101\ldots0 \\ \ldots..\ldots.. \\ \ldots..\ldots.. \\ 00..011 \\ 111\ldots0 \\ 1101..0 \\ 11001.0 \\ \ldots..\ldots..\ldots \\ \ldots..\ldots..\ldots \\ \ldots..\ldots..\ldots \\ 111111 \end{array} \right| \quad (6)$$

An algorithm for constructing the matrix **A** as follows:

- in the first row is placed in the first column 1, and the rest 0,
- in the second row in the second column is put 1 and 0 in the other,
- and so on until the last 1column,
- then put 1 in the first two columns, and the rest 0,
- 1 is then placed in the first and third columns, and the remaining 0,
- 1 is then placed in the first and fourth columns, and the remaining 0,
- and so on until the last two in one of the two columns,
- then put 1 in the first three columns, and the rest 0,
- then put 1 in the first, third and fourth columns, and the rest 0,
- 1 is then placed in the first, fourth and fifth columns, and the remaining 0,
- and so on until one in three of the last three columns,
- and so on until they are in all columns 1.

Naturally, in such a way that the resulting system of equations for a matrix type mod 2 (4) will have a large dimension. However, in real CNS robots, not all components of the equation (not all combinations of logical variables) is physically realizable and can be discarded. As a result of this reduction, we obtain a matrix system of equations for mod 2 smaller dimension [7]:

$$\mathbf{C} * \mathbf{R} = \mathbf{G}, \tag{7}$$

where, $\mathbf{C} \subset \mathbf{A}$, $\mathbf{R} \subset \mathbf{F}$, $\mathbf{G} \subset \mathbf{B}$.

The data logical type (x_{ij}, y_{ij}, z_{ij}, u_{ij}, v_{ij}, w_{ij}), are extracted from the data or signals from the sensors senses of robots by their fuzzification [7].

For example, the logical variables $v3_j$ formed by the quantization of all temperature and assign the sensor range quanta received $\Delta 3_i$ names $v3_j$ logical variables is True (1) or False (0). Then, if the input variable—T the temperature may range from −20 °C to +20 °C, then introducing a quantum of 10 °C, the entire range of possible temperature changes into four quantum $\Delta 3_1$ = [−20, −10], $\Delta 3_2$ = [−10, 0], $\Delta 3_3$ = [0, +10], $\Delta 3_4$ = [+ 10, +20]. Then, quantum $\Delta 3_1$ can name $v3_1$ is {very cold}, quantum $\Delta 3_2$ to name $v3_2$ {cold}, quantum $\Delta 3_3$ to name $v3_3$ {cool} and quantum $\Delta 3_4$ to name $v3_4$ {heat}. Wherein,

- covering the logic variable $v3_1$ corresponds to the interval: [(−20 + 20)/(20 + 20), (−10 + 20)/(20 + 20)] = [0, 0.25]
- covering the logic variable $v3_2$ corresponds to the interval: [(−10 + 20)/(20 + 20), (0 + 20)/(20 + 20)] = [0.25, 0.5]
- covering the logic variable $v3_3$ corresponds to the interval: [(0 + 20)/(20 + 20), (10 + 20)/(20 + 20)] = [0.5, 0.75]
- covering the logic variable $v3_4$ corresponds to the interval: [(10 + 20)/(20 + 20), (20 + 20)/(20 + 20)] = [0.75, 1].

In particular, if, for example, the sensor shows a temperature t = + 50 °C, after fuzzification in CNSR database are entered following values of logic variables: $v3_1$ = 0, $v3_2$ = 0, $v3_3$ = 1, $v3_4$ = 0 and the corresponding ranges described above as attributes these logical variables.

In more complex cases, the attributes may be the probability (P $\{x_{ij} = 1\}$ or membership functions $\mu(x_{ij})$. In this case, the data from the sensor senses the robots are stored in memory in the form of logical—probabilistic or logical-linguistic variables [8] when as attributes obtained after fuzzification logic variables in the database CNSR data will be stored probabilities, or membership functions. In this case, the inference machine CNSR almost always will get not one solution, but several with varying degrees of certainty.

If: $x_{ij} = 1$ with probability P_x and $y_{ij} = 1$ with probability P_y and $z_i = 1$ with probability P_z and $u_{ij} = 1$ with probability P_u and $v_{ij} = 1$ with probability P_v and $w_{ij} = 1$ with probability P_w, the $q_{ij} = 1$ P_q likely.

Also not any solution received from the system (7) is doable particular robot in the current environment (the state of the operational environment). This means that

the solution obtained from CNSR (7) must satisfy the constraints, which can also be expressed as a systems logic equations [9]:

$$\mathbf{C_i} * \mathbf{R_i} = \mathbf{H} \tag{8}$$

$$\mathbf{C_j} * \mathbf{R_j} = \mathbf{D} \tag{9}$$

where: $\mathbf{C_i}$ and $\mathbf{C_j}$—constraint matrix obtained by analogy with the matrix **C**, **H** and **D**—a binary vector obtained by analogy with the vector **G**, $\mathbf{R_i} \subset \mathbf{F_i}$ и $\mathbf{R_j} \subset \mathbf{F_j}$.

In this case vector $\mathbf{F_i}$ and $\mathbf{F_j}$ are formed similarly to the vector **A**:

$$\begin{aligned}\mathbf{F_i^T} = |&s_{11}, s_{12}, \ldots, s_{1n}, s_{21}, \ldots, s_{mn}, s_{11} * s_{12}, \ldots, s_{11} * s_{12} * \ldots * s_{mn},\\ &\times s_{11} * q_{11}, \ldots, s_{11} * s_{12} * \ldots * s_{mn} * g_{11} * \ldots * g_{mn}, 1|\end{aligned} \tag{10}$$

$$\begin{aligned}\mathbf{F_j^T} = |&s_{11}, s_{12}, \ldots, s_{1n}, s_{21}, \ldots, s_{mn}, s_{11} * s_{12}, \ldots, s_{11} * s_{12} * \ldots * s_{mn},\\ &\times s_{11} * q_{11}, \ldots, s_{11} * s_{12} * \ldots * s_{mn} * l_{11} * \ldots * l_{mn}, 1|\end{aligned} \tag{11}$$

where: g_{ij}—logical variables characterizing the technical limitations associated with the design of the robot, and l_{ij}—logical variables characterizing the technical limitations associated with the environment (environment functioning of the robot at the moment).

The set of solutions obtained CNSR in solving Eqs. (7)–(9), of course, will lead to ambiguous behavior of the robot. A man in this situation it is advisable to behave purposefully or intuitively, based on our own experience, or genetically inherent behavioral patterns [10]. The task empowering robots skills purposeful behavior is still at a very early stage. Currently, the most thoroughly studied the problem of choosing the optimal decisions under conditions of incomplete certainty interval, probabilistic or linguistic type [11].

The man in the process of thinking and decision-making on the basis of the available information processing normally adheres to one of two styles of deductive or inductive. There is also a third, poorly understood, and rarely encountered, the type of thinking—Abductive. Consider options for use in CNSR each of these types of decision-making.

3 Methods of Decision-Making

When deductive thinking in decision making CNSR process begins with a global level and then goes down to the local movement [12]. Technical analog of this kind of thinking can be the optimization process when initially on the basis of the available information is searched for the best solution of all possible, and then by checking on the basis of available information, all the restrictions made solutions correction.

Selection of the optimal solutions of all y_i solutions obtained from (7) can be carried out in various ways. The most simple in this case, to use the methods of mathematical programming [13]. Then, when the logical-probabilistic description of uncertainty [11], i.e., when the attributes of the logical variables in Eqs. (7)–(9) are the probabilities

$P\{y_i = 1\}$, the quality criterion can be expressed as follows:

$$f_0(Y) = P\{y_i = 1\} \rightarrow \max \tag{12}$$

In this case probabilities $P\{y_i = 1\}$ can be calculated approximately by the procedure described in [7, 14, 15] algorithm.

If the result of the analysis CNSR reveals that the influence of certain component y_i, for her behavior is different, the quality criterion (12) it is advisable to bring to mind:

$$f_0(Y) = b_i\, P\{y_i = 1\} \rightarrow \max \tag{13}$$

where b_i—assigned weights.

When the logical-linguistic description of uncertainties [11], i.e. when the attributes of the logical variables in Eqs. (7)–(9) are membership functions $\mu(y_i)$, a quality criterion can be expressed as follows:

$$f_0(Y) = \mu(y_i) \rightarrow \max \tag{14}$$

The values of the membership functions $\mu(y_i)$ can be calculated as described in [7] algorithms.

$$f_0(Y) = \beta_i \mu(y_i) \rightarrow \max \tag{15}$$

When the logical-interval description of the uncertainties [11], i.e., when the attributes of the logical variables in Eqs. (7)–(9) are the intervals $\Delta_{ij} = [a_{ji}, b_{ji}]$, the quality criterion can be expressed as the following expressions:.

$$f_0(Y) = k_{ji}(b_{ji} - a_{ji}) \rightarrow \min \tag{16}$$

$$f_0(Y) = k_{ji}(b_{ji} - a_{ji}) - c_{ji}]^2 \rightarrow \min \tag{17}$$

$$f_0(Y) = [k_{ji}^b(b_{ji} - b_{ji}^0)^2 + (a_{ji} - a_{ji}^0)^2] \rightarrow \min \tag{18}$$

$$f_0(Y) = [k_{ji}^b(b_{ji} - b_{ji}^0)^2 + k_{ji}^a(a_{ji} - a_{ji}^0)^2] \rightarrow \min \tag{19}$$

where: k_{ji}, k_{ji}^b, k_{ji}^a—coefficients of preference decision makers (DMP) of optimality, c_{ji}—DMP desired width of the interval, b_{ji}^0, a_{ji}^0—the boundaries of your DMP intervals.

After calculating the quality criteria of all possible solutions in accordance with the Eqs. (12) and (13)—with logic-probabilistic description of uncertainties, or (14) and (15)—with the logical-linguistic description of uncertainties, or (16)–(19)—when describing the logic-interval uncertainty all the solutions are ranked. Then the solutions are checked for feasibility constraints (8) and (9) from the first, having the highest quality criterion. In this case the first of the audited solutions satisfying the constraints is considered optimal.

When inductive thinking in decision making CNSR process starts with analysis of individual decisions to continue the search for common, global solution [12]. Technical analog of this kind of thinking can be the optimization process when initially on the basis of available information checked all the decisions on the feasibility constraints of the form (8) and (9), and then looking for the best solution of all possible under the terms of the decisions of restrictions on the type of criteria (12)–(19).

When abductive decision making, according to Pierce cognitive activity in CNSR is reacting abduction, induction and deduction [16, 17]. In this case abduction carries adoption of plausible hypotheses by explaining the facts by induction implemented testing hypotheses, and by deduction of the accepted hypotheses derived investigation. Technical analog of this kind of thinking can be the process of finding the optimal solution, by analogy, when of all the possible solutions derived from the Eqs. (7)–(9), first selected by means of pattern recognition [18], the decisions that are closest to the existing solutions, stored in the database CNSR data and give good results in the past. You could then deductive methods and/or inductive action on quality criteria for decisions (16)–(19) to choose the best.

In more complex cases, typical of intelligent systems that are unable to form a scalar quality criterion, the choice of the optimal solution of all y_i solutions obtained from (7) can be carried out by means of mathematical programming in the ordinal scale, generalized mathematical programming or multistep generalized mathematical programming [7, 11, 19, 20]. Comparing the decision described methods can be concluded that the abduction is the fastest method by analogy with intuition, but its reliability depends on the completeness of the database good solutions from the past, i.e. strongly depends on the operating time of such robots in the environment similar conditions. The deductive method is faster with a relatively stable inductance with a large number of restrictions, because they do not require testing restrictions for all solutions. When the complex criteria of quality and a small number of restrictions inductive method can provide results faster as throw finding solutions for complex quality criteria for unacceptable restrictions on the making.

4 Conclusion

The proposed principles of deductive, inductive and abduction of decision-making based on the information from the central nervous system using algebraization and matrix solving logical equations apply effectively in the formation of strategy and

tactics of control intelligent robots in a not complete determination. Thus the most rapid decision-making is by using the principle of abduction, including elements of deductive and inductive reasoning. Validity and reliability of decision-making in such an approach may be increasing in the operation of the robot, if included in the self-controls system collects data sampled good solutions, given in the past, the right solutions.

Acknowledgements The author would like to thank the Russian Foundation for Basic Researches (grants 14-07-00257, 15-07-04760, 15-07-02757, 16-29-04424, and 16-29-12901) for partial funding of this research.

References

1. Dobrynin, D.A.: Intelligent robots yesterday, today, tomorrow. In: X natsional'naia konferentsiia po iskusstvennomu intellektu s mezhdunarodnym uchastiem KII-2006 (25–28 sentiabria 2006g., Obninsk) [X National Conference on Artificial Intelligence with International Participation (25–28 September 2006, Obninsk)], Conference Proceedings. V.2. M: FIZMATLIT, 2006 (in Russian)
2. Ackoff, R., Emery, F.: O tseleustremlennykh sistemakh [On Purposeful Systems], 269 p. M.: Sov. Radio (1974) (in Russian)
3. Gorodetskiy, A.E., Erofeev, A.A.: Principles of intelligent control systems mobile objects. Avtomatika i telemekhanika [Automation and Remote Control]. **9** (1997) (in Russian)
4. Gorodetskiy, A.E., Dubarenco, V.V., Erofeev, A.A.: Algebraic approach to the solution of logical control problems. Avtomatika i telemekhanika [Automation and Remote Control]. **2**, 127–138 (2000) (in Russian)
5. Zhegalkin, I.I.: Arifmetizatsiia simvolicheskoi logiki [Arithmetization symbolic logic]. Matematicheskii sbornik [Mathematical Collection]. **35**(3–4) (1928) (in Russian)
6. Dubarenco, V.V., Kurbanov, V.G.: The method of bringing the systems of logical equations in the form of linear sequential machines. Informatsionno – izmeritel'nye i upravliaiushchie sistemy [Information—Measuring and Control Systems]. **7**(4), 37–40 (2009) (M. Publish. Radiotechnika) (in Russian)
7. Gorodetsky, A.E., Tarasova, I.L.: Nechetkoe matematicheskoe modelirovanie plokho formalizuemykh protsessov i system [Fuzzy Mathematical Modeling Badly Formalized Processes and Systems], 336 p. SPb. : Publishing House of the Polytechnic, University Press (2010) (in Russian)
8. Gorodetskiy, A.: Osnovy teorii intellektual'nykh sistem upravleniia [Foundations of the Theory of Intelligent Control Systems], 313 p. LAP LAMBERT Academic Publishing GmbH @ Co. KG (2011) (in Russian)
9. Gorodetskiy, A.E., Kurbanov, V.G., Tarasova, I.L.: Ergatic operating instructions manual methods of analysis and decision-making processes in injuries and accidents of power. Informatsionno-upravliaiushchie sistemy [Information and Control Systems]. **6**, 29–36 (2013) (in Russian)
10. Gorodetsky, A.E.: Fuzzy decision making in design on the basis of the habituality situation application. In: Reznik, L., Dimitrov, V., Kacprzyk, J. (eds.) Fuzzy Systems Design. Social and Engineering Applications, pp. 63–73. Physica-Verlag, A Springer-Verlag Company, New York (1998)
11. Gorodetskiy, A.E., Kurbanov, V.G., Tarasova, I.L.: Methods of synthesis of optimal intelligent control systems SEMS. In: Gorodetskiy, A.E. (ed.) Smart Electromechanical Systems, 277 p. Springer International Publishing (2016). doi:10.1007/978-3-319-27547-5

12. Kondakov, N.I.: Logicheskii slovar'-spravochnik [Logical Dictionary-Reference Book], 720 p. M.: Nauka (1975)
13. Tobacco, D., Kuo, B.: Optimal'noe upravlenie i matematicheskoe programmirovanie [Optimal Control and Mathematical Programming], 280 p. M.: Nauka (1975) (in Russian)
14. Gorodetskiy, A.E., Dubarenko, V.V.: Combinatorial method of calculating the probabilities of complex logic functions. Zhurnal vychislitel'noi matematiki i matematicheskoi fiziki [Journal of Computational Mathematics and Mathematical Physics]. **39**(7), 1246–1249 (1999) (in Russian)
15. Dubarenko, V.V., Kurbanov, V.G., Kuchmin, A.Y.: A method of calculating the probabilities of logic functions. Informatsionno-upravliaiushchie sistemy [Information and Control Systems]. (5), 2–7 (2010) (in Russian)
16. Vagin, V.N., Golovina, E.Yu., Zagoryansky, A.A., Fomin, M.V.: Dostovernyi i pravdopodobnyi vyvod v intellektual'nykh sistemakh [Reliable and plausible conclusion in intelligent systems]. In: Vagin, V.N., Pospelov, D.A. (eds.) 2nd Edition Revised and Enlarged, 712 p. FIZMATLIT (2008) (in Russian)
17. Peirce, Ch.S.: Rassuzhdenie i logika veshchei [Reasoning and Logic of Things], Lectures for the Cambridge Conference, 1898 (in Russian)
18. Gorodetskiy, A.E.: 18. The use of a situation accustomed to accelerate the adoption of intellectual solutions in information and measuring systems. In: Physical Metrology: Theoretical and Applied Aspects, pp. 141–151. SPb.: Publishing, KN, 1996 (in Russian)
19. Gorodetskiy, A.E., Tarasova, I.L.: Upravlenie i neironnye seti [Control and Neural Networks], 312 p. SPb.: Publishing house of the Polytechnic, University Press (2005) (in Russian)
20. Iudin, D.B.: Vychislitel'nye metody teorii priniatiia reshenii [Computational Methods of Decision Theory], 320 p. Nauka Publ., Moscow (1989) (in Russian)

Behavioral Decisions of a Robot Based on Solving of Systems of Logical Equations

Andrey E. Gorodetskiy, I.L. Tarasova and Vugar G. Kurbanov

Abstract *Purpose*: The expedient behavior of a robot based on the information obtained from the Central Nervous System of a Robot (CNSR) about the environment and conditions of the system, in many respects, is defined by the ability of this robot to form the language of feelings and reflexive reasoning. The purpose of the article is to describe approaches to adopt behavioral (reflexive) solutions of a robot on the basis of the language of feelings similar to a human. The language is formed of information obtained by the central nervous system of robots from being its part of sensory system. *Results*: New methods of adoption of behavioral decisions and formation of language of feelings of the type "friend–foe", "dangerous–safe", "loved–unloved", "pleasant–unpleasant", etc., in the framed central nervous system of the robot which is under construction on the basis of SEMS modules are suggested. *Practical importance*: The principles and approaches to decision-making offered in article on the basis of information from the central nervous system can be used to form laws of control of expedient behavior of intelligent robots.

Keywords Language of feelings · Smart electromechanical systems · Sensory organs of a human · Central nervous system of a human · Central nervous system of a robot · Reflexive reasoning · Systems of logical equations

A.E. Gorodetskiy (✉) · I.L. Tarasova · V.G. Kurbanov
Institute of Problems of Mechanical Engineering,
Russian Academy of Sciences, Saint Petersburg, Russia
e-mail: g27764@yandex.ru

I.L. Tarasova
e-mail: g17265@yandex.ru

V.G. Kurbanov
e-mail: vugar_borchali@yahoo.com

A.E. Gorodetskiy and V.G. Kurbanov (eds.), *Smart Electromechanical Systems: The Central Nervous System*, Studies in Systems, Decision and Control 95,
DOI 10.1007/978-3-319-53327-8_5

1 Introduction

Expedient the behavior of intelligent robot based on information from its sensor systems with respect to the environment and the state of the robot. Without this information, it can not determine the functioning purpose and reach this goals [1]. However, for what would robots, created on the basis of SEMS modules, can independently, without needing human intervention, formulate objectives and successfully fulfill them, it must be able to understand the language of feelings. So they must have feelings the type "is dangerous–safely", "favorite–unloved", "pleasant–unpleasant" and others. Then, by solving the system of logical equations, formed on the basis of this language, the robots can acquire the ability to reflective reasoning. At presence of these abilities in the central nervous system of the robot (CNSR) the robot becomes possible of independent decision-making with respect to expedient behavior [2, 3].

2 Stages of the Formation of Behavioral Decisions

After collecting numerical information from the sensor system in the robot becomes possible go to the formation of sensations language. In this case the following steps (operation) necessary to execute of the software:

- fuzzification numerical data received from the sensor system, i.e., to obtain qualitative data logical type;
- selection of images by combining qualitative data using rules of inference;
- the formation of binary estimates of images such as "dangerous–not dangerous", "strong–weak", "bad–good" and others, using solving systems of logic equations that make up binary relations;
- the formation of reflective reasoning based on logical analysis of binary estimates image is surrounded a robot;
- the formation of the goals of the robot operation based on a selection of reflective reasoning corresponding maximum (minimum) quality criteria used;
- deciding whether the behavior in order to achieve the objectives formed on the basis of solving optimization problems with constraints.

Operation fuzzification numerical data is widely used in intelligent control systems [4] and, accordingly, in the intelligent robot control systems. For example, in the formation of databases of expert controls [5]. After performing fuzzification for each sensor of the measuring channel are formed a plurality of X_i, containing sets of logical variables x_{ij}. For example, for channel brightness measurement can be obtained following logical variables: x11—«very dark», x12—«dark», x13—«semi-dark», x14—«semi-light», x15—«light», x16—«semi-bright», x17—«bright», x18—«very bright». These logical variables for different points surrounding space robot can be true ($x_{ijk} = 1$) or false ($x_{ijn} = 0$). At that can often

originate situations when fuzzification numerical data about the truth or falsity of the received one or another of logical variables can only speak with some confidence. In this case, each received a logical variable x_{ijk} supplied with the appropriate attribute in the form of the probability $P\{x_{ijk} = 1\}$ or membership functions $\mu(x_{ijk})$ [6], which are stored in a database together with their data. Also with logical variables are stored in the database the coordinates of points of the surrounding space of the robot corresponding to each logical variable. Naturally, when you change the environment of the robot contents of the database is updated.

Operation separation images in the space surrounding the robot is widely used in the vision systems of intelligent robots [7]. In the simplest case, this operation is reduced to unite into a single set those points of spaces which have the same set of logical variables with the same attributes and provided that the distance to the nearest neighboring points with the same parameters does not exceed a predetermined value. It also determined the coordinates of the center of gravity of the resulting images. After association a plurality of points, the latter can receive additional quality parameters as a logical variables y_{ij}, obtained for example after the analysis of geometrical parameters of images (areas, volumes, contours, etc.). These additional parameters:. y_{11}—«large volume», y_{21}—«smooth contour», etc. are recorded in the database in the profile set of images together with other logical parameters and sets the coordinates of their centers of gravity. The content of this database partition is also updated when you change the environment of the robot. In the event of situations not complete certainty in the process of unification of points in space in a certain set (image) due to, for example the probability attributes of logical of variables, necessary in addition to the geometric measures proximity of points introduce additional measures proximity, for example a valid spread of values of probability of logical variables of the neighboring points.

Formation of the binary estimates of images carried out by the logical analysis of image parameters. To do this, you must first create a rule assigned to this image of a binary estimation of, for example, if the image is very bright, large and quickly moved to the side of the robot, this image (object) is very dangerous. The system of this rules introduced in CNSR knowledge base at the stage of creating a robot. In some cases, it can be corrected during use of the robot by means of training or self-study [8]. With a large number of such rules is expedient to bring them to a system of algebraic equations modulo two or algebra Zhegalkin logic [9]. In this case we obtain the matrix equation whose solutions are easily parallelized matrix processors. This allows sharply to speed up the logical analysis of the parameters of the images. The resulting binary estimation of images are also recorded in the database of images about the surrounding space of the robot. When you change the environment of the robot binary evaluation and the images themselves are updated.

Formation of reflective robot reasoning is based on the logical analysis of binary estimates of images that are around him. To do this, you must create rules like "if-then" reaction to a particular binary estimation of image, given its location and status of the robot. For example:

1. if the image is very dangerous and is near, the robot has to move away from him;
2. if the image is very dangerous, is close by and nearby there is a large image of the good, the robot has to hide behind him.

These rules are drawn up and recorded in the knowledge base at the stage of creating a robot. They can be very much and they can be corrected during operation. At that as well it is advisable to bring them to a system of algebraic equations modulo two or algebra Zhegalkin logic for parallel computing. The translation program of rules in a system algebraic equations modulo two to come into software CNSR

Formation goals of the robot operation on the based selection reflexive reasoning obtained after analysis of binary estimates of the images surrounding the robot is a complex problem, related to decision of bad formalized multicriteria optimization tasks [10]. It is often necessary to select more than one specific goal, a sequence of consecutive goals in the successful implementation previous goals. In the robot design stage it is impossible to foresee all situations that may be a robot when decision-making of functioning purposes. Therefore, in the robot's memory are entered possible on the proposed conditions of use situation and corresponding possible targets with index of their efficiency. Then CNSR should be such software which could be by evaluating acceptable reflexive reasoning and available suitable most effective targets of functioning in this situation the choice to make a sequence of goals that would ensure the maximum (minimum) quality criteria, expressed numerically. Formation of such a quality criterion is a complex and time-consuming task. Solution to this problem is primarily associated with the formation and solution of a number of logical problems, leading to the formula of calculating the quality criterion [11]. Most good results in solving this problem can be obtained using multistep generic programming [12], and programming environments such as A-life [13]. After completion of the formation of functioning sequence of goals is necessary deciding- making with respect to purposeful behavior to achieve the formulated goals. Selected expedient behavior is realized forming block the control actions on the working bodies of the robot. In the CNSR need to implement the decision of optimization problems with constraints. The basis for the solution of these problems may have different methods of mathematical programming, mathematical programming on an ordinal scale, generalized mathematical programming and multistep generalized mathematical programming [12]. A number of new approaches to solving optimization tasks under interval uncertainty is described in [14].

3 Features of Recognition, Described by Equations in Algebra Modulo Two

The decision making process in the formation of the goals the operation and purposeful behavior can be greatly accelerated by the recognition formed an image M_i i.e. at the expense their allocation to the different classes of images $C_j^{M,}$ containing

the so-called ideal images M_i^*, for which the best known solutions earlier adopted ($M_i^* \ni C_j^M$). In this case, you can use the method of habitualness of the situation [15] (the analogue of intuition in man), and replace the desired solution to the analogue.

Pattern recognition procedure in the event of their representation in the algebra modulo 2 requires the task of rules or algorithms for language processing of the attribute that characterizes the logical variables at carrying out over them the operations of addition and multiplication modulo 2. Linguistic attributes are generally form the nonmetrizable sets B_i characterizing images. In this case, the recognition of the choice of the best class of the plurality of alternative may be based on the search procedure of binary relations $B_i g B_{cj}$, where B_{cj}—the set that characterizes the ideal image of the class under consideration C_j^M to which we want as close as possible and g—double predicate on the analyzed sets, which for example can be set by an indication of formulas logical-mathematical language, or by specifying a formal linguistic expression [6]. The problem of revealing the best approximation is reduced to two problems. The first is the problem of obtaining sets B_i, B_{cj}, and the second—the construction of the optimal procedure g, which allows to obtain a quantitative estimate of the proximity to the B_i to B_{cj}.

Creating a source database for the construction of g appropriate to start with the selection in each of the compared sets of subsets of metrizable (an example of making the probability subsets), for elements that may be specified ratio and numerical measure of proximity. Next, the most difficult step is the ordering of the elements nonmetrizable subsets. It is very likely that this task will need to build a new system of logic equations, the solution of which will lead either to a metrizable sets or to the orderly. In the first case we immediately obtain numerical measure of proximity. In the second of these measures will have to be built anew. Possible numerical estimates can be power sets, the number of matching elements, the number of groups matched elements, etc. There are no recommendations on the selection of those or other assessments currently unavailable due to insufficient study of such models. If you can not arranging nonmetrizable sets decision to proximity most of a set to the standard must accept himself a developer or operator, based on their preferences, experience and intuition [6].

The most frequently used and easily constructed-functional binary relationship are the following:

– Estimation of by the maximum deflection power sets:

$$\sum_i x_i - \sum_i y_i = \Delta, \tag{1}$$

where $x_i = 1$ and $y_i = 1$ for non-zero (not empty) elements of set being compared and thus $x_i = 0$ and $y_i = 0$ for zero (empty) elements of set being compared, and Δ—numerical estimate proximity.

– Estimate the standard deviation power sets:

$$\sqrt{(\sum_i x_i)^2 - (\sum_i y_i)^2} = \delta, \tag{2}$$

where δ—proximity numerical estimate

– Probability estimate for the maximum deviation of the power sets:

$$\sum_i P(x_i = 1)x_i - \sum_i P(y_i = 1)y_i = \Delta_P \tag{3}$$

where P(.)—the probability, Δ_P—numerical probabilistic estimate proximity

– Probability estimate for the standard deviation power sets:

$$\sqrt{(\sum_i (P(x_i = 1)x_i)^2 - (\sum_i P(y_i = 1)y_i)^2} = \delta_P \tag{4}$$

where δ_P—numerical probabilistic estimate proximity

The use of these binary functional relationship makes it easy to rank the images Bi model for their proximity to B_{cj} standards and at the same time allows you to enter a numerical estimate of the proximity.

4 Features of the Optimization Solutions of the Problems Described by Equations in Algebra Modulo Two

When selecting the optimal reflective reasoning described by systems of logical equations in algebra Zhegalkin, as well as in making the best decision on the advisability of behavior in order to achieve the goals formed, requires solution of optimization problems with constraints. The most simple solutions will be when there is a possibility of constructing a scalar quality criterion, taking into account the attributes of logical variables. In this case, you can search for the optimum reduced to problems of mathematical programming (MP) [16].

The problem MP is required to calculate the n—dimensional vector X, optimizing (refer to the maximum or minimum, depending on the substantive statement of the problem) quality criteria solutions $f_0(x)$ subject to the restrictions $f_j(x) \leq u_j$, $j \in 1, 2, \ldots, r$, $x \in G$, where f_j—known scalar functional, u_j—given numbers, G—a predetermined the set n-dimensional space R_n.

Thus, the MP problem has the form:

$$f_0(x) \rightarrow ext / f_j(x) \leq u_j, \quad j \in 1, 2, \ldots, r, \quad x \in G \subseteq R^n \tag{5}$$

If probabilistic attribute of the logical variables in these systems in order to optimize can be the search the identification matrix rows of system logic equations describing the decision, which give true value y_i logic functions with maximum values of probabilities $P\{y_i = 1\}$. Then the quality criterion can be expressed as follows:

$$f_0(Y) = \sum_{i=1}^{n} P\{y_i = 1\} \rightarrow \max \tag{6}$$

At the same probabilities $P\{y_i = 1\}$ can be calculated approximately from the [10] described an algorithm.

If the analysis of a complex CNSR is revealed that the influence of those or other component y_i on its behavior is different, the quality criterion (6) it is expedient to the form:

$$f_0(Y) = \sum_{i=1}^{n} \beta_i P\{y_i = 1\} \rightarrow \max \tag{7}$$

where βi—assigned the weighting coefficients.

If the attribute of the logical variables in these systems of equations [10] will be the membership function, purpose of optimization can be the search the identity matrix rows of system logic equations describing the decision, which give values y_i logic functions with maximum values of membership functions $\mu(y_i)$. Then the quality criterion can be expressed as follows:

$$f_0(Y) = \sum_{i=1}^{n} \mu(y_i) \rightarrow \max \tag{8}$$

The values of the membership functions $\mu(y_i)$ can be calculated as described by Gorodetskiy et al. [10] algorithms.

If the analysis of a complex CRNG is revealed that the influence of those or other component y_i on it behavior is different, the quality criterion (8) it is expedient to the form:

$$f_0(Y) = \sum_{i=1}^{n} \beta_i \mu(y_i) \rightarrow \max \tag{9}$$

where β_i—assigned the weighting coefficients.

If the attribute of the logical variables in these equations systems [10] are the intervals $[a_{ji}, b_{ji}]$, the following scalar functionals can be used:

$$J_1 = \sum_{j}^{m} \sum_{i}^{n} k_{ji}(b_{ji} - a_{ji}) \rightarrow \min \tag{10}$$

$$J_2 = \sum_{j}^{n} \sum_{i}^{n} [k_{ji}(b_{ji} - a_{ji}) - c_{ji}]^2 \rightarrow \min \tag{11}$$

$$J_3 = \sum_{j}^{m} \sum_{i}^{n} k_{ji}[(b_{ji} - a_{ji}) - (b_{ji}^0 - a_{ji}^0)]^2 \rightarrow \min \tag{12}$$

$$J_4 = \sum_{j}^{m} \sum_{i}^{n} [k_{ji}^b (b_{ji} - b_{ji}^0)^2 + k_{ji}^a (a_{ji} - a_{ji}^0)^2] \rightarrow \min \tag{13}$$

where: k_{ji}—coefficients of preference decision makers (DM) of optimality, c_{ji}—the desired for DM width of the interval, b_{ji}^0, a_{ji}^0—the desired for DM the boundaries intervals.

But available in various literature [10, 17–19] recommendations for the calculation of the intervals of complex logic functions, at known intervals of logical variables is still very contradictory. They can give a completely unacceptable results. In more detail this question is considered in [14].

In the central nervous system Human (CNSH) solutions for optimality are usually made on the basis of the concept of a consistent preference for one of the other variants compared. For him it is a more natural way to select a rational alternative than the formulation of the objectives and the approach to it. When using this approach CNSR feasible set of alternatives it is expedient not to ask inequalities, and some of conditions of preference selectable variants. To solve such problems can be generalized scheme of mathematical programming, shifting from quantitative scales to the sequence, that is, shifting from models that require functionals assignment, defining the objectives and constraints of the problem, to models, takes into account the preferences of the persons participating in choosing decision. This extends the range of applications of the theory of extreme problems and may prove useful in a number of situations of choice [4, 12]. Going to the problems of mathematical programming in the ordinal scale (MPOS), generalized mathematical programming (GMP) and multistep generalized mathematical programming (MsGMP) described in more detail in [10]. In this case, when choosing the optimal solution of a system of logical equations part logic variable attributes can be linguistic expressions, describing the preferences in the form of, for example ballroom estimates formed by analyzing the views of decision-makers. And there is a principal possibility of ordering preferences.

5 Conclusion

Are described and discussed the stages of formation sensations language CNSR based on the use systems of equations modulo two or systems of logical equations in algebra Zhegalkin and the features of recognition, described by equations in algebra modulo two. It is shown that the effective use of method situation habitualness in CNSR, which is analogous of human intuition and allows the desired solution to replace analogue. Then, sharply increases the rate of formation of reflective reasoning. When selecting the optimal reflective reasoning described by systems of logical equations in algebra Zhegalkin and in making the best decision on the advisability of conduct for achieving of formulated goals it is desirable to find the optimum reduced to a well-studied problem of mathematical programming (MP). In the case when part attributes of logical variables in the system of equations CNSR are linguistic expressions, more naturally choice of the best solution is the transition to the concept of a consistent preference for one of the other variants compared. To solve such problems can be generalized scheme of mathematical programming, shifting from quantitative scales to the ordinal, or shifting from models that require functionals assignment, defining goals and constraints of the problem, to models, taking into account the preferences of the persons participating in choosing decision.

Acknowledgements The author would like to thank the Russian Foundation for Basic Researches (grants 14-07-00257, 15-07-04760, 15-07-02757, 16-29-04424, and 16-29-12901) for partial funding of this research.

References

1. Dobrynin, D.A.: Intellektual'nye roboty vchera, segodnia, zavtra [Intelligent robots yesterday, today, tomorrow]. X natsional'naia konferentsiia po iskusstvennomu intellektu s mezhdunarodnym uchastiem KII-2006 (25–28 sentiabria 2006 g., Obninsk): Trudy konferentsii. V 3-t. T.2. Fizmatlit, Moscow (2006) (In Russian)
2. Khakhalin, G.K.: Prikladnaia ontologiia na iazyke gipergrafov [Applied ontology in the language of hypergraphs]. Trudy vtoroi Vserossiiskoi Konferentsii s mezhdunarodnym uchastiem "Znaniia-Ontologii-Teorii" (ZONT-09), pp. 223–231. 20–22 oktiabria 2009 g., Novosibirsk 2009 (In Russian)
3. Akkof, R., Emeri, F.: O tseleustremlennykh sistemakh [About the Purposeful Systems], 269 p. Sov. Radio, Moscow (1974) (In Russian)
4. Gorodetsky, A.E.: (RU) Osnovy teorii intellektual'nyh sistem upravleniia [Fundamentals of the Theory of Intelligent Control Systems], 314 p. LAP LAMBERT Academic Publ, Berlin (2011)
5. Gorodetskii, A.E., Erofeev, A.A.: Printsipy postroeniia intellektual'nykh sistem upravleniia podvizhnymi ob"ektami [Principles of intellectual control systems of mobile objects]. Automation Remote Control **58**(9), 1485–1491 (1997) (In Russian)
6. Gorodetskiy, A.E., Tarasova, I.L.: Nechetkoe matematicheskoe modelirovanie plokho formalizuemykh protsessov i system [Fuzzy Mathematical Modeling of Poorly Formalized Processes and Systems.]. Izd-vo Politekhn, SPb, un-ta, 336 s (2010) (In Russia)

7. Moshkin, V.I., Petrov, A.A., Titov, V.S., Iakushenkov, I.G.: Tekhnicheskoe zrenie robotov. [The Technical Vision of Robots], 272 p. Mashinostroenie, Moskva (1990) (In Russian)
8. Nikolenko, S.I., Tulup'ev A.L.: Samoobuchaiushchiesia sistemy [Self-Learning Systems], 288 p. MTsNMO, Izdatel'stvo (Moskovskii tsentr nepreryvnogo matematicheskogo obrazovaniia) (2009) (In Russian)
9. Gorodetskiy, A.E., Dubarenko, V.V., Erofeev, A.A.: Algebraicheskii podkhod k resheniiu zadach logicheskogo upravleniia [Algebraic approach to the solution of tasks of logical control]. Automation Remote Control **61**(2), 295–305 (2000) (In Russian)
10. Gorodetskiy, A.E., Kurbanov, V.G., Tarasova, I.L.: Methods of synthesis of optimal intelligent control systems SEMS. In: Gorodetskiy, A.E. (ed.) Smart Electromechanical Systems, 277 p. Springer International Publishing (2016). doi:10.1007/978-3-319-27547-5
11. Gorodetsky, A.E., Kurbanov, V.G., Tarasova, I.L.: Ergatic methods of analysis of exploitation processes and decision-making in case of damage and accidents of power facilities. IUS **67**(6), 29–36 (2013) (In Russian)
12. Iudin, D.B.: Vychislitel'nye metody teorii priniatiia reshenii [Computational Methods of Decision Theory], 320 p. Nauka, Moscow (1989) (In Russian)
13. Gorodetskii, A.E., Dubarenko, V.V., Tarasova, I.L., Shereverov, A.V.: Programmnye sredstva intellektual'nykh sistem [Software Intelligent Systems], 171 p. Izdatel'stvo SPbGTU, SPb (2000) (In Russian)
14. Kuchmin, A.Y.: Ob odnom metode nelineinogo programmirovaniia s proizvolnymi ogranicheniiami [A method for nonlinear programming with arbitrary constraints]. Informatsionno-upravliaiushchie sistemy/Inf. Control Syst. (2), 2–9 (2016) (In Russian)
15. Gorodetsky, A.E.: Fuzzy decision making in design on the basis of the habituality situation application. In: Reznik, L., Dimitrov, V., Kacprzyk, J. (eds.) Fuzzy Systems Design. Social and Engineering Applications, pp. 63–73. Physica-Verlag, A Springer-Verlag Company, New York (1998)
16. Tabak, D., Kuo, B.: Optimal'noe upravlenie i matematicheskoe programmirovanie [Optimal Control and Mathematical Programming], 280 p. Nauka, Moscow (1975) (In Russian)
17. Alefel'd, G., Khertsberger, I.: Vvedenie v interval'nye vychisleniia, 360 s. Mir, Moscow (1987). [Introduction to the Interval Calculation], 360 p. Mir, Moscow (1987) (In Russia)
18. Levin, V.I.: Raschet dinamicheskikh protsessov v diskretnykh avtomatakh s neopredelennymi parametrami s pomoshch'iu nedeterministskoi beskonechnoznachnoi logiki / Kibernetika i sistemnyi analiz [Calculation of dynamic processes in discrete machines with uncertain parameters using non-deterministic infinite-logic], № 3, pp. 15–30 (1992) (In Russian)
19. Levin, V.I.: Nepreryvnaia logika i ee primenenie [Continuous logic and its application]. Informatsionnye tekhnologii. № 1, pp. 17–21 (1997) (In Russian)

Hierarchical Data Fusion Architecture for Unmanned Vehicles

I.L. Ermolov

Abstract *Purpose* effective functioning of unmanned vehicles demands to process large amounts of various data. In order to systemize such data processing special so-called data fusion architectures are used (e.g. JDL, Waterfall, Boyd etc.). However, those have some shortages restricting their wide usage. A goal of this paper is to develop a new date fusion architecture which could be used on board of unmanned vehicles. *Result* this paper presents new hierarchical date fusion architecture for unmanned vehicles. This architecture has some advantages in comparison to those already in use. *Practical results* the developed data fusion architecture can be used for building complex data fusion systems on board of unmanned vehicles as well as of group of vehicles and even of systems of higher hierarchy.

Keywords Data fusion · Sensor fusion · Unmanned vehicles

1 Introduction

In [1] a topic of Unmanned Vehicles (UV) autonomy was discussed. It proves emergency to provide UV with autonomy, in first term through multi-agent usage and further expansion of their applications. It is postulated that in order to implement autonomy of Unmanned Vehicles it is efficient to increase their information supply and intelligence level.

Both of these directions are connected with processing of data coming from sensors of UV and of environment. Due to specifics of sensors used in UVs it is necessary to use data fusion. Importance of data fusion is especially emerging for mobile systems.

I.L. Ermolov (✉)
Institute for Problems in Mechanics of the Russian Academy of Sciences,
Moscow State Technological University "STANKIN", Moscow, Russia
e-mail: ermolov@ipmnet.ru

A.E. Gorodetskiy and V.G. Kurbanov (eds.), *Smart Electromechanical Systems: The Central Nervous System*, Studies in Systems, Decision and Control 95,
DOI 10.1007/978-3-319-53327-8_6

2 Data Fusion

Data fusion by itself is widely known for centuries. Actually the most perfect creature, a human widely uses data fusions (fusion of five senses, distribution and doubling of sensors etc.).

Data fusion by itself can be defined as a process of information generalization based on more than once source of information.

Speaking about advantages which data fusion gives to robotists one should mention following:

- it's cheaper to produce new information by developing software than by installing extra sensors;
- considerable energy savings as information processing requires less energy than hardware of sensors;
- minimization of UVs' mass and sizes, this is especially crucial for UVs working in severe environment;
- decrease of wires and other interfaces, this higher reliability;
- decrease of negative interference among UVs' components;
- possibility to use lower performance (i.e. cheaper) sensors with higher quality of information got from them;
- compensation of restricted working space and spectrum of sensors;
- transfer of computational load from human-operator to on-board control system;
- unification increase through using same set of sensors for various functional tasks.

3 Data Fusion in UVs

In this paper it's proposed to distinguish following cases of data fusion in Unmanned systems:

Time-based data fusion. While tracking variation of some parameter in time sequences it becomes possible to estimate other parameters of UV. Another case of such data fusion is data filtering [2]. For more details see [3].

Reliability-based data fusion. While fusing data from several sensors with low-reliability characteristics it becomes possible to get highly reliable information.

Space-based data fusion. By fusing information from several sensors each one with narrow working space (Fig. 1) we may get information of the large working space. Another case of space-based data fusion is fusing date from dispensed sensors which gives us new information.

Sensor-type data fusion. Fusion of data from sensors measuring same parameter but functioning on various principles gives information with higher reliability factor (Fig. 2).

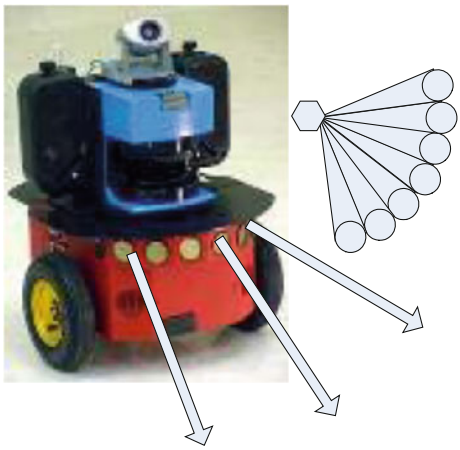

Fig. 1 Space-based data fusion (fusion of ultrasonics data at Pioneer P3DX platform by Adept Mobilerobots)

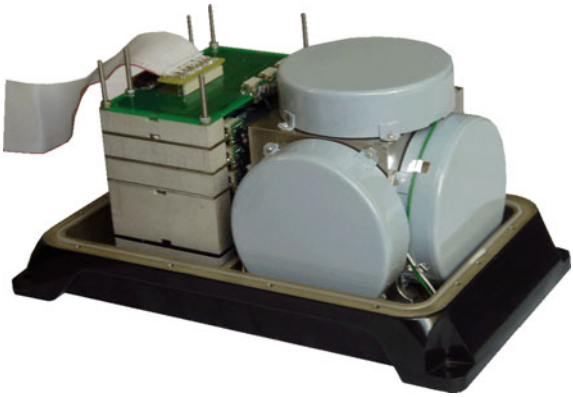

Fig. 2 Navigation data from various types of sensors is fused directly on board of 120/3 navigation system from Perm Instrument Making Company

Data-type data fusion. This one is used to produce information basing on data of various type (e.g. fusing information from video sensor with information from laser sensor). This type of fusion is intensively used especially for object recognition.

Summarizing this classification it can be said that most of the data fusion cases in unmanned systems can be described by these fusion cases or by their combination.

Data fusion architectures. Modern UVs are extremely complex systems with large number of data flows [4]. In order to analyze such amount of data flow it is necessary to adjust those data flows.

This is known as data fusion architectures. There exists variety of such architectures: JDL, Boyd model, LAAS, The Omnibus Model, Waterfall model and some others [5].

One of the most popular solutions in this area was the JDL (Joint Directors of Laboratories) Architecture [6] which was developed in 1985.

This architecture includes 5 level data hierarchy and a data base connected with common bus. Those levels may act both in sequence and in parallel.

However JDL architecture has some restrictions [6]:

- each time model is organized basing on some specific data or information. E.g. it's difficult to recombine a JDL-model for other applications.
- Outlook of the model seems to be rather abstract, what creates an obstacle for its interpretation;
- This architecture doesn't correlate with some specific data processing algorithms, this impedes its implementation in real system.

Speaking of data fusion architecture mostly suitable for Unmanned Vehicles one may formulate following criteria for such architecture:

- Data fusion architecture should have hierarchical structure, as only hierarchy allows to control large-scale systems;
- Data fusion architecture should demonstrate all processes in their hierarchy, be easily understandable, even intuitive for its user;
- Such architecture should allow various feedback and counter-current data flows;
- In some cases architecture should permit data transfer omitting some hierarchical layers.

4 Hierarchical Data Fusion Architecture

Hierarchy is inherent with some data fusion architectures presented above. However the distinction between layers is not demonstrative there.

Author of this paper proposes following *Hierarchical data fusion architecture* (Fig. 3).

Here author describes layers' term as following:

Parameter—predicate which describes as a rule quantitatively property of a single component of a UV or of environment. Input of this level usually comes directly from sensors.

Mathematically it can be described as following:

$$p_i = \sum_{j=1}^{z} a_{ji}^{gp} g_j + \sum_{k=1}^{y} a_{ki}^{pp} p_k,$$

where

p_i i-th parameter,
a_{ji}^{gp} coefficient considering influence of j-th sensor to i-th parameter,
gj input from j-th sensor,
z number of sensors in system,

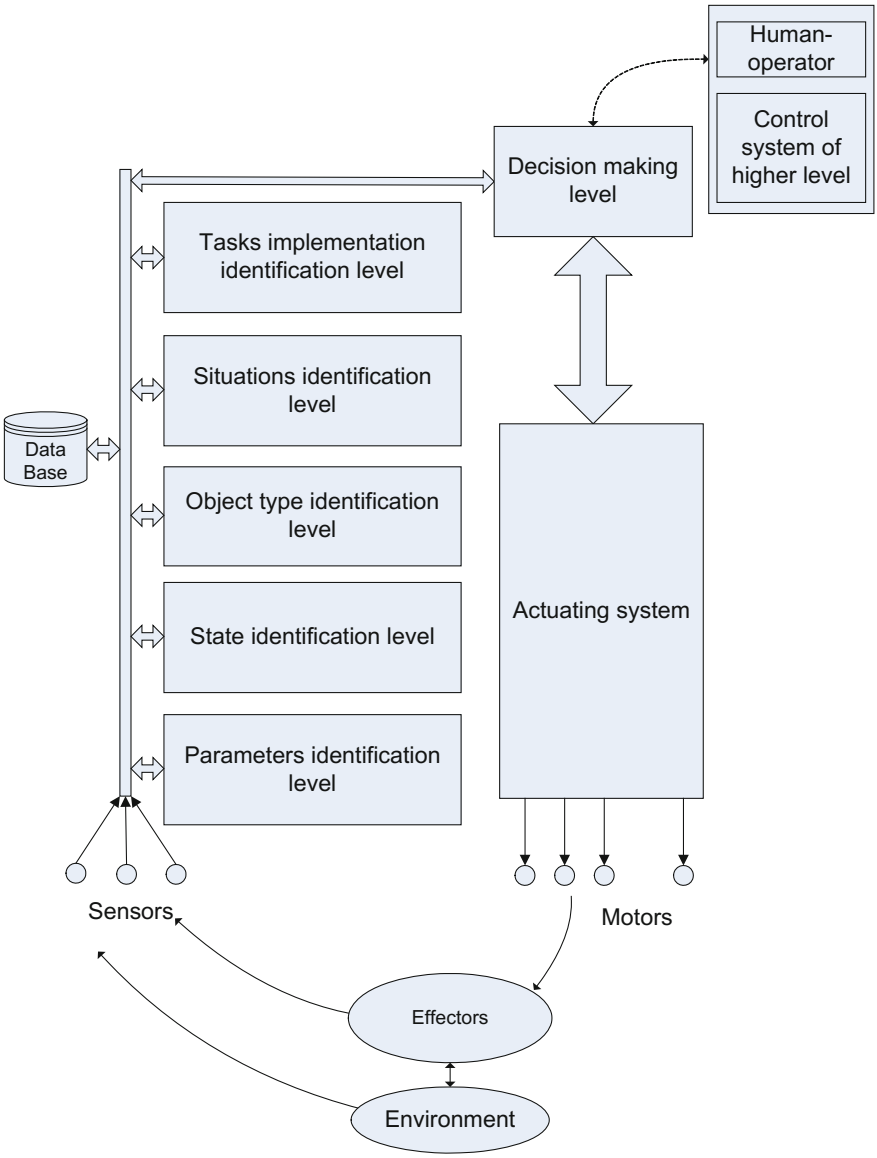

Fig. 3 Hierarchical data fusion architecture

a_{ki}^{pp} coefficient considering influence of k-th parameter to i-th parameter (in k = i it is predicate's "inertia"),
p_k value of k-th parameter,
y number of parameters in system.

State—predicate which describes quantitatively or relatively property of a whole UV or of environment. Input for this predicate comes from *parameters* or from sensors directly.

Mathematically it can be described as following:

$$s_i = \sum_{j=1}^{y} a_{ji}^{ps} p_j + \sum_{k=1}^{x} a_{ki}^{ss} s_k + \sum_{h=1}^{w} a_{hi}^{os} o_h,$$

where

s_i i-th state,
a_{ji}^{ps} coefficient considering influence of j-th parameter on i-th state,
a_{ki}^{ss} coefficient considering influence of k-th state on i-th state,
o_h *h*-th instruction,
x number of states in system,
a_{hi}^{os} coefficient considering influence of h-th instruction on i-th statee *cocmoue*,
w number of instructions in system.

Object type—generalized identification of an object present in environment, which is defined by its typical data and by its potential interaction with UV.

Mathematically it can be described as following:

$$m_i = \sum_{j=1}^{y} a_{ji}^{pm} p_j + \sum_{k=1}^{x} a_{ki}^{sm} s_k + \sum_{h=1}^{v} a_{hi}^{mm} m_h + \sum_{l=1}^{u} a_{li}^{cm} c_l + \xi_i^m + \psi_i^m,$$

where

m_i i-th type of object,
a_{ji}^{pm} coefficient considering influence of j-th parameter on identification of i-th type of objects,
a_{ki}^{sm} coefficient considering influence of k-th state on identification of i-th type of objects,
a_{hi}^{mm} coefficient considering influence various other types of objects presented in environment to the identification of i-th object type,
v number of objects type predicates in system,
a_{li}^{cm} coefficient considering influence of l-th state identification of i-th object type,
c_l l-th situation predicate,
u number of situations in system,
ξ_i^m information from data base on trends of i-th type of objects presence,
ψ_i^m information from tasks on the possibility of i-th type of objects presence.

Situation—is a generalized notion which describes complex of interaction between robot and environment.

Mathematically it can be described as following:

$$c_i = \sum_{j=1}^{y} a_{ji}^{pc} p_j + \sum_{k=1}^{x} a_{ki}^{sc} s_k + \sum_{h=1}^{v} a_{hi}^{mc} m_h + \sum_{l=1}^{u} a_{li}^{cc} c_l + \xi_i^c + \psi_i^c,$$

where

c_i i-th situation
a_{ji}^{pc} coefficient considering influence of j-th parameter on identification of i-th situation,
a_{ki}^{sc} coefficient considering influence of k-th state on identification of i-th situation,
a_{hi}^{mc} coefficient considering influence of various types of objects presented on identification of i-th situation,
a_{li}^{cc} coefficient considering influence of l-th situation on identification of i-th situation,
ξ_i^c information from data base on trends of i-th situation,
ψ_i^c information from tasks on the possibility i-th situation.

Tasks—a set of situations in serial-parallel order. These situations must be achieved (implemented) by robot in order for a task to be fulfilled.

Mathematically it can be described as following:

$$t_i = \sum_{j=1}^{y} a_{ji}^{pt} p_j + \sum_{k=1}^{x} a_{ki}^{st} s_k + \sum_{h=1}^{u} a_{hi}^{ct} c_h + \sum_{l=1}^{q} a_{li}^{tt} t_l + \xi_i^t,$$

where

t_i i-th task implementation,
a_{ji}^{pt} coefficient considering influence of j-th parameter on identification of i-th task implementation,
a_{ki}^{st} coefficient considering influence of k-th state on identification of i-th task implementation,
a_{hi}^{ct} coefficient considering influence of h-th situation on identification of i-th task implementation,
a_{li}^{tt} coefficient considering influence of l-th task implementation on identification of i-th task implementation,
q number of tasks in system,
ξ_i^t information from data base on trends i-th task implementation

Now let's see how it works.

Data from various sensors of UV and of environment flows to the common bus. An important advantage of this scheme is that it can use data from both on-board and stand-alone sensors.

Usage of common data bus is also an important advantage as it allows to exchange data and information among various levels freely. As it was mentioned before data may flow to the next level and also to higher levels directly.

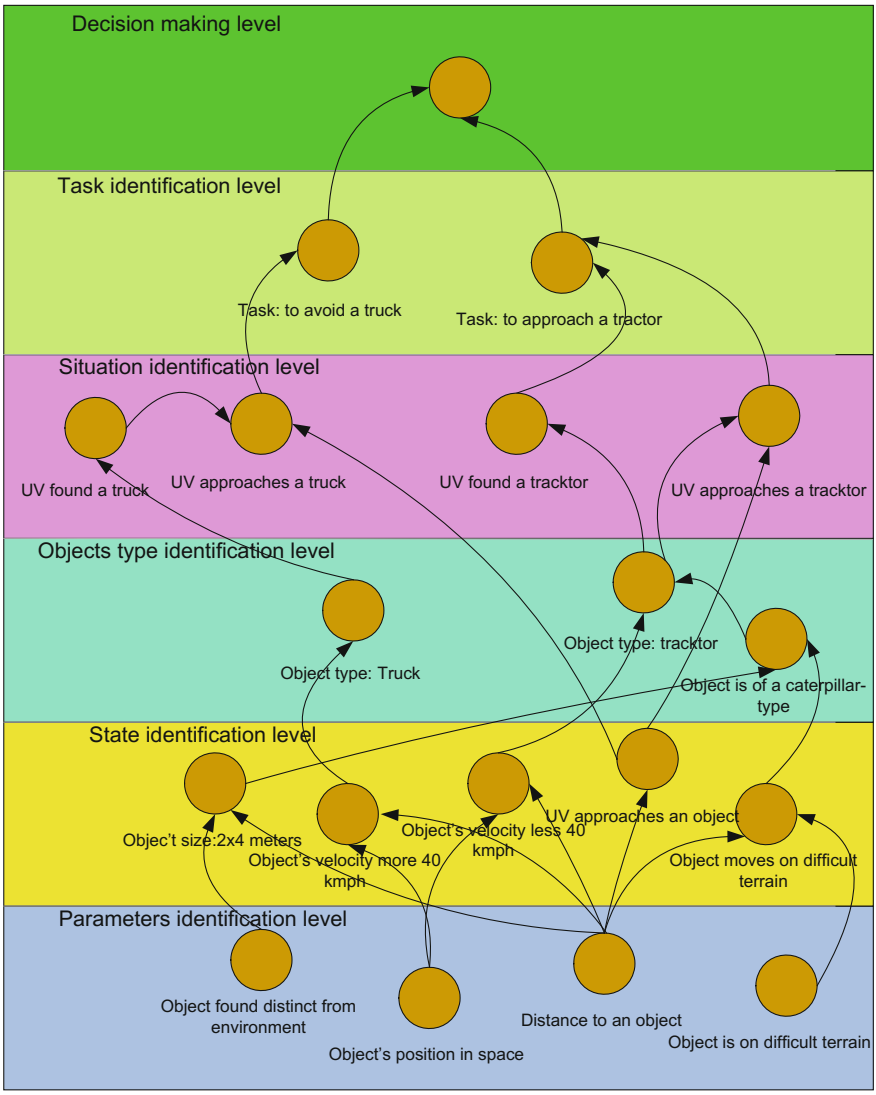

Fig. 4 Example of a model built upon *Hierarchical data fusion architecture*

This also allows in case human-operator needs it to receive information on any predicate directly.

All the data is fused in bottom-up direction. However it's obvious that some more simple or primitive systems may omit some of the higher levels. However highly autonomous systems will involve all the levels.

When needed extra data will be acquired from data base.

Final output comes to the decision making level which sends instructions to actuators and sub-systems. It also may be built on same approach.

Figure 4 presents example of model built on *Hierarchical data fusion architecture.* In this example UV has a goal to approach tractor, while avoiding a truck. This scheme shows only some of the data fusion components and data flows.

Let's outline advantages of the proposed *Hierarchical data fusion architecture*:

- it is appropriate to modern UV structure;
- it has good demonstrable and visual properties, which allow operator to use it intuitively;
- wide usage of various data flows and feedbacks including transient flows;
- modularity which allows various ready-to-use solutions be transferred from one scheme to another.

Software implementation of proposed architecture involves intelligent control approaches, such as neural networks, fuzzy cognitive maps, expert systems [7, 8].

5 Conclusions

Data fusion is an important technology implementing high autonomy of UV. Hierarchical data fusion architecture has good properties of modularity, visualization and hierarchy. It allows to systemize data processing in complex system of modern UVs.

Research supported by Russia Academy of Sciences grant: "Emerging Problems of Robotics".

References

1. Ermolov, I.L.: Robots' Autonomy, its Measures and How To Increase it. Mechantron. Autom. Control, № 528 (2008)
2. Zenkevich, S.L., Minin, A.A.: Mapping by UV with a lidar basing recurrent filtration method. Зенкевич С.Л., Минин А.А., Mechantron. Autom. Control, № 8 (2007)
3. Fomichev, A.A., Uspensky, V.B., Stchastlivets, K.Y., et al.: Data fusion in integrated navigation system with laser gyroscopes based on generalized Kalman filter. In: Proceedings of International Conference on Integrated Navigation Systems, St. Petersburg, 26–28 May 2003
4. Ermolov, I.L.: Factors affecting UGVs spacious autonomy level, Vestnik YuFU, № 1, 2016
5. Gorodetsky, V.I., Karsaev, O.V., Samoylov, V.V.: Data fusion in complex situations analysis and understanding. In: Proceedings of "Perspective Systems and Control Tasks", Dombai, Russia (2008)
6. Elmenreich Wilfried, Sensor Fusion in Time-Triggered Systems, Technischen Universitat Wien, Wien, im Oktober 2002
7. Makarov, I.M., Lokhin, V.M. (eds.): Intelligent Control Methods. Physmatlit, Moscow (2001)
8. Martchenko Anna, S., Ermolov Ivan, L., Groumpos Peter, P., Poduraev Jury, V., Stylios Chrysostomos, D.: Investigating stability analysis issues for fuzzy cognitive maps. In: Proceedings of IEEE MED-2003 Conference, Rhodes, Greece (2003)

Part III
Sensor Systems

Automatic 3D Human Body Modelling

A.Yu. Kuchmin and Somar Karheily

Abstract *Objective* 3-layers adaptive system that detects, extracts, analyzes and models human bodies existed in video stream, it uses different detection methods in parallel and evaluates each detection result according to correctness measurements, and controls method's work and priorities according to dynamic parameters; these parameters are updated continuously depending on the system's statistics. The system gathers the information gradually; builds complete model based on already existed and trusted results, and waits for the missing information to update. *Results* introducing effective way to use different detection methods in parallel and control them adaptively, then make decision based on these unrelated sources, reducing the ambiguity in high complex environments by depending on all features of the human body, which leaded to more accurate and trustful results. *Practical importance* The automatic 3D human body modeling system is presented; this system takes RGB video stream input, and extract the human body inside the video, then model this body with no depth information. This system can be used as an electronic vision system for mobile robots.

Keywords Human detection · Contour deformation · Human pose estimation · Parallel detection · 3D human model

A.Yu. Kuchmin (✉)
Institute of Problems in Mechanical Engineering, Russian Academy of Sciences, Saint-Petersburg, Russia
e-mail: radiotelescope@yandex.ru

S. Karheily
Peter the Great St. Petersburg Polytechnic University, Saint Petersburg, Russia

A.E. Gorodetskiy and V.G. Kurbanov (eds.), *Smart Electromechanical Systems: The Central Nervous System*, Studies in Systems, Decision and Control 95,
DOI 10.1007/978-3-319-53327-8_7

1 Introduction

1.1 Main Goal

The main goal is to get the contour of the human body and subtract it from the background, then using these results to build a 3D human model, this way allows us to gather the information from several methods, evaluate each result, then make a decision about closest results to the body.

The known methods depend on specific features in the body, some on color, some on histograms, some on contour feature and others, so they give different results depending on working circumstances, so by gathering them, we are using all known features, and choose the best depending on working results [1–12].

- Input of the system: a video stream coming from RGB camera.
- Output: 3D model for human bodies that appear in the video.

This main goal is distributed into sub goals:

- Detection of the body: using the known techniques and algorithms.
- Extracting of body contour: after detecting the candidate areas of the body, the contour of the body should be extracted using appropriate filters and contour detection algorithms.
- Tracking body area: to follow detected body every frame in video stream.
- Pose estimation: after getting the contour, analyzing the body pose is needed for parts division and determining the individual features of the body.
- Modeling: depending on the gathered information from the previous steps, we build the model for the detected body.

1.2 Methods of Study

The work was done first by studying the methods of detection, and theories about human body classification and features, this study took in consideration the differences in accuracy, speed and the features they depend on to detect the body.

The theoretical study gave us the idea of building the system, which can use any method in detection phase, with ability to add new methods, then evaluate results, and analyze the body pose, then adapt the whole system flow depending on previous results and how much accurate they were.

Building and implementing the system was done by using OpenCV libraries, and IDE of Visual Studio 2013, and tested in the different ordinary environments using Intel® Core™ i5-4200M CPU @ 2.50 GHz, RAM 4 GB, graphic card NVIDIA GeForce 840M.

1.3 Main Results

The effect of working environment on detection methods, and body features leads us to the importance of using more than one source of detection methods, and the need to separate the detection from analyzing in a way that allows us to add any new method to the system, that work gave us ability to integrate several methods together in an intelligent system that controls working flow of each method and adapts decision-making parameters, reducing the ambiguity in high complex environments by depending on all features of the human body and extracting the nearest candidate.

The new results:

- Increasing the accuracy of existing method.
- Efficient parallel detecting.
- Modeling body using RGB video input, with no depth information.
- Pose analyzing of the body.

2 Previous Work

The object classification methods could be divided into three categories: shape-based, motion-based and texture-based (Table 1). Shape-based approaches first describe the shape information of moving regions such as points, boxes and blobs. Then, it is commonly considered as a standard template-matching issue. However, the articulation of the human body and the differences in observed viewpoints lead to a large number of possible appearances of the body, making it difficult to accurately distinguish a moving human from other moving objects using the shape-based approach. This challenge could be overcome by applying part-based template matching. Texture-based methods such as histograms of oriented gradient (HOG) use high dimensional features based on edges and use support vector machine (SVM) to detect human regions.

- Gaussian mixture model, self-adaptive cluster background subtraction (CBS-GMS).
- Histograms of Oriented Gradients (HOG).
- Convolutional Neural Networks (CNN).
- Principle Component Analysis (PCA).
- Bayesian similarity measurements (BSM).

Table 1 Texture-based methods to detect human regions

	CNNs	CBS-GMM	HOG	PCA
Accuracy	90%	Between 80 and 99% depending on body part	80–90% depending on the environment	98% relating to face recognition
Complexity	2	4	3	1
Time	Real time	Almost real time	Almost real time	Real time
Notes	Generalized to all object	For humans	For humans	For face
Camera moving	Yes	Needs optimization	Needs optimization	Optimized

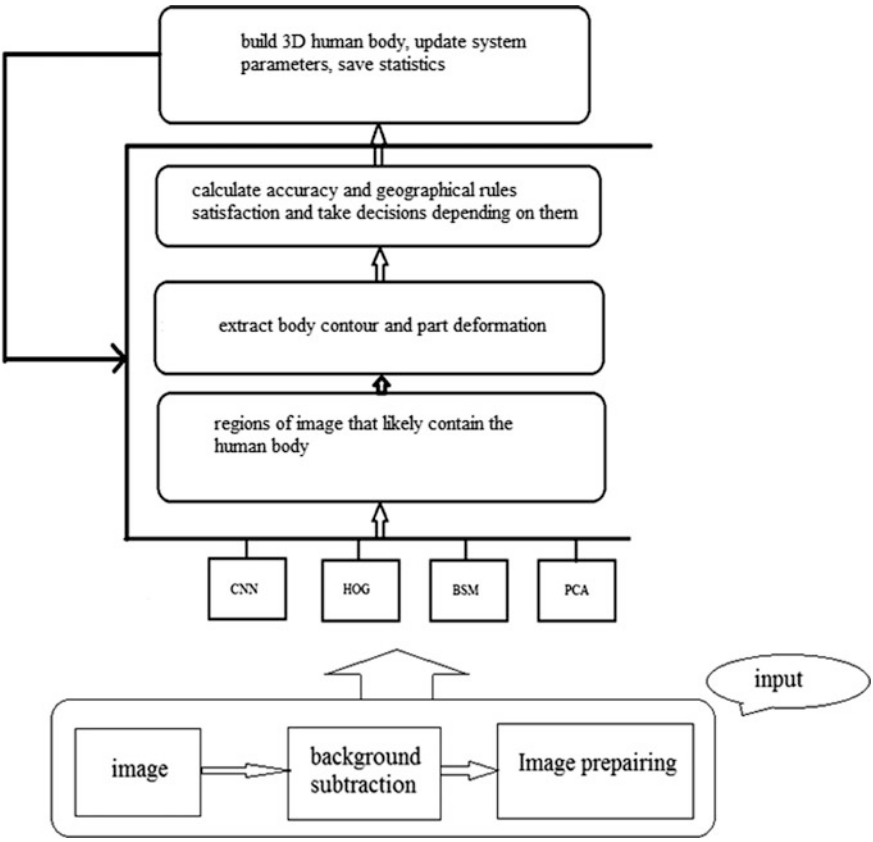

Fig. 1 System architecture

3 System Design

3.1 System Architecture

The work flow of the system can be divided into three main steps (Fig. 1):

- Body detection.
- Decision making about human features.
- Modeling and adapting the parameters.

This main steps in organized in system architecture as three layers, each one of this layer is responsible for specific missions, and passes the result to upper layer.

The division of system work flow makes it easier to modify in future, and update the way of work in each step, especially in the detection where we depend on more than one technique.

3.2 System Layers

3.2.1 Layer 1

Uses the previous techniques described before (Fig. 2).

Each one of these techniques works depending on different features of the body, so they differ in results according to the work environment, so here by gathering information from more than one method, we reduce the effect of environment as much as possible.

- Input of this layer is the image frame coming from the video.
- Output of this layer is number of areas that contain human bodies; these areas are presented as rectangles.

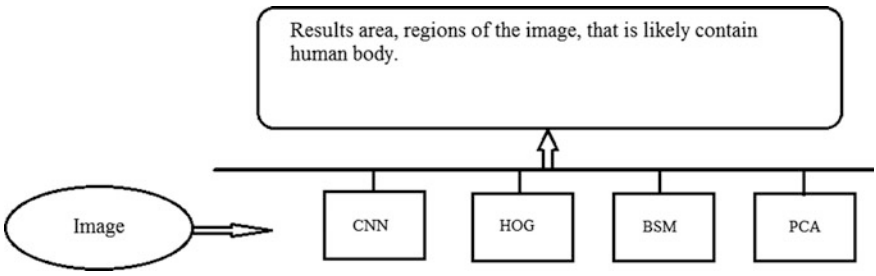

Fig. 2 Layer 1 diagram

3.2.2 Layer 2

The decision about body pose and features is taken in this layer depending on the constraints of the human body, and how close the extracted contour is to the human models, so we extract the human contour out of the area detected in first layer, and then we deform it into parts, using the curve salience study (Fig. 3).

- Input: rectangles of the candidate areas from layer 1.
- Output: deformed body and texture of each part.

A correctness function will take the input, and use mathematical formulas to calculate the trust and accuracy of each result from previous layer.

3.2.3 Layer 3

- Input is the feature of human body detected, with the results evaluation made in layer 2.
- Output is 3D model of the body and the updated parameters of the system.

The system here in this layer does these tasks:

- Extract body texture.
- Build 3D model.
- Save statistics.
- Update system parameters.
- Estimate confidence of each method depending on statistics of cost function.

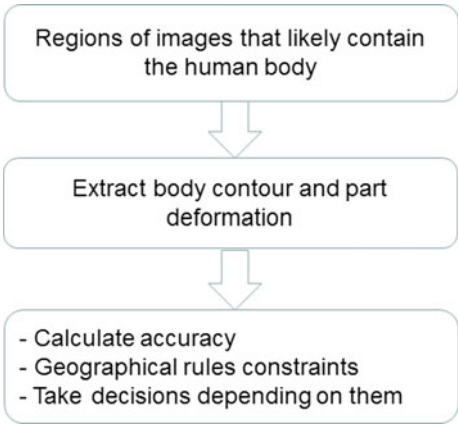

Fig. 3 Layer 2 diagram

4 System Implementation

4.1 Layer 1

In the first layer we implement the methods:

- HOG
- PCA
- Haar-like Features

4.2 Layer 2

Layer Tasks:

– Apply image processing algorithms for contour detecting.
– Subtract contour from the background.
– Analyze the body contour.
– Evaluate the result.
– Take decision about correct results.

So first we subtract the contour from the background, and that would be represented as a sequence of points $[a_1 \ldots a_n]$, then the system deforms this contour into parts.

In order to deform the contour, first step is to smooth the contour which excludes the extreme points, then the system determined the basic points in the contour, which are the "negative curvature minima (NCM)" which is calculated by scanning all points of the contour.

Each one of these points is likely located on body part edge. (Hoffman and Richards's minima rule.)

Then System searches for the shortest cut for each point of NCM.

Let S be a silhouette, C be the boundary of S, P be a point on C with NCM, and P_m be a point on C so that P and P_m divide the boundary C into two curves C_l, C_r of equal arc length. The ends P_l and P_r of the two cuts are located as follows:

$$p_l = \arg\min_{p'}\left(\left|\left|\overline{pp'}\right|\right|\right) \quad s.t \frac{\left\|\widehat{pp'}\right\|}{\left|\left|\overline{pp'}\right|\right|} > T_p, \quad p' \in C_l, \ \overline{pp'} \in S$$

$$p_r = \arg\min_{p'}\left(\left|\left|\overline{pp'}\right|\right|\right) \quad s.t \frac{\left\|\widehat{pp'}\right\|}{\left|\left|\overline{pp'}\right|\right|} > T_p, \quad p' \in C_r, \ \overline{pp'} \in S$$

where T_p is a experimental threshold.

We find the two points P_l and P_r which are the edges of the body part.

After searching for those points, we get the required cuts for the body, but we still have extra cuts that we do not need, so we remove the overloaded cuts.

The system executes these operations for each area sent from layer 1, and in next step, it evaluates the results to take the decisions and adopt the best of them.

4.2.1 Correctness Function

Assume that n ribbons are extracted from a contour C = {c_1, c_2, …, c_n}, and that the human model consists of m model body parts: F = {f_1, f_2, …, f_m}.

Let H = (h_1, h_2, …; h_m, view) represent a match hypothesis, where

view$^{\in}$ {front/back, side} and

$$hi = \begin{cases} j & \text{if } cj \text{ corresponds to } f \\ 0 & \text{if no point corresponds to } f \end{cases}$$

This is not a one to one mapping; it allows some body parts to be occluded and also allows some ribbons to not correspond to any body parts. The maximum (MAP) hypothesis H* is selected from the hypothesis space H such that, given a person is present in the image,

$$H = \arg\max_{\mathrm{H}} P(H, C\backslash person)$$

where $P(H, C\backslash person)$ is number of identical points in H when comparing C to person (model).

Accordingly, the goodness function that rates the hypothesis is defined as follows:

$$G(H) = P(C\backslash H, person)p(person\backslash H)$$

where $P(C\backslash H, person)$ evaluates the degree of resemblance between the matched pairs, while $(person\backslash H)$ is proportional to the number of identified body parts.

In order to calculate the goodness function G(H), two terms need to be estimated: the likelihood P(C\H, person) and the posterior probability p(person\H).

Let $\widehat{A'}, \widehat{S'}, \widehat{U'}$ be the aspect ratios, relative sizes, and relative positions of the identified body parts, respectively. They are estimated with the parameters of the corresponding ribbons, so:

$$P(C\backslash H, person) = N(\widehat{A'}\backslash \widehat{A)} * N(\widehat{S'}\backslash \widehat{S)} * N(\widehat{U'}\backslash \widehat{U)}$$

And the second $p(person\backslash H)$ represents the number of body parts that was selected, we attach a weight for every body parts (here we can give big weight for the face if it was detected by PCA also), so:

$$p(person\backslash H) = \sum d_i w_i$$

Depending on the measurements of the goodness function, we took the decision about the chosen results, and send them to the next layer.

4.2.2 System Knowledge Base

A knowledge base refers to a repository of entities and rules that can be used for decision making, the entities in our KB consist of object and attributes.

We use three types of attributes to describe an object (which is a body part in our system).

- Visual attributes: correspond to knowledge acquired from visual perception and system calculation.
- Physical attributes: constitute a form of knowledge from the physical world. Each physical attribute is a measurable quantity that describes one aspect of the object. We use properties such as width and height, to describe the objects.
- Categorical attributes: reflect the semantic understanding of the object (generalization). Object categories form a hierarchy consisting of several levels of abstraction, and the object relation with other objects.

Rules are defined to model the human body parts features and its relations and constraints. The rules are divided into two major parts:

- System rules that are taken from parameters which are calculated in the system during work, such as priority for each method, and previous results of the part (e.g., position and texture), such rules are useful while tracking the body.
- Human constraints: which are taken from the structure of the human body and each part priority, such as positional and orientation constraints between adjacent parts, as torso-upper limb connection, or upper-lower limb connection.

4.3 Layer 3

System in this layer, gather the extracted features that outputted from previous layer, and construct the 3D model depending on the information of:

- Position and orientation (given through series of points for each part).
- Texture extracted from matching with the original photo.

The system saves the statistics for each method in layer 1, and calculates the priority of working depending on how correct and accurate this method is working.

The priority is calculated as follow:

$$p = \frac{1}{2}\left[E_d + E_p\right]$$

where E_d is detection statistics, starts at certain value (ex 80%) calculated by previous statistics, and update its value by the system forward working.

$$E_d = \frac{E_0 + \frac{N_g}{N_{tot}}}{2}.100$$

where E_0 is the starting statistic value of detection method.

N_g is the number of the correct detection results, and N_{tot} is the total number of all results.

$$E_p = \sum_{i \in parts} w_i Q_i$$

where E_p is parts detection statistics, where w_i is the part weight (importance), and Q_i is part detection correctness.

The priority factor is used to control working method priorities in layer 1.

Every method also has statistics about each part extraction results, in order to analyze its results for each part:

$$Q_m = [Q_1, Q_2, \ldots, Q_n]$$

The velocity of each part V_p also needed for evaluating result.

Saving these statistics for each method are used to control methods priorities, and making decisions in layer 2, where two methods give different results while working.

5 Experimental

Layer 1, gives us the regions that likely contain the human body, these regions are transferred into layer 2, which analyses each one, and deforms the body parts.

In order to estimate the results of our work, we calculate the number of frames in which there is a detected body, and then we divide this number on the total number of the frames.

Let R the detection rate and D the number of frames where we detected the human body,

$$\mathrm{R} = \mathrm{D}/\mathrm{total}_{\mathrm{frame}}$$

By comparing results between our work and previous work and methods, we can see that for every period of time, we get the maximum rate at least from both methods, and as long as the detected frames is not always identical in both methods,

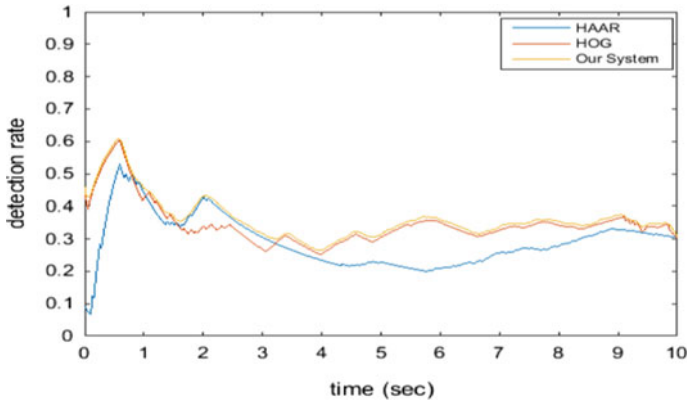

Fig. 4 Our result in comparison with known methods

so the overall result is the maximum with a little shift (because the methods may detect different frames) Fig. 4.

6 Conclusion

In our work, we presented automatic 3D human body modeling system; this system takes RGB video stream input, and extract the human body inside the video, then model this body. The system accomplished tasks:

- Specify human area in video.
- Show contour of the body.
- Analyze human parts and pose.
- Extract features: dimension, orientation, position, texture.
- Build 3D model identical to the extracted features.

These tasks were achieved by adaptive 3-layers structure that organizes the sub-tasks of the system in a way that allows us to improve the results by adding/removing methods to system structure.

References

1. Zhu, Q., Avidan, S., Yeh, M.-C., Cheng, K.-T.: Fast Human Detection Using a Cascade of Histograms of Oriented Gradients (2006)
2. Chen, B., Perona, P., Bourdev, L.: Hierarchical Cascade of Classifiers for Efficient Poselet Evaluation (2014)
3. Jiang, Y., Ma, J.: Combination Features and Models for Human Detection (2015)

4. Takayanagi, Y., Katto, J.: Human Body Detection using HOG with Additional Color Features (2010)
5. https://en.wikipedia.org/wiki/Histogram_of_oriented_gradients
6. Dalal, N., Triggs, B.: Histograms of Oriented Gradients for Human Detection (2005)
7. Xiong, Y.: Automatic 3D Human Modeling: An Initial Stage Towards 2-way Inside Interaction in Mixed Reality (2011)
8. http://docs.opencv.org/2.4/doc/tutorials/imgproc/imgtrans/canny_detector/canny_detector.html
9. https://en.wikipedia.org/wiki/Eigenface
10. https://en.wikipedia.org/wiki/Pedestrian_detection
11. Dollár, P., Wojek, C., Schiele, B., Perona, P.: Pedestrian Detection: An Evaluation of the State of the Art (2011)
12. Walk, S., Majer, N., Schindler, K., Schiele, B.: New Features and Insights for Pedestrian Detection (2010)

Optoelectronic Autocollimating Video Sensor for a Mobile Robot

I.A. Konyakhin, Van Phong Hoang and A.I. Konyakhin

Abstract *Purpose* developing of the structure and metrological parameters of the autocollimating video sensor to generate SEMS control signals at mobile robot arm tool for high-precision operations. Analyzing the method to increase the pitch and yaw angular measuring range of the autocollimating sensor. *Results* autocollimating video sensor using a sight target compose of three reflectors designed as glass tetrahedrons with angles of 90° between reflecting edges allows for generation of SEMS control signals for steering the mobile robot and its operating arm in all motion modes: movement between target objects, approaching to the stop point, steering during performance of operations. If the reflecting edge of one of reflectors of the sight target is designed as a conical surface its retro-reflection property is preserved and the processing of the image of reflected beam allows for high precision positioning of the mobile SEMS platform of a mobile robot. *Practical value* universal autocollimating video-sensor for independent generation of control signals in three main movement modes: movement between target objects, approaching the stop point near the next target object, steering of the mobile robot or arm tool to perform required operation.

Keywords Mobile robot · Autocollimator · Pitch and yaw measurements · Tetrahedral reflector · Matrix photo receiver · Invariant axis · Angular shifts of the robot arm tool

I.A. Konyakhin (✉) · V.P. Hoang · A.I. Konyakhin
ITMO University, Saint Petersburg, Russia
e-mail: igor@grv.ifmo.ru

V.P. Hoang
e-mail: vanphongkqh@yahoo.com

A.I. Konyakhin
e-mail: aligkon@yandex.ru

A.E. Gorodetskiy and V.G. Kurbanov (eds.), *Smart Electromechanical Systems: The Central Nervous System*, Studies in Systems, Decision and Control 95,
DOI 10.1007/978-3-319-53327-8_8

1 Introduction

Mobile robots are commonly used for transport operations in the remote areas in the industry and power generation facilities and in the hazardous conditions for example under water or under high temperature and in high radiation zones.

Universal mobile robots designed as self-propelled systems and provided with all required devices and interchangeable equipment have a strong potential. Mobile robots are typically used for transport operations, preventive maintenance and repairs in deterministic environment which is characterized by a priori knowledge of the position of the target objects with which the robot can interact.

For high precision operations and movement along a complex trajectory in many cases the mobile robot contains a special module based on the hexapod structures of smart electromechanical systems (SEMS). The robot arm tool for high-precision operations is mounted on a mobile hexapod structure and the base as fixed platform is attached to the rigid structural element of the robot.

Video-sensors are commonly used to control SEMS and motion of the arm tool. The information from video-sensors allows for independent generation of control signals in three main movement modes: movement between target objects, approaching the stop point near the next target object, steering of the robot or arm tool to perform required operation. For ensuring required precision of the approach and steering the sighting targets are placed in the stop points which are read by SEMS video sensor. Let us consider an universal autocollimating video sensor that enables SEMS to steer mobile robot or its arm tool in all motion and operating modes.

2 Structure of Autocollimating Video Sensor

Autocollimating video sensor includes optoelectronic automatic collimator mounted on the transport robot and sight target located in the stop point.

Optoelectronic automatic collimator consists of emitting collimator and receiving channel—see Fig. 1.

Collimator includes emitting mark 1, for example IR emitting diode installed in the focal plane of lens 2. Collimator produces optical beam with required parameters and directs it towards the sight target consisting of three reflectors 3, 4, 5. Basic distances l_1, l_2 determine relative position of reflectors of the sight target.

Beams reflected from the sight target pass lens 2 as a receiver and produce images of reflectors in the focal plane formed by beam splitter 6. The sensor of the matrix photodetector 7—matrix CCD or CMOS is aligned with the focal plane of the receiving channel. Microprocessor 8 processes video frames from matrix photodetector and calculates coordinates and characteristics of the images of reflectors which allows for estimation of the parameters determining the position of the transport robot relative to the sight target. Based on the parameters of spatial orientation the command unit 9 generates control signals that control movement of the robot relative to the stop point.

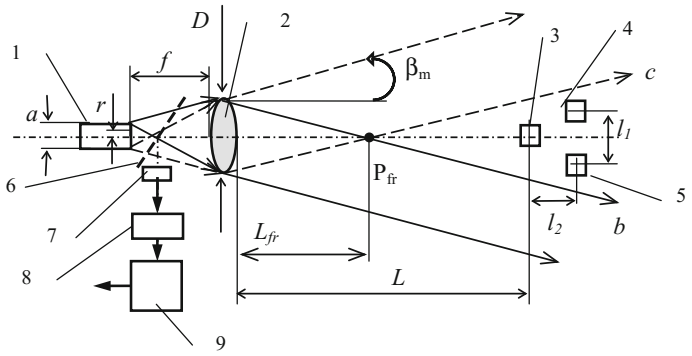

Fig. 1 Structure of autocollimating video sensor

3 Autocollimating Sensor Functioning Algorithm

Sensor collimator produces a beam composed by a multitude of elementary parallel beams. Each elementary beam is generated from the emission of one point of emitting mark 1; the axis of the beam forms angle of β_0 with lens 2:

$$\beta_0 = arctg(r/f) \tag{1}$$

where r is the distance from optical axis to the considered point of mark 1; f is focal distance of lens 2 of collimator.

If a is a diameter of mark 1 then full parallel beam of collimator (Fig. 1) propagates a cone with angle β_m, which is determined by the dimensional beams emitted from extreme points of mark 1.

$$\beta_m = arctg(a/f) \tag{2}$$

On Fig. 1 the dimensional beams from the upper point of the mark are shown by the solid lines, dimensional beams from the lower point of the cross section are shown by dashed lines.

Complete beam of collimator has internal and external areas [1]. The internal area is limited by the conical surface; beam emitted from the edge of the exit pupil with diameter of D_1 at an angle of β_k to optical axis of lens and intersecting the axis in point P_{fr} (beams c and b) is its generatrix. Distance L_{fr} from the center of the exit pupil to point P_{fr} is a distance of generation of the beam. Value L_{fr} is calculated using ratio (3):

$$L_{fr} = D/(2 \cdot tg(\beta_m)) \tag{3}$$

Internal conical are includes two cones: far and near. The axis of the near cone is formed by optical axis of lens at the distance of $L < L_{fr}$, the base of the cone is the

aperture of lens 2 of collimator, point P_{fr} is located at the vertex of the cone—Fig. 1. The axis of the far cone is formed by optical lens at the distance of $L > L_{fr}$, point P_{fr} is located at the vertex of the cone.

Heterogeneous structure of the beam collimator is a reason for transforming the beams reflected from the sight target during movement of the robot.

Reflectors 3, 4, 5 of the sight target are realized as glass tetrahedrons with angles of 90° between reflective edges forming a corner reflector with retro-reflection property. The beam reflected from corner reflector is directed oppositely to the incident beam. This property allows for setting the position of corner reflector using automatic collimator in a broad spatial angle $\Omega = \pm 35°$ [2].

At the stage of approaching the destination point reflectors 3, 4, 5 stay in the far zone of the beam of collimator. In this case each reflector is in the area of elementary parallel beams produced from the limited number of points of the emitting mark. In the result the reflected beams on the photodetection matrix generate three pointed images of the apertures of reflectors 3, 4, 5 as secondary small-size emitters —Fig. 2. Images of reflectors 3′, 4′, 5′ are marked by a solid line.

Microprocessor system is used for calculation of coordinates x_i, y_i ($i = 3 \ldots 5$) of three images and then using known base distances l_1, l_2 and focal distance f of lens 1 the linear and angular coordinates determining position of the robot with automatic collimating sensor relative to the sight target with an error of up to 0.1 … 0.5 mm [3].

At the stage of performance of a special mobile operation transport robot is positioned at the distance $L < L_{fr}$ and in the result the sight target is positioned in the near zone of the beam collimator. In this case the reflectors are located in the area of elementary parallel beams formed by all points of the emitting mark 1. In the result the reflected beams form images of emitting mark on the photodetection

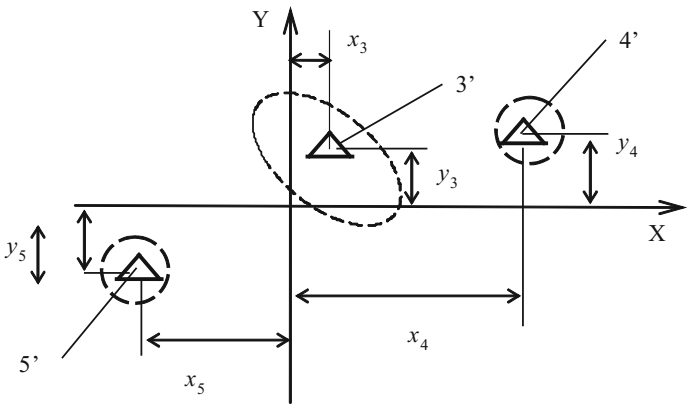

Fig. 2 Images of reflectors 3′, 4′, 5′ on matrix photodetector: *solid lines* show location of the sight line in the far zone, *dashed lines* show location in the near zone

matrix and the shape of these images is determined by the reflection of the beams inside the reflector. Images of mark 3′, 4′, 5′ on Fig. 2 of reflectors are shown by dashed line.

One of corner reflectors, for example reflector 3 features minor deviation from the nominal cubic shape. The shape of the tag image that it forms depends on the position of the automatic collimating sensor relative to the axis of reflector 3. The microprocessor system is used to calculate parameters of shapes of the image 3′ and then known optical parameters of reflector 3 are used to determine the position of the robot with automatic collimating sensor relative to sight target with high precision (up to seconds of arc).

4 Analysis of Performance of the Reflector with Deviation of Angles Between Reflecting Edges from 90°

Reflector for high-precision positioning should support retroreflection of the light beam and form an image with parameters that determine the angular position of the reflector relative to the beam collimator.

Assume that autocollimator 1 is linked with conditionally fixed coordinate system of axes OXYZ, reflector 2 is linked with coordinate system $O_1X_1Y_1\ Z_1$ (Fig. 3). It is necessary to synthesize reflector that allows to measure angles of rotation Θ_1, Θ_2 of reflector 2 with system $O_1X_1Y_1\ Z_1$ relative to axes OX, OY.

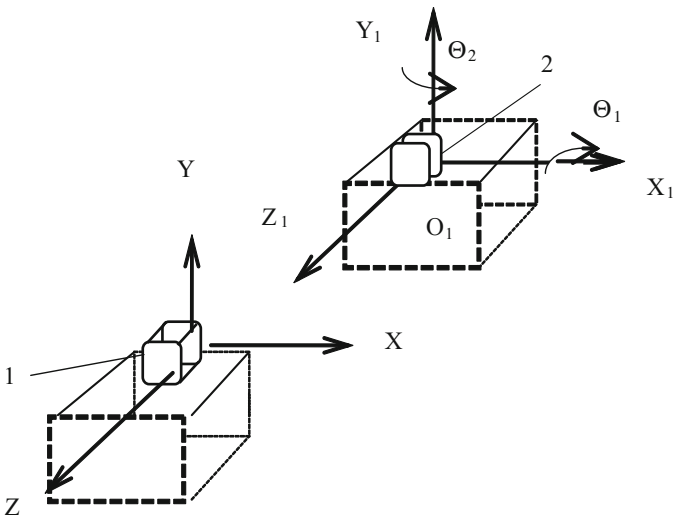

Fig. 3 Coordinate systems

Let us analyze properties of reflector using common equation for unit axis **B** of reflected elementary beam [4]:

$$\mathbf{B} = \mathrm{M_r} \cdot \mathrm{M_d} \cdot \mathrm{M_r^{-1}} \cdot \mathbf{A}, \tag{4}$$

where A is unit vector of incident beam, $\mathrm{M_d}$ is a reflection matrix of the reflector, $\mathrm{M_r}$ and $\mathrm{M_r^{-1}}$ are matrices of the direct and reverse conversions of the coordinates corresponding to respective turn of the reflector [5].

Matrix $\mathrm{M_d}$ of reflector with retro-reflection property is expressed by equation [5]:

$$\mathrm{M_d} = \cos(\mathrm{w}) \cdot \mathrm{E} - (1 + \cos(\mathrm{w})) \cdot \mathrm{m_u} + \sin(\mathrm{w}) \cdot \mathrm{M_u} \tag{5}$$

where E is a single matrix; components $\mathrm{M_u}$ and $\mathrm{m_u}$, are matrices with elements determined by coordinates $\mathrm{u_1}$, $\mathrm{u_2}$, $\mathrm{u_3}$ of unit vector **u** of invariant axis of reflector, ω is an angle of rotation of unit vector of beam in case of reflection around invariant axis:

Let edge 3 of reflector is formed as a part of conical surface, edges 1 and 2 are planes with angle between them equal to 90°.

$$M_u = \begin{bmatrix} 0 & -u_3 & u_2 \\ u_3 & 0 & -u_1 \\ -u_2 & u_1 & 0 \end{bmatrix} \tag{6}$$

$$m_u = \begin{bmatrix} u_1^2 & u_2 \cdot u_1 & u_1 \cdot u_3 \\ u_2 \cdot u_1 & u_2^2 & u_2 \cdot u_3 \\ u_1 \cdot u_3 & u_2 \cdot u_3 & u_3^2 \end{bmatrix} \tag{7}$$

Link auxiliary coordinate system $\mathrm{X_0Y_0Z_0}$ with the edges of the considered reflector—Fig. 4.

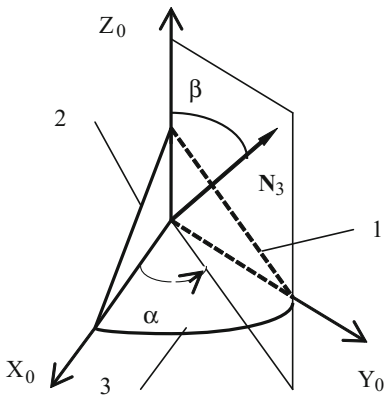

Fig. 4 Structure of reflector

Unit vector of normal to conical edge is described by common expression:

$$N_3 = (\sin(\beta) \cdot \cos(\alpha) \quad \sin(\beta)\cdot, \sin(\alpha) \quad \cos(\beta))^{\mathrm{T}} \tag{8}$$

Angle α ranges from 0 to 90°. This angle determines the position of the plane containing generatrix of surface. Angle β between axis OZ_0 and normal unit vector has a permanent vertex and is equal to the deflection of the angle at the vertex of the cone from the straight angle—Fig. 4.

Rotation angle ω of reflected beam and unit vector of invariant axis for various successive reflections from the edges is calculated as follows:

$$\omega = \pi + 2 \cdot \beta \tag{9}$$

$$u_{213\_123} = \left(\sin(\varepsilon) \quad -\tfrac{\sqrt{3}}{3} \cdot \cos(\varepsilon) \quad \tfrac{\sqrt{6}}{3} \cdot \cos(\varepsilon)\right)^{\mathrm{T}} \tag{10}$$

$$u_{132} = \left(\cos(\varepsilon) \quad -\tfrac{\sqrt{3}}{3} \cdot \sin(\varepsilon) \quad \tfrac{\sqrt{6}}{3} \cdot \sin(\varepsilon)\right)^{\mathrm{T}} \tag{11}$$

where:

$$\varepsilon = (1/4)\pi + \alpha \tag{12}$$

Indices determine the succession of the reflection from edges 1, 2, 3.

The reflection matrices are determined by expressions (5)–(7) in case of insertion of ratios (9)–(11) with required attention to different position of axes $X_0Y_0Z_0$ and $X_1Y_1Z_1$.

Expression (4) is used to determine coordinates of the unit vector of reflected beam. The image generated by the beam can be approximated by an ellipse—Fig. 5, dotted line.

Coordinates of the points of the image are described by the equations:

$$X_0(\varepsilon, \beta) = -a(\beta) \cdot \cos(\varepsilon); \quad Y_0(\varepsilon, \beta) = -b(\beta)\sin(\varepsilon), \tag{13}$$

where:

$$a(\beta) = -\frac{\sqrt{3}}{3}\cdot, \sin(2\beta) \quad b(\beta) = \sin(2\beta) \tag{14}$$

In case of rotation of reflector by an angle Θ_1 relative to axis OX the size of the ellipse along axis OX and semi-axis a(β) will change proportionately to angle Θ_1; the size along axis OY and semi-axis b(β) do not change—Fig. 5, thin line:

$$a(\beta)_{\Theta 1} = K_{\Theta 1} \cdot a(\beta) \quad K_{\Theta 1} = \sin(\Theta_1) \cdot \sqrt{2} + \cos(\Theta_1) \tag{15}$$

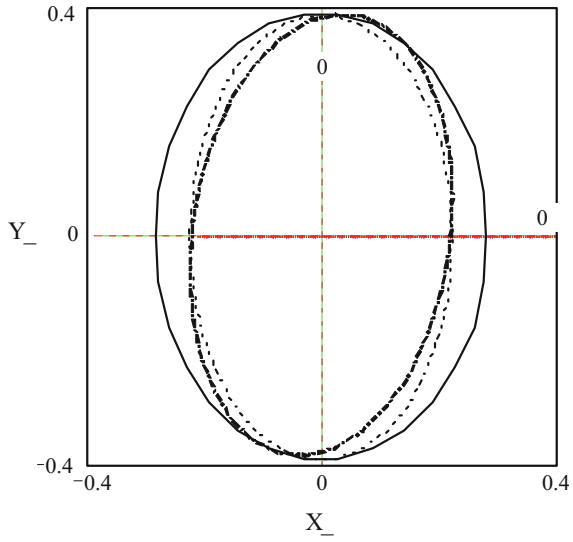

Fig. 5 Image generated by the reflector with conical edge

For the ranges of measured angles of around several degrees with an error of 1% it is possible to use an approximated expression:

$$a(\beta)_{\Theta 1} = \left(1 + \Theta_1 \cdot \sqrt{2}\right) \cdot a(\beta) \tag{16}$$

Large semi-axis b(ε) and orientation of the elliptical image do not change.

In case of rotation of the reflector by collimating angle of Θ_2 relative to axis OY_1 the image will turn relative to center O of angular field of receiving system by an angle Ξ—Fig. 5, bold dashed line:

$$\Xi(\Theta_2) = -\left(\frac{1}{2}\right) arctg\left(2\sqrt{2} \cdot \frac{\sin(\Theta_2)}{1 + (\cos(\Theta_2))^2}\right) \tag{17}$$

Large semi-axis b(ε) of the ellipse does not change; small semi-axis a(β) of ellipse will slightly change the value:

$$a(\beta)_{\Theta 2} = a(\beta) \cdot \cos(\Theta_2) \tag{18}$$

With low angles Θ_2 with an error of not more than 1% it is possible to use an approximate expression:

$$\Xi(\Theta_2) = -\left(\frac{\sqrt{2}}{2}\right) \cdot \Theta_2 \tag{19}$$

Algorithm of measurement of angles in case of usage of reflector includes the following stages.

1. The coordinates of the points of the recorded fragment of the image are measured.
2. The parameters of the ellipse corresponding to them are determined.
3. The measured angles are calculated based on the obtained values of the axes of the ellipse and their rotation angle using expressions (15)–(19).

Computer modeling of functioning of reflector with conical edge showed that with focal distance of lenses of receiving channel of video sensor $f \geq 300$ mm and reflector cone angle $\beta = 2°$ the error of computing of the angular position of the mobile robot does not exceed 15 arc sec over a range of 4°.

5 Conclusion

Autocollimating video sensor using a sight target compose of three reflectors designed as glass tetrahedrons with angles of 90° between reflecting edges allows for generation of SEMS control signals for steering the mobile robot and its operating arm in all motion modes: movement between target objects, approaching to the stop point, steering during performance of operations.

If the reflecting edge of one of reflectors of the sight target is designed as a conical surface its retro-reflection property is preserved and this reflector also generates a beam of elliptical shape. Processing of the image of this beam allows for high precision positioning of the mobile SEMS platform of a mobile robot.

Computer modeling of operation of the reflector of video sensor confirmed the correctness of theoretical assumptions.

Acknowledgements This work was financially supported by Government of Russian Federation, Grant 074-U01.

References

1. Konyakhin, I., Molev, F., Ezhova, K.: Determination of parameters and research autoreflection scheme to measurement errors relative position of the optical elements of the space telescope. In: Proceedings SPIE 9131, 91311 V (2014). doi:10.1117/12.2052127
2. Vanderwerf, D.F.: Applied prismatic and reflective optics, vol. 303. SPIE, Bellingham, Washington (2010)
3. Kaliteevskiy, I., Konyakhin, I.: Optoelectronic system for deformation measurement of radio-telescope counter-reflector computer modeling. Proc. SPIE **7133**, 71333X (2009). doi:10.1117/12.807666

4. Konyakhin, I., Van Phong, H., Artemenko, Y., Li, R., Smekhov, A.: Optic-electronic system for measuring the three-dimensional angular deformation of pipe sections at large constructions. In: Proceedings SPIE 9525, 952540 (2015). doi:10.1117/12.2184824
5. Korn, G.A., Korn, T.M.: Mathematical Handbook for Scientists and Engineers: Definitions, Theorems, and Formulas for Reference and Review, pp. 1152. Dover Publications, New York (2000)

Method of Constructing a System of Optical Sensors for Mutual Orientation of Industrial Robots for Monitoring of the Technosphere Objects

A.V. Petrochenko and I.A. Konyakhin

Abstract *Purpose* Developing of the methods of relative orientation of industrial robots and construction of three-dimensional scenes areas of interest using optical sensors. *Results* Developed the method of construction of the relative orientation of industrial robots to meet the challenges of reconstruction of three-dimensional mapping and image-set received from the optical sensors. The basis of this technique is the problem of finding the solution of the global position of each industrial robot on the relative orientation of each of them. The global position of the industrial robot characterized by a matrix of rotation and transfer vector in a coordinate system (adopted as a global). As a result of the global positioning possible to solve the major problems of vision such as detection, tracking and classification of objects of the space in which these systems and robots operate. *Practical significance* Continuous qualitative monitoring of technosphere objects.

Keywords Three-dimensional reconstruction · Optical sensor · Localization and building card system · Technical vision

1 Introduction

In connection with the development of robotics have become increasingly popular variety of three-dimensional reconstruction of the system mapping and image-set received from the optical sensors. The main objective of technical and robot vision is the detection, tracking and classification of objects of the space in which these systems and robots operate. Two-dimensional images sometimes don't contain sufficient information to address those or other problems: the construction of the map

A.V. Petrochenko · I.A. Konyakhin (✉)
ITMO University, Saint-Petersburg, Russia
e-mail: igor@grv.ifmo.ru

A.V. Petrochenko
e-mail: andrew.petrochenko@gmail.com

A.E. Gorodetskiy and V.G. Kurbanov (eds.), *Smart Electromechanical Systems: The Central Nervous System*, Studies in Systems, Decision and Control 95,
DOI 10.1007/978-3-319-53327-8_9

of the surrounding area for a route; object identification, tracking their relative position and movement; selection of objects and their attributes to complement the knowledge base. Three-dimensional reconstruction of the surrounding space allows you to obtain information on the relative positions of objects, their shape, surface texture. Systems, providing training on the basis of three-dimensional reconstruction of the results of the comparison can produce two-dimensional images of three-dimensional model that allows for the recognition of volume objects on flat images. The problem of the relative orientation of industrial robots with the ability to build three-dimensional scenes of controlled surfaces is becoming actual nowadays.

2 The Principle of the Interaction of the Optical Sensor Group of Mobile Robots

Let monitoring of the surface an object of the technosphere, for example, the mesh construction, is realized by group of the mobile robots, each of them is equipped by the smart electromechanical systems (SEMS). A special optical sensor is commonly used to generate the SEMS control signals for motion the robot tools.

The optical sensor has two optical-electronic blocks: the first is the target point in the form of point-emitting labels, the second is the measuring video system, which includes an object-glass and the matrix photodetector, located in its focal plane.

Optical sensors detect the relative position of each of the robot group in relation to other robots, next to it. At the same time the measuring video system of each robot in the local coordinate system by the method of reverse angular serifs determine the coordinates of the target points located on a nearby robot.

The concept interaction of optical sensors for mobile robot is shown in Fig. 1.

Depending on the amount and direction of sighting of sensors used to monitor a given node grid structure deformation changes the direction of further measurements neighboring node, and the maximum measurement error is minimized by averaging each channel found spatial positions of the same node structure.

Based on the above, consider the structure of the measuring sensor.

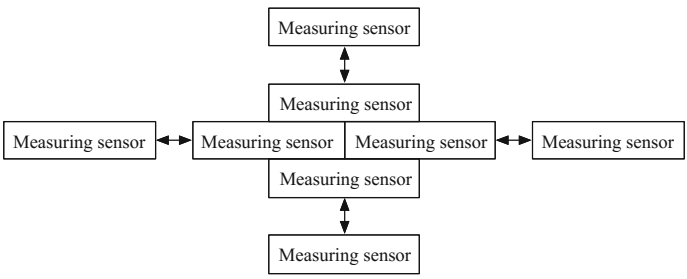

Fig. 1 The block diagram of the measuring system (*MS*—measuring system of the optical sensor emitting nating the target is not shown)

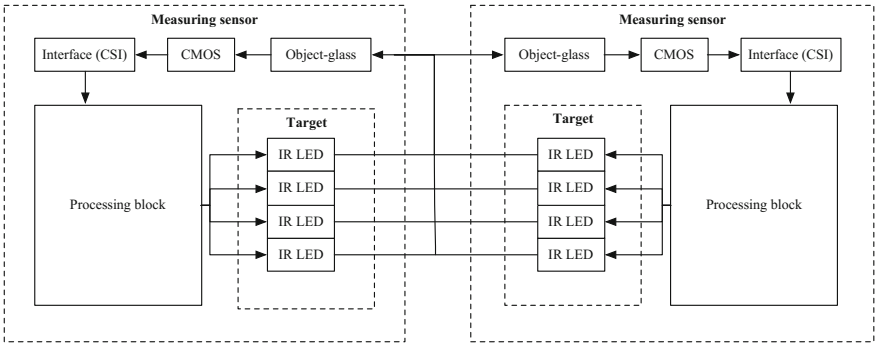

Fig. 2 Block diagram of the optical sensor

Assume that as a target sighting mark is a group made of four infrared emitting diode, then this basic scheme can be represented as show in Fig. 2.

The composition includes a sensor information processing unit that performs the following functions:

- capture images from a matrix receiver of optical radiation;
- image processing and calculation of local spatial position of the sensor;
- on/off control target reticle, which is part of the measuring sensor;
- the implementation of teams sharing the main robot control unit.

3 Methods of Determining the Spatial Position of the Measuring Sensor

Methods of determining the spatial position of the sensor is based on the projective transformation, is used as a model of the camera obscura (pinhole camera).

Fig. 3 Coordinate system of sensor

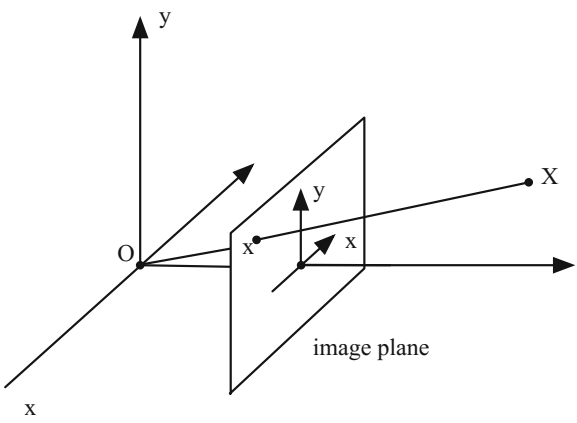

Let consider the sequence of steps that form this transformation between coordinate systems three-camera image-space.

1. Camera: perspective projection (Fig. 3)
   This type of transformation can be represented as:

$$\begin{bmatrix} x_c \\ y_c \\ f \end{bmatrix} = \lambda \begin{bmatrix} X_c \\ Y_c \\ Z_c \end{bmatrix} \tag{1}$$

   where $= \frac{Z_c}{f}$.
   This can be written as a linear mapping between homogeneous coordinates (the equation is only up to a scale factor):

$$\begin{bmatrix} x_c \\ y_c \\ f \end{bmatrix} = \begin{bmatrix} 1 & 0 & 0 & 0 \\ 0 & 1 & 0 & 0 \\ 0 & 0 & 1 & 0 \end{bmatrix} \begin{bmatrix} X_c \\ Y_c \\ Z_c \\ 1 \end{bmatrix} \tag{2}$$

   where 3×4 **projection matrix** represents a map from 3D to 2D.

2. **Image**: (intrinsic/internal camera parameters)

At this stage, the transformation of the local coordinate system of image (two-dimensional space), shown in Fig. 4.

This type of transformation can be represented as:

$$\begin{cases} k_u x_c = u - u_0 \\ k_v y_c = v_0 - v \end{cases} \tag{3}$$

where k_u, k_v—scale coefficients in pixels/length.

Combination of Eqs. (1) and (2) can be represented as:

$$x_i = \begin{bmatrix} u \\ v \\ 1 \end{bmatrix} = \begin{bmatrix} fk_u & 0 & u_0 \\ 0 & -fk_v & v_0 \\ 0 & 0 & 1 \end{bmatrix} \begin{bmatrix} x_c \\ y_c \\ f \end{bmatrix} = C \begin{bmatrix} x_c \\ y_c \\ f \end{bmatrix} \tag{4}$$

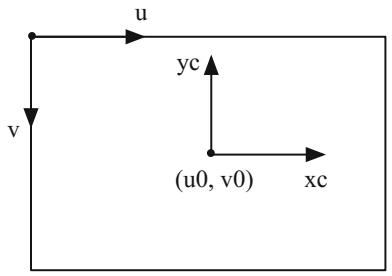

Fig. 4 Coordinate system of image

where C—is a 3 × 3 upper triangular matrix, called the **camera matrix**.

$$C = \begin{bmatrix} \alpha_u & 0 & u_0 \\ 0 & \alpha_v & v_0 \\ 0 & 0 & 1 \end{bmatrix} \tag{5}$$

where $\alpha_u = fk_u, \alpha_v = -fk_v$.

Matrix C provides the transformation between an image point and a ray in Euclidean 3-space.

The basic parameters of the camera calibration matrix:

1. The scaling in the image x and y directions—α_u и α_v.
2. The *principal point* (u_0, v_0), which is the point where the optic axis intersects the image plane.
3. The *aspect ratio* is α_v/α_u.

Once is known the camera is termed *calibrated*. A calibrated camera is a *direction sensor*, able to measure the direction of rays.

4. **World**: (extrinsic/external camera parameters)

The Euclidean transformation between the camera and world coordinates is Fig. 5.

$$X_c = RX_w + T \tag{6}$$

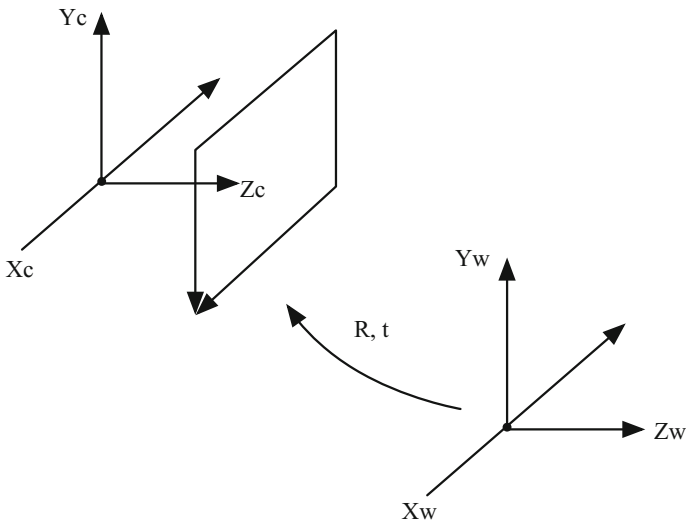

Fig. 5 Transformation of local coordinate system to global

$$\begin{bmatrix} X_c \\ Y_c \\ Z_c \\ 1 \end{bmatrix} = \begin{bmatrix} R & T \\ 0^T & 1 \end{bmatrix} \begin{bmatrix} X_w \\ Y_w \\ Z_w \\ 1 \end{bmatrix} \tag{7}$$

Finally, concatenating the three matrices:

$$x_i = \begin{bmatrix} u \\ v \\ 1 \end{bmatrix} = C \begin{bmatrix} 1 & 0 & 0 & 0 \\ 0 & 1 & 0 & 0 \\ 0 & 0 & 1 & 0 \end{bmatrix} \begin{bmatrix} R & T \\ 0^T & 1 \end{bmatrix} \begin{bmatrix} X_w \\ Y_w \\ Z_w \\ 1 \end{bmatrix} = C[R|T] \begin{bmatrix} X_w \\ Y_w \\ Z_w \\ 1 \end{bmatrix} \tag{8}$$

which defines the 3 × 4 projection matrix from Euclidean 3-space to an image:

$$x = P \begin{bmatrix} X \\ 1 \end{bmatrix}, \tag{9}$$

where $P = C[R|T]$—projection matrix.

4 Methods of Estimation Global Orientation of Sensors

Begin with a brief summary of the relevant concepts in Multiview geometry. A thorough treatment of this subject can be found in [1]. Let $I_1, I_2, \ldots, I_n$ denote a collection of images of a stationary scene, and let $t_i \in \mathbb{R}^3$ and $R_i \in SO(3)$ $(1 \le i \le n)$ respectively denote the focal points and orientations of the n cameras in some global coordinate frame. Let f_i denote the focal length of the ith camera. To produce the ith image a scene point $P = (X, Y, Z)^T$ is transformed to $P_i = R_i^T(P - t)$ and projected to $p_i = (x_i, y_i, f_i)$ in I_i with $p_i = (f_i/Z_i)P_i$, where Z_i is the depth coordinate of P_i.

For a pair of images I_i and $I_j (1 \le i, j \le n)$ define $R_{ij} = R_i^T R_j$ and $t_{ij} = R_i^T(t_j - t_i)$. It can readily be verified that $P_j = R_{ij}^T\left(P_i - t_{ij}\right)$. Therefore, R_{ij} and t_{ij} are rotation and translation that relate the coordinate frame of image j with that of image i. Clearly, $R_{ji} = R_{ij}^T$ and $t_{ji} = -R_{ij}^T t_{ij}$.

By a standard construction, the Essential Matrix E_{ij} is defined as $E_{ij} = [t_{ij}]_\times R_{ij}$, where $[t_{ij}]_\times$ denotes the skew-symmetric matrix corresponding to the cross product with t_{ij}. This construction ensures that for every point $P \in \mathbb{R}^3$ its projections onto I_i and I_j, denoted p_i and p_j, satisfy the epipolar constraints

$$p_i^T E_{ij} p_j = 0. \tag{10}$$

A proper Essential Matrix E_{ij} can be decomposed into a rotation R_{ij} and a translation t_{ij}. This provides two possible rotations and a scale (and sign) ambiguity for the translation, which are determined by the chirality constraint.

5 Estimating Camera Orientation

Our formulation is based on recent estimation methods shown in the context of 3D structure determination of macro-molecules in cryo-electron microscopy (EM) images [2, 3]. That work has assumed that pairwise rotations are known for every image pair. We focus on the SFM case where many of the pairwise rotations are missing. Our objective function is similar to that in [4], with our objective function allowing to additionally derive a tighter SDP relaxation.

Other works that take a global approach for recovery of camera rotation include using a reference plane (e.g. [5]) or quaternions [6, 7], which were shown in [4] to be inferior to Frobenius-based techniques. Hartley [8] uses a non-linear L1 minimization for rotation estimation.

We estimate camera orientation for a set of n images $I_1, I_2, \ldots, I_n$. Suppose we are given estimates of some of the $\binom{n}{2}$ Essential Matrices, $\widehat{E}_{ij}$. (Below we use the hat accent to denote measurements inferred from the input images.) We factorize each Essential Matrix and obtain a unique pairwise rotation denoted $\widehat{R}_{ij}$. We can further use [9] to detect motion degeneracies, in which case $\widehat{E}_{ij}$ is ignored. Our aim is to recover camera orientation in each of the n images, $R_1, R_2, \ldots, R_n$, based on the pairwise rotations $\widehat{R}_{ij}$.

Suppose all $\widehat{R}_{ij}$ are known. Then, following [4], we can cast this problem as an over-constrained optimization:

$$\min_{\{R_1,\ldots,R_n\}} \sum_{i,j=1}^{n} \left\| R_i^T R_j - \widehat{R}_{ij} \right\|_F^2 \tag{11}$$

where $\|\cdot\|_F^2$ denotes the Frobenius norm of a matrix. We further require each matrix $R_j (1 \leq i \leq n)$ to be a rotation, obtaining seven constraints for each of the rotations—six orthonormality constraints of the form $R_i^T R_i = E$ and one for the determinant (to distinguish it from reflections).

We solve the optimization problem using the following observation. Let G be a symmetric matrix constructed by concatenating the pairwise rotation matrices, namely,

$$G = \begin{bmatrix} I & R_{12} & \dots & R_{1n} \\ R_{21} & I & \dots & R_{2n} \\ \dots & & & \dots \\ R_{n1} & R_{n2} & \dots & I \end{bmatrix} \tag{12}$$

Let R be a matrix constructed by concatenating rotations relative to a universal coordinate system $R = [R_1 \quad R_2 \quad \dots \quad R_n]$. Then,

Claim 1 *G has rank 3 and its three eigenvectors of nonzero eigenvalues are given by the columns of R^T.*

Proof By definition $R_{ij} = R_i^T R_j$, and so $G = R^T R$ with rank 3. Since, and hence the three columns of R^T form the eigenvectors of G with the same eigenvalue, n.

Usually, in SFM problems some of the pairwise rotations are missing. We then modify G to contain zero blocks for the missing rotations. Let d_i denote the number of available rotations R_{ij} in the ith block row of G, and let D be the diagonal matrix constructed as

$$D = \begin{bmatrix} d_1 I & 0 & \dots & 0 \\ 0 & d_2 I & \dots & 0 \\ \dots & & & \dots \\ 0 & 0 & \dots & d_n I \end{bmatrix} \tag{13}$$

It can be readily verified that, and so the columns of R^T form three eigenvectors of $D^{-1}G$ with eigenvalue 1.

More generally, the construction of G and D can be modified to incorporate weights $(0 \le \omega_{ij} \le 1)$ that reflect our confidence in the available pairwise rotations R_{ij}.

In practice, however, the relative rotations $\widehat{R}_{ij}$ that are extracted from the estimated Essential Matrices may deviate from the ground truth underlying R_{ij}. This is both because of mismatched corresponding points and errors in their estimated location. Similarly to G, we define $\widehat{G}$ as the matrix containing the *observed* pairwise rotations $\widehat{R}_{ij}$.

Claim 2 *An approximate solution to* (2)*, under relaxed orthonormality and determinant constraints, is determined by the three leading eigenvectors of the matrix $\widehat{G}$.*

Details and a proof are provided in the appendix. Note that, in general, the noisy input reduces the spectral gap between the top three eigenvalues of $\widehat{G}$ and the rest of its eigenvalues.

To extract the rotation estimates, we denote by M the matrix containing the eigenvectors as in Claim 2. M comprises n submatrices of size 3×3, $M = [M_1 \quad M_2 \quad \dots \quad M_n]$.

Each M_i is an estimate for the rotation of the ith camera. Due to the relaxation, each M_i is not guaranteed to satisfy $M_i^T M_i = I$. Therefore, we find the nearest rotation (in the Frobenius norm sense) by applying the singular value decomposition and setting $\widehat{R}_i^T = U_i V_i^T$ [10]. We further enforce $\det\left(\widehat{R}_i^T\right) = 1$ by negating if needed. Note that this solution is determined up to a global rotation, corresponding to a change in orientation of the global coordinate system.

6 Estimating Camera Location

Once camera orientations $\widehat{R}_1, \ldots, \widehat{R}_n$ are recovered we turn to recovering the camera location parameters, $t_1, \ldots, t_n$. We do this using an efficient linear approach.

Previous approaches for estimating camera locations typically exploit the pairwise translations derived from the Essential Matrices (1) to construct a system of equations in the unknown translation parameters, and often also in the un- known depth coordinates. Such methods commonly involve a large excessive number of unknowns either involving 3D point positions for all feature points or additional pairwise scaling factors. Solving such systems can be computationally demanding and sensitive to errors.

For example, Govindu [7] uses the pairwise translations t_{ij} to estimate the camera location using $t_{ij} = \gamma_{ij} R_i^T (t_i - t_j)$ where γ_{ij} are unknown scale factors separate for each pair of images. He then shows that eliminating these scaling factors lead to unstable results, and so he estimates them us- ing an iterative reweighting approach. Crandall et al. [11] uses an MRF to solve simultaneously for camera locations and structure, but relies on prior geotag locations and assumes 2D translations. Kahl and Hartley [12] and subsequently also [4, 6] define a nonlinear, quasiconvex system of equations in the translations and point locations and use SOCP to solve the system under the l1 norm. Rother [5] proposes a linear system for solving simultaneously for both camera and 3D point locations. This adds a large number of unknowns to the equations.

Below we propose an alternative approach to solving for the translation parameters. Our approach is based on a simple but effective change of coordinates, which leads to a linear system with a large number of linear equations—an equation for every pair of corresponding points—in a *minimal* number of unknowns, the sought translations $t_1, \ldots, t_n$.

Claim 4 *The Essential Matrix can be expressed in terms of the location and orientation of each camera:*

$$E_{ij} = R_i^T (T_i - T_j) R_j \tag{14}$$

where $1 \leq i, j \leq n$, *and* $T_i = [t_i]_\times$, $T_j = [t_j]_\times$. *This expression generalizes over the usual decomposition of the Essential Matrix; if we express the Essential Matrix in*

the coordinate frame of the ith image then $t_i = 0$ *and* $R_i = I$*, and we are left with* $E_{ij} = [t_{ij}]_\times R_{ij}$.

Proof We derive an expression for the Essential Matrix in terms of a global coordinate system. The construction is similar to the usual derivation of the Essential Matrix. Let P denote a point in $\mathbb{R}^3$. Let $P_i = R_i^T(P - t_i)$ and $p_i = (x_i, y_i, f_i)$ denote its projection onto the image $I_i (1 \leq i \leq n)$. For a pair of images I_i and I_j we eliminate P to obtain:

$$R_j P_j - R_i P_i = t_i - t_j \tag{15}$$

Taking the cross product with $t_i - t_j$ and the inner product with $R_i P_i$ we obtain

$$P_i^T R_i^T \left(\left(t_i - t_j \right) \times R_j P_j \right) = 0 \tag{16}$$

and, due to the homogeneity of this equation, we can replace the points with their projections

$$p_i^T R_i^T \left(\left(t_i - t_j \right) \times R_j p_j \right) = 0 \tag{17}$$

This defines the epipolar relations between I_i and I_j. Consequently,

$$E_{ij} = R_i^T (T_i - T_j) R_j \tag{18}$$

The advantage of this representation of the Essential matrix is that it includes only the location and orientation of each camera; pairwise information (R_{ij}, t_{ij}) is no longer required. Let $p_i^{(1)}, \ldots, p_i^{(M_{ij})}$ and $p_j^{(1)}, \ldots, p_j^{(M_{ij})}$ be M_{ij} corresponding image points from images I_i and I_j respectively. Then, the expression in (8) defines a homogenous epipolar line equation for every pair of corresponding points $p_i^{(m)}$ and $p_j^{(m)}$, $m = 1 \ldots M_{ij}$:

$$p_i^{(m)\,T} R_i^T \left(t_i - t_j \right) R_j p_j^{(m)} = 0 \tag{19}$$

This equation is linear in the translation parameters.

This epipolar equation system can further be written as follows. Note that the left hand side defines a triple product between the rotated points $R_i p_i^{(m)}$, $R_j p_j^{(m)}$ and the translation $t_i - t_j$. A triple product is invariant to permutation (up to a change of sign if the permutation is non-cyclic). Consequently, can be written as

$$\left(t_i - t_j \right)^T \left(R_i p_i^{(m)} \times R_j p_j^{(m)} \right) = 0 \tag{20}$$

Therefore, *every* point pair contributes a linear equation in six unknowns (three for t_i and three for t_j). As such, the location of each camera is linearly constrained

by each of its feature correspondences. Weighting $\omega_{ij}^{(m)}$ can be easily incorporated to reflect the certainty of each such equation.

Clearly, $t_i = (1, 0, 0)$, $t_i = (0, 1, 0)$ and $t_i = (0, 0, 1)$ for all (1,0,0) i, are three trivial solutions of this linear system. Therefore, the sought solution is the optimal solution orthogonal to this trivial subspace. This allows recovering the camera locations up to a global translation and a single global scaling factor; these are inherent to the problem and cannot be resolved without external measurements. Unlike alternative linear methods [5, 7], our linear system is compact: the only unknowns are the camera locations. Thus, employing linear methods for its solution allows for an extremely efficient implementation. Moreover, despite the obvious drawbacks of using an L2 approach, its highly over-constrained formulation plays a main role in promoting its robustness, as is demonstrated in our experiments. Further robustness can be achieved, e.g., by minimizing the L1 norm, e.g., by applying iterative reweighted least squares.

7 Conclusion

In the process of research, we have developed a mathematical model of the interaction of the optical sensor group of mobile robots deformation nonlinear surface mesh type and confirmed the possibility of practical implementation of the system.

On the basis of a mathematical model was developed an algorithm for determining nonlinear distortion of the surface by using a global method for calculating the spatial position of the intermediate points of the surface of the parameters group mutual arrangement of robots.

The data obtained in the course of the experiment showed that the developed algorithm can be applied in high-speed optical sensors of mobile robots.

Acknowledgements This work was financially supported by Government of Russian Federation, Grant 074-U01.

References

1. Hartley, R.I., Zisserman, A.: Multiple View Geometry in Computer Vision. Cambridge University Press (2000)
2. Singer, A.: Angular synchronization by eigenvectors and semidefinite programming. Appl. Comput. Harmonic Anal. **30**(1), 20–36 (2011)
3. Singer, A., Shkolnisky, Y.: Three-dimensional structure determination from common lines in cryo-em by eigenvectors and semidefinite programming. SIAM J. Imaging Sci. **4**(2), 543–572 (2011)
4. Martinec, D., Padjla, T.: Robust rotation and translation estimation in multiview reconstruction. In CVPR (2007)

5. Rother, C.: Linear multi-view reconstruction of points, lines, planes and cameras using a reference plane. ICCV (2003)
6. Enqvist, O., Kahl, F., Olsson, C.: Non-sequential structure from motion. OMNIVIS (2011)
7. Govindu, V.: Combining two-view constraints for motion estimation. CVPR (2001)
8. Hartley, R., Aftab, K., Trumpf, J.: L1 rotation averaging using the weiszfeld algorithm. CVPR (2011)
9. Torr, P., Zisserman, A., Maybank, S.: Robust detection of degenerate configurations while estimating the fundamental matrix. Comput. Vis. Image Underst. **71**(3), 312–333 (1998)
10. Fan, K., Hoffman, A.J.: Some metric inequalities in the space of matrices. Proc. Am. Math. Soc. **6**(1), 111–116 (1955)
11. Crandall, D., Owens, A., Snavely, N., Huttenlocher, D.P.: Discrete-continuous optimization for large-scale structure from motion. CVPR (2011)
12. Kahl, F., Hartley, R.I.: Multiple-view geometry under the l_1-norm. PAMI **30**, 1603–1617 (2008)
13. Longuet-Higgins, H.C.: A computer algorithm for reconstructing a scene from two projections. Nature **293**(2) (1981)

Part IV
Working Bodies

Adaptive Capture

I.L. Tarasova, Vugar G. Kurbanov and Andrey E. Gorodetskiy

Abstract *Purpose* when solving modern problems of robotics, designing of tiny adaptive captures is becoming urgent for the medical micro robots equipped by controlled tiny and energy-efficient propellers imitating human hands. The purpose of this work is to develop new structure of the adaptive capture adjusting to the taken object by means of changing the form and rigidity of fingers. *Results* a new type of the tiny adaptive capture imitating work of hands and allowing to adapt to the environment by means of control over rigidity and shape of phalanxes of fingers is suggested in the article. The algorithm of work of its system of automatic control is also suggested. *Practical importance* the suggested adaptive capture with the controlled rigidity and form is supplied with the corresponding system of automatic control and can be used in micro robots of different function. The offered algorithms of work of system of automatic control of the developed captures with the controlled form and rigidity can be easily modified to capture objects of various shapes and forms.

Keywords Adaptive capture · Biological systems · A hand · Fingers · Phalanxes · Tiny propeller · System of automatic control · Computer modeling · Control over rigidity and form

I.L. Tarasova (✉) · V.G. Kurbanov · A.E. Gorodetskiy
Institute of Problems of Mechanical Engineering, Russian Academy of Sciences, Moscow, Russia
e-mail: g17265@yandex.ru

V.G. Kurbanov
e-mail: vugar_borchali@yahoo.com

A.E. Gorodetskiy
e-mail: g27764@yandex.ru

A.E. Gorodetskiy and V.G. Kurbanov (eds.), *Smart Electromechanical Systems: The Central Nervous System*, Studies in Systems, Decision and Control 95,
DOI 10.1007/978-3-319-53327-8_10

1 Introduction

In recent years, robots that imitate the complexity and adaptability of biological systems become one of the main objectives in the field of robotics research [1, 2]. This applies particularly to medical micro-robots that can move through the blood vessels [3]. Obviously, it is expedient to provide such micro-robots of capture for manipulating in the working environment, for example for the removal of plaque in blood vessels. The effective functioning of such captures depends essentially on the ability to adapt to capture subjects. At the same time one of the most complex and difficult to solve the problems is to provide a controlled miniature and energy-efficient mechanisms for capturing and adaptation. In solving this problem SEMS modules may be used, simulating operation of animal and human muscle [4]. Adaptability of such captures may be carried out by controlling the shape ST5 SEMS module platforms [5], forming a phalanx gripping fingers, as well as by controlling the rigidity of special modules hardness [6] placed between the gripping fingers phalanges.

2 Structure of Adaptive Capture

Known finger gripping robot [7], which comprises a plurality of phalanges, each of which is driven by a controllable electric drive. The finger has a touch sensor, which are incorporated in control system of the electric drive as feedback sensors. It uses two level sensors, provides information about the orientation of the grip parts (Fig. 1).

The disadvantage of this device is the low reliability of capturing the transported objects because of the inability to adapt form of the finger surface to the shape of the transported object.

It is also known adaptive three-fingered capture [8]. It comprises a control system and the housing mounted with its three fingers, arranged at the vertices of an isosceles or equilateral triangle (Fig. 2).

Each finger has three phalanges with actuators. The first phalanx rotates relative to the housing. The second and third phalanges are rotated relative to the first and second, respectively, through individual rotary actuators with parallel axes of rotation. And two fingers may be rotatable about an axis perpendicular to the installation plane and perpendicular fingers pivot axes of the phalanges. Each finger is rotatable relative to the housing by an angle of at least 90° by means of individual drive. The housing includes a rotary actuator that rotates the housing with fingers respect to the constructive housing component by means of which the gripping device is attached to the manipulator. As an individual drives used actuators with integrated torque Sensing. The contact surface of the phalanges are equipped with tactile sensors.

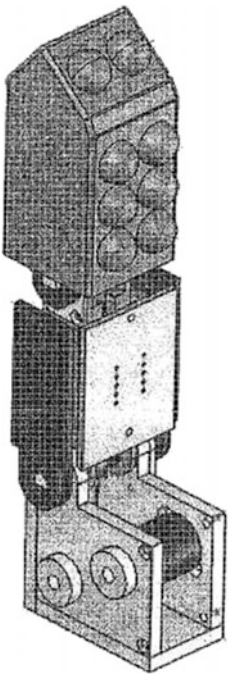

Fig. 1 View of the robot gripping finger

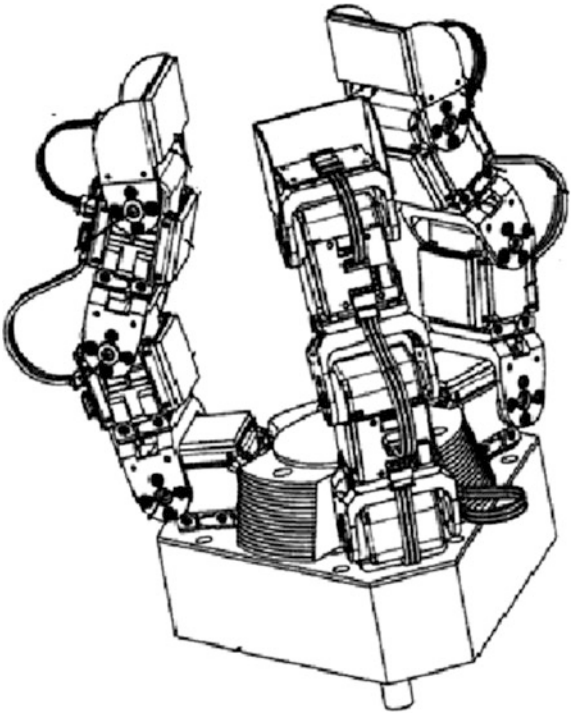

Fig. 2 Adaptive three-fingered capture

The main disadvantage of this device is its low reliability capture objects transported. This is due to the absence adaptation of the finger surface form to the shape of the transported object. This is due to the inability to change the size of the housing unit and the fingers. The latter also restricts the size of the captured object.

Improving the reliability of capture of transported objects and expand their range of sizes can be provided as follows. As discussed above capture comprises a control system and electromechanical system, comprising a housing (a palm) with the drives and installed fingers on it. Each finger consists phalanges with individual actuators, controllers and tactile sensors on the contact surfaces. But, unlike the previous capture palm and finger phalanges are designed as modules of the same type. These modules contain the lower and upper platforms, each of which consists of a base pad and at least three mounting pads. Each mounting pad is associated with neighboring telescopic rods and base pads—control rods containing actuators, gears, movement sensors and force sensors. Thus the tactile sensors are mounted on the outer surfaces of mounting pads.

The upper and lower platforms are linked by six legs-actuators. Its contain lower hinges that attach the mounting pads lower platform and upper hinges that attach the mounting pads of the upper platform. In addition, they contain linear actuators with reduction gears, displacement sensors and force sensors.

Driving these modules is shown in Fig. 3. Module comprises a lower 1 and an upper 2 platform, each of which comprises a support pad 3 and at least three mounting pads 4. The support pads 3 through the joints 5 are connected to the control rods 6 with drives and through the joints 8 with the mounting pads 4. This allows you to change the size and shape of the platforms 1 and 2. Lower 1 and upper one 2 platform are interconnected by six legs-actuators 9 with drives 10 through the bottom 11 and top 12 joints. Mounting pads 4 are bonded to adjacent telescopic rods 13. The drives 10 are equipped regulators, displacement sensors and force sensors (not shown here).

Fingers are arranged as follows (Fig. 4). By mounting pads 4 of the upper platform 2 modules third phalanges are attached mounting pad 4 of the lower platform 1 modules second phalanges. By mounting pads 4 of the upper platform 2 modules second phalanges are attached mounting pad 4 of the lower platform 1 module of the first phalanges. Number of finger and phalanges if necessary can be varied in a large and downwards. On the outer surfaces of the mounting pads 4 modules phalanges located tactile sensors 14.

Between the phalanges of fingers can be mounted units with controllable rigidity. Fixing finger to the palm can be of two types: independent (Fig. 5) and dependent (Fig. 6).

When mounting an independent phalanges (Fig. 5) on each mounting pad 4 of the upper platform 2 modules palm, fixed mounting pad 4 lower platform 1 modules third phalanges.

When a dependent attachment phalanges (Fig. 6) two mounting pad 4 lower platform 1 modules third phalanges, are fixed directly to the two mounting pads 4 of the upper platform 2 modules palm.

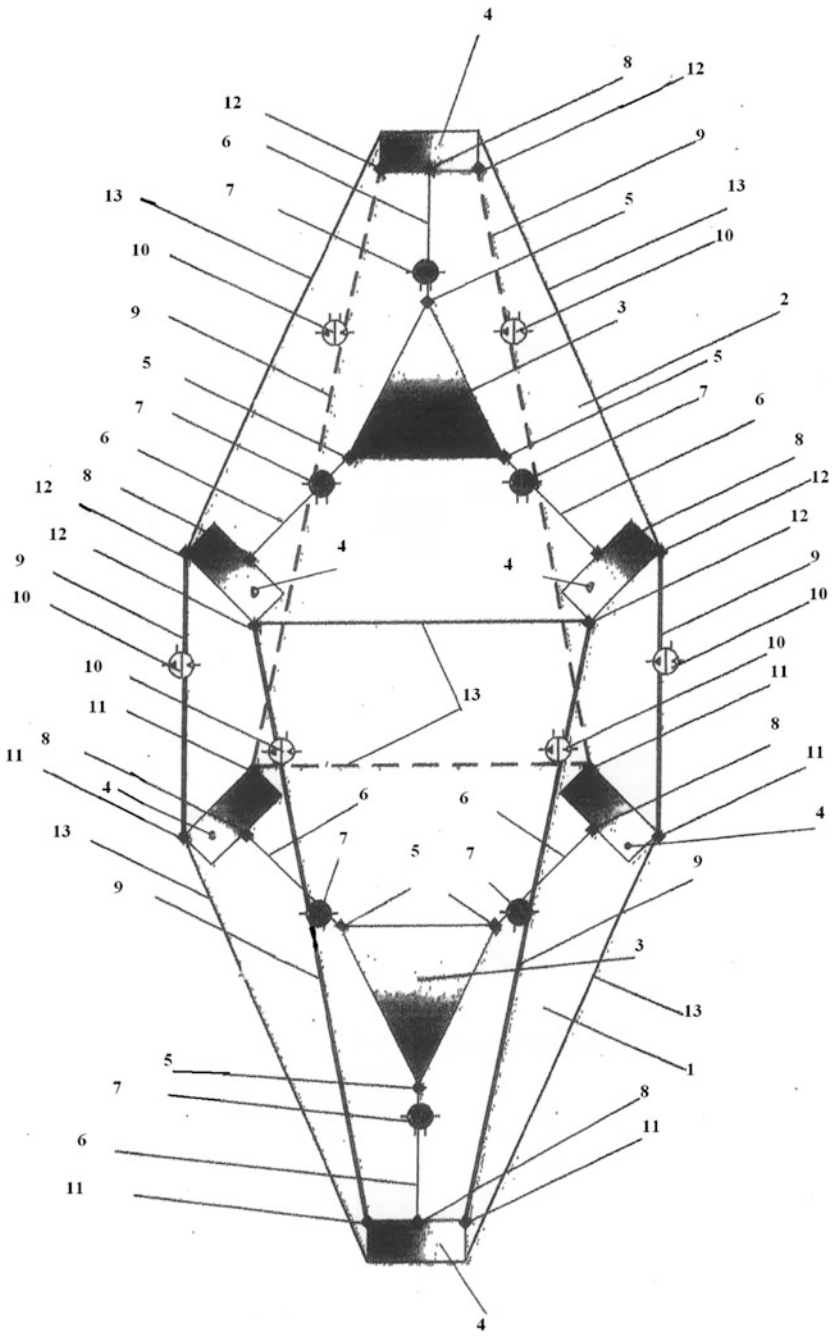

Fig. 3 View of the module palm and phalanges

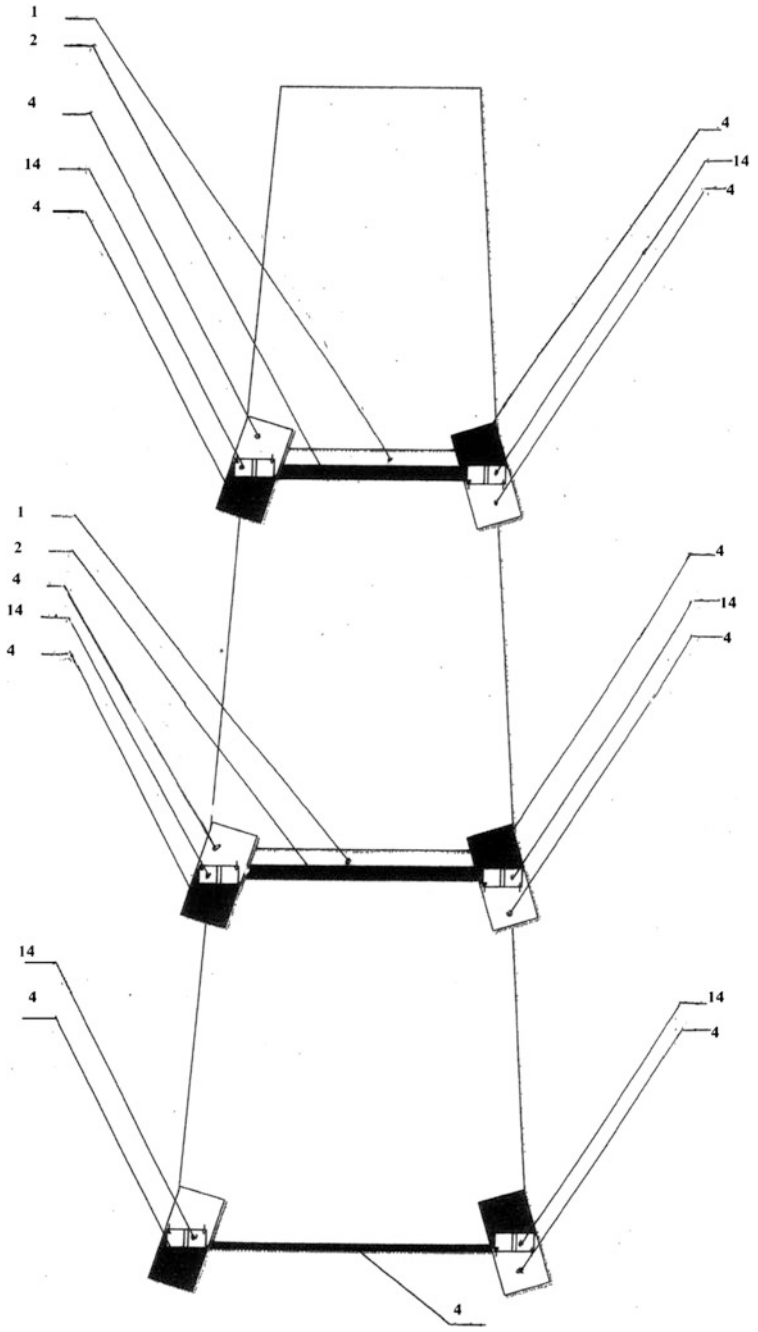

Fig. 4 General view of the finger

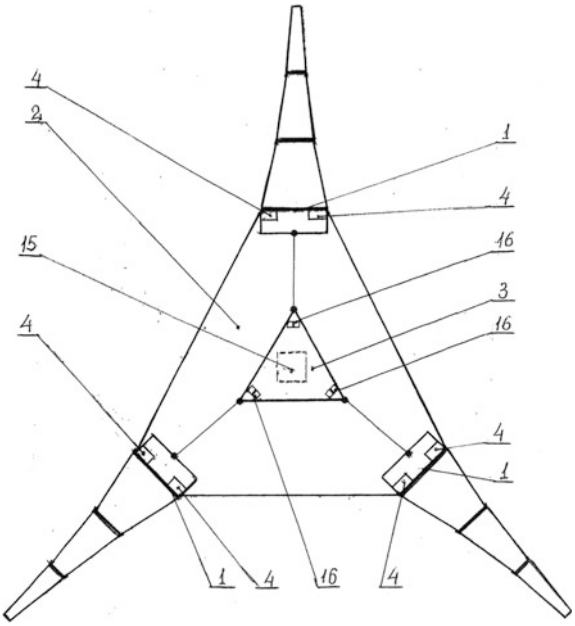

Fig. 5 General view of the capture of an independent fastening fingers

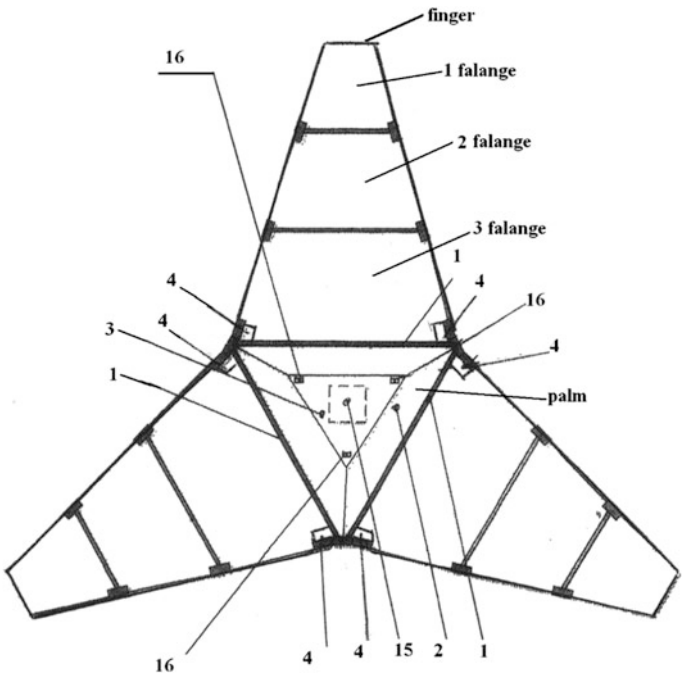

Fig. 6 General view of the capture of an independent fastening fingers

On the supporting pad 3 of the upper platform 2 module (Figs. 5 and 6) palm, located on the inner side control block 15, and the outer surface of the tactile sensors 16 are arranged.

The operation of such capture is as follows.

Control block 15 with the included in its composition vision system assesses the size and shape of the transport object. Then, on command from the control block 15

- with the help of the drive 7 rods 6 palm platform module 2 changes its size in accordance with the size of the transported object;
- with the help of the drive 10 legs-actuators 9 modules phalanges finger changes its length in accordance with the size of the transported object;
- with the help of the drive 7 rods 6 platforms 1 and 2 modules finger phalanges change its width and shape in accordance with the size and shape of the transported object.

Thus, capture adapts to the size and shape of the transported object.

Further on command from the control block 15 is made to capture the movement of the point of capture. Then, on command from the control block 15 with the help of the drives 10 of the legs-actuators 9-center platform 2 module palm with using correction signals from the tactile sensor 16 of this platform brought into contact with the transported object.

Finally, on command from the control block 15 with the help of the drives 10 legs-actuators 9 modules phalanges of the fingers last, using correction signals from the tactile sensors 14 platform 1 and module 2 phalanges are introduced into contact with the captured object.

Required gripping force develops drives a 10-foot-actuators 9 modules phalanges and drive 7 rods 6 of the platforms 1 and 2 modules phalanges. This is done by signals from the control block 15 and in accordance with the correction signals from the force sensors in the legs-actuators 9 and rods 6 platforms 1 and 2 modules phalanges. Thereafter, upon commands from the control block 15 can increase rigidity of the fingers with the help of the controlled rigidity blocks. Then transported object gets up and moves to the desired point of shipment.

Thus, objects made transportable in delivery point with a high efficiency of shipment.

3 Algorithms of the Automatic Control System

The control block 15 is automatic control system (ACS) of the considered adaptive capture. It is built as a multi-processor system architecture “tree” type [4].

Consider algorithms ACS of the adaptive capture, equipped with stepper motors for example movement of a convex object (the box).

Algorithm 1 ***Positioning the upper platform module palm***

1. Setting the upper platform module palm parallel to the top plane of the capture object (Fig. 7)

   1.1. Measurement of angles u_p and v_p between the upper palm module platform and the upper surface of the object relative to the axes X and Y, respectively.

   1.2. Calculating the changes of the legs lengths of the module palm corresponding to the measured angle u_p by formulas [9]:

$$\Delta L_i(x, y, z, u_p) = L_i(x, y, z, u_p) - L_i(0) \tag{1}$$

$$L_i(x, y, z, u_p) = \left(\left(r_{iu}^x(x, y, z, u_p) - r_{id}^x \right)^2 + \left(r_{iu}^y(x, y, z, u_p) - r_{id}^y \right)^2 + \left(r_{iu}^z(x, y, z, u_p) - r_{id}^z \right)^2 \right)^{1/2} \tag{2}$$

$$\mathbf{r_{iu}}(x, y, z, u_p) = \mathbf{C_{up}} \mathbf{r_{iu}}(0) \tag{3}$$

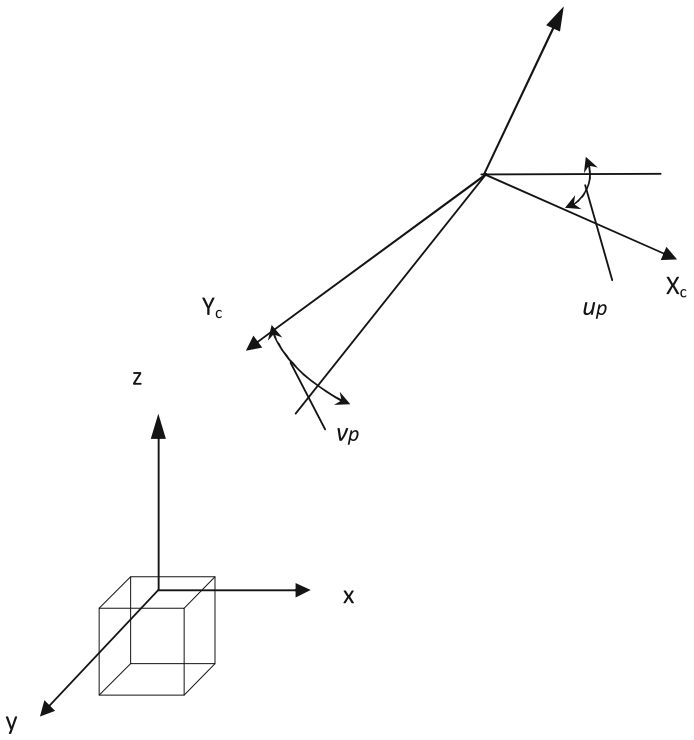

Fig. 7 Positioning the capture

$$C_{u_\pi} = \begin{vmatrix} 1 & 0 & 0 \\ 0 & \cos(u_p(t)) & -\sin(u_p(t)) \\ 0 & \sin(u_p(t)) & \cos(u_p(t)) \end{vmatrix} \quad (4)$$

where:

i	number of leg-actuator (LA);
r_{iu}	vector from point O to point iu (Fig. 8);
r_{id}	vector from point O_1 to point id (Fig. 8);
u	the upper platform;
d	the lower platform;
$r^x_{iu} r^x_{id}$; r^y_{iu}, r^y_{id}; r^z_{iu}, r^z_{id}	projection vectors on the axis X, Y, Z.

1.3. The calculation of the number of steps N_{Li} drive legs-actuator of the module palm corresponding calculated changes in length ΔL_i according to the formula:

$$N_{Li} = \Delta L_i / h_{Li} \quad (5)$$

where: h_{Li}—step drive of the i leg-actuator.

1.4. Feeding to drive of the legs-actuators of the module palm numbers pulses equal to the calculated step numbers.

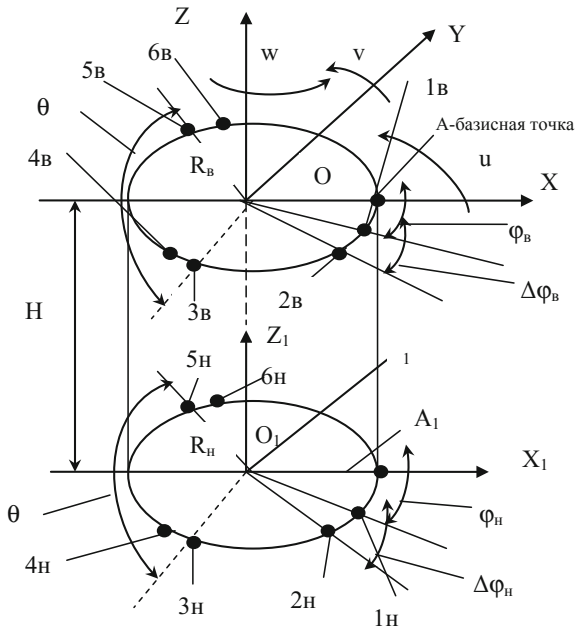

Fig. 8 Scheme of module SEMS

1.5. Calculating the changes of the legs lengths of the module palm corresponding to the measured angle v_p by the formulas (1), (2) and the following [9]:

$$\mathbf{r_{iu}}(x, y, z, u, v_p) = \mathbf{C_{vp}}(\mathbf{r_{iB}}(x, y, z, u_p)) \tag{6}$$

$$C_{v_p} = \begin{vmatrix} \cos(v_p(t)) & 0 & \sin(v_p(t)) \\ 0 & 1 & 0 \\ -\sin(v_p(t)) & 0 & \cos(v_p(t)) \end{vmatrix} \tag{7}$$

1.6. The calculation of the number of steps N_{Li} drive legs-actuator of the module palm corresponding calculated changes in length according to the formula (5).

1.7. Feeding to drive of the legs-actuators of the module palm numbers pulses equal to the calculated step numbers.

2. Installation of the fingers parallel to the upper platform palm module

2.1 Measuring angles u_{f1}, u_{f2}, u_{f3} and v_{f1}, v_{f2}, v_{f3} between the upper platform module palm and upper platforms of third phalanges fingers modules.

2.2 Calculation of changes in leg length modules third phalanges fingers ΔL_{if} by formulas such as (1)–(4) and (6), (7).

2.3 The calculation of the number of steps N_{Li} drive legs-actuator of the module third phalanges fingers corresponding calculated changes in length according to the formula (5).

2.4 Feeding to drive of the legs-actuators of the module third phalanges fingers numbers pulses equal to the calculated step numbers.

3. Move the platform on the axis X, Y and Z (Fig. 7).

3.1 Getting coordinates of the center of the upper the palm platform X_{pc}, Y_{pc}, Z_{pc} and the center of the object X_O, Y_O, Z_O, the size of the object L_X, L_Y, L_Z (the maximum size of the object), positioning steps h_X, h_Y, h_Z from the upper level system (measuring system), as well as the geometric parameters of possible obstacles and their coordinates.

3.2 Calculation of the required displacements l_X, l_Y, l_Z the upper platform the capture on the axes X, Y, Z:

3.2.1 If there are no obstructions between the capture and the capture object, the displacement computation according to the following equations:

$$\begin{cases} l_X = X_{pc} - X_0 - L_X/2 \\ l_Y = Y_{pc} - Y_0 - L_Y/2 \\ l_Z = Z_{pc} - Z_0 - L_Z/2 \end{cases} \tag{8}$$

3.2.2 If there are obstacles, the methods of mathematical programming calculation of the optimal trajectory moving to the capture point within the constraints. Then, an approximation of the trajectory Nth number of the linear sections. Then, for each section jth calculation movement Δl_{Xj}, Δl_{Yj}, Δl_{Zj} the corresponding calculation of the trajectory.

3.3 Formation of control actions:

3.3.1 If there are no obstacles between the capture and the capture an object, then the calculation of the number of steps capture drive on the coordinates on following equations:

$$\begin{cases} N_X = l_X/h_X \\ N_Y = l_Y/h_Y \\ N_Z = l_Z/h_Z \end{cases} \tag{9}$$

and feeding into drive: N_X pulses on the X axis, N_Y pulses on Y axis, N_Z pulses on Z axis.

(i) If there are obstacles, the

1. The calculation of the number of steps drives of the capture on the coordinates for the first part of the trajectory for j = 1:

$$\begin{cases} N_{Xj} = \Delta l_{Xj}/h_X \\ N_{Yj} = \Delta l_{Yj}/h_Y \\ N_{Zj} = \Delta l_{Zj}/h_Z \end{cases} \tag{10}$$

and feeding into drive N_{Xj} pulses on the X axis, N_{Yj} pulses on Y axis, N_{Zj} pulses on Z axis.

2. Calculating equations of type (10) the number of steps for the second section (j = 2) the trajectory and feed in the drives along the axes X, Y, Z corresponding number N_{Xj}, N_{Yj}, N_{Zj} pulses.
And so on until j = N.

4. Rotate the upper of the module platform palm about the Z axis

4.1 Measurement (calculation) of all the angles ak between the sides of the upper platform module palm and the upper surface of the object (Fig. 9).

4.2 Determination of the required angle of rotation of the upper platform module palm Z axis relative to the formula:

$$w_p = \min(\alpha_1, \alpha_2, \ldots, \alpha_k)$$

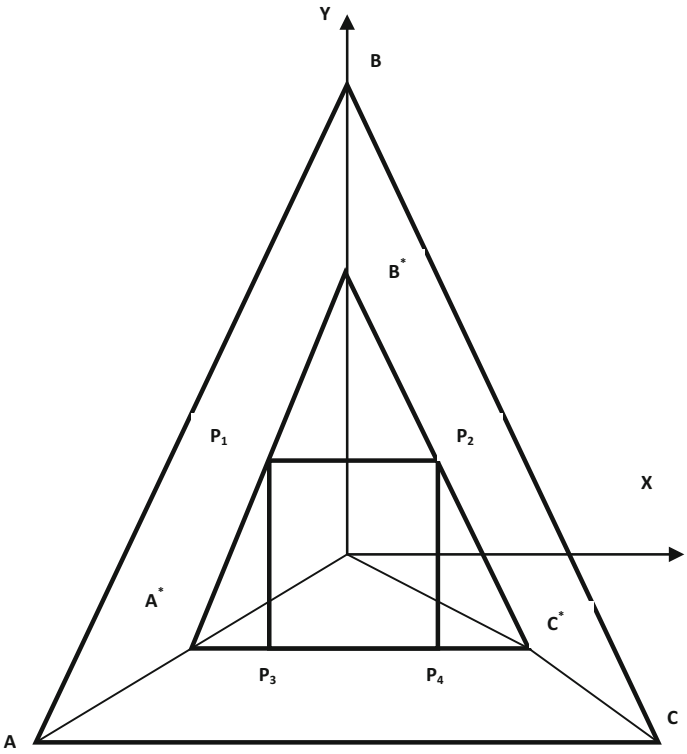

Fig. 9 Change the size of the palm of the capture

4.3 Computation changes legs lengths of the module palm corresponding obtained angle w_p by formulas (1), (2) and the following [9]:

$$\mathbf{r_{iu}}(x, y, z, u, v, w_p) = \mathbf{C_w}(\mathbf{r_{iu}}(x, y, z, u, v_p)) \tag{11}$$

$$C_{wp} = \begin{vmatrix} \cos(w_p(t)) & -\sin(w_p(t)) & 0 \\ \sin(w_p(t)) & \cos(w_p(t)) & 0 \\ 0 & 0 & 1 \end{vmatrix} \tag{12}$$

4.4 The calculation of the number of steps N_{Li} drive legs-actuator of the module palm corresponding calculated changes in length ΔL_i according to the formula (5).

4.5 Feeding to drive of the legs-actuators of the module palm numbers pulses equal to the calculated step numbers, providing palm position relative to the object, as shown in Fig. 9 (a triangle with vertices A, B, C).

End of the algorithm

Algorithm 2 ***Resizing palm the capture***

1. Measurement of the three coordinates of extreme points of the surface of the palm of A(x_A, y_A); B(x_B, y_B); C(x_C, y_C) (Fig. 9) and the four coordinates of extreme points of the object $P_1(a_2, b_2)$, $P_2(a_2, b_2)$, $P_3(a_3, b_3)$, $P_4(a_4, b_4)$.
2. The calculation of the required coordinates of the three extreme points of the surface of the palm of $A^*(x_A^*, y_A^*)$; $B^*(x_B^*, y_B^*)$; $C^*(x_C^*, y_C^*)$ (Fig. 9), provided that the upper platform palm module will be in the form of an equilateral triangle, one side of which is adjacent to one side of the upper surface of the object, the other two sides pass through the top of the rectangle the upper surface of the object, forms another sides, using the following equation:

$$x_{A^*} = \frac{a_3(b_4 - b_3) - b_3(a_4 - a_3) + \sqrt{3}(a_4 - a_3)(b_1 - \sqrt{3}a_1)}{(b_4 - b_3) - \sqrt{3}(a_4 - a_3)} \tag{13}$$

$$y_{A^*} = \frac{(b_4 - b_3)(b_1 - \sqrt{3}a_1) + \sqrt{3}[a_3(b_4 - b_3) - b_3(a_4 - a_3)]}{(b_4 - b_3) - \sqrt{3}(a_4 - a_3)} \tag{14}$$

$$x_{B^*} = \frac{(b_2 + \sqrt{3}a_2) - (b_1 - \sqrt{3}a_1)}{2\sqrt{3}} \tag{15}$$

$$y_{B^*} = \frac{(b_2 + \sqrt{3}a_2) + (b_1 - \sqrt{3}a_1)}{2} \tag{16}$$

$$x_{C^*} = \frac{(a_4 - a_3)(b_2 + \sqrt{3}a_2) + a_3(b_4 - b_3) - b_3(a_4 - a_3)}{(b_4 - b_3) + \sqrt{3}(a_4 - a_3)} \tag{17}$$

$$y_{C^*} = \frac{-\sqrt{3}\left[(a_4 - a_3)(b_2 + \sqrt{3}a_2) + a_3(b_4 - b_3) - b_3(a_4 - a_3)\right]}{(b_4 - b_3) + \sqrt{3}(a_4 - a_3)} + (b_2 + \sqrt{3}a_2) \tag{18}$$

3. The calculation of the required changes in the lengths of the control rod the upper palm platform module (Fig. 9):

$$\Delta R_A = \left[(x_A - x_{A^*})^2 + (y_A - y_{A^*})^2\right]^{\frac{1}{2}} \tag{19}$$

$$\Delta R_B = \left[(x_B - x_{B^*})^2 + (y_B - y_{B^*})^2\right]^{\frac{1}{2}} \tag{20}$$

$$\Delta R_C = \left[(x_C - x_{C^*})^2 + (y_C - y_{C^*})^2\right]^{\frac{1}{2}} \tag{21}$$

(Since the triangle palm is equilateral, then $\Delta R_A = \Delta R_B = \Delta R_C$).

4. The calculation of the number of steps N_R drive control rod corresponding calculated changes in length ΔR_B according to the formula (5).
5. The calculation of the required changes in the lengths ΔL_i of legs of the module palms (Fig. 3) according to the equations [9]:

$$\Delta L_i(\Delta R_u(t), \Delta R_d(t)) = L_i((\Delta R_u, \Delta R_d) - L_i(0)) \tag{22}$$

where:

$$\begin{aligned} L_i(\Delta R_B, \Delta R_H) = ((r^x_{iB}(\Delta R_B) - r^x_{iH}(\Delta R_H))^2 + (r^y_{iB}(\Delta R_B) - r^y_{iH}(\Delta R_H))^2 \\ + (r^z_{iB}(\Delta R_B) - r^z_{iH}(\Delta R_H))^2)^{1/2} \end{aligned} \tag{23}$$

$$\mathbf{r_{iu}}(\Delta R_u(t)) = /r^x_{iu}; r^y_{iu}; r^z_{iu}/^T + \mathbf{B_{iu}}(t) = /r^x_{iu}(\Delta R_u); r^y_{iu}(\Delta R_u); r^z_{iu}(\Delta R_u)/^T \tag{24}$$

$$\mathbf{r_{id}}(\Delta R_d(t)) = /r^x_{id}; r^y_{id}; r^z_{id}/^T + \mathbf{B_{id}}(t) = /r^x_{id}(\Delta R_d); r^y_{id}(\Delta R_d); r^z_{id}(\Delta R_d)/^T \tag{25}$$

$$\mathbf{B_{1u}}(t) = /\Delta R_u(t) \sin \varphi_u; \Delta R_u(t) \cos \varphi_u; 0/^T \tag{26}$$

$$\mathbf{B_{2u}}(t) = /\Delta R_u(t) \sin(\varphi_u + \Delta\varphi_u); \Delta R_u(t) \cos(\varphi_u + \Delta\varphi_u); 0/^T \tag{27}$$

$$\mathbf{B_{3B}}(t) = /\Delta R_B(t) \sin(\varphi_B + 30^\circ); \Delta R_B(t) \cos(\varphi_B + 30^\circ); 0/^T \tag{28}$$

$$\mathbf{B_{4u}}(t) = /\Delta R_u(t) \sin(\varphi_u + \Delta\varphi_u + 30^\circ); \Delta R_u(t) \cos(\varphi_u + \Delta\varphi_u + 30^\circ); 0/^T \tag{29}$$

$$\mathbf{B_{5u}}(t) = /\Delta R_u(t) \sin(\varphi_u + 60^\circ); \Delta R_u(t) \cos(\varphi_u + 60^\circ); 0/^T \tag{30}$$

$$\mathbf{B_{6u}}(t) = /\Delta R_u(t) \sin(\varphi_u + \Delta\varphi_u + 30^\circ); \Delta R_u(t) \cos(\varphi_u + \Delta\varphi_u + 30^\circ); 0/^T \tag{31}$$

$$\mathbf{B_{1d}}(t) = /\Delta R_d(t) \sin \varphi_d; \Delta R_d(t) \cos \varphi_d; 0/^T \tag{32}$$

$$\mathbf{B_{2d}}(t) = /\Delta R_d(t) \sin(\varphi_d + \Delta\varphi_d); \Delta R_d(t) \cos(\varphi_d + \Delta\varphi_d); 0/^T \tag{33}$$

$$\mathbf{B_{3d}}(t) = /\Delta R_d(t) \sin(\varphi_d + 30^\circ); \Delta R_d(t) \cos(\varphi_d + 30^\circ); 0/^T \tag{34}$$

$$\mathbf{B_{4d}}(t) = /\Delta R_d(t) \sin(\varphi_d + \Delta\varphi_d + 30^\circ); \Delta R_d(t) \cos(\varphi_d + \Delta\varphi_d + 30^\circ); 0/^T \tag{35}$$

$$\mathbf{B_{5d}}(t) = /\Delta R_d(t) \sin(\varphi_d + 60^\circ); \Delta R_d(t) \cos(\varphi_d + 60^\circ); 0/^T \tag{36}$$

$$\mathbf{B_{6d}}(t) = /\Delta R_d(t)\sin(\varphi_d + \Delta\varphi_d + 30^\circ); \Delta R_d(t)\cos(\varphi_d + \Delta\varphi_d + 30^\circ); 0/^T \tag{37}$$

$$\Delta R_d(t) = 0 \tag{38}$$

6. The calculation of the number of steps N_{Li} drive legs-actuator corresponding calculated changes in length ΔL_i according to the formula (5).
7. Feeding to the drives control rods number pulses of equal to the calculated in p4, the number of steps and at the same time in the drives legs-actuators number of pulses equal to the calculated in p.6 the number of steps.

End of the algorithm

Algorithm 3 ***Positioning phalanges***

1. Calculation of changes in the lengths legs $\Delta L_i^2(x, y, z, u_2)$ module of the third phalanx of the second finger for the angle $u_2 = 30^\circ$ (see Fig. 10) according to Eqs. (4)–(7).
2. The calculation of the number of steps N_{Li} drives legs-actuator of this module corresponding calculated changes in length ΔL_i^2 according to the formula (5).
3. Feeding to this drives numbers pulses equal to the calculated step numbers.

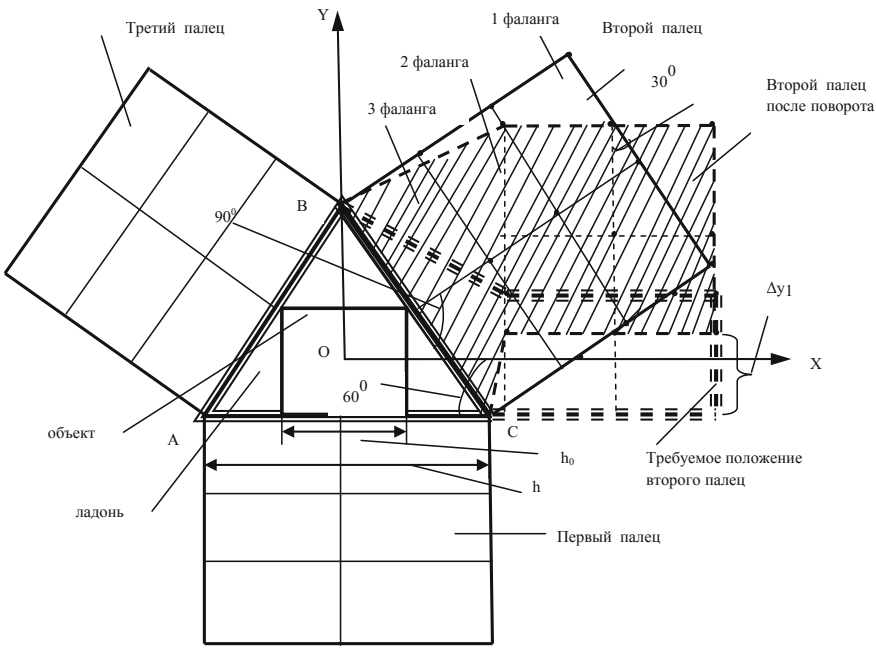

Fig. 10 Positioning of fingers

4. Calculation of changes in the lengths legs $\Delta L_i^3(x, y, z, u_3)$ module of the third phalanx of the third finger for the angle $u_3 = -30°$ (see Fig. 10) according to Eqs. (4)–(7).
5. The calculation of the number of steps N_{Li} drives legs-actuator of this module corresponding calculated changes in length ΔL_i^3 according to the formula (5).
6. Feeding to this drives numbers pulses equal to the calculated step numbers.

End of the algorithm

Algorithm 4 ***Changing the size and shape of the phalanges of the first finger***

1. The calculation of the change of the lengths ΔR of the control rod of the upper platform of the third phalanx as well as lower and upper platforms of the first and second phalanx (Fig. 11) according to the formula:

$$\Delta R = R - Rh/h_o \tag{39}$$

where: h_o and h—the width of the object and the original width of the finger, respectively, R—original length control rods.
2. The calculation of the number of steps N_{Ri} drives control rod corresponding calculated changes in length ΔR according to the formula (5).
3. Calculation of the displacement Δx of the upper platform of the third phalanx, and upper and lower platforms of the first and second phalanges of a finger (see Fig. 11) by the formula:

$$\Delta x = \Delta R x/R$$

where x—the starting coordinates of the center platform of the phalanges of the first finger.
4. Calculation of changes in length legs phalanges corresponding displacements calculated according to the formulas of the type (1), (2), as well as the following:

$$\mathbf{r_{iu}}(x(t), y(t), z(t), \Delta x_u, \Delta R_u) = \mathbf{r_{iu}}(0) + \Delta x_u + \mathbf{B_{iu}}(t) \tag{40}$$

$$\mathbf{r_{id}}(x(t), y(t), z(t), \Delta x_d, \Delta R_d) = \mathbf{r_{id}}(0) + \Delta x_d + \mathbf{B_{id}}(t) \tag{41}$$

where: B_{iu} (t) and B_{id} (t)—are calculated by equations of the type (26)–(37).
5. The calculation of the number of steps N_{Li} drives legs-actuator corresponding calculated changes in length according to the formula (5).
6. Feeding to the drives control rods number pulses of equal to the calculated in p2, the number of steps and at the same time in the drives legs-actuators number of pulses equal to the calculated in p.5 the number of steps.

End of the algorithm

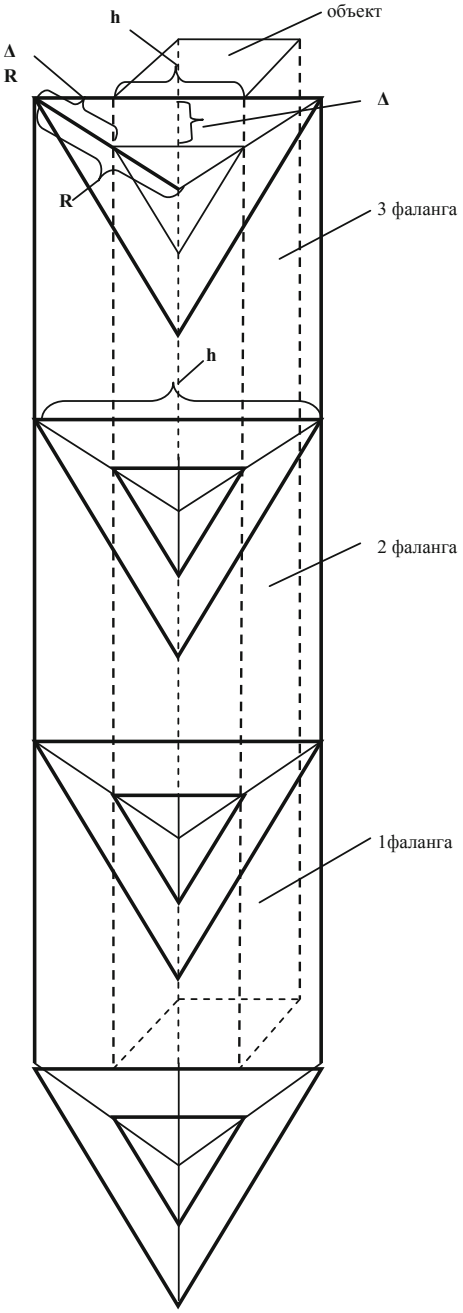

Fig. 11 Change the size and shape of the phalanges of the first finger

Algorithm 5 ***Changing the size and shape of the phalanges of the second and third finger***

1. The calculation of the change of the lengths ΔR of the control rod of the upper platform of the third phalanx as well as lower and upper platforms of the first and second phalanx (Fig. 10) according to the formula (39).
2. The calculation of the number of steps N_{Ri} drives control rod corresponding calculated changes in length ΔR according to the formula (5).
3. Calculation of the displacement Δy of the upper platform of the third phalanx, and upper and lower platforms of the first and second phalanges of a fingers (see Fig. 10) by the formula:

$$\Delta y = \Delta R y / R$$

   where: y—the starting coordinates of the center platform of the phalanges of the second and third fingers
4. Calculation of changes in length legs phalanges corresponding displacements calculated according to the formulas of the type (1), (2), as well as the following:

$$\mathbf{r_{iu}}(x(t), y(t), z(t), \Delta y_u, \Delta R_u) = \mathbf{r_{iu}}(0) + \Delta y_u + \mathbf{B_{iu}}(t) \quad (42)$$

$$\mathbf{r_{id}}(x(t), y(t), z(t), \Delta y_d, \Delta R_d) = \mathbf{r_{id}}(0) + \Delta y_d + \mathbf{B_{id}}(t) \quad (43)$$

   where: $B_{iu}(t)$ and $B_{id}(t)$—are calculated by equations of the type (26)–(37).
5. The calculation of the number of steps N_{Li} drives legs-actuator corresponding calculated changes in length according to the formula (5).
6. Feeding to the drives control rods number pulses of equal to the calculated in p2, the number of steps and at the same time in the drives legs-actuators number of pulses equal to the calculated in p.5 the number of steps.

End of the algorithm

Algorithm 6 ***Changing the length phalanges***

1. Measure the height H_o of the object.
2. Calculation of changes in length phalanges by the equation:

$$\Delta z = \Delta H = H_o/3 - H - h_z$$

3. Calculation of changes in leg length ΔLi modules phalanges using Eqs. (1), (2) and the following:

$$\mathbf{r_{iB}}(x(t), y(t), z(t), \Delta z) = \mathbf{r_{iB}}(0) + \Delta z$$

4. The calculation of the number of steps N_{Li} drives legs-actuator of the modules phalanges corresponding calculated changes in length according to the formula (5).

5. Feeding to the drives legs-actuators of the modules phalanges number of pulses equal to the calculated the number of steps.

End of the algorithm

Algorithm 7 ***Capture object***

1. Positioning of the phalanx of the first finger

1.1. The task for the first finger elementary angular displacement Δu phalanx.
1.2. Calculating changes in length of legs actuator ΔL_i^1 module of the third phalanx of the first finger on Eqs. (1)–(4).
1.3. The calculation of the number ΔN_i^1 of steps drive of leg actuator module of the third phalanx of Eq. (5).
1.4. Feeding in the drives legs-actuators of the third phalanx of the first finger the number of pulses equal to the calculated number of steps ΔN_i^1.
1.5. If the signal from the touch sensor of the third phalanx $\xi_{31} = 0$ (no connection), then the transition to n. 1.4 of this algorithm, until $\xi_{31} = 1$ (there is contact).
1.6. Feeding in the drives legs-actuators of the second phalanx of the first finger the number of pulses equal to the calculated number of steps ΔN_i^1.
1.7. If the signal from the touch sensor of the second phalanx $\xi_{21} = 0$ (no connection), then the transition to n. 1.6 of this algorithm, until $\xi_{21} = 1$ (there is contact).
1.8. Feeding in the drives legs-actuators of the first phalanx of the first finger the number of pulses equal to the calculated number of steps ΔN_i^1.
1.9. If the signal from the touch sensor of the first phalanx $\xi_{11} = 0$ (no connection), then the transition to n. 1.8 of this algorithm, until $\xi_{11} = 1$ (there is contact).

2. Positioning of the phalanx of the second finger

2.1. The task for the second finger elementary angular displacement Δv phalanx.
2.2. Calculating changes in length of legs actuator ΔL_i^2 module of the third phalanx of the second finger on Eqs. (1), (2), (6), (7).
2.3. The calculation of the number ΔN_i^2 of steps drive of leg actuator module of the third phalanx of Eq. (5).
2.4. Feeding in the drives legs-actuators of the third phalanx of the second finger the number of pulses equal to the calculated number of steps ΔN_i^2.
2.5. If the signal from the touch sensor of the third phalanx $\xi_{32} = 0$ (no connection), then the transition to n. 2.4 of this algorithm, until $\xi_{32} = 1$ (there is contact).
2.6. Feeding in the drives legs-actuators of the second phalanx of the second finger the number of pulses equal to the calculated number of steps ΔN_i^2.
2.7. If the signal from the touch sensor of the second phalanx $\xi_{22} = 0$ (no connection), then the transition to n. 2.6 of this algorithm, until $\xi_{22} = 1$ (there is contact).

2.8. Feeding in the drives legs-actuators of the first phalanx of the second finger the number of pulses equal to the calculated number of steps ΔN_i^2.
2.9. If the signal from the touch sensor of the first phalanx $\xi_{12} = 0$ (no connection), then the transition to n. 2.8 of this algorithm, until $\xi_{12} = 1$ (there is contact).

3. Positioning of the phalanx of the third finger

3.1. The task for the third finger elementary angular displacement—Δv phalanx.
3.2. Calculating changes in length of legs actuator ΔL_i^3 module of the third phalanx of the third finger on Eqs. (1), (2), (6), (7).
3.3. The calculation of the number ΔN_i^3 of steps drive of leg actuator module of the third phalanx of Eq. (5).
3.4. Feeding in the drives legs-actuators of the third phalanx of the third finger the number of pulses equal to the calculated number of steps ΔN_i^3.
3.5. If the signal from the touch sensor of the third phalanx $\xi_{33} = 0$ (no connection), then the transition to n. 3.4 of this algorithm, until $\xi_{33} = 1$ (there is contact).
3.6. Feeding in the drives legs-actuators of the second phalanx of the third finger the number of pulses equal to the calculated number of steps ΔN_i^3.
3.7. If the signal from the touch sensor of the second phalanx $\xi_{23} = 0$ (no connection), then the transition to n. 3.6 of this algorithm, until $\xi_{23} = 1$ (there is contact).
3.8. Feeding in the drives legs-actuators of the first phalanx of the third finger the number of pulses equal to the calculated number of steps ΔN_i^3.
3.9. If the signal from the touch sensor of the first phalanx $\xi_{13} = 0$ (no connection), then the transition to n. 3.8 of this algorithm, until $\xi_{13} = 1$ (there is contact).

End of the algorithm

Algorithm 8 ***Compression object***

1. Positioning of the first finger

1.1. The task for the first finger elementary angular displacement Δu phalanx
1.2. Calculating changes in length of legs actuator ΔL_i^1 module of the phalanx of the first finger on Eqs. (1)–(4).
1.3. The calculation of the number ΔN_i^1 of steps drive of leg actuator module of the phalanx of Eq. (5).
1.4. Feeding in the drives legs-actuators of the third phalanx of the first finger the number of pulses equal to the calculated number of steps ΔN_i^1.
1.5. If the signal from the force sensor of the third phalanx $\mu_{31} < f$ (f—a predetermined force), the transition to n. 1.4 of this algorithm until $\mu_{31} > f$.
1.6. Feeding in the drives legs-actuators of the second phalanx of the first finger the number of pulses equal to the calculated number of steps ΔN_i^1.
1.7. If the signal from the force sensor of the second phalanx $\mu_{21} < f$ (f—a predetermined force), the transition to n. 1.4 of this algorithm until $\mu_{31} > f$.

1.8. Feeding in the drives legs-actuators of the first phalanx of the first finger the number of pulses equal to the calculated number of steps ΔN_i^1.
1.9. If the signal from the force sensor of the first phalanx $\mu_{11} < f$ (f—a predetermined force), the transition to n. 1.4 of this algorithm until $\mu_{11} > f$.
1.10. Feeding to the modules with variable rigidity of the first finger given the strength of the current I.

2. Positioning of the second finger

2.1. The task for the second finger elementary angular displacement Δv phalanx.
2.2. Calculating changes in length of legs actuator ΔL_i^2 module of the phalanx of the second finger on Eqs. (1), (2), (6), (7).
2.3. The calculation of the number ΔN_i^2 of steps drive of leg actuator module of the phalanx of Eq. (5).
2.4. Feeding in the drives legs-actuators of the third phalanx of the second finger the number of pulses equal to the calculated number of steps ΔN_i^2.
2.5. If the signal from the force sensor of the third phalanx $\mu_{32} < f$ (f—a predetermined force), the transition to n. 2.4 of this algorithm until $\mu_{32} > f$.
2.6. Feeding in the drives legs-actuators of the second phalanx of the second finger the number of pulses equal to the calculated number of steps ΔN_i^2.
2.7. If the signal from the force sensor of the second phalanx $\mu_{22} < f$ (f—a predetermined force), the transition to n. 2.6 of this algorithm until $\mu_{22} > f$.
2.8. Feeding in the drives legs-actuators of the first phalanx of the second finger the number of pulses equal to the calculated number of steps ΔN_i^2.
2.9. If the signal from the force sensor of the first phalanx $\mu_{12} < f$ (f—a predetermined force), the transition to n. 2.8 of this algorithm until $\mu_{12} > f$.
2.10. Feeding to the modules with variable rigidity of the second finger given the strength of the current I.

3. Positioning of the third finger

3.1. The task for the third finger elementary angular displacement—Δv phalanx.
3.2. Calculating changes in length of legs actuator ΔL_i^3 module of the phalanx of the third finger on Eqs. (1), (2), (6), (7).
3.3. The calculation of the number ΔN_i^3 of steps drive of leg actuator module of the phalanx of Eq. (5).
3.4. Feeding in the drives legs-actuators of the third phalanx of the third finger the number of pulses equal to the calculated number of steps ΔN_i^3.
3.5. If the signal from the force sensor of the third phalanx $\mu_{33} < f$ (f—a predetermined force), the transition to n. 3.4 of this algorithm until $\mu_{33} > f$.
3.6. Feeding in the drives legs-actuators of the second phalanx of the third finger the number of pulses equal to the calculated number of steps ΔN_i^3.
3.7. If the signal from the force sensor of the second phalanx $\mu_{23} < f$ (f—a predetermined force), the transition to n. 3.6 of this algorithm until $\mu_{23} > f$.

3.8. Feeding in the drives legs-actuators of the first phalanx of the third finger the number of pulses equal to the calculated number of steps ΔN_i^3.
3.9. If the signal from the force sensor of the first phalanx $\mu_{13} < f$ (f—a predetermined force), the transition to n. 2.8 of this algorithm until $\mu_{13} > f$.
3.10. Feeding to the modules with variable rigidity of the third finger given the strength of the current I.

End of the algorithm

Algorithm 9 ***Moving object***

This algorithm is similar to n. 3 Move the platform on the axis X, Y and Z in Algorithm 1.

Algorithm 10 ***Releasing the object***

1. Reducing the current supplied to the modules with a controlled rigidity to the value I = 0.
2. Install the phalanges in parallel the palm similar to the n. 2 Installation of the fingers parallel to the upper platform palm module. **Algorithm** 1.

End of the algorithm

4 Conclusion

Analysis of the existing design solutions of captures for robots and manipulators that mimic the work of the hands revealed, their effectiveness can be significantly improved by providing the possibility of changing the size of the palm and fingers, and by adapting to the shape of the object captured. To do this, palm and phalanges is better to build on the basis of the structures of the standard module SM5 SEMS.

Automatic control system (ACS) for such captures built as much processor system with the architecture of the "tree". Control algorithm using stepper drives is reduced to the logic control. Rules-based selection sequence incorporating electric drives and calculating the number of steps each drive.

Acknowledgements The author would like to thank the Russian Foundation for Basic Researches (grants 14-07-00257, 15-07-04760, 15-07-02757, 16-29-04424, and 16-29-12901) for partial funding of this research.

References

1. Zhang, L., Abbott, J.J., Dong, L., Kratochvil, B.E., Bell, D., Nelson, B.J.: Artificial bacterial flagella: fabrication and magnetic control. Appl. Phys. Lett. **94**, 064107 (2009). doi:10.1063/1.3079655
2. Gradetsky, V., Solovtsov, V., Kniazkov, M., Rizzotto, G., Amato, P.: Modular design of electro-magnetic mechatronic microrobots. In: Proceedings of the 6-th International Conference CLAWAR 2003, pp. 651–658, Catania, Italy, 2003

3. Agapov, V.A. (RU), Gorodetskiy, A.E. (RU), Kuchmin, A.J. (RU), Selivanova, E.N. (RU): Medical microrobot. Patent RU, no. 2469752, 2011
4. Gorodetskiy, A.E.: Smart Electromechanical Systems, 277 p. Springer International Publishing (2016). doi:10.1007/978-3-319-27547-5
5. Gorodetskiy, A.E.: Smart Electromechanical Systems Modules. In: Gorodetskiy, A.E. (ed.) Smart Electromechanical Systems, 277 p. Springer International Publishing (2016). doi:10.1007/978-3-319-27547-5
6. Gorodetskiy, A.E., Kurbanov, V.G., Tarasov, I.L., Kuchmin, A.J.: Flagellate Propulsor (in this volume)
7. Torres-Jara, E.R.: Dexterous and compliant robotic finger. Patent US, no. 20120013139 A1, 2012
8. Modiagin, A.I. (RU), Priadko, A.I. (RU), Rogov, A.V. (RU), Ushakov, F.G. (RU): Adaptivnoe trekhpaloe zakhvatnoe ustroistvo (Adaptive three-fingered catching device). Patent RU no. 2481942 C2, 2013
9. Gorodetskiy, A.E., Kurbanov, V.G., Tarasova, I.L.: The direct problem of kinematics SM8 SEMS. In: Gorodetskiy, A.E. (ed.) Smart Electromechanical Systems, 277 p. Springer International Publishing (2016). doi:10.1007/978-3-319-27547-5

Controlled Ciliated Propulsion

I.L. Tarasova, Andrey E. Gorodetskiy and Vugar G. Kurbanov

Abstract *Purpose* when modern problems of robotics are being solved, the bionic approach where robots imitate complexity and adaptability of biological systems gains more ground nowadays. Particularly, it is urgent for the medical micro robots equipped by controlled tiny and energy-efficient propellers. The purpose of this article is to develop new structures of controlled propellers imitating muscle work of animals and people. *Results* new types of the tiny controlled propellers imitating operation of the ciliary apparatus of a human's eye and its intellectual systems of automatic control are suggested. With the use of computer modeling, it is shown that the suggested type of the propeller allows reaching the dynamic characteristics required for medical micro robots. *Practical importance* the suggested controlled ciliary propellers supplied with the corresponding systems of automatic control can be used in micro robots of different function. At the same time, they can adapt to the environment due to control over rigidity and forms of elements of the propeller.

Keywords Biological systems · Ciliary apparatus · Controlled propeller · System of automatic control · Control over rigidity and form · Adaptation

1 Introduction

In recent years, advances in robotics can be partly explained by the interaction with the biological sciences. Robots that mimic the complexity and adaptability of biological systems, becoming one of the main objectives in the field of robotics

I.L. Tarasova (✉) · A.E. Gorodetskiy · V.G. Kurbanov
Institute of Problems of Mechanical Engineering,
Russian Academy of Sciences, Moscow, Russia
e-mail: g17265@yandex.ru

A.E. Gorodetskiy
e-mail: g27764@yandex.ru

V.G. Kurbanov
e-mail: vugar_borchali@yahoo.com

A.E. Gorodetskiy and V.G. Kurbanov (eds.), *Smart Electromechanical Systems: The Central Nervous System*, Studies in Systems, Decision and Control 95,
DOI 10.1007/978-3-319-53327-8_11

research. Of particular note is the use of bionic approach when creating a medical robotic systems for various applications. An example of micro-robots can be designed to deliver drugs to the infected tissue [1, 2] or micro-robots able to move through the blood vessels [3].

When establishing such micro robots one of the most complex and difficult problem to be solved is to create for its controlled miniature and energy-efficient propulsion. To solve this problem is actual use of propulsion that mimic the work of human and animal muscles. In particular, its can imitate the work ciliary apparatus [4–6].

The effective functioning of these propulsion can be significantly improved by controlling the rigidity and the form of its elements.

2 Muscles

Muscles have strictly ordered structure. This provides a highly efficient energy conversion of adenosine triphosphate (ATP) into mechanical work. The nucleotide coenzyme ATP is the most important form of saving chemical energy in cells. The splitting of ATP—high ekzoergicheskaya reaction. The chemical energy of ATP hydrolysis can be used to interface with endoergic processes such as biosynthesis, traffic and transport.

Packaging contractile proteins in muscle comparable with packing of atoms and molecules in the crystal composition. Fusiform muscle consists of bundles of muscle fibers. The myofibrils of skeletal muscles is observed regular alternation of lighter and darker areas. So often skeletal muscle called striated transversely. Myofibril consists of identical repetitive elements, the so-called sarcomeres (see Fig. 1). Sarcomere is bounded on two sides Z-drives. These disks are attached to both sides of the thin actin filaments [7, 8].

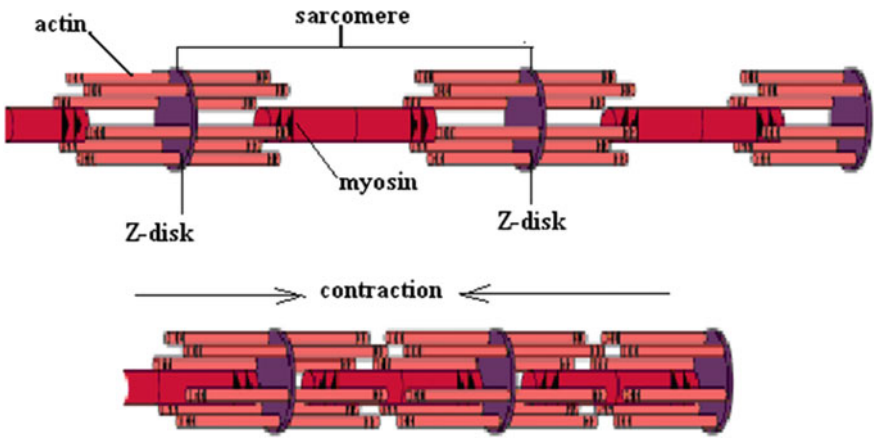

Fig. 1 Muscle structure

In the course of ATP hydrolysis is available myosin is able to interact with actin and actin filament begins to pull to the center of the sarcomere (see Fig. 1). As a result of this motion decreases the length of each sarcomere and all muscle, respectively. Importantly, at such system of generating motion does not change the length of the filaments (actin filaments and myosin filaments). Shortening is a consequence of a movement of the filaments relative to each other. The signal for the beginning of muscle contractions is to increase the concentration of Ca^{2+} in the cell. The calcium concentration in the cell is regulated by means of special calcium pumps. Its are embedded in the outer membrane and the membrane of the sarcoplasmic reticulum (Ca^{2+} storage), which twist around the myofibrils.

3 Ciliary Apparatus

Cilium is the outgrowth of cells covered the plasma membrane. Cilia thickness lies in the range 0.2–0.25 μm, length of 5–10 μm [4]. Under the membrane is axoneme consisting of 9 pairs of microtubules, which is a cylindrical formation. In the center of axoneme are two other microtubules, enclosed in a shell. Therefore, the cilia are the structural model: 9 + 2. The nine peripheral doublets are connected to a central tube by radial "spokes". At the base lies basal body (Fig. 2).

Energy supply mechano-chemical process in the microtubule is also carried out at the expense of ATP hydrolysis. Thus ATP activity exhibit globular head dynein [4].

The movement type of cilia, according to most researchers, can be described as a stroke or a rowing paddle movement, which consists of two phases—an effective and return. Cilia speed oscillations approximately 160–250 times per minute and significantly depends on the body temperature. Direct measurements and indirect calculations found that effective cilium movement is 3–6 times faster than the return [4, 5].

The effective phase of calcium ions that pass through the channels in the membrane cilia move to the negatively charged end of the microtubules, interact with dynein and participate in the hydrolysis of ATP. With further increase in the concentration of calcium, when involved all dynein handle then the flow of calcium into the end stops. Calcium concentration increases near the cell membrane and closes the calcium pump.

After that comes the return phase. It begins with the recovery of ATP with release of free calcium. It displayed across the cytoplasmic membrane into the priciliano liquid.

Selection of calcium through the plasma membrane makes to operate calcium pump of microtubules located opposite the microtubules involved in phase "stroke." Involved dynein handle returns cilium to its original position with less than the effective phase of the hydrodynamic resistance.

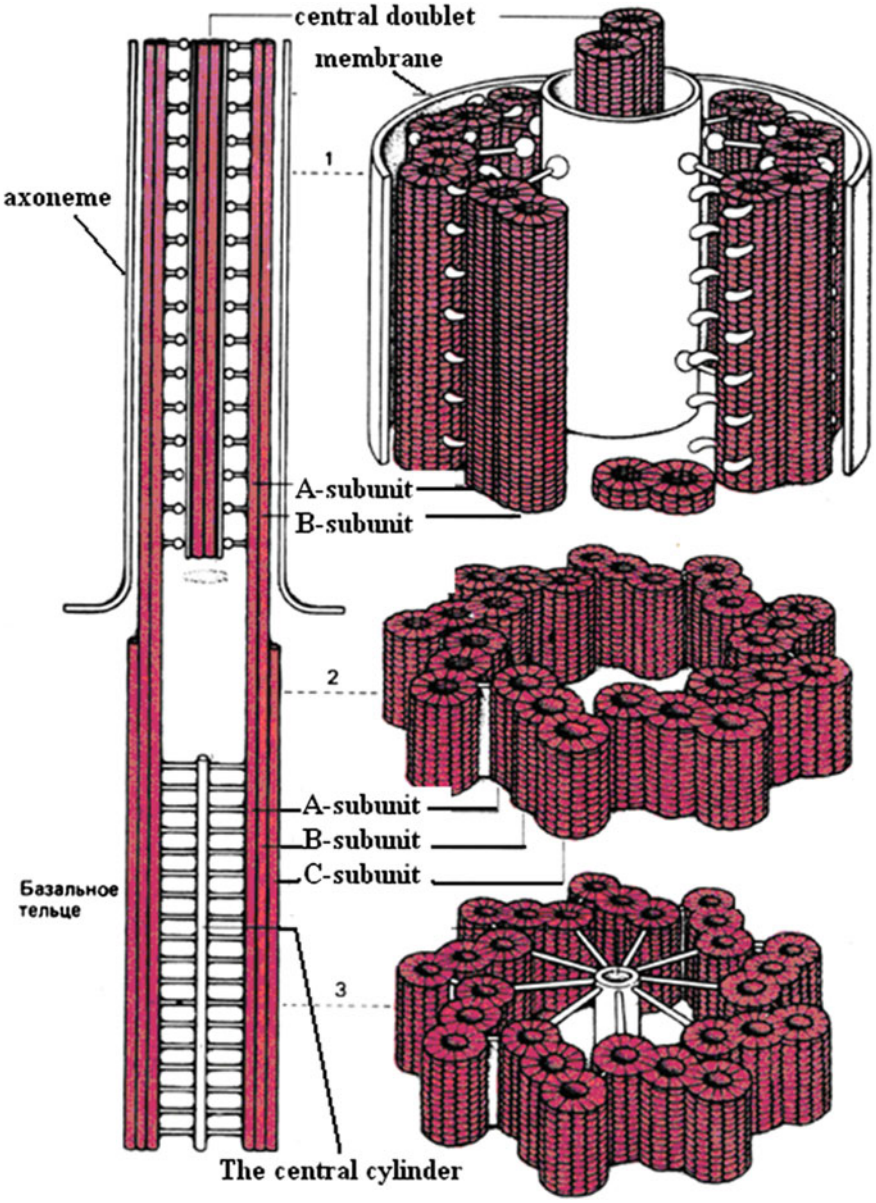

Fig. 2 Structure of cilia

4 Ciliary Propulsion

Comparing the structure of the muscle (Fig. 1) with the structure of the standard module of SEMS (Fig. 3) [9] is easy to see the similarities. It is the presence of two discs (platforms), interconnected filaments (legs), the ability to change its size by the action of the control signals.

Serial connection of these modules will be very similar to the structure of cilia. Therefore, a simple analogy of cilia would be controlled ciliated propulsion (CCP) (Fig. 4), simulating the vibrations of cilia of ciliated cells containing electromechanical cilia (EMC) in the form of serial connection Standard Module (SM) SEMS [10] and the automatic control system (ACS) in the form of Platform Coordinates Controller (PCC) of these modules [11].

In this form of fluctuations in the EMC can be set different in three-dimensional space by setting the sequences of pulse from the PCC for linear xi, yi, zi and angular ui, vi, wi coordinate platform i-x modules.

Such a propulsion device may be used in the medical micro-robots [3] as rowing oars.

The automatic control system of the propulsion device has generally the architecture of the "tree" (see Fig. 5). It is just as SEMS control system [11] comprising a central control computer (CCC) and the following subsystems: block modeling (BM); block optimization (BO); block decision making (BDM); block cilia coordinates control (BCCC); vision system (VS) and automatic control system standard modules (ACS SM) SEMS.

CCC provides a solution to problems of choice of strategy implementation required by the operator and/or systems of higher-level jobs in the frequency and

Fig. 3 Standard SEMS module (PI firm hexapod)

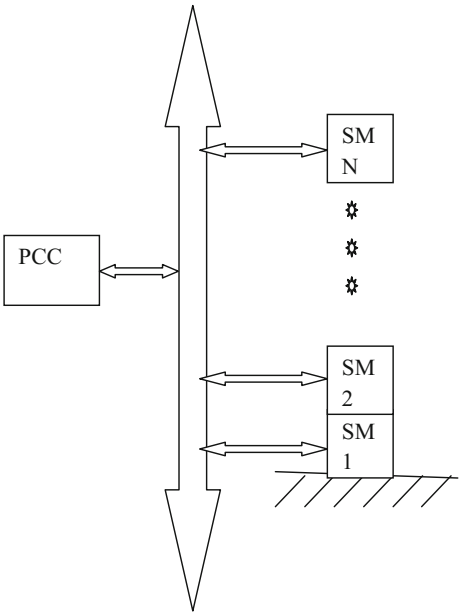

Fig. 4 Structure control ciliary propulsion

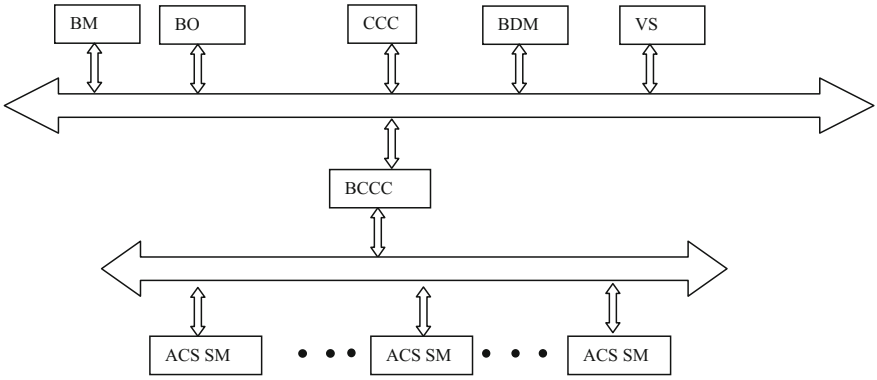

Fig. 5 Architecture ACS CP

waveform and the formation of the algorithms, required for its implementation. In addition, it should ensure a prompt correction of behavior depending on the information about the change of the environment coming from the VS, and coordination of the subsystems. Operation CCC requires advanced skills to acquire knowledge of the laws governing the environment, to the interpretation, classification and identification of emerging situations, to analyze and memorize the consequences of their actions on the basis of experience (self-learning property).

VS through from controllers on commands CCC controls its parameters, collects information, on the basis of the information collected makes identification of surrounding objects and the state of the operational environment and transmits this information to the CCC. VS can be provided with a pixel matrix switches, which can change the shape and size of the pixels on commands from CCC, ensuring their adaptation to the parameters of the identifiable objects [12, 13].

Subsystems BM, BO, BDM and BCCC usually in the form of neuroprocessor modules, algorithms that are realized in software.

BO, based on the input from the VS information about the state of the environment and in accordance with the algorithms of behavior formed CCC, performs the planning of optimal trajectories SEMS module platforms. At the same time the operational restructuring of the trajectories subject to restrictions and dynamics of the executive subsystems must be ensured.

BM provides a prediction of the dynamics of the executive subsystems for issuing corrections planned BO optimal trajectories and adaptation parameters computed control actions. At the same time, the BDM determines the conditions under which correction will be made BCCC.

BCCC on incoming information from BW, BM and BDM, and in accordance with algorithms coming from CCC produces control actions for ACS SM. Recent are control the required movement of the platform in the surrounding area.

ACS SM have the same architecture type “tree” [14, 15], and contains a block calculation of optimal movement (BCOM), which by the information received from BCCC calculates optimal elongation without jamming standard module legs. Calculated in BCOM linear and angular movements act on the appropriate group controls legs (GCL). GCL generates and provides control actions of the automatic control system legs (ACSL). Legs controllers available in GCL, using feedback signals sensors (linear encoders, angular encoders, force sensors and tactile sensor) calculating error signals. Then they produce at a predetermined control laws (e.g. laws PID) control inputs to the respective legs drives. The last performed needed legs extension, providing EMC oscillations according to the time diagram example shown in Fig. 6.

Figure 6 illustrates the simplest version of oscillation, namely quick turn in one plane from 0 to 180° at an effective phase and then slow return from 180 to 0°.

5 Ciliary Propulsion with Controllable Rigidity

The effectiveness of the ciliated propellers can be greatly increased by controlling the rigidity EMC. For this purpose modules with controlled rigidity (MCR) can be set between SM2 modules (Fig. 7) [16]. In this case, the propulsion efficiency is increased by reducing the resistance of the medium when returning EMC. By forming control law in the ACS such propulsion can be obtained waveform his EMR similar form of oscillations of biological cilia (Fig. 8).

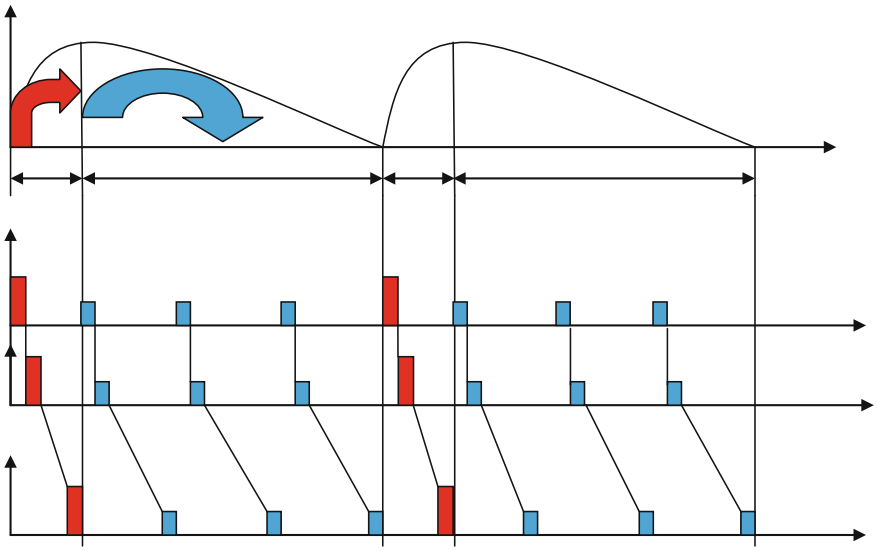

Fig. 6 Timing diagram of the modules

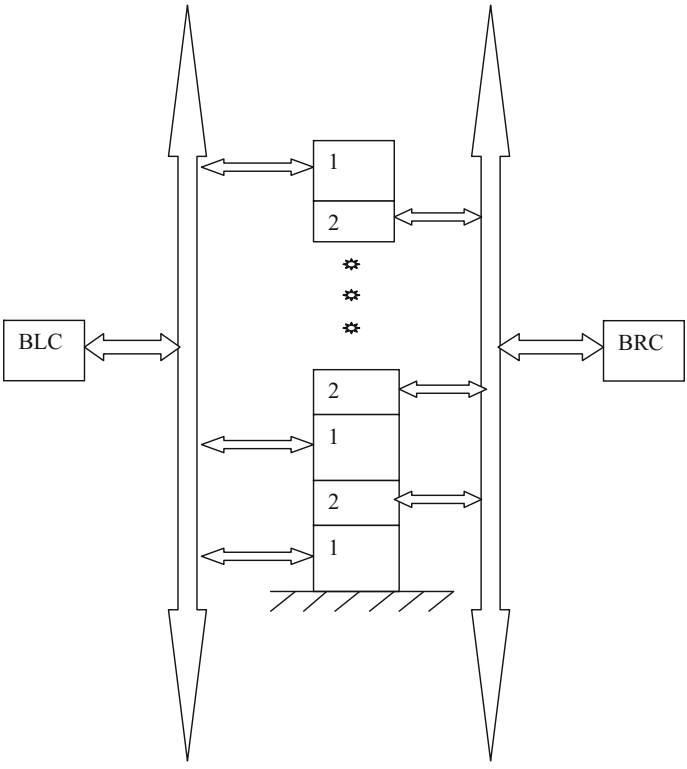

Fig. 7 Structure of ciliary propulsion with controllable rigidity. *BLC* block fluctuations control, *BRC* block rigidity control, *1* SM2 SEMS modules, *2* modules with controlled rigidity

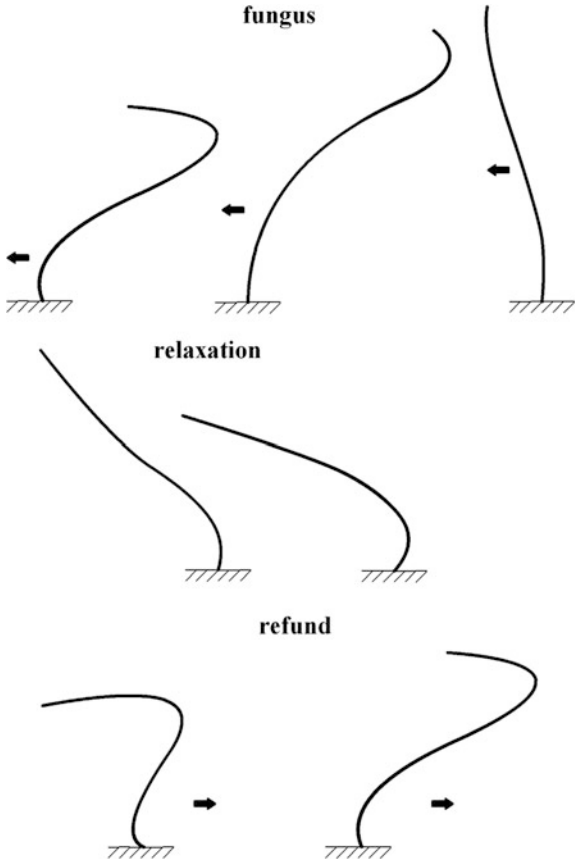

Fig. 8 Form of biological cilia vibrations

During biological cilia fluctuations stroke occurs in about 3–5 times faster than return. Moreover, during stroke rigidity much greater than during the return. This reduces energy costs on the return movement and increasing rowing effort.

Modules with controlled rigidity can be made of laminates with controlled rigidity. These layers contain conductive filaments electrically separated by a flexible porous material impregnated with an electrorheological suspension [16]. The magnitude of the laminate rigidity varies depending on a control electric current supplied to the wires from the BRC.

Automatic control systems ciliary propulsion with controllable stiffness (ACS CPCS) as well as ACS ciliary propulsion described in the above usually has the architecture of the "tree" (Fig. 9). Its contain a central control computer (CCC) and the following subsystems: block modeling (BM); block optimization (BO); block decision making (BDM); block control coordinates the cilia (BCCC) vision system (VS) and automatic control system standard modules (ACS CM) SEMS. To control the rigidity of ACS CPCS additional supplied the BRC and automatic control systems modules with controlled rigidity (ACS MCR).

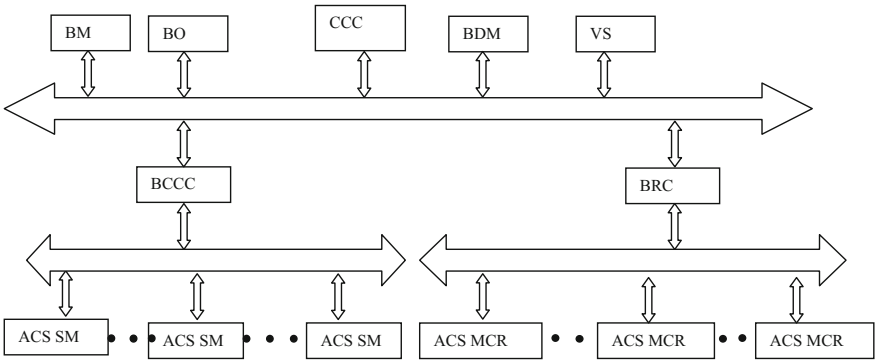

Fig. 9 ACS CPCS architecture

BRC according to the information received from the BO, BM and BDM, and in accordance with algorithms coming from CCC generates control feedback for ACS MCR, which carry out the required changes to their rigidity.

ACS MCR has an architecture of the "tree" (see Fig. 10) and contains a block calculation of optimal rigidity (BCOR), which by the information received from the BRC calculates optimum rigidity for MCR and transmits this information to the controllers rigidity (CR), which generate corresponding control electric current supplied to the MCR.

Algorithms work ACS MCR explains timing diagram shown in Fig. 11, where V—angle of rotation of the cilia, and c1, c2, … cn—rigidity modules with controlled rigidity.

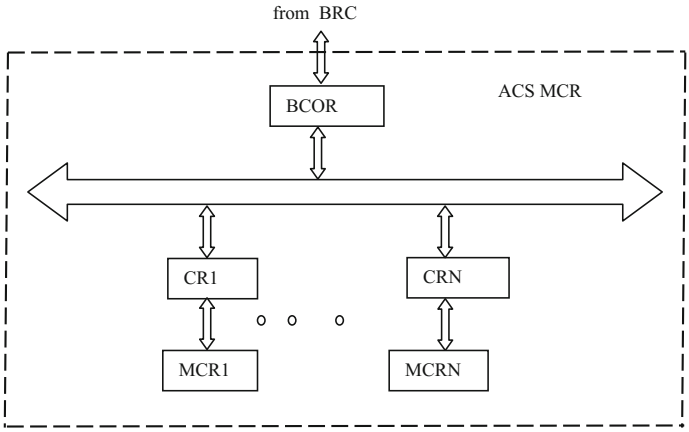

Fig. 10 Structure ACS MCR

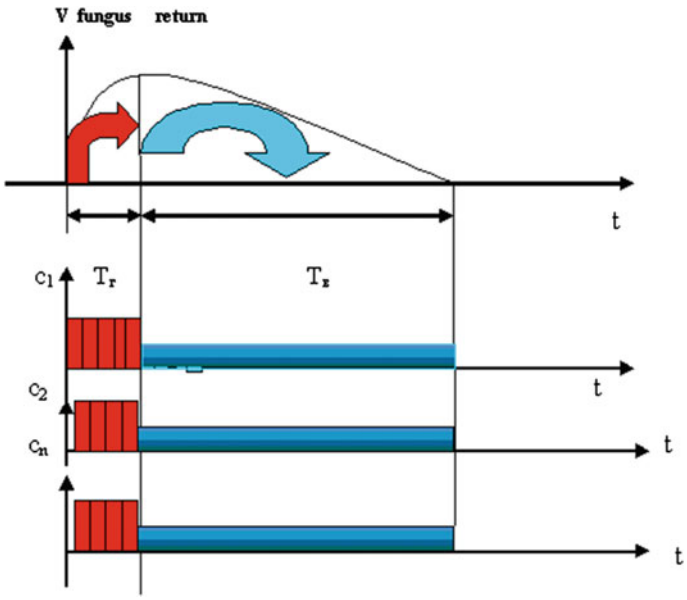

Fig. 11 Timing diagram MCR

6 Ciliary Propulsion with Controllable Rigidity and Shape

Efficiency of functioning of the considered ciliary can be even more increased due to control of a form of its rowing elements. For this purpose in his design it is possible to use SM5 SEMS [9] modules which platforms contain the control rods with motors. Such modules allow the control rods to increase the surface area of the EMC at the stroke and decrease when returning by changing a control voltage; supplied to the motors-driven rods.

SM5 SEMS module platform is shown in Fig. 12. It contains control rods 1–3 with electric-driver 4–6, that allow you to change its length and thereby change the shape of the rowing surface propulsion.

Usually electric-driver contain gears (R), displacement sensors (DS), such as opto-electronic sensors, force sensors (FS), such as piezoelectric and controllers (C).

The system of automatic control of ciliary propulsion with controllable rigidity and shape (ACS CPRS) as well as ACS propulsion described above may have the architecture of the "tree" (Fig. 13). It contains a central control computer (CCC) and the following subsystems: block modeling (BM); block optimization (BO); block decision making (BDM); vision system (VS); block control coordinates of the cilia (BCCC), automatic control system of standard modules (ACS SM) of SEMS, block control rigidity (BCR) and automatic control system modules with controlled rigidity (ACS MCR). To control form the ACS CPRS also be provided

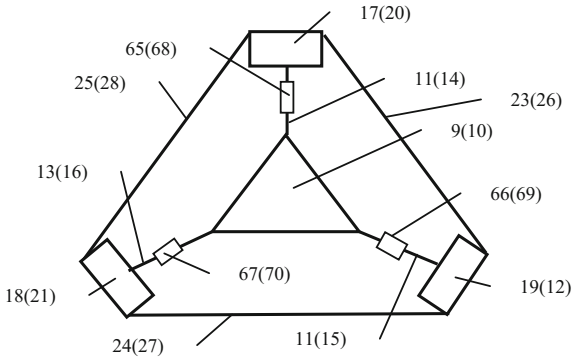

Fig. 12 Platform module SM5 SEMS with the control rod

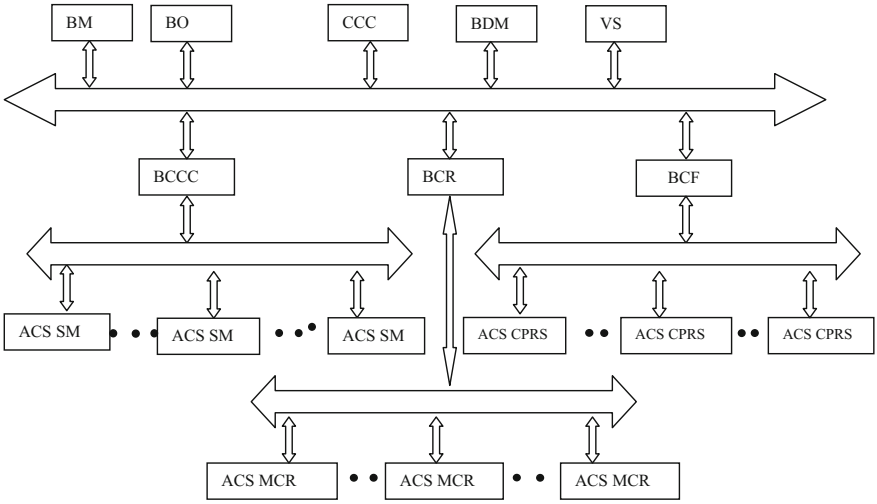

Fig. 13 Architecture ACS CPRS

with block control form (BCF) and automatic control systems motors of control rods (ACS MCR).

BCF according to information received from the BM, BO, BDM, and in accordance with algorithms coming from CCC produces control actions for ACS MCR which carry out the required changes in the shape SM5 SEMS module platforms.

ACS MCR has the architecture of "tree" type (see Fig. 14) and contains a block calculation of optimal elongation (BCOE). It on incoming information from the BCF calculates the optimal elongation of the control rod (CR) and transmits this information to the motor controller of the control rod (MCCR), which generate corresponding control voltage supplied to the motor of control rods (MCR).

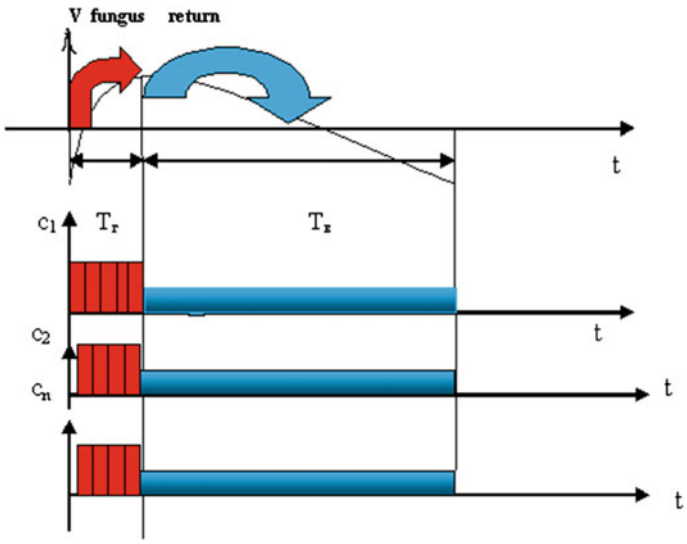

Fig. 14 Timing diagram changes SM5 SEMS module platform sizes

Algorithms work of automatic control system of form explains a timing diagram shown in Fig. 6, where V—cilia rotation angle, and c1, c2, … cn—the size of the propeller surface (platform module SM5 SEMS).

We consider the simplest variant, namely, quick turn in one plane from 0 to 180° when the stroke and then slow return from 180 to 0°.

In this case, for control form at the time of the stroke Tg in the MCR provides control signals to increase the surface of the stroke and during the start of the return —control signals to reduce the surface return.

7 Conclusion

Analysis of the structure and function of human muscle and ciliary apparatus showed similarities with modules SEMS and c series connection of the such modules. It is allowed to offer ciliated propulsor having an electromechanical structure consisting of a series connection of modules SEMS. The work of the such propulsion is similar to fluctuations in the cilia. Therefore, such a propulsor, equipped with a corresponding automatic control system (ACS), can be used as controlled ciliary propulsion (CCP) in micro robots.

As the results of the research the effectiveness of the functioning of ciliated propulsion can be significantly improved by controlling the rigidity of its elements. For this purpose, in the electromechanical structure from series connection of modules SEMS placed between the modules SEMS modules with controlled

rigidity (MCR). In this case, the automatic control system of ciliary propulsion is complemented by the automatic control system of modules with controllable rigidity. Micro robots with such propulsion more efficient use of energy reserves by reducing energy consumption during the return movement.

In addition the efficiency of the ciliated propulsion can be greatly increased by simultaneously controlling the shape and rigidity of its elements. For this purpose, the electromechanical structure of propulsor build of a series connection SM5 SEMS-type modules and between the modules are placed modules with controlled rigidity. In this case, the automatic control system of ciliary propulsion is complemented by the automatic control system of the control rods of platform module SM5 SEMS. Micro robots with such propulsion more efficient use of energy reserves by reducing energy consumption during the return movement and increase the efforts of the stroke.

Acknowledgements The author would like to thank the Russian Foundation for Basic Researches (grants 14-07-00257, 15-07-04760, 15-07-02757, 16-29-04424, and 16-29-12901) for partial funding of this research.

References

1. Zhang, L., Abbott, J.J., Dong, L., Kratochvil, B.E., Bell, D., Nelson, B.J.: Artificial bacterial flagella: fabrication and magnetic control. Appl. Phys. Lett. **94**, 064107 (2009). doi:10.1063/1.3079655
2. Gradetsky, V., Solovtsov, V., Kniazkov, M., Rizzotto, G., Amato, P.: Modular design of electro-magnetic mechatronic microrobots. In: Proceedings of the 6-th International Conference CLAWAR 2003, pp. 651–658, Catania, Italy, 2003
3. Agapov, V.A. (RU), Gorodetskiy, A.E. (RU), Kuchmin, A.J. (RU), Selivanova, E.N. (RU): Medical microrobot. Patent RU, no. 2469752, 2011
4. Zakharova, G.P., Ianov, I.K., Shabalin, V.V. SPb.: Mukotsiliarnaia sistema verkhnikh dykhatel'nykh putei (Mucociliary system of the upper respiratory tract) 360 s. «Dialog» (2010, in Russia)
5. Alekseev, D.S., Badu, E.I., Gorodetsky, A.E., Dubarenko, V.V., Tarasova, I.L., Kuchmin, A. Y.: Simulation of the ciliary apparatus of ciliated epithelial cells. Math. Mod. Comput. Simul. **1**(6), 757–767 (2009)
6. Selivanova, E.N., Gorodetskii, A.E.: Computer modeling of processes of excitation and syncing of oscillations of the cilia ciliated of cells (Komp'iuternoe modelirovanie protsessov vozbuzhdeniia i sinkhronizatsii kolebanii resnichek mertsatel'nykh kletok). In: Informatsionno-upravliaiushchie sistemy (Information and Control Systems) №4, pp. 29–34 (2010, in Russia)
7. Meditsinskaia biofizika (Medical biophysics) Samoilov V.O. Uchebnik dlia vuzov Izd. 2-e, ispr., dop., SPb: SpetsLit (2007, in Russia)
8. Gusev, N.B.: Molekuliarnye mekhanizmy myshechnogo sokrashchaniia (Molecular mechanisms of muscle contraction). Sorosovskii obrazovatel'nyi zhurnal (Soros Educational Journal), tom 6, № 8, pp. 24–32 (2000, in Russia)
9. Gorodetskiy, A.E.: Smart electromechanical systems modules. In: Gorodetskiy, A.E. (ed.) Smart Electromechanical Systems, 277 p. Springer International Publishing (2016). doi:10.1007/978-3-319-27547-5

10. Gorodetsky, A.E.: Smart electromechanical systems architectures. In: Gorodetskiy, A.E. (ed.) Smart Electromechanical Systems, 277 p. Springer International Publishing (2016). doi:10.1007/978-3-319-27547-5
11. Kurbanov, V.G., Gorodetskiy, A.E., Tarasova, I.L.: Automatic control systems of SEMS. In: Gorodetskiy, A.E. (ed.) Smart Electromechanical Systems, 277 p. Springer International Publishing (2016). doi:10.1007/978-3-319-27547-5
12. Gorodetskiy, A.E., Kurbanov, V.G., Tarasova, I.L., Agapov, V.A.: Problems of increase of efficiency of use of matrix receivers for radio images in astronomy. Radio Eng. (1), 88–96 (2015, in Russia)
13. Gorodetskiy, A.E., Tarasova, I.L.: Detection and identification of dangerous space objects using adaptive matrix radio receivers. In: Informatsionno-upravliaiushchie sistemy (Information and Control Systems), № 5, pp. 18–23 (2014, in Russia)
14. Tarasova, I.L., Gorodetskiy, A.E., Kurbanov, V.G.: Neuroprocessor automatic control system of the module SEMS. In: Gorodetskiy, A.E. (ed.) Smart Electromechanical Systems, 277 p. Springer International Publishing (2016). doi:10.1007/978-3-319-27547-5
15. Gorodetsky, A.E., Tarasova, I.L., Kurbanov, V.G., Agapov, V.A.: Mathematical model of automatic control system for SEMS module. In: Informatsionno-upravliaiushchie sistemy (Information and Control Systems), no. 3(59), pp. 40–45 (2015, in Russian)
16. Boikov, V.I. (RU), Bystrov, S.V. (RU), Smirnov, A.V. (RU), Chezhin, M.S. (RU): Sloistyi materials izmeniaemoi zhestkost'iu (A laminate variable rigidity). Patent RU, no. 1749056, 1992

Flagella Propeller

I.L. Tarasova, Andrey E. Gorodetskiy, Vugar G. Kurbanov and A.Yu. Kuchmin

Abstract *Purpose*: when modern problems of robotics are being solved, the bionic approach where robots imitate complexity and adaptability of biological systems gains more ground nowadays. Particularly, it is urgent for the medical micro robots equipped by controlled tiny and energy-efficient propellers. The purpose of this article is to develop new structure of flagella propellers imitating the work of biological flagella propeller. *Results*: a new type of the tiny flagella propeller imitating operation of the biological flagella propeller and allowing adapting to the environment due to control over rigidity and forms of elements of the propeller is suggested here, as well as its intellectual system of automatic control. With the use of computer modeling, it is shown that the suggested type of the propeller allows reaching the dynamic characteristics required for medical micro robots. *Practical importance*: the suggested adaptive flagella propeller with controlled rigidity is supplied with the corresponding systems of automatic control can be used in micro robots of different function. Development of dynamics and setup of parameters of flagella propellers with the controlled form and rigidity by means of computer modeling can be improved by inclusion of the model of SEMS module into the constructed model designed by authors earlier.

Keywords Biological systems · Biological flagella · Adaptive propeller · System of automatic control · Computer modeling · Control over rigidity and form

I.L. Tarasova (✉) · A.E. Gorodetskiy (✉) · V.G. Kurbanov · A.Yu.Kuchmin
Institute of Problems of Mechanical Engineering, Russian Academy of Sciences, Saint-Petersburg, Russia
e-mail: g17265@yandex.ru

A.E. Gorodetskiy
e-mail: g27764@yandex.ru

V.G. Kurbanov
e-mail: vugar_borchali@yahoo.com

A.Yu.Kuchmin
e-mail: radiotelescope@yandex.ru

A.E. Gorodetskiy and V.G. Kurbanov (eds.), *Smart Electromechanical Systems: The Central Nervous System*, Studies in Systems, Decision and Control 95,
DOI 10.1007/978-3-319-53327-8_12

1 Introduction

In recent years robots which imitate complexity and adaptability of biological systems become one of main goals of researches in the field of robotics [1, 2]. At the same time one, from the most difficult, and difficult solved problem is creation of the operated tiny and energy efficient propulsions for such robots. At the solution of this problem the propulsions imitating work of a flagellum- an organella of the movement at bacteria and archaeal (Fig. 1) can be used [3, 4].

2 The Biological Flagellum

Flagellum of an eukaryotic cell—the outgrowth similar to an cilium [3] having thickness about 0.25 μm and length to 150 μm, dressed by a plasmatic membrane. Inside there is an axonema—the cylinder which wall is constructed of 9 couples of microtubules connected among themselves by "handles". In the center of an axonema microtubules settle down 2 (more rare 1, 3 or more) (so-called structure 9 + 2). In the basis of a flagellum two mutually perpendicular basal little bodies lie. Flagellum, unlike cilium, wavy move or it is funneled, due to sliding of microtubules of the next couples relatively each other by means of "handles", using energy of ATP [3].

Absolutely other molecular mechanism is the base of the movement of a bacterial cell [4]. Ability of bacteria to fast and the directed movement is caused by presence at these organisms of special body of the movement—the bacterial flagellum (BF), structure and which functioning codes about 50 genes. BF, penetrating a cellular wall, leaves under a cytoplasmatic membrane. He has the discrete structure consisting of a basal body, long external thread and the "hook" connecting these two parts (see Fig. 2).

The basal body which located inside the cellular wall during rotating sets the external semifixed spiral proteinaceous thread providing generation of hydrodynamic force in motion it is directed the pushing cell. A long time as a part of BF looked for ATPase, but haven't found her. Relatively recently (the end 70-th years) it has become clear that the basal body of a flagellum represents a tiny electric motor thanks to which the bacterial cell is capable to gather very high speed—

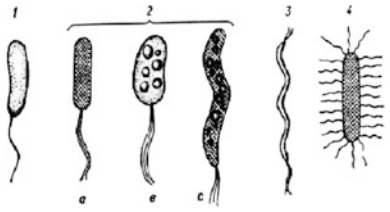

Fig. 1 Types of biological flagella

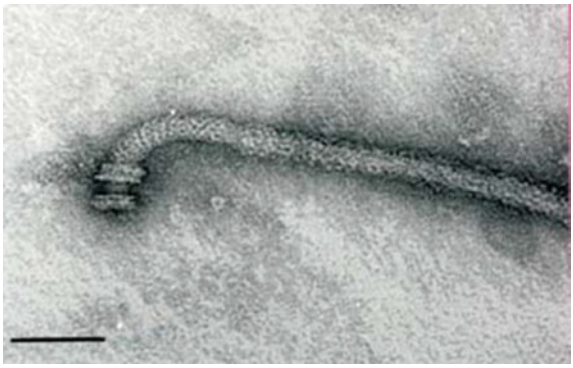

Fig. 2 The electron microscope picture of a bacterial flagellum

100 μm/s, that is more than 50 lengths of a body of a cell per second. The power of this process was unique for systems of mobility—the transmembrane potential of ions of hydrogen (or sodium) on a membrane.

Morphologically flagellum is constructed of three main parts: the basal body rotating inside the cellular wall and which is carrying out a role of a tiny electric motor, the external semifixed spiral thread constructed of protein of a flagellin and playing a screw role at the movement of bacteria in the environment and so-called "hook", the flexible proteinaceous structure tying a basal body and external thread [5–7]. However it doesn't exhaust all structure of the motive device of a bacterium. There is still an additional amount of proteins and proteinaceous educations in the cytoplasm and a cytoplasmatic membrane participating in rotation of a flagellum. However, accumulate them in the structure these three main parts.

The motor system of a flagellum contains about 25 various proteins, including the specific proteins switching the direction of rotation of the motor. Recently a number of proofs is received that these proteins form two main parts of the motor—a rotor and the stator.

The special attention is deserved by protein of external thread of a flagellum—flagellin. Properties of subunit of a flagellin in a thread allow to take a proteinaceous spiral of BF thread the different forms (flagellum has the form of a semifixed spiral like the screw), thereby providing movement of a cell in the environment.

3 The Structure of Flagellated Propulsion

Consecutive connections of SEMS [8] modules very similar to the structure of BF. Therefore the simplest electromechanical analog of BF is controlled flagellated propulsion (Fig. 3), which imitates the wavy or funneled movement of a flagellum and contains the electric drive of rotation (EDR) fixed on the basis, electromechanical flagellum (EMF) connected with EDR through a reducer (R) and the

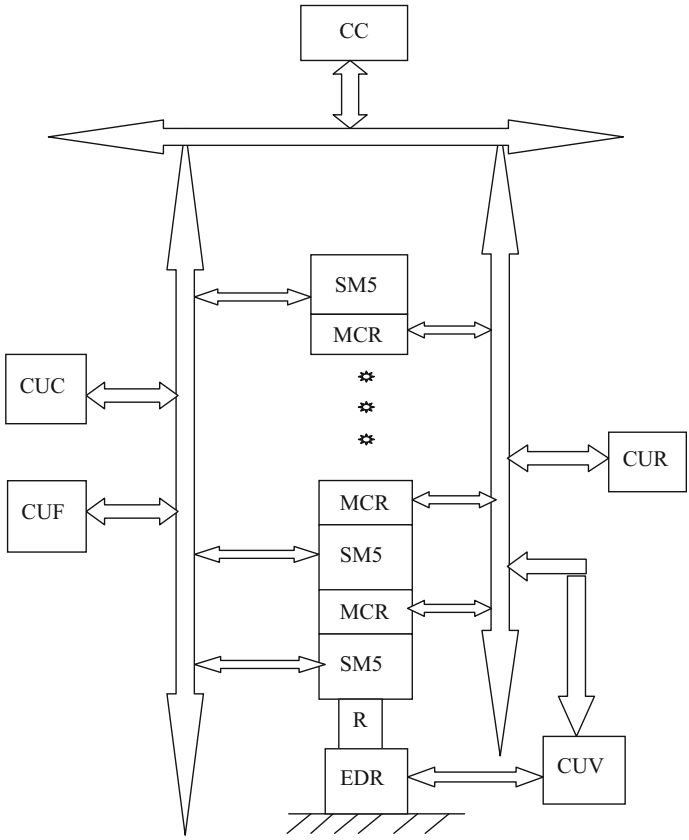

Fig. 3 The scheme of EMF

system of automatic control (SAC). EMF has the form of consecutive connection of SM5 SEMS [9] modules. Modules with the controlled rigidity (MCR) are installed between SM5 [10].

In 3D space the kind of motion of EMF can be defined by set the sequences of the control impulses from the control unit of coordinates (CUC) of SAC to engines of legs of SM5 SEMS modules for linear displacements x_i, y_i, z_i and angles u_i, v_i, w_i of each platform. The angular velocity EMF can be changed by voltages of EDR from control unit of velocity (CUV) of SAC. The Control Computer (CC) generates the goals of control of EMF.

The shape of EMF can be changed due to giving of the control influences from the control unit of a form (CUF) of SAC in the engines of the controlled bars (ECB) of platforms of SM5 modules of SEMS, and rigidity of EMF can be changed due to giving of the operating influences from the control unit of rigidity (CUR) of SAC in the MCR [10].

Such propulsion can be used in the medical micro robot [11] as the screw propulsion.

4 The System of Automatic Control

Let's consider architecture of system of automatic control of the flagellated propulsion (SAC FP) on the example of use it in the medical microrobot (Fig. 4) [11]. The SAC FP has as general architecture like "tree" (see Fig. 5). It consists of

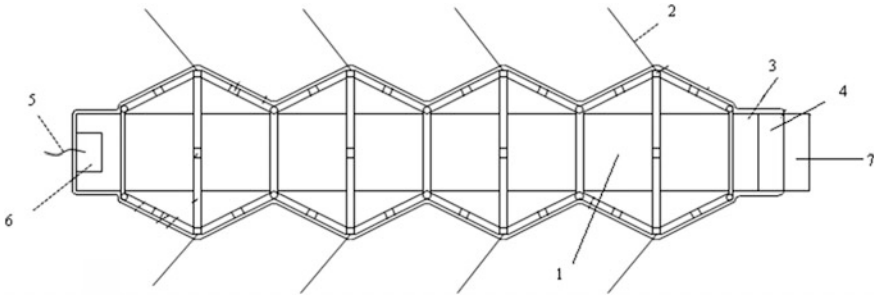

Fig. 4 Medical microrobot. *1*—The SM5 modules of SEMS, *2*—the cilium propulsions, *3*—the control computer, *4*—the electronic vision system, *5*—the flagellated propulsion, *6*—the control unit of rigidity, *7*—the adaptive grab

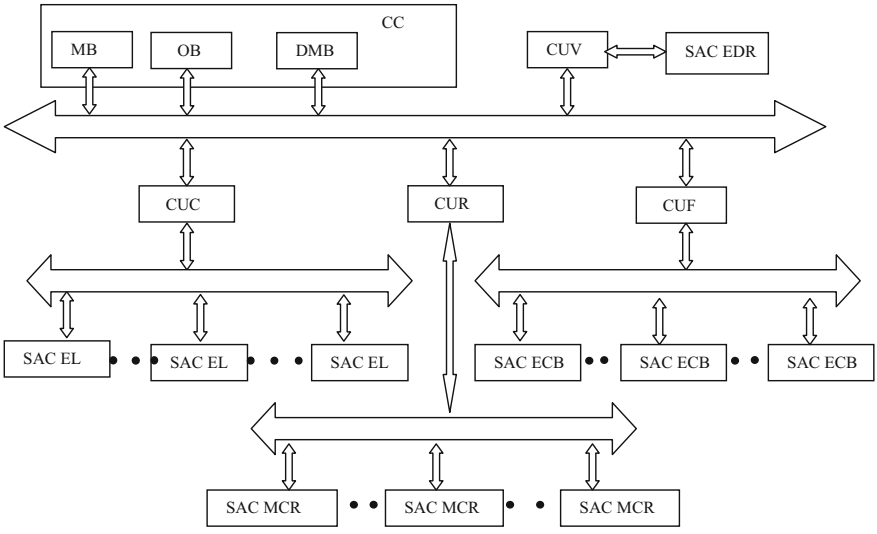

Fig. 5 The architecture of SAC FP

the operating computer (OC) containing the following modules: modeling block (MB); optimization block (OB); decision-making block (DMB); and control blocks: control unit of coordinates (CUC), control unit of a form (CUF), control unit of rigidity (CUR) and control unit of velocity (CUV). Each of the listed control units is connected with the corresponding systems of automatic control. The CUC has link with system of automatic control of engines of legs (SAC EL) of standard SEMS modules. The CUR has link with system of automatic control of modules with the control rigidity (SAC CUR). The CUF has link with system of automatic control of engines of the controlled bars (SAC ECB) of standard SEMS modules. The CUV has link with system of automatic control of the electric drive of rotation (SAC EDR).

The CC provides the solution of problems of the choice of strategy of the performance demanded from the operator and/or system of higher level of a task for type and form of motion and formations of the sequence of actions (algorithms) necessary for his realization. Besides, it has to provide real time correction of subsystems depending on information on change of the external environment arriving from the electronic vision system (EVS) of the microrobot and coordination of functioning of all subsystems.

The modules of CC: MB, OB and DMB as usual have been done as a neuroprocessor module, which algorithms of work are implemented programmatically.

The BO proceeds information about state of environment getting from EVS of the microrobot and according to the requirements of control algorithms created in CC performs planning of optimum trajectories of movement of platforms of SEMS modules, their reconfiguration and change of rigidity of MCR and velocities of EDR. At the same time operational reorganization of trajectories taking into account restrictions and dynamics of executive subsystems shall be provided.

The MB provides forecasting of dynamics of executive subsystems for issue of corrections of the planned OB of optimum trajectories and adaptation of parameters of the calculated corrective actions. At the same time DMB determines conditions under which in CUC, CUF, CUR and the CUV adjustments will be made.

The CUC according to the getting information from OB, MB and DMB and according to the algorithms getting from CC develops the operating influences for SAC EL which carry out the required movements of the SM5 SEMS platforms in surrounding space. The CUF according to the getting information from OB, MB and DMB and according to the algorithms getting from CC develops the operating influences for SAC EDR which carry out the required reconfigurations of the SM5 SEMS platforms. The CUR according to the getting information from OB, MB and DMB and according to the algorithms getting from CC develops the operating influences for SAC MCR which carry out the required changes of their rigidity. The CUV according to the getting information from OB, MB and DMB and according to the algorithms getting from CC develops the operating influences for SAC EDR which carry out the required changes of velocity of rotation.

The structure and work of SAC EL, SAC DUS and SAC MCR are described in [10], and SAC EDR—in [12].

5 The Computer Modeling

Computer modeling of subsystems automatic control of rigidity and a form, is described in [13], and SAC of the standard SEMS module—in [14].

The simplest computer model of system of automatic control of an angle of rotation of one of links, that is one of SM5 modules, bodies of a flagellum at rotation of the flagellum from EDR (see Fig. 3) is shown in Fig. 6. The model contains the chain 1 imitating an output signal from the sensor of the angle of rotation giving a sawtooth signal of a corner from 0° to 360° (see Fig. 7), the chain 2 imitating a module angle of rotation from a starting position to the maximum angle, the chain 3 imitating an angle of rotation from the maximum value to minimum and the chain 4 imitating an angle of rotation from the minimum angle to initial (see Fig. 8). Besides at the exit of model the block (Transfer for 3) imitating influence on an angle of rotation of the liquid environment is installed.

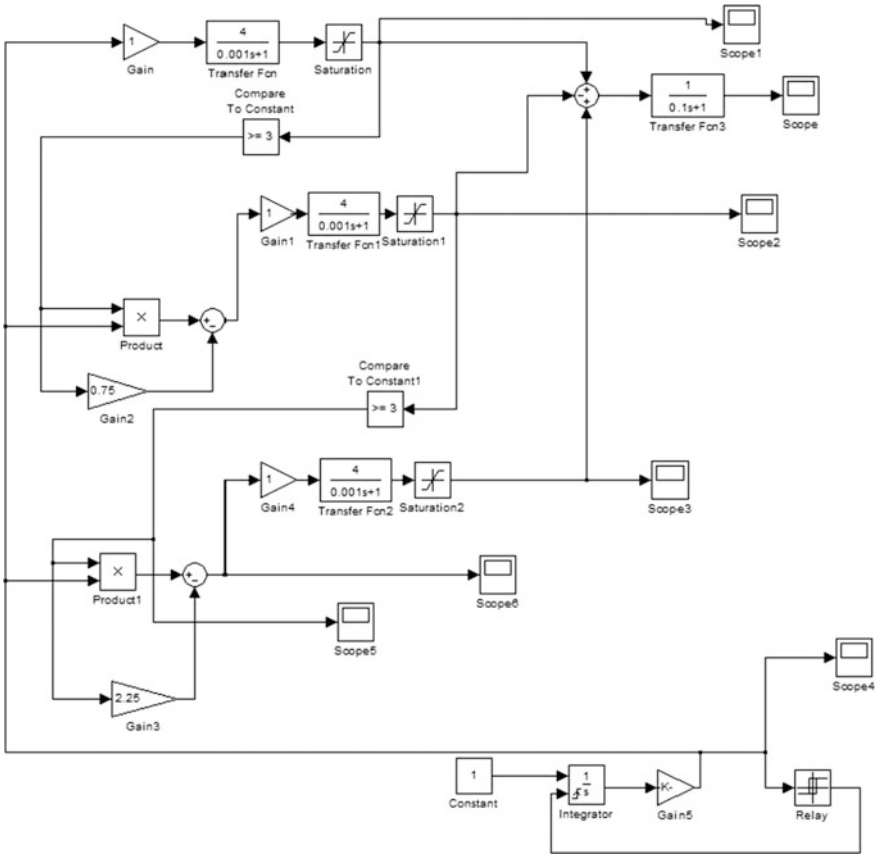

Fig. 6 The scheme of model of SAC of rotating of section of EMF

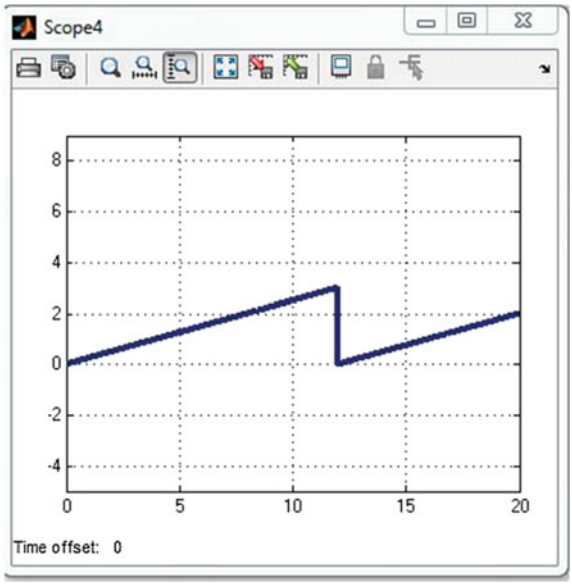

Fig. 7 The time diagram of sensor of rotation angle

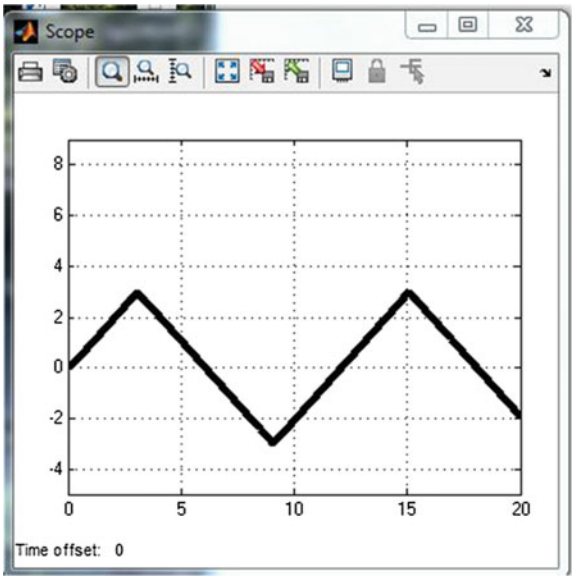

Fig. 8 The time diagram of changing of an angle of section of flagellated propulsion

The circuit 1 contains the unit (Constant) with a signal input of the unit (Integrator) which output is connected to an input of the unit (Gain 5). The output of this unit is connected to an input of the unit (Relay) which output is connected to the second (controlling) input of the unit (Integrator). The signal from an output of a circuit 1, i.e. from an output of the unit (Gain 5), arrives on an input of a circuit 2,

i.e. on an input of the unit (Gain), on an input of a circuit 3, i.e. on an input of the unit (Product), and on an input of a circuit 4, i.e. on an input of the unit (Product 1)

The circuit 2 contains the unit (Gain) which output is connected to an input of the unit (Transfer for) which output is connected to an input of the unit (Saturation) which output is connected via the unit (Compare To Constant) to the second input of the unit (Product) of a circuit 3, and via the adder to an input of the unit (Transfer for 3) which output is a model output.

The circuit 3 contains the unit (Product) which output is connected to the first input of the adder of a circuit 3 to which second input the output of the unit (Gain 2) which input is connected to an output of the unit (Compare To Constant) of a circuit 2 is connected. Counter total exit of a circuit 3 is connected to an input of the unit (Gain 2) which output is connected to an input of the unit (Transfer for 1) the Output of this unit is connected to an input of the unit (Saturation 1) which output is connected via the unit (Compare To Constant 1) to the second input of the unit (Product 1) of a circuit 4, and via the adder of a circuit 2 to an input of the unit (Transfer for 3) which output is a model output.

The circuit 4 contains the unit (Product 1) which output is connected to the first input of the adder of a circuit 4 to which second input the output of the unit (Gain 3) which input is connected to an output of the unit (Compare To Constant 1) of a circuit 3 is connected. Counter total exit of a circuit 4 is connected to an input of the unit (Gain 4) which output is connected to an input of the unit (Transfer for 2) the Output of this unit is connected to an input of the unit (Saturation 2) which output is connected via the adder of a circuit 2 to an input of the unit (Transfer for 3) which output is a model output.

Besides, for observation of an output signal of a chain 1 (see Fig. 7) the block (Scope) is connected to an exit of the block (Gain 5), and for observation of change of an angle of rotation of one of links of a flagellum at his rotation (see Fig. 8) to an exit of the block (Transfer for 3), the being model exit, has connected the block (Scope 1).

From Figs. 7 to 8 it is visible that during rotation of a flagellum from 0° to 360° links of a flagellum make a full cycle of turn in other plane, the perpendicular plane of rotation of a flagellum. And the phase of turn of each subsequent link is shifted rather previous that creates force of the movement directed along a flagellum or a body of the robot. An initial phase of each link of a flagellum, for example it is possible to change due to introduction of a delay to an output signal of a chain 1, that is to a signal from the sensor of an angle of rotation.

6 Conclusion

The analysis of structure and the principle of action of a biological flagellum showed their similarity to consecutive connections by SEMS modules. It allowed to offer the flagellated propulsion having electromechanical structure from consistently connection of SEMS modules and modules with the controlled rigidity which

work is similar to a biological flagellum. Therefore such propulsion supplied with the corresponding system of automatic control (SAC) can be used as the controlled propulsion in micro robots.

Efficiency of functioning the flagellated propulsions can be significantly increased due to adaptation to the surrounding liquid environment by control of rigidity and a form of links.

Results of computer modeling of systems of automatic control showed that the offered type of propulsions allows to reach the dynamic characteristics required for medical micro robots.

Acknowledgements The author would like to thank the Russian Foundation for Basic Researches (grants 14-07-00257, 15-07-04760, 15-07-02757, 16-29-04424, and 16-29-12901) for partial funding of this research.

References

1. Zhang, L., Abbott, J.J., Dong, L., Kratochvil1, B.E., Bell, D., Nelson, B.J.: Artificial Bacterial Flagella: Fabrication and Magnetic Control (2009)
2. Gradetsky, V., Solovtsov, V., Kniazkov, M., Rizzotto, G.: Amato P. Modular design of electro-magnetic mechatronic microrobots. In: Proceedings of the 6-th International Conference CLAWAR 2003, vol. 3, pp. 651–658. Catania, Italy (2003)
3. Cappuccinelli, P.: Motility of Living Systems. 79 S., 45 Abb., 3 Tab. London-New York. Chapman and Hall (1980)
4. Metlina, A.L.: Flagellum of procaryote as system of biological mobility. Achievements Biol. Chem. **41**, 229–282 (2001)
5. Poglazov, B.F., Metlina, A.L., Novikov, V.V.: News Acad. Sci. USSR, Biol. **5**, 672–690 (1981)
6. De Phamphilis, M.L.: Adler J. // J. Bacteriol. **105**, 376–407 (1971)
7. Jones, C.J.: Aizawa S. // Advan. Microbial. Physiol. **32**, 109—172
8. Gorodetskiy, A.E.: Smart Electromechanical Systems. Springer International Publishing, p. 277 (2016). doi:10.1007/978-3-319-27547-5
9. Gorodetskiy, A.E.. Smart electromechanical systems modules. In: Gorodetskiy, A.E. (eds.) Smart Electromechanical Systems. Springer International Publishing, p. 277 (2016). doi:10.1007/978-3-319-27547-5
10. Controlled cilium propulsion (In the volume)
11. Medical microrobot. Russian Federation patent № 2469752
12. Yu, A.N., Gorodetskiy, A.E., Dubarenko, V.V., Yu, K.A., Agapov, V.A.: Analysis of dynamics of automatic control system of space radio-telescope subdish actuators. Informatsionno-upravliaiushchie Sistemy **55**(6):2–6 (2011) (In Russian)
13. Kurbanov, V.G., Gorodetskiy, A.E., Tarasova, I.L.: Computer simulation of automatic control system ciliated propulsion (In the volume)

Linearized Model of the Mechanism with Parallel Structure

A.Yu. Kuchmin and V.V. Dubarenko

Abstract *Purpose* The mode of tracking is one of the main operating modes of electromechanical systems of parallel architecture, for example adaptive platforms (Smart Electromechanical Systems—SEMS). The systems are nonlinear and non-stationary plants therefore control of them requires use of adaptive regulators for the purpose of increase in accuracy, speed and reliability of such systems. A research purpose is development of a technique of development of the linear models for synthesis of adaptive regulator of a platform moved by group of actuators, taking into account change of the line of action of these actuators in the tracking mode. *Results* the non-stationary model of the adaptive platform moved by group of n actuators working in the tracking mode is received, formulas of calculation of matrixes of parameters of this model depending on the chosen stationary point or a basic trajectory in phase space are received. It is shown that for such adaptive platforms it is necessary to consider change of length and the line of action of actuators. *Practical importance* the offered algorithms of calculation of a matrix of parameters of non-stationary model of an adaptive platform are effective in case of implementation of the predictive model allowing to estimate not measured components of a state vector of a platform and calculation of parameters of regulators that will lead to increase in accuracy and reliability of a control system in the tracking mode.

Keywords The SEMS platform · An actuator · The equations of dynamics of an SEMS

A.Yu. Kuchmin (✉) · V.V. Dubarenko
Institute of Problems in Mechanical Engineering,
Russian Academy of Sciences, Saint-Petersburg, Russia
e-mail: radiotelescope@yandex.ru

V.V. Dubarenko
e-mail: vladimir.dubarenko@gmail.com

A.E. Gorodetskiy and V.G. Kurbanov (eds.), *Smart Electromechanical Systems: The Central Nervous System*, Studies in Systems, Decision and Control 95,
DOI 10.1007/978-3-319-53327-8_13

1 Introduction

Development of the linearized non-stationary models of the adaptive platforms on the mobile basis moved by group of actuators taking into account change of the line of action of these actuators working in the mode of tracking is an urgent task which plays an important role during the calculating of parameters of regulators and estimation of not measured platform state vector components.

Recently there was an interest in use of electromechanical systems of parallel architecture, for example SEMS [1–5], in high-precision instrument making, robotics, adaptive antennas, etc. Benefits, using and the description of such mechanisms have been considered in prior publications [1, 2, 4].

One of the main operating modes of an adaptive platform is tracking of which smooth trajectories of movement are characteristic that allows by consideration of system in small deviations to pass to the non-stationary linearized models of dynamics of such platforms.

In the previous article [2] kinematic and dynamic models of an adaptive platform for a case of n of actuators in detail were considered. The mainframe of similar systems consisting of two mobile platforms [the basis and the adaptive platform (AP)] connected with each other by electromechanical actuators has been for this purpose considered. Each actuator consists of a bar with the linear electric drive allowing to change its length. Each actuator is connected to the lower and top platforms two hinges allowing pushers to rotate freely on anglers.

Let's describe the main definitions and formulas of kinematic model according [2]. The basis moves on three linear displacements (x_0, y_0, z_0) and three anglers (β_0, θ_0, α_0) about an basic coordinate system (BCS), where β_0—angler of rotation about an axis x, θ_0—angler of rotation about an axis y, α_0—angler of rotation about an axis z. The adaptive platform moves on three linear displacements (x, y, z) and three anglers (β, θ, α) about an coordinate system of basis (CS BAS), where β—angler of rotation about an axis x, θ—angler of rotation about an axis y, α—angler of rotation about an axis z.

Let's describe BCS $E_0 = (\mathbf{o}_0, [\mathbf{e}_0])$, where $\mathbf{o}_0$—the origin of coordinates of BCS; $[\mathbf{e}_0]$—the orts of BCS (Fig. 1). For the angles, vectors and matrixes of rotation the lower index is number of the coordinates system (CS), the top index is number of CS relative which is defined angular and linear displacements, the second top index designates number CS in which coordinates of vectors are calculated. Matrixes of rotation $\mathbf{c}_j^i$ are described by $\mathbf{c}_j^i\left(\varphi_j^i\right) = \mathbf{c}_1(\beta_j^i) \cdot \mathbf{c}_2(\theta_j^i) \cdot \mathbf{c}_3(\alpha_j^i)$, where $\varphi_j^i = \left[\begin{array}{ccc} \beta_j^i & \theta_j^i & \alpha_j^i \end{array}\right]^{\mathrm{T}}$, β_j^i, θ_j^i and α_j^i—angles of the elementary rotations about axes x, y and z respectively; matrixes of the elementary rotations are described by:

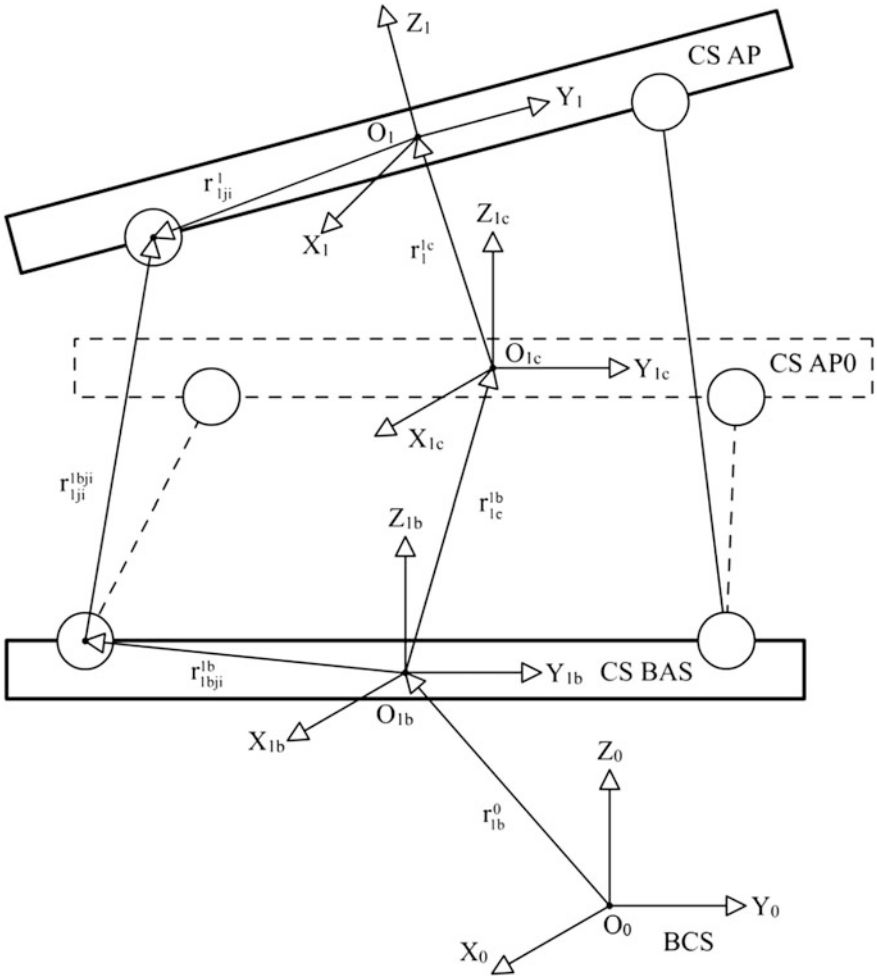

Fig. 1 The coordinates system of basic block of SEMS

$$\mathbf{c}_1(\beta_j^i) = \begin{bmatrix} 1 & 0 & 0 \\ 0 & \cos(\beta_j^i) & -\sin(\beta_j^i) \\ 0 & \sin(\beta_j^i) & \cos(\beta_j^i) \end{bmatrix}; \mathbf{c}_2(\theta_j^i) = \begin{bmatrix} \cos(\theta_j^i) & 0 & \sin(\theta_j^i) \\ 0 & 1 & 0 \\ -\sin(\theta_j^i) & 0 & \cos(\theta_j^i) \end{bmatrix}; \mathbf{c}_3(\alpha_j^{jc})$$
$$= \begin{bmatrix} \cos(\alpha_j^i) & -\sin(\alpha_j^i) & 0 \\ \sin(\alpha_j^i) & \cos(\alpha_j^i) & 0 \\ 0 & 0 & 1 \end{bmatrix}.$$

Let's define the bound coordinate system for basis CS BAS $E_{1b} = (\mathbf{o}_{1b}, [\mathbf{e}_{1b}])$, where $\mathbf{o}_{1b}$—the origin of CS BAS, it is described relative the BCS by coordinates

$\mathbf{r}_{1b}^{0,0}$; [$\mathbf{e}_{1b}$]—the orts of CS BAS, φ_{1b}^{0}—the anglers of rotation of CS BAS relative the BCS.

Let's define the CS AP0 which describe the initial location of AP E_{1c} = ($\mathbf{o}_{1c}$, [$\mathbf{e}_{1c}$]), where $\mathbf{o}_{1c}$—the origin of CS AP0, it is described relative the CS BAS by coordinates $\mathbf{r}_{1c}^{1b,1b}$; [e_{1c}]—the orts of CS AP0, φ_{1c}^{1b}—the anglers of rotation of CS AP0 relative the CS BAS.

Let's define the bound CS AP which describe the location of AP E_1 = ($\mathbf{o}_1$, [$\mathbf{e}_1$]), where $\mathbf{o}_1$—the origin of CS AP, it is described relative the CS AP0 by coordinates $\mathbf{r}_1^{1c,1c}$; [$\mathbf{e}_1$]—the orts of CS AP, φ_1^{1c}—the anglers of rotation of CS AP relative the CS AP0.

The linear displacements of CS AP relative the BCS are described by vector $\mathbf{r}_1^0$, the coordinates in the BCS can be calculated by formula $\mathbf{r}_1^{0,0} = \mathbf{r}_{1b}^{0,0} + \mathbf{c}_{1b}^{0}\left[\mathbf{r}_{1c}^{1b,1b} + \mathbf{c}_{1c}^{1b}\mathbf{r}_1^{1c,1c}\right]$, and rotation can be obtained by $\mathbf{c}_1^0 = \mathbf{c}_{1b}^{0}\mathbf{c}_{1c}^{1b}\mathbf{c}_1^{1c}$, where $\mathbf{c}_i^j$—matrixes of rotation of anglers φ_i^j respectively.

Let's define the coordinates of fastening of hinges on the basis in CS BAS: $\mathbf{r}_{1bj1}^{1b,1b}, \mathbf{r}_{1bj2}^{1b,1b}, \ldots, \mathbf{r}_{1bji}^{1b,1b}, \ldots, \mathbf{r}_{1bjn}^{1b,1b}$, where the lower index designates the number of hinges on the basis. Let's similarly define coordinates of fastening of hinges on an adaptive platform into CS AP: $\mathbf{r}_{1j1}^{1,1}, \mathbf{r}_{1j2}^{1,1}, \ldots, \mathbf{r}_{1ji}^{1,1}, \ldots, \mathbf{r}_{1jn}^{1,1}$, where the lower index designates the number of hinge on the AP.

The current lengths of actuators can be determined as distance between the corresponding hinges of the basis and AP by a formula $l_{1ji}^{1bji} = \left|\mathbf{r}_{1ji}^{1bji,1b}\right| = \left|\mathbf{r}_{1ji}^{1b,1b} - \mathbf{r}_{1bji}^{1b,1b}\right|, i = 1\ldots6$, where $\mathbf{r}_{1ji}^{1b,1b}$—coordinates of a point of fastening of hinges on the lower platform in CS BAS, it can be calculated as follows: $\mathbf{r}_{1ji}^{1b,1b} = \mathbf{r}_{1c}^{1b,1b} + \mathbf{c}_{1c}^{1b}\left[\mathbf{r}_1^{1c,1c} + \mathbf{c}_1^{1c}\mathbf{r}_{1ji}^{1,1}\right], i = 1\ldots n$. As a result expression for the current lengths will take a form:

$$l_{1ji}^{1bji} = \left|\mathbf{r}_{1c}^{1b,1b} + \mathbf{c}_{1c}^{1b}\left[\mathbf{r}_1^{1c,1c} + \mathbf{c}_1^{1c}\mathbf{r}_{1ji}^{1,1}\right] - \mathbf{r}_{1bji}^{1b,1b}\right| = l_{0i} + \Delta l_{ai}, i = 1\ldots n, \qquad (1)$$

where l_{0i}—the initial values of lengths of actuators, $l_{0i} = \left|\mathbf{r}_{1c}^{1b,1b} + \mathbf{c}_{1c}^{1b}\mathbf{r}_{1ji}^{1,1} - \mathbf{r}_{1bji}^{1b,1b}\right|$; Δl_{ai}—the current lengthenings of rods of actuators; $\Delta l_{ai} = \tau_i + \frac{\psi_i}{I_i}$, τ_i—the deformation of the actuator, ψ_i—the actuator engine rotor angle, I_i—transmission ratio of a reducer.

Having differentiated $\mathbf{r}_1^{0,0}$ and $\mathbf{c}_1^0$, and having considered properties of skew-symmetric matrixes, we will receive expressions for the linear $\mathbf{v}_1^{0,0}$ and angular $\boldsymbol{\omega}_1^{0,0}$ velocities of AP in BCS:

$$\mathbf{v}_1^{0,0} = \mathbf{v}_{1b}^{0,0} + \mathbf{c}_{1b}^{0}\left\langle\mathbf{r}_{1c}^{1b,1b} + \mathbf{c}_{1c}^{1b}\mathbf{r}_1^{1c,1c}\right\rangle^{\mathrm{T}}\boldsymbol{\omega}_{1b}^{0,1b} + \mathbf{c}_{1b}^{0}\mathbf{c}_{1c}^{1b}\mathbf{v}_1^{1c,1c}, \boldsymbol{\omega}_1^{0,0} = \mathbf{c}_{1b}^{0}\boldsymbol{\omega}_{1b}^{0,1b} + \mathbf{c}_1^{0}\boldsymbol{\omega}_1^{1c,1}, \qquad (2)$$

where $\mathbf{v}_{1b}^{0,0}$—the linear velocity of BAS into BCS; $\boldsymbol{\omega}_{1b}^{0,1b}$—the angular velocity of BAS relative the BCS into CS BAS; <…>—the skew-symmetric matrix of type $\left\langle [x,y,z]^{\mathrm{T}} \right\rangle = \begin{bmatrix} 0 & -z & y \\ z & 0 & -x \\ -y & x & 0 \end{bmatrix}$; $\mathbf{v}_1^{1c,1c}$—the linear velocity of AP into CS AP0; $\boldsymbol{\omega}_1^{1c,1}$—the angular velocity of AP relative the CS AP0 into CS AP.

The angular velocities $\boldsymbol{\omega}_1^{0,0}$, $\boldsymbol{\omega}_{1b}^{0,1b}$ and $\boldsymbol{\omega}_1^{1c,1}$ can be defined by using velocities of elementary rotations $\dot{\boldsymbol{\varphi}}_1^0$, $\dot{\boldsymbol{\varphi}}_{1b}^0$ и $\dot{\boldsymbol{\varphi}}_1^{1c}$:

$$\boldsymbol{\omega}_{1b}^{0,1b} = \boldsymbol{\varepsilon}_{1b}^0 \dot{\boldsymbol{\varphi}}_{1b}^0; \quad \boldsymbol{\omega}_1^{1c,1} = \boldsymbol{\varepsilon}_1^{1c} \dot{\boldsymbol{\varphi}}_1^{1c}; \quad \boldsymbol{\omega}_1^{0,0} = \mathbf{c}_1^0 \boldsymbol{\varepsilon}_1^0 \dot{\boldsymbol{\varphi}}_1^0,$$

where $\boldsymbol{\varepsilon}_j^i$—the Euler's matrix $\boldsymbol{\varepsilon}_j^i = \left[\mathbf{c}_3^{\mathrm{T}}\left(\alpha_j^i\right) \mathbf{c}_2^{\mathrm{T}}\left(\theta_j^i\right) \mathbf{e}_x | \mathbf{c}_3^{\mathrm{T}}\left(\alpha_j^i\right) \mathbf{e}_y | \mathbf{e}_z \right]$, $\mathbf{e}_x = [1\ 0\ 0]^{\mathrm{T}}$, $\mathbf{e}_y = [0\ 1\ 0]^{\mathrm{T}}$, $\mathbf{e}_z = [0\ 0\ 1]^{\mathrm{T}}$.

Let's find velocities of lengthenings of actuators $\dot{l}_{1ji}^{1bji}$ as a result of differentiation of (1):

$$\dot{l}_{1ji}^{1bji} = \frac{\mathbf{v}_{1ji}^{1bji,1b,\mathrm{T}} \mathbf{r}_{1ji}^{1bji,1b}}{l_{1ji}^{1bji}} = v_{ai} + \dot{\tau}_i, i = 1 \ldots n, \tag{3}$$

where v_{ai}—the velocities of lengthening of rods of actuators which in case of the screw gear can be determined by a formula $v_{ai} = \frac{\Omega_i}{I_i}$, Ω_i—the angular velocity of the engine; $\dot{\tau}_i$—velocity of deformation of the actuator; $\mathbf{v}_{1ji}^{1bji,1b} = \mathbf{c}_{1c}^{1b} \mathbf{v}_1^{1c,1c} + \mathbf{c}_{1c}^{1b} \mathbf{c}_1^{1c} \left\langle \mathbf{r}_{1ji}^{1,1} \right\rangle^{\mathrm{T}} \boldsymbol{\varepsilon}_1^{1c} \dot{\boldsymbol{\varphi}}_1^{1c}$—the velocities of the relative linear displacements of hinges of one actuator in CS BAS.

2 Linearized Dynamical Equations of the SEMS Block with n Actuators Without Forces and Torque

Dynamical equations of SEMS platform have an form of [2]:

$$\boldsymbol{\Theta} \dot{\mathbf{V}}_1^{0,1} + \boldsymbol{\Phi}\, \boldsymbol{\Theta}\, \mathbf{V}_1^{0,1} = \boldsymbol{\Xi},$$
$$\mathbf{V}_1^{0,1} = \begin{bmatrix} \mathbf{v}_1^{0,1} \\ \boldsymbol{\omega}_1^{0,1} \end{bmatrix}, \boldsymbol{\Xi} = \begin{bmatrix} \mathbf{F}_1 \\ \mathbf{M}_1 \end{bmatrix}, \boldsymbol{\Phi} = \begin{bmatrix} \left\langle \boldsymbol{\omega}_1^{0,1} \right\rangle & 0 \\ \left\langle \mathbf{v}_1^{0,1} \right\rangle & \left\langle \boldsymbol{\omega}_1^{0,1} \right\rangle \end{bmatrix}, \boldsymbol{\Theta} = \begin{bmatrix} \mathbf{m}_1 & 0 \\ 0 & \mathbf{I}_1 \end{bmatrix}, \tag{4}$$
$$\mathbf{m}_1 = diag(\, m_1 \quad m_1 \quad m_1 \,),$$

where $\boldsymbol{\Theta}$—the matrix of inertia of AP; $\mathbf{v}_1^{0,1}$—the linear velocities of AP relative the BCS into CS AP $\mathbf{v}_1^{0,1} = \mathbf{c}_1^{0,\mathrm{T}} \mathbf{v}_{1b}^{0,0} + \mathbf{c}_1^{0,\mathrm{T}} \mathbf{c}_{1b}^0 \left\langle \mathbf{r}_{1c}^{1b,1b} + \mathbf{c}_{1c}^{1b} \mathbf{r}_1^{1c,1c} \right\rangle^{\mathrm{T}} \boldsymbol{\omega}_{1b}^{0,1b} + \mathbf{c}_1^{1c,\mathrm{T}} \mathbf{v}_1^{1c,1c}$; $\boldsymbol{\omega}_1^{0,1}$—the angular velocity of AP relative the BCS into CS AP

$\boldsymbol{\omega}_1^{0,1} = \mathbf{c}_1^{0,\mathrm{T}}\mathbf{c}_{1b}^{0}\boldsymbol{\omega}_{1b}^{0,1b} + \boldsymbol{\omega}_1^{1c,1}$; $\mathbf{V}_1^{0,1}$—the vector of velocities of AP; $\mathbf{F}_1$—the vector of forces operating on AP in CS AP; $\mathbf{M}_1$—the vector of torques operating on AP in CS; $\boldsymbol{\Xi}$—the vector of forces and the torques operating on AP in CS AP; m_1—mass of AP; $\mathbf{I}_1$—the moment of inertia matrix of AP.

Taking into account the kinematic scheme (Fig. 1.) the vector of velocities $\mathbf{V}_1^{0,1}$ can be defined as follows:

$$\begin{gathered}\mathbf{V}_1^{0,1} = \mathbf{M}_1^{1c}\dot{\mathbf{q}}_1^{1c} + \mathbf{L}_1^{1c,\mathrm{T}}\mathbf{L}_{1c}^{1b,\mathrm{T}}\mathbf{M}_{1b}^{0}\dot{\mathbf{q}}_{1b}^{0},\\ \mathbf{M}_1^{1c} = \begin{bmatrix}\mathbf{c}_1^{1c,\mathrm{T}} & 0\\ 0 & \boldsymbol{\varepsilon}_1^{1c}\end{bmatrix},\ \mathbf{L}_1^{1c} = \begin{bmatrix}\mathbf{c}_1^{1c} & 0\\ \left\langle \mathbf{r}_1^{1c,1c}\right\rangle \mathbf{c}_1^{1c} & \mathbf{c}_1^{1c}\end{bmatrix},\\ \mathbf{L}_{1c}^{1b} = \begin{bmatrix}\mathbf{c}_{1c}^{1b} & 0\\ \left\langle \mathbf{r}_{1c}^{1b,1b}\right\rangle \mathbf{c}_{1c}^{1b} & \mathbf{c}_{1c}^{1b}\end{bmatrix},\ \mathbf{M}_{1b}^{0} = \begin{bmatrix}\mathbf{c}_{1b}^{0,\mathrm{T}} & 0\\ 0 & \boldsymbol{\varepsilon}_{1b}^{0}\end{bmatrix},\ \mathbf{q}_1^{1c} = \begin{bmatrix}\mathbf{r}_1^{1c,1c}\\ \varphi_1^{1c}\end{bmatrix},\ \mathbf{q}_{1b}^{0} = \begin{bmatrix}\mathbf{r}_{1b}^{0,0}\\ \varphi_{1b}^{0}\end{bmatrix},\end{gathered} \tag{5}$$

where $\mathbf{M}_1^{1c}$ and $\mathbf{M}_{1b}^{0}$—the matrixes of transformation of velocities of AP to the generalized velocities; $\mathbf{L}_1^{1c}$ and $\mathbf{L}_{1c}^{1b}$—the transformation matrixes of CS; $\mathbf{q}_1^{1c}$—generalized coordinates of AP; $\mathbf{q}_{1b}^{0}$—the generalized coordinates of the BAS.

To define accelerations $\dot{\mathbf{V}}_1^{0,1}$, we will differentiate (5):

$$\begin{aligned}\dot{\mathbf{V}}_1^{0,1} &= \mathbf{M}_1^{1c}\ddot{\mathbf{q}}_1^{1c} + \mathbf{L}_1^{1c,\mathrm{T}}\mathbf{L}_{1c}^{1b,\mathrm{T}}\mathbf{M}_{1b}^{0}\ddot{\mathbf{q}}_{1b}^{0} + \dot{\mathbf{M}}_1^{1c}\dot{\mathbf{q}}_1^{1c} + \mathbf{L}_1^{1c,\mathrm{T}}\mathbf{L}_{1c}^{1b,\mathrm{T}}\dot{\mathbf{M}}_{1b}^{0}\dot{\mathbf{q}}_{1b}^{0} + \dot{\mathbf{L}}_1^{1c,\mathrm{T}}\mathbf{L}_{1c}^{1b,\mathrm{T}}\mathbf{M}_{1b}^{0}\dot{\mathbf{q}}_{1b}^{0}\\ &= \mathbf{M}_1^{1c}\ddot{\mathbf{q}}_1^{1c} + \dot{\mathbf{M}}_1^{1c}\dot{\mathbf{q}}_1^{1c} + \mathbf{L}_1^{1c,\mathrm{T}}\mathbf{L}_{1c}^{1b,\mathrm{T}}\mathbf{M}_{1b}^{0}\ddot{\mathbf{q}}_{1b}^{0} + \left[\boldsymbol{\Lambda}_1^{1c,\mathrm{T}}\mathbf{L}_{1c}^{1b,\mathrm{T}}\dot{\mathbf{M}}_{1b}^{0} + \boldsymbol{\Phi}_1^{1c,1,\mathrm{T}}\mathbf{L}_1^{1c,\mathrm{T}}\mathbf{L}_{1c}^{1b,\mathrm{T}}\mathbf{M}_{1b}^{0}\right]\dot{\mathbf{q}}_{1b}^{0},\end{aligned} \tag{6}$$

where $\dot{\mathbf{L}}_1^{1c} = \mathbf{L}_1^{1c}\boldsymbol{\Phi}_1^{1c,1}$. Having substituted (5) and (6) in (4) we will get:

$$\begin{aligned}&\boldsymbol{\Theta}_1^{1}\mathbf{M}_1^{1c}\ddot{\mathbf{q}}_1^{1c} + \left[\boldsymbol{\Theta}_1^{1}\dot{\mathbf{M}}_1^{1c} + \boldsymbol{\Phi}_1^{0,1}\boldsymbol{\Theta}_1^{1}\mathbf{M}_1^{1c}\right]\dot{\mathbf{q}}_1^{1c} = \boldsymbol{\Xi}_1^{1} - \boldsymbol{\Theta}_1^{1}\mathbf{L}_1^{1c,\mathrm{T}}\mathbf{L}_{1c}^{1b,\mathrm{T}}\mathbf{M}_{1b}^{0}\ddot{\mathbf{q}}_{1b}^{0}\\ &\quad - \left[\boldsymbol{\Phi}_1^{0,1}\boldsymbol{\Theta}_1^{1}\mathbf{L}_1^{1c,\mathrm{T}}\mathbf{L}_{1c}^{1b,\mathrm{T}}\mathbf{M}_{1b}^{0} + \boldsymbol{\Theta}_1^{1}\mathbf{L}_1^{1c,\mathrm{T}}\mathbf{L}_{1c}^{1b,\mathrm{T}}\dot{\mathbf{M}}_{1b}^{0} + \boldsymbol{\Theta}_1^{1}\boldsymbol{\Phi}_1^{1c,1,\mathrm{T}}\mathbf{L}_1^{1c,\mathrm{T}}\mathbf{L}_{1c}^{1b,\mathrm{T}}\mathbf{M}_{1b}^{0}\right]\dot{q}_{1b}^{0}.\end{aligned} \tag{7}$$

Having multiplied (7) by a matrix $\mathbf{M}_1^{1c,\mathrm{T}}$ we will pass to the generalized forces:

$$\begin{aligned}&\mathbf{M}_1^{1c,\mathrm{T}}\boldsymbol{\Theta}_1^{1}\mathbf{M}_1^{1c}\ddot{\mathbf{q}}_1^{1c} + \mathbf{M}_1^{1c,\mathrm{T}}\left[\boldsymbol{\Theta}_1^{1}\dot{\mathbf{M}}_1^{1c} + \boldsymbol{\Phi}_1^{0,1}\boldsymbol{\Theta}_1^{1}\mathbf{M}_1^{1c}\right]\dot{\mathbf{q}}_1^{1c}\\ &\quad = \mathbf{M}_1^{1c,\mathrm{T}}\boldsymbol{\Xi}_1^{1} - \mathbf{M}_1^{1c,\mathrm{T}}\boldsymbol{\Theta}_1^{1}\mathbf{L}_1^{1c,\mathrm{T}}\mathbf{L}_{1c}^{1b,\mathrm{T}}\mathbf{M}_{1b}^{0}\ddot{\mathbf{q}}_{1b}^{0}\\ &\quad - \mathbf{M}_1^{1c,\mathrm{T}}\left[\boldsymbol{\Phi}_1^{0,1}\boldsymbol{\Theta}_1^{1}\mathbf{L}_1^{1c,\mathrm{T}}\mathbf{L}_{1c}^{1b,\mathrm{T}}\mathbf{M}_{1b}^{0} + \boldsymbol{\Theta}_1^{1}\mathbf{L}_1^{1c,\mathrm{T}}\mathbf{L}_{1c}^{1b,\mathrm{T}}\dot{\mathbf{M}}_{1b}^{0} + \boldsymbol{\Theta}_1^{1}\boldsymbol{\Phi}_1^{1c,1,\mathrm{T}}\mathbf{L}_1^{1c,\mathrm{T}}\mathbf{L}_{1c}^{1b,\mathrm{T}}\mathbf{M}_{1b}^{0}\right]\dot{\mathbf{q}}_{1b}^{0}.\end{aligned} \tag{8}$$

Having entered new designations, we will pass to more compact record:

$$\mathbf{A}\left(\mathbf{q}_1^{1c}\right)\ddot{\mathbf{q}}_1^{1c} + \mathbf{B}\left(\mathbf{q}_1^{1c}, \dot{\mathbf{q}}_1^{1c}, \mathbf{q}_{1b}^{0}, \dot{\mathbf{q}}_{1b}^{0}\right)\dot{\mathbf{q}}_1^{1c} = \mathbf{Q}_{\xi}\left(\boldsymbol{\theta}_1^{1c}, \dot{\mathbf{q}}_1^{1c}, \mathbf{q}_{1b}^{0}, \mathbf{u}, \mathbf{p}\right) + \mathbf{Q}_0\left(\mathbf{q}_1^{1c}, \dot{\mathbf{q}}_1^{1c}, \mathbf{q}_{1b}^{0}, \dot{\mathbf{q}}_{1b}^{0}, \ddot{\mathbf{q}}_{1b}^{0}\right), \tag{9}$$

where $\mathbf{u} = [\psi_1, \ldots, \psi_n, \Omega_1, \ldots, \Omega_n]^{\mathrm{T}}$—data-ins in platform model from models of electric drives, $\mathbf{p}$—data-ins in platform model from models of external loadings,

$$\begin{gathered}\mathbf{A}\left(\mathbf{q}_1^{1c}\right) = \mathbf{M}_1^{1c,\mathrm{T}}\boldsymbol{\Theta}_1^1\mathbf{M}_1^{1c}, \mathbf{B}\left(\mathbf{q}_1^{1c}, \dot{\mathbf{q}}_1^{1c}, \mathbf{q}_{1b}^0, \dot{\mathbf{q}}_{1b}^0\right) = \mathbf{M}_1^{1c,\mathrm{T}}\left[\boldsymbol{\Theta}_1^1\dot{\mathbf{M}}_1^{1c} + \boldsymbol{\Phi}_1^{0,1}\boldsymbol{\Theta}_1^1\mathbf{M}_1^{1c}\right], \\ \mathbf{Q}_0\left(\mathbf{q}_1^{1c}, \dot{\mathbf{q}}_1^{1c}, \mathbf{q}_{1b}^0, \dot{\mathbf{q}}_{1b}^0, \ddot{\mathbf{q}}_{1b}^0\right) = -\mathbf{A}_0\left(\mathbf{q}_1^{1c}, \mathbf{q}_{1b}^0\right)\ddot{\mathbf{q}}_{1b}^0 - \mathbf{B}_0\left(\mathbf{q}_1^{1c}, \dot{\mathbf{q}}_1^{1c}, \mathbf{q}_{1b}^0, \dot{\mathbf{q}}_{1b}^0\right)\dot{\mathbf{q}}_{1b}^0, \\ \mathbf{Q}_\xi\left(\mathbf{q}_1^{1c}, \dot{\mathbf{q}}_1^{1c}, \mathbf{q}_{1b}^0, \mathbf{u}, \mathbf{p}\right) = \mathbf{M}_1^{1c,\mathrm{T}}\boldsymbol{\Xi}_1^1, \mathbf{A}_0\left(\mathbf{q}_1^{1c}, \mathbf{q}_{1b}^0\right) = \mathbf{M}_1^{1c,\mathrm{T}}\boldsymbol{\Theta}_1^1\mathbf{L}_1^{1c,\mathrm{T}}\mathbf{L}_{1c}^{1b,\mathrm{T}}\mathbf{M}_{1b}^0, \\ \mathbf{B}_0\left(\mathbf{q}_1^{1c}, \dot{\mathbf{q}}_1^{1c}, \mathbf{q}_{1b}^0, \dot{\mathbf{q}}_{1b}^0\right) = \mathbf{M}_1^{1c,\mathrm{T}}\left[\boldsymbol{\Theta}_1^1\mathbf{L}_1^{1c,\mathrm{T}}\mathbf{L}_{1c}^{1b,\mathrm{T}}\dot{\mathbf{M}}_{1b}^0 + \boldsymbol{\Theta}_1^1\boldsymbol{\Phi}_1^{1c,1,\mathrm{T}}\mathbf{L}_1^{1c,\mathrm{T}}\mathbf{L}_{1c}^{1b,\mathrm{T}}\mathbf{M}_{1b}^0 + \boldsymbol{\Phi}_1^{0,1}\boldsymbol{\Theta}_1^1\mathbf{L}_1^{1c,\mathrm{T}}\mathbf{L}_{1c}^{1b,\mathrm{T}}\mathbf{M}_{1b}^0\right].\end{gathered}$$

We linearize Eq. (9) in a stationary point $\mathbf{X}_{fix} = \left[\mathbf{q}_{1,fix}^{1c}; \dot{\mathbf{q}}_{1,fix}^{1c}; \ddot{\mathbf{q}}_{1,fix}^{1c}; \mathbf{q}_{1b,fix}^0; \dot{\mathbf{q}}_{1b,fix}^0; \ddot{\mathbf{q}}_{1b,fix}^0; \mathbf{u}_{fix}; \mathbf{p}_{fix}\right]$ by an expansion in a series of Taylor.

We linearize the first item:

$$\mathbf{A}\left(\mathbf{q}_1^{1c}\right)\ddot{\mathbf{q}}_1^{1c} \approx \mathbf{A}\left(\mathbf{q}_{1,fix}^{1c}\right)\ddot{\mathbf{q}}_{1,fix}^{1c} + \mathbf{J}_{\mathbf{q}_1^{1c}}\left(\mathbf{A}\left(\mathbf{q}_1^{1c}\right)\ddot{\mathbf{q}}_1^{1c}\right)_{\mathbf{X}_{fix}}\delta\mathbf{q}_1^{1c} + \mathbf{J}_{\ddot{\mathbf{q}}_1^{1c}}\left(\mathbf{A}\left(\mathbf{q}_1^{1c}\right)\ddot{\mathbf{q}}_1^{1c}\right)_{\mathbf{X}_{fix}}\delta\ddot{\mathbf{q}}_1^{1c}, \tag{10}$$

which in case of coincidence of a center of mass with origin of CS AP has a form:

$$\begin{aligned}\mathbf{A}\left(\mathbf{q}_1^{1c}\right)\ddot{\mathbf{q}}_1^{1c} &= \mathbf{M}_1^{1c,\mathrm{T}}\boldsymbol{\Theta}_1^1\mathbf{M}_1^{1c}\ddot{\mathbf{q}}_1^{1c} = \begin{bmatrix}\mathbf{c}_1^{1c} & 0\\ 0 & \boldsymbol{\varepsilon}_1^{1c,\mathrm{T}}\end{bmatrix}\begin{bmatrix}\mathbf{m}_1 & 0\\ 0 & \mathbf{I}_1\end{bmatrix}\begin{bmatrix}\mathbf{c}_1^{1c,\mathrm{T}} & 0\\ 0 & \boldsymbol{\varepsilon}_1^{1c}\end{bmatrix}\begin{bmatrix}\ddot{\mathbf{r}}_1^{1c,1c}\\ \ddot{\varphi}_1^{1c}\end{bmatrix} \\ &= \begin{bmatrix}\mathbf{m}_1 & 0\\ 0 & \boldsymbol{\varepsilon}_1^{1c,\mathrm{T}}\mathbf{I}_1\boldsymbol{\varepsilon}_1^{1c}\end{bmatrix}\begin{bmatrix}\ddot{\mathbf{r}}_1^{1c,1c}\\ \ddot{\varphi}_1^{1c}\end{bmatrix} = \begin{bmatrix}\mathbf{m}_1\ddot{\mathbf{r}}_1^{1c,1c} & 0\\ 0 & \boldsymbol{\varepsilon}_1^{1c,\mathrm{T}}\mathbf{I}_1\boldsymbol{\varepsilon}_1^{1c}\ddot{\varphi}_1^{1c}\end{bmatrix},\end{aligned} \tag{11}$$

then the first variation from (11) is defined as follows:

$$\begin{aligned}\delta\left(\mathbf{A}\left(\mathbf{q}_1^{1c}\right)\ddot{\mathbf{q}}_1^{1c}\right) &= \begin{bmatrix}\mathbf{m}_1\delta\ddot{\mathbf{r}}_1^{1c,1c} & 0\\ 0 & \delta\boldsymbol{\varepsilon}_1^{1c,\mathrm{T}}\mathbf{I}_1\boldsymbol{\varepsilon}_1^{1c}\ddot{\varphi}_1^{1c} + \boldsymbol{\varepsilon}_1^{1c,\mathrm{T}}\mathbf{I}_1\delta\boldsymbol{\varepsilon}_1^{1c}\ddot{\varphi}_1^{1c} + \boldsymbol{\varepsilon}_1^{1c,\mathrm{T}}\mathbf{I}_1\boldsymbol{\varepsilon}_1^{1c}\delta\ddot{\varphi}_1^{1c}\end{bmatrix} \\ &= \begin{bmatrix}0 & 0\\ 0 & \delta\boldsymbol{\varepsilon}_1^{1c,\mathrm{T}}\mathbf{I}_1\boldsymbol{\varepsilon}_1^{1c}\ddot{\varphi}_1^{1c} + \boldsymbol{\varepsilon}_1^{1c,\mathrm{T}}\mathbf{I}_1\delta\boldsymbol{\varepsilon}_1^{1c}\ddot{\varphi}_1^{1c}\end{bmatrix} + \begin{bmatrix}\mathbf{m}_1 & 0\\ 0 & \boldsymbol{\varepsilon}_1^{1c,\mathrm{T}}\mathbf{I}_1\boldsymbol{\varepsilon}_1^{1c}\end{bmatrix}\delta\ddot{\mathbf{q}}_1^{1c},\end{aligned} \tag{12}$$

where $\delta\boldsymbol{\varepsilon}_1^{1c}$ has a form:

$$\begin{gathered}\delta\boldsymbol{\varepsilon}_1^{1c} = \boldsymbol{\lambda}_{1,1}^{1c}\delta\beta_1^{1c} + \boldsymbol{\lambda}_{1,2}^{1c}\delta\theta_1^{1c} + \boldsymbol{\lambda}_{1,3}^{1c}\delta\alpha_1^{1c}, \boldsymbol{\lambda}_{1,1}^{1c} = 0, \\ \boldsymbol{\lambda}_{1,2}^{1c} = \begin{bmatrix}-\cos\left(\alpha_1^{1c}\right)\sin\left(\theta_1^{1c}\right) & 0 & 0\\ \sin\left(\alpha_1^{1c}\right)\cos\left(\theta_1^{1c}\right) & 0 & 0\\ \cos\left(\theta_1^{1c}\right) & 0 & 0\end{bmatrix}, \boldsymbol{\lambda}_{1,3}^{1c} = \begin{bmatrix}-\sin\left(\alpha_1^{1c}\right)\cos\left(\theta_1^{1c}\right) & \cos\left(\alpha_1^{1c}\right) & 0\\ -\cos\left(\alpha_1^{1c}\right)\cos\left(\theta_1^{1c}\right) & -\sin\left(\alpha_1^{1c}\right) & 0\\ 0 & 0 & 0\end{bmatrix}.\end{gathered} \tag{13}$$

Taking into account (13) we will calculate expression:

$$\delta\left(\boldsymbol{\varepsilon}_1^{1c,\mathrm{T}}\mathbf{I}_1\boldsymbol{\varepsilon}_1^{1c}\right)\ddot{\varphi}_1^{1c} = \boldsymbol{\lambda}_{1,1}^{1c}\ddot{\varphi}_1^{1c}\delta\beta_1^{1c} + \left[\boldsymbol{\lambda}_{1,2}^{1c,\mathrm{T}}\mathbf{I}_1\boldsymbol{\varepsilon}_1^{1c} + \boldsymbol{\varepsilon}_1^{1c,\mathrm{T}}\mathbf{I}_1\boldsymbol{\lambda}_{1,2}^{1c}\right]\ddot{\varphi}_1^{1c}\delta\theta_1^{1c}$$
$$+ \left[\boldsymbol{\lambda}_{1,3}^{1c,\mathrm{T}}\mathbf{I}_1\boldsymbol{\varepsilon}_1^{1c} + \boldsymbol{\varepsilon}_1^{1c,\mathrm{T}}\mathbf{I}_1\boldsymbol{\lambda}_{1,3}^{1c}\right]\ddot{\varphi}_1^{1c}\delta\alpha_1^{1c} = \boldsymbol{\gamma}_1\delta\varphi_1^{1c},$$
$$\boldsymbol{\gamma}_1 = \left[\boldsymbol{\lambda}_{1,1}^{1c}\ddot{\varphi}_1^{1c}|\boldsymbol{\lambda}_{1,2}^{1c,\mathrm{T}}\mathbf{I}_1\boldsymbol{\varepsilon}_1^{1c}\ddot{\varphi}_1^{1c} + \boldsymbol{\varepsilon}_1^{1c,\mathrm{T}}\mathbf{I}_1\boldsymbol{\lambda}_{1,2}^{1c}\ddot{\varphi}_1^{1c}|\boldsymbol{\lambda}_{1,3}^{1c,\mathrm{T}}\mathbf{I}_1\boldsymbol{\varepsilon}_1^{1c}\ddot{\varphi}_1^{1c} + \boldsymbol{\varepsilon}_1^{1c,\mathrm{T}}\mathbf{I}_1\boldsymbol{\lambda}_{1,3}^{1c}\ddot{\varphi}_1^{1c}\right]. \tag{14}$$

Then Jacobians in (10) are calculated on formulas:

$$\mathbf{J}_{\mathbf{q}_1^{1c}}\left(\mathbf{A}\left(\mathbf{q}_1^{1c}\right)\ddot{\mathbf{q}}_1^{1c}\right)_{\mathbf{X}_{fix}} = \begin{bmatrix} 0 & 0 \\ 0 & \boldsymbol{\gamma}_1 \end{bmatrix}, \mathbf{J}_{\ddot{\mathbf{q}}_1^{1c}}\left(\mathbf{A}\left(\mathbf{q}_1^{1c}\right)\ddot{\mathbf{q}}_1^{1c}\right)_{\mathbf{X}_{fix}} = \begin{bmatrix} \mathbf{m}_1 & 0 \\ 0 & \boldsymbol{\varepsilon}_1^{1c,\mathrm{T}}\mathbf{I}_1\boldsymbol{\varepsilon}_1^{1c} \end{bmatrix}. \tag{15}$$

We linearize the second item in (9):

$$\mathbf{B}\left(\mathbf{q}_1^{1c}, \dot{\mathbf{q}}_1^{1c}, \mathbf{q}_{1b}^0, \dot{\mathbf{q}}_{1b}^0\right)\dot{\mathbf{q}}_1^{1c} \approx \mathbf{B}\left(\mathbf{q}_{1,fix}^{1c}, \dot{\mathbf{q}}_{1,fix}^{1c}, \mathbf{q}_{1b,fix}^0, \dot{\mathbf{q}}_{1b,fix}^0\right)\dot{\mathbf{q}}_{1,fix}^{1c}$$
$$+ \mathbf{J}_{\mathbf{q}_1^{1c}}\left(\mathbf{B}\dot{\mathbf{q}}_1^{1c}\right)_{\mathbf{X}_{fix}}\delta\mathbf{q}_1^{1c} + \mathbf{J}_{\dot{\mathbf{q}}_1^{1c}}\left(\mathbf{B}\dot{\mathbf{q}}_1^{1c}\right)_{\mathbf{X}_{fix}}\delta\dot{\mathbf{q}}_1^{1c} + \mathbf{J}_{\mathbf{q}_{1b}^0}\left(\mathbf{B}\dot{\mathbf{q}}_1^{1c}\right)_{\mathbf{X}_{fix}}\delta\mathbf{q}_{1b}^0 + \mathbf{J}_{\dot{\mathbf{q}}_{1b}^0}\left(\mathbf{B}\dot{\mathbf{q}}_1^{1c}\right)_{\mathbf{X}_{fix}}\delta\dot{\mathbf{q}}_{1b}^0, \tag{16}$$

which in case of coincidence of a center of mass with origin of CS AP has a form:

$$\mathbf{B}\left(\mathbf{q}_1^{1c}, \dot{\mathbf{q}}_1^{1c}, \mathbf{q}_{1b}^0, \dot{\mathbf{q}}_{1b}^0\right)\dot{\mathbf{q}}_1^{1c} = \mathbf{M}_1^{1c,\mathrm{T}}\boldsymbol{\Theta}_1^1\dot{\mathbf{M}}_1^{1c}\dot{\mathbf{q}}_1^{1c} + \mathbf{M}_1^{1c,\mathrm{T}}\boldsymbol{\Phi}_1^{0,1}\boldsymbol{\Theta}_1^1\mathbf{M}_1^{1c}\dot{\mathbf{q}}_1^{1c}$$
$$= \begin{bmatrix} \mathbf{m}_1\left\langle\boldsymbol{\omega}_{1b}^{0,1c}\right\rangle & 0 \\ \mathbf{m}_1\boldsymbol{\varepsilon}_1^{1c,\mathrm{T}}\mathbf{c}_1^{1c,\mathrm{T}}\left\langle\mathbf{v}_1^{0,1c}\right\rangle & \boldsymbol{\varepsilon}_1^{1c,\mathrm{T}}\mathbf{I}_1\dot{\boldsymbol{\varepsilon}}_1^{1c} + \boldsymbol{\varepsilon}_1^{1c,\mathrm{T}}\left\langle\boldsymbol{\omega}_1^{0,1}\right\rangle\mathbf{I}_1\boldsymbol{\varepsilon}_1^{1c} \end{bmatrix}\begin{bmatrix} \dot{\mathbf{r}}_1^{1c,1c} \\ \dot{\boldsymbol{\varphi}}_1^{1c} \end{bmatrix}, \tag{17}$$

then the first variation from (17) is defined as follows:

$$\delta\left(\mathbf{B}\left(\mathbf{q}_1^{1c}, \dot{\mathbf{q}}_1^{1c}, \mathbf{q}_{1b}^0, \dot{\mathbf{q}}_{1b}^0\right)\dot{\mathbf{q}}_1^{1c}\right)$$
$$= \begin{bmatrix} \mathbf{m}_1\left\langle\delta\boldsymbol{\omega}_{1b}^{0,1c}\right\rangle & 0 \\ \mathbf{m}_1\delta\left(\boldsymbol{\varepsilon}_1^{1c,\mathrm{T}}\mathbf{c}_1^{1c,\mathrm{T}}\left\langle\mathbf{v}_1^{0,1c}\right\rangle\right) & \delta\left(\boldsymbol{\varepsilon}_1^{1c,\mathrm{T}}\mathbf{I}_1\dot{\boldsymbol{\varepsilon}}_1^{1c}\right) + \delta\left(\boldsymbol{\varepsilon}_1^{1c,\mathrm{T}}\left\langle\boldsymbol{\omega}_1^{0,1}\right\rangle\mathbf{I}_1\boldsymbol{\varepsilon}_1^{1c}\right) \end{bmatrix}\begin{bmatrix} \dot{\mathbf{r}}_1^{1c,1c} \\ \dot{\boldsymbol{\varphi}}_1^{1c} \end{bmatrix}$$
$$+ \begin{bmatrix} \mathbf{m}_1\left\langle\boldsymbol{\omega}_{1b}^{0,1c}\right\rangle & 0 \\ \mathbf{m}_1\boldsymbol{\varepsilon}_1^{1c,\mathrm{T}}\mathbf{c}_1^{1c,\mathrm{T}}\left\langle\mathbf{v}_1^{0,1c}\right\rangle & \boldsymbol{\varepsilon}_1^{1c,\mathrm{T}}\mathbf{I}_1\dot{\boldsymbol{\varepsilon}}_1^{1c} + \boldsymbol{\varepsilon}_1^{1c,\mathrm{T}}\left\langle\boldsymbol{\omega}_1^{0,1}\right\rangle\mathbf{I}_1\boldsymbol{\varepsilon}_1^{1c} \end{bmatrix}\begin{bmatrix} \delta\dot{\mathbf{r}}_1^{1c,1c} \\ \delta\dot{\boldsymbol{\varphi}}_1^{1c} \end{bmatrix}, \tag{18}$$

where $\delta\boldsymbol{\omega}_{1b}^{0,1c}$ can be got as:

$$\delta\boldsymbol{\omega}_{1b}^{0,1c} = \mathbf{c}_{1c}^{1b,\mathrm{T}}\delta\boldsymbol{\varepsilon}_{1b}^0\dot{\boldsymbol{\varphi}}_{1b}^0 + \mathbf{c}_{1c}^{1b,\mathrm{T}}\boldsymbol{\varepsilon}_{1b}^0\delta\dot{\boldsymbol{\varphi}}_{1b}^0 = \mathbf{c}_{1c}^{1b,\mathrm{T}}\boldsymbol{\gamma}_2\delta\varphi_{1b}^0 + \mathbf{c}_{1c}^{1b,\mathrm{T}}\boldsymbol{\varepsilon}_{1b}^0\delta\dot{\boldsymbol{\varphi}}_{1b}^0,$$
$$\delta\boldsymbol{\varepsilon}_{1b}^0 = \boldsymbol{\lambda}_{1b,1}^0\delta\boldsymbol{\beta}_{1b}^0 + \boldsymbol{\lambda}_{1b,2}^0\delta\theta_{1b}^0 + \boldsymbol{\lambda}_{1b,3}^0\delta\alpha_{1b}^0, \boldsymbol{\gamma}_2 = \left[\boldsymbol{\lambda}_{1b,1}^0\dot{\boldsymbol{\varphi}}_{1b}^0|\boldsymbol{\lambda}_{1b,2}^0\dot{\boldsymbol{\varphi}}_{1b}^0|\boldsymbol{\lambda}_{1b,3}^0\dot{\boldsymbol{\varphi}}_{1b}^0\right]. \tag{19}$$

Let's calculate the item $\delta\left(\boldsymbol{\varepsilon}_1^{1c,\mathrm{T}}\mathbf{c}_1^{1c,\mathrm{T}}\left\langle\mathbf{v}_1^{0,1c}\right\rangle\right)$ on a formula:

$$\begin{aligned}\delta\left(\boldsymbol{\varepsilon}_1^{1c,\mathrm{T}}\mathbf{c}_1^{1c,\mathrm{T}}\left\langle\mathbf{v}_1^{0,1c}\right\rangle\right) &= \delta\,\boldsymbol{\varepsilon}_1^{1c,\mathrm{T}}\mathbf{c}_1^{1c,\mathrm{T}}\left\langle\mathbf{v}_1^{0,1c}\right\rangle + \boldsymbol{\varepsilon}_1^{1c,\mathrm{T}}\delta\mathbf{c}_1^{1c,\mathrm{T}}\left\langle\mathbf{v}_1^{0,1c}\right\rangle + \boldsymbol{\varepsilon}_1^{1c,\mathrm{T}}\mathbf{c}_1^{1c,\mathrm{T}}\left\langle\delta\mathbf{v}_1^{0,1c}\right\rangle \\ &= \delta\boldsymbol{\varepsilon}_1^{1c,\mathrm{T}}\mathbf{c}_1^{1c,\mathrm{T}}\left\langle\mathbf{v}_1^{0,1c}\right\rangle - \boldsymbol{\varepsilon}_1^{1c,\mathrm{T}}\langle\boldsymbol{\varepsilon}_1^{1c}\delta\varphi_1^{1c}\rangle\mathbf{c}_1^{1c,\mathrm{T}}\left\langle\mathbf{v}_1^{0,1c}\right\rangle + \boldsymbol{\varepsilon}_1^{1c,\mathrm{T}}\mathbf{c}_1^{1c,\mathrm{T}}\left\langle\delta\mathbf{v}_1^{0,1c}\right\rangle.\end{aligned} \tag{20}$$

As $\mathbf{v}_1^{0,1c}$ is described by expression (21):

$$\mathbf{v}_1^{0,1c} = \mathbf{c}_{1c}^{1b,\mathrm{T}}\mathbf{c}_{1b}^{0,\mathrm{T}}\dot{\mathbf{r}}_{1b}^{0,0} + \mathbf{c}_{1c}^{1b,\mathrm{T}}\left\langle\mathbf{r}_{1c}^{1b,1b} + \mathbf{c}_{1c}^{1b}\mathbf{r}_1^{1c,1c}\right\rangle^{\mathrm{T}}\boldsymbol{\varepsilon}_{1b}^{0}\dot{\boldsymbol{\varphi}}_{1b}^{0} + \dot{\mathbf{r}}_1^{1c,1c}, \tag{21}$$

then will be:

$$\begin{aligned}\delta\mathbf{v}_1^{0,1c} = {} & \mathbf{c}_{1c}^{1b,\mathrm{T}}\left[\left\langle\mathbf{c}_{1b}^{0,\mathrm{T}}\dot{\mathbf{r}}_{1b}^{0,0}\right\rangle\boldsymbol{\varepsilon}_{1b}^{0} + \left\langle\mathbf{r}_{1c}^{1b,1b} + \mathbf{c}_{1c}^{1b}\mathbf{r}_1^{1c,1c}\right\rangle^{\mathrm{T}}\boldsymbol{\gamma}_2\right]\delta\varphi_{1b}^{0} \\ & + \mathbf{c}_{1c}^{1b,\mathrm{T}}\left\langle\mathbf{r}_{1c}^{1b,1b} + \mathbf{c}_{1c}^{1b}\mathbf{r}_1^{1c,1c}\right\rangle^{\mathrm{T}}\boldsymbol{\varepsilon}_{1b}^{0}\delta\dot{\boldsymbol{\varphi}}_{1b}^{0} + \mathbf{c}_{1c}^{1b,\mathrm{T}}\mathbf{c}_{1b}^{0,\mathrm{T}}\delta\dot{\mathbf{r}}_{1b}^{0,0} \\ & + \left\langle\mathbf{c}_{1c}^{1b,\mathrm{T}}\boldsymbol{\varepsilon}_{1b}^{0}\dot{\boldsymbol{\varphi}}_{1b}^{0}\right\rangle\delta\mathbf{r}_1^{1c,1c} + \delta\dot{\mathbf{r}}_1^{1c,1c}.\end{aligned} \tag{22}$$

Let's calculate the item $\delta\left(\boldsymbol{\varepsilon}_1^{1c,\mathrm{T}}\mathbf{I}_1\dot{\boldsymbol{\varepsilon}}_1^{1c}\right)$ on a formula:

$$\delta\left(\boldsymbol{\varepsilon}_1^{1c,\mathrm{T}}\mathbf{I}_1\dot{\boldsymbol{\varepsilon}}_1^{1c}\right) = \delta\boldsymbol{\varepsilon}_1^{1c,\mathrm{T}}\mathbf{I}_1\dot{\boldsymbol{\varepsilon}}_1^{1c} + \boldsymbol{\varepsilon}_1^{1c,\mathrm{T}}\mathbf{I}_1\delta\dot{\boldsymbol{\varepsilon}}_1^{1c}, \tag{23}$$

where $\delta\dot{\boldsymbol{\varepsilon}}_1^{1c}$ is described as $\dot{\boldsymbol{\varepsilon}}_1^{1c} = \boldsymbol{\lambda}_{1,1}^{1c}\dot{\beta}_1^{1c} + \boldsymbol{\lambda}_{1,2}^{1c}\dot{\theta}_1^{1c} + \boldsymbol{\lambda}_{1c,3}^{1}\dot{\alpha}_1^{1c}$ therefore:

$$\begin{aligned}\delta\dot{\boldsymbol{\varepsilon}}_1^{1c} &= \delta\boldsymbol{\lambda}_{1,1}^{1c}\dot{\beta}_1^{1c} + \delta\boldsymbol{\lambda}_{1,2}^{1c}\dot{\theta}_1^{1c} + \delta\boldsymbol{\lambda}_{1c,3}^{1}\dot{\alpha}_1^{1c} + \boldsymbol{\lambda}_{1,1}^{1c}\delta\dot{\beta}_1^{1c} + \boldsymbol{\lambda}_{1,2}^{1c}\delta\dot{\theta}_1^{1c} + \boldsymbol{\lambda}_{1c,3}^{1}\delta\dot{\alpha}_1^{1c} \\ &= \boldsymbol{\phi}_{1,1}^{1c}\delta\beta_1^{1c} + \boldsymbol{\phi}_{1,2}^{1c}\delta\theta_1^{1c} + \boldsymbol{\phi}_{1,3}^{1c}\delta\alpha_1^{1c} + \boldsymbol{\lambda}_{1,1}^{1c}\delta\dot{\beta}_1^{1c} + \boldsymbol{\lambda}_{1,2}^{1c}\delta\dot{\theta}_1^{1c} + \boldsymbol{\lambda}_{1c,3}^{1}\delta\dot{\alpha}_1^{1c}, \\ \boldsymbol{\phi}_{1,1}^{1c} &= 0, \\ \boldsymbol{\phi}_{1,2}^{1c} &= \begin{bmatrix} -\cos\left(\alpha_1^{1c}\right)\cos\left(\theta_1^{1c}\right)\dot{\theta}_1^{1c} + \sin\left(\alpha_1^{1c}\right)\sin\left(\theta_1^{1c}\right)\dot{\alpha}_1^{1c} & 0 & 0 \\ -\sin\left(\alpha_1^{1c}\right)\sin\left(\theta_1^{1c}\right)\dot{\theta}_1^{1c} + \cos\left(\alpha_1^{1c}\right)\sin\left(\theta_1^{1c}\right)\dot{\alpha}_1^{1c} & 0 & 0 \\ -\sin\left(\theta_1^{1c}\right)\dot{\theta}_1^{1c} & 0 & 0 \end{bmatrix}, \\ \boldsymbol{\phi}_{1,3}^{1c} &= \begin{bmatrix} \sin\left(\alpha_1^{1c}\right)\sin\left(\theta_1^{1c}\right)\dot{\theta}_1^{1c} - \cos\left(\alpha_1^{1c}\right)\cos\left(\theta_1^{1c}\right)\dot{\alpha}_1^{1c} & -\sin\left(\alpha_1^{1c}\right)\dot{\alpha}_1^{1c} & 0 \\ \cos\left(\alpha_1^{1c}\right)\cos\left(\theta_1^{1c}\right)\dot{\theta}_1^{1c} + \sin\left(\alpha_1^{1c}\right)\cos\left(\theta_1^{1c}\right)\dot{\alpha}_1^{1c} & -\cos\left(\alpha_1^{1c}\right)\dot{\alpha}_1^{1c} & 0 \\ 0 & 0 & 0 \end{bmatrix}.\end{aligned} \tag{24}$$

Let's get $\delta\left(\boldsymbol{\varepsilon}_1^{1c,\mathrm{T}}\left\langle\boldsymbol{\omega}_1^{0,1}\right\rangle\mathbf{I}_1\boldsymbol{\varepsilon}_1^{1c}\right)$ by formula:

$$\delta\left(\boldsymbol{\varepsilon}_1^{1c,\mathrm{T}}\left\langle\boldsymbol{\omega}_1^{0,1}\right\rangle\mathbf{I}_1\boldsymbol{\varepsilon}_1^{1c}\right) = \delta\boldsymbol{\varepsilon}_1^{1c,\mathrm{T}}\left\langle\boldsymbol{\omega}_1^{0,1}\right\rangle\mathbf{I}_1\boldsymbol{\varepsilon}_1^{1c} + \boldsymbol{\varepsilon}_1^{1c,\mathrm{T}}\left\langle\delta\boldsymbol{\omega}_1^{0,1}\right\rangle\mathbf{I}_1\boldsymbol{\varepsilon}_1^{1c} + \boldsymbol{\varepsilon}_1^{1c,\mathrm{T}}\left\langle\boldsymbol{\omega}_1^{0,1}\right\rangle\mathbf{I}_1\delta\boldsymbol{\varepsilon}_1^{1c}, \tag{25}$$

where $\delta\boldsymbol{\omega}_1^{0,1}$ is described as $\boldsymbol{\omega}_1^{0,1} = \mathbf{c}_1^{1c,\mathrm{T}}\mathbf{c}_{1c}^{1b,\mathrm{T}}\boldsymbol{\varepsilon}_{1b}^{0}\dot{\boldsymbol{\varphi}}_{1b}^{0} + \boldsymbol{\varepsilon}_1^{1c}\dot{\boldsymbol{\varphi}}_1^{1c}$ therefore:

$$\begin{aligned}\delta\boldsymbol{\omega}_1^{0,1} &= \delta\mathbf{c}_1^{1c,\mathrm{T}}\mathbf{c}_{1c}^{1b,\mathrm{T}}\boldsymbol{\varepsilon}_{1b}^{0}\dot{\boldsymbol{\varphi}}_{1b}^{0} + \mathbf{c}_1^{1c,\mathrm{T}}\mathbf{c}_{1c}^{1b,\mathrm{T}}\delta\boldsymbol{\varepsilon}_{1b}^{0}\dot{\boldsymbol{\varphi}}_{1b}^{0} + \mathbf{c}_1^{1c,\mathrm{T}}\mathbf{c}_{1c}^{1b,\mathrm{T}}\boldsymbol{\varepsilon}_{1b}^{0}\delta\dot{\boldsymbol{\varphi}}_{1b}^{0} + \delta\boldsymbol{\varepsilon}_1^{1c}\dot{\boldsymbol{\varphi}}_1^{1c} + \boldsymbol{\varepsilon}_1^{1c}\delta\dot{\boldsymbol{\varphi}}_1^{1c}\\ &= \left[\left\langle\mathbf{c}_1^{1c,\mathrm{T}}\mathbf{c}_{1c}^{1b,\mathrm{T}}\boldsymbol{\varepsilon}_{1b}^{0}\dot{\boldsymbol{\varphi}}_{1b}^{0}\right\rangle\boldsymbol{\varepsilon}_1^{1c} + \boldsymbol{\gamma}_3\right]\delta\varphi_1^{1c} + \boldsymbol{\varepsilon}_1^{1c}\delta\dot{\boldsymbol{\varphi}}_1^{1c} + \mathbf{c}_1^{1c,\mathrm{T}}\mathbf{c}_{1c}^{1b,\mathrm{T}}\boldsymbol{\gamma}_2\delta\varphi_{1b}^{0} + \mathbf{c}_1^{1c,\mathrm{T}}\mathbf{c}_{1c}^{1b,\mathrm{T}}\boldsymbol{\varepsilon}_{1b}^{0}\delta\dot{\boldsymbol{\varphi}}_{1b}^{0},\\ \boldsymbol{\gamma}_3 &= \left[\boldsymbol{\lambda}_{1,1}^{1c}\dot{\boldsymbol{\varphi}}_1^{1c}|\boldsymbol{\lambda}_{1,2}^{c1}\dot{\boldsymbol{\varphi}}_1^{1c}|\boldsymbol{\lambda}_{1,3}^{1c}\dot{\boldsymbol{\varphi}}_1^{1c}\right].\end{aligned} \tag{26}$$

The first variation from (17) is defined with the above by expression:

$$\delta\left(\mathbf{B}\left(\mathbf{q}_1^{1c},\dot{\mathbf{q}}_1^{1c},\mathbf{q}_{1b}^{0},\dot{\mathbf{q}}_{1b}^{0}\right)\dot{\mathbf{q}}_1^{1c}\right) = \begin{bmatrix}\mathbf{b}_1\\ \mathbf{b}_2\end{bmatrix}, \tag{27}$$

where $\mathbf{b}_1$ can be got as:

$$\begin{aligned}\mathbf{b}_1 &= \mathbf{m}_1\left\langle\delta\boldsymbol{\omega}_{1b}^{0,1c}\right\rangle\dot{\mathbf{r}}_1^{1c,1c} + \mathbf{m}_1\left\langle\boldsymbol{\omega}_{1b}^{0,1c}\right\rangle\delta\dot{\mathbf{r}}_1^{1c,1c} = -\mathbf{m}_1\left\langle\dot{\mathbf{r}}_1^{1c,1c}\right\rangle\delta\boldsymbol{\omega}_{1b}^{0,1c} + \mathbf{m}_1\left\langle\boldsymbol{\omega}_{1b}^{0,1c}\right\rangle\delta\dot{\mathbf{r}}_1^{1c,1c}\\ &= \mathbf{m}_1\left\langle\boldsymbol{\omega}_{1b}^{0,1c}\right\rangle\delta\dot{\mathbf{r}}_1^{1c,1c} - \mathbf{m}_1\left\langle\dot{\mathbf{r}}_1^{1c,1c}\right\rangle\mathbf{c}_{1c}^{1b,\mathrm{T}}\boldsymbol{\gamma}_2\delta\varphi_{1b}^{0} - \mathbf{m}_1\left\langle\dot{\mathbf{r}}_1^{1c,1c}\right\rangle\mathbf{c}_{1c}^{1b,\mathrm{T}}\boldsymbol{\varepsilon}_{1b}^{0}\delta\dot{\boldsymbol{\varphi}}_{1b}^{0}.\end{aligned} \tag{28}$$

The vector $\mathbf{b}_2$ can be got as:

$$\begin{aligned}\mathbf{b}_2 &= \mathbf{m}_1\delta\left(\boldsymbol{\varepsilon}_1^{1c,\mathrm{T}}\mathbf{c}_1^{1c,\mathrm{T}}\left\langle\mathbf{v}_1^{0,1c}\right\rangle\right)\dot{\mathbf{r}}_1^{1c,1c} + \delta\left(\boldsymbol{\varepsilon}_1^{1c,\mathrm{T}}\mathbf{I}_1\dot{\boldsymbol{\varepsilon}}_1^{1c}\right)\dot{\boldsymbol{\varphi}}_1^{1c} + \delta\left(\boldsymbol{\varepsilon}_1^{1c,\mathrm{T}}\left\langle\boldsymbol{\omega}_1^{0,1}\right\rangle\mathbf{I}_1\boldsymbol{\varepsilon}_1^{1c}\right)\dot{\boldsymbol{\varphi}}_1^{1c}\\ &+ \mathbf{m}_1\boldsymbol{\varepsilon}_1^{1c,\mathrm{T}}\mathbf{c}_1^{1c,\mathrm{T}}\left\langle\mathbf{v}_1^{0,1c}\right\rangle\delta\dot{\mathbf{r}}_1^{1c,1c} + \left[\boldsymbol{\varepsilon}_1^{1c,\mathrm{T}}\mathbf{I}_1\dot{\boldsymbol{\varepsilon}}_1^{1c} + \boldsymbol{\varepsilon}_1^{1c,\mathrm{T}}\left\langle\boldsymbol{\omega}_1^{0,1}\right\rangle\mathbf{I}_1\boldsymbol{\varepsilon}_1^{1c}\right]\delta\dot{\boldsymbol{\varphi}}_1^{1c},\end{aligned} \tag{29}$$

where $\mathbf{m}_1\delta\left(\boldsymbol{\varepsilon}_1^{1c,\mathrm{T}}\mathbf{c}_1^{1c,\mathrm{T}}\left\langle\mathbf{v}_1^{0,1c}\right\rangle\right)\dot{\mathbf{r}}_1^{1c,1c}$ can be got as:

$$\begin{aligned}&\mathbf{m}_1\delta\left(\boldsymbol{\varepsilon}_1^{1c,\mathrm{T}}\mathbf{c}_1^{1c,\mathrm{T}}\left\langle\mathbf{v}_1^{0,1c}\right\rangle\right)\dot{\mathbf{r}}_1^{1c,1c} = \mathbf{m}_1\delta\boldsymbol{\varepsilon}_1^{1c,\mathrm{T}}\mathbf{c}_1^{1c,\mathrm{T}}\left\langle\mathbf{v}_1^{0,1c}\right\rangle\dot{\mathbf{r}}_1^{1c,1c}\\ &-\mathbf{m}_1\boldsymbol{\varepsilon}_1^{1c,\mathrm{T}}\left\langle\boldsymbol{\varepsilon}_1^{1c}\delta\varphi_1^{1c}\right\rangle\mathbf{c}_1^{1c,\mathrm{T}}\left\langle\mathbf{v}_1^{0,1c}\right\rangle\dot{\mathbf{r}}_1^{1c,1c} + \mathbf{m}_1\boldsymbol{\varepsilon}_1^{1c,\mathrm{T}}\mathbf{c}_1^{1c,\mathrm{T}}\left\langle\delta\mathbf{v}_1^{0,1c}\right\rangle\dot{\mathbf{r}}_1^{1c,1c}\\ &= \mathbf{m}_1\boldsymbol{\gamma}_4\delta\varphi_1^{1c} + \mathbf{m}_1\boldsymbol{\varepsilon}_1^{1c,\mathrm{T}}\left\langle\mathbf{c}_1^{1c,\mathrm{T}}\left\langle\mathbf{v}_1^{0,1c}\right\rangle\dot{\mathbf{r}}_1^{1c,1c}\right\rangle\boldsymbol{\varepsilon}_1^{1c}\delta\varphi_1^{1c} - \mathbf{m}_1\boldsymbol{\varepsilon}_1^{1c,\mathrm{T}}\mathbf{c}_1^{1c,\mathrm{T}}\left\langle\dot{\mathbf{r}}_1^{1c,1c}\right\rangle\delta\mathbf{v}_1^{0,1c}\\ &= \mathbf{m}_1\left[\boldsymbol{\gamma}_4 + \boldsymbol{\varepsilon}_1^{1c,\mathrm{T}}\left\langle\mathbf{c}_1^{1c,\mathrm{T}}\left\langle\mathbf{v}_1^{0,1c}\right\rangle\dot{\mathbf{r}}_1^{1c,1c}\right\rangle\boldsymbol{\varepsilon}_1^{1c}\right]\delta\varphi_1^{1c} - \mathbf{m}_1\boldsymbol{\varepsilon}_1^{1c,\mathrm{T}}\mathbf{c}_1^{1c,\mathrm{T}}\left\langle\dot{\mathbf{r}}_1^{1c,1c}\right\rangle\left\langle\mathbf{c}_{1c}^{1b,\mathrm{T}}\boldsymbol{\varepsilon}_{1b}^{0}\dot{\boldsymbol{\varphi}}_{1b}^{0}\right\rangle\delta\mathbf{r}_1^{1c,1c}\\ &-\mathbf{m}_1\boldsymbol{\varepsilon}_1^{1c,\mathrm{T}}\mathbf{c}_1^{1c,\mathrm{T}}\left\langle\dot{\mathbf{r}}_1^{1c,1c}\right\rangle\delta\dot{\mathbf{r}}_1^{1c,1c}\\ &-\mathbf{m}_1\boldsymbol{\varepsilon}_1^{1c,\mathrm{T}}\mathbf{c}_1^{1c,\mathrm{T}}\left\langle\dot{\mathbf{r}}_1^{1c,1c}\right\rangle\mathbf{c}_{1c}^{1b,\mathrm{T}}\left[\left\langle\mathbf{c}_{1b}^{0,\mathrm{T}}\dot{\mathbf{r}}_{1b}^{0,0}\right\rangle\boldsymbol{\varepsilon}_{1b}^{0} + \left\langle\mathbf{r}_{1c}^{1b,1b} + \mathbf{c}_{1c}^{1b}\mathbf{r}_1^{1c,1c}\right\rangle^{\mathrm{T}}\boldsymbol{\gamma}_2\right]\delta\varphi_{1b}^{0}\\ &-\mathbf{m}_1\boldsymbol{\varepsilon}_1^{1c,\mathrm{T}}\mathbf{c}_1^{1c,\mathrm{T}}\left\langle\dot{\mathbf{r}}_1^{1c,1c}\right\rangle\mathbf{c}_{1c}^{1b,\mathrm{T}}\left\langle\mathbf{r}_{1c}^{1b,1b} + \mathbf{c}_{1c}^{1b}\mathbf{r}_1^{1c,1c}\right\rangle^{\mathrm{T}}\boldsymbol{\varepsilon}_{1b}^{0}\delta\dot{\boldsymbol{\varphi}}_{1b}^{0} - \mathbf{m}_1\boldsymbol{\varepsilon}_1^{1c,\mathrm{T}}\mathbf{c}_1^{1c,\mathrm{T}}\left\langle\dot{\mathbf{r}}_1^{1c,1c}\right\rangle\mathbf{c}_{1c}^{1b,\mathrm{T}}\mathbf{c}_{1b}^{0,\mathrm{T}}\delta\dot{\mathbf{r}}_{1b}^{0,0},\end{aligned} \tag{30}$$

where $\boldsymbol{\gamma}_4 = \left[\boldsymbol{\lambda}_{1,1}^{1c,\mathrm{T}}\left\langle\mathbf{v}_1^{0,1}\right\rangle\mathbf{c}_1^{1c,\mathrm{T}}\dot{\mathbf{r}}_1^{1c,1c}|\boldsymbol{\lambda}_{1,2}^{1c,\mathrm{T}}\left\langle\mathbf{v}_1^{0,1}\right\rangle\mathbf{c}_1^{1c,\mathrm{T}}\dot{\mathbf{r}}_1^{1c,1c}|\boldsymbol{\lambda}_{1,3}^{1c,\mathrm{T}}\left\langle\mathbf{v}_1^{0,1}\right\rangle\mathbf{c}_1^{1c,\mathrm{T}}\dot{\mathbf{r}}_1^{1c,1c}\right]$.

The item $\delta\left(\boldsymbol{\varepsilon}_1^{1c,\mathrm{T}}\mathbf{I}_1\dot{\boldsymbol{\varepsilon}}_1^{1c}\right)\dot{\boldsymbol{\varphi}}_1^{1c}$ can be got by formula:

$$\begin{aligned}\delta\left(\boldsymbol{\varepsilon}_1^{1c,\mathrm{T}}\mathbf{I}_1\dot{\boldsymbol{\varepsilon}}_1^{1c}\right)\dot{\boldsymbol{\varphi}}_1^{1c} &= \delta\boldsymbol{\varepsilon}_1^{1c,\mathrm{T}}\mathbf{I}_1\dot{\boldsymbol{\varepsilon}}_1^{1c}\dot{\boldsymbol{\varphi}}_1^{1c} + \boldsymbol{\varepsilon}_1^{1c,\mathrm{T}}\mathbf{I}_1\delta\dot{\boldsymbol{\varepsilon}}_1^{1c}\dot{\boldsymbol{\varphi}}_1^{1c} \\ &= \left[\boldsymbol{\gamma}_5 + \boldsymbol{\varepsilon}_1^{1c,\mathrm{T}}\mathbf{I}_1\boldsymbol{\gamma}_6\right]\delta\varphi_1^{1c} + \boldsymbol{\varepsilon}_1^{1c,\mathrm{T}}\mathbf{I}_1\boldsymbol{\gamma}_3\delta\dot{\boldsymbol{\varphi}}_1^{1c},\end{aligned} \tag{31}$$

where

$\boldsymbol{\gamma}_5 = \left[\boldsymbol{\lambda}_{1,1}^{1c,\mathrm{T}}\mathbf{I}_1\dot{\boldsymbol{\varepsilon}}_1^{1c}\dot{\boldsymbol{\varphi}}_1^{1c}|\boldsymbol{\lambda}_{1,2}^{1c,\mathrm{T}}\mathbf{I}_1\dot{\boldsymbol{\varepsilon}}_1^{1c}\dot{\boldsymbol{\varphi}}_1^{1c}|\boldsymbol{\lambda}_{1,3}^{1c,\mathrm{T}}\mathbf{I}_1\dot{\boldsymbol{\varepsilon}}_1^{1c}\dot{\boldsymbol{\varphi}}_1^{1c}\right]$, $\boldsymbol{\gamma}_6 = \left[\boldsymbol{\phi}_{1,1}^{1c}\dot{\boldsymbol{\varphi}}_1^{1c}|\boldsymbol{\phi}_{1,2}^{1c}\dot{\boldsymbol{\varphi}}_1^{1c}|\boldsymbol{\phi}_{1,3}^{1c}\dot{\boldsymbol{\varphi}}_1^{1c}\right]$.

The item $\delta\left(\boldsymbol{\varepsilon}_1^{1c,\mathrm{T}}\left\langle\boldsymbol{\omega}_1^{0,1}\right\rangle\mathbf{I}_1\boldsymbol{\varepsilon}_1^{1c}\right)\dot{\boldsymbol{\varphi}}_1^{1c}$ can be got by formula:

$$\begin{aligned}&\delta\left(\boldsymbol{\varepsilon}_1^{1c,\mathrm{T}}\left\langle\boldsymbol{\omega}_1^{0,1}\right\rangle\mathbf{I}_1\boldsymbol{\varepsilon}_1^{1c}\right)\dot{\boldsymbol{\varphi}}_1^{1c} \\ &= \delta\boldsymbol{\varepsilon}_1^{1c,\mathrm{T}}\left\langle\boldsymbol{\omega}_1^{0,1}\right\rangle\mathbf{I}_1\boldsymbol{\varepsilon}_1^{1c}\dot{\boldsymbol{\varphi}}_1^{1c} + \boldsymbol{\varepsilon}_1^{1c,\mathrm{T}}\left\langle\delta\boldsymbol{\omega}_1^{0,1}\right\rangle\mathbf{I}_1\boldsymbol{\varepsilon}_1^{1c}\dot{\boldsymbol{\varphi}}_1^{1c} + \boldsymbol{\varepsilon}_1^{1c,\mathrm{T}}\left\langle\boldsymbol{\omega}_1^{0,1}\right\rangle\mathbf{I}_1\delta\boldsymbol{\varepsilon}_1^{1c}\dot{\boldsymbol{\varphi}}_1^{1c} \\ &= \left[\boldsymbol{\gamma}_7 + \boldsymbol{\varepsilon}_1^{1c,\mathrm{T}}\left\langle\boldsymbol{\omega}_1^{0,1}\right\rangle\mathbf{I}_1\boldsymbol{\gamma}_3\right]\delta\varphi_1^{1c} - \boldsymbol{\varepsilon}_1^{1c,\mathrm{T}}\left\langle\mathbf{I}_1\boldsymbol{\varepsilon}_1^{1c}\dot{\boldsymbol{\varphi}}_1^{1c}\right\rangle\delta\boldsymbol{\omega}_1^{0,1} \\ &= \left[\boldsymbol{\gamma}_7 + \boldsymbol{\varepsilon}_1^{1c,\mathrm{T}}\left\langle\boldsymbol{\omega}_1^{0,1}\right\rangle\mathbf{I}_1\boldsymbol{\gamma}_3 - \boldsymbol{\varepsilon}_1^{1c,\mathrm{T}}\left\langle\mathbf{I}_1\boldsymbol{\varepsilon}_1^{1c}\dot{\boldsymbol{\varphi}}_1^{1c}\right\rangle\left[\left\langle\mathbf{c}_1^{1c,\mathrm{T}}\mathbf{c}_{1c}^{1b,\mathrm{T}}\boldsymbol{\varepsilon}_{1b}^0\dot{\boldsymbol{\varphi}}_{1b}^0\right\rangle\boldsymbol{\varepsilon}_1^{1c} + \boldsymbol{\gamma}_3\right]\right]\delta\varphi_1^{1c} \\ &\quad -\boldsymbol{\varepsilon}_1^{1c,\mathrm{T}}\left\langle\mathbf{I}_1\boldsymbol{\varepsilon}_1^{1c}\dot{\boldsymbol{\varphi}}_1^{1c}\right\rangle\boldsymbol{\varepsilon}_1^{1c}\delta\dot{\boldsymbol{\varphi}}_1^{1c} - \boldsymbol{\varepsilon}_1^{1c,\mathrm{T}}\left\langle\mathbf{I}_1\boldsymbol{\varepsilon}_1^{1c}\dot{\boldsymbol{\varphi}}_1^{1c}\right\rangle\mathbf{c}_1^{1c,\mathrm{T}}\mathbf{c}_{1c}^{1b,\mathrm{T}}\boldsymbol{\gamma}_2\delta\varphi_{1b}^0 \\ &\quad -\boldsymbol{\varepsilon}_1^{1c,\mathrm{T}}\left\langle\mathbf{I}_1\boldsymbol{\varepsilon}_1^{1c}\dot{\boldsymbol{\varphi}}_1^{1c}\right\rangle\mathbf{c}_1^{1c,\mathrm{T}}\mathbf{c}_{1c}^{1b,\mathrm{T}}\boldsymbol{\varepsilon}_{1b}^0\delta\dot{\boldsymbol{\varphi}}_{1b}^0,\end{aligned} \tag{32}$$

where $\boldsymbol{\gamma}_7 = \left[\boldsymbol{\lambda}_{1,1}^{1c,\mathrm{T}}\left\langle\boldsymbol{\omega}_1^{0,1}\right\rangle\mathbf{I}_1\boldsymbol{\varepsilon}_1^{1c}\dot{\boldsymbol{\varphi}}_1^{1c}|\boldsymbol{\lambda}_{1,2}^{1c,\mathrm{T}}\left\langle\boldsymbol{\omega}_1^{0,1}\right\rangle\mathbf{I}_1\boldsymbol{\varepsilon}_1^{1c}\dot{\boldsymbol{\varphi}}_1^{1c}|\boldsymbol{\lambda}_{1,3}^{1c,\mathrm{T}}\left\langle\boldsymbol{\omega}_1^{0,1}\right\rangle\mathbf{I}_1\boldsymbol{\varepsilon}_1^{1c}\dot{\boldsymbol{\varphi}}_1^{1c}\right]$.

Proceeding from the above, the Jacobian $\mathbf{J}_{\mathbf{q}_1^{1c}}\left(\mathbf{B}\dot{\mathbf{q}}_1^{1c}\right)_{\mathbf{X}_{fix}}$ in (16) is calculated on a formula:

$$\begin{aligned}\mathbf{J}_{\mathbf{q}_1^{1c}}\left(\mathbf{B}\dot{\mathbf{q}}_1^{1c}\right)_{X_{fix}} &= \begin{bmatrix}\mathbf{J}_{\mathbf{q}_1^{1c}}\left(\mathbf{B}\dot{\mathbf{q}}_1^{1c}\right)_{11} & \mathbf{J}_{\mathbf{q}_1^{1c}}\left(\mathbf{B}\dot{\mathbf{q}}_1^{1c}\right)_{12} \\ \mathbf{J}_{\mathbf{q}_1^{1c}}\left(\mathbf{B}\dot{\mathbf{q}}_1^{1c}\right)_{21} & \mathbf{J}_{\mathbf{q}_1^{1c}}\left(\mathbf{B}\dot{\mathbf{q}}_1^{1c}\right)_{22}\end{bmatrix}, \\ \mathbf{J}_{\mathbf{q}_1^{1c}}\left(\mathbf{B}\dot{\mathbf{q}}_1^{1c}\right)_{11} &= 0,\ \mathbf{J}_{\mathbf{q}_1^{1c}}\left(\mathbf{B}\dot{\mathbf{q}}_1^{1c}\right)_{12} = 0, \\ \mathbf{J}_{\mathbf{q}_1^{1c}}\left(\mathbf{B}\dot{\mathbf{q}}_1^{1c}\right)_{21} &= -\mathbf{m}_1\boldsymbol{\varepsilon}_1^{1c,\mathrm{T}}\mathbf{c}_1^{1c,\mathrm{T}}\left\langle\dot{\mathbf{r}}_1^{1c,1c}\right\rangle\left\langle\mathbf{c}_{1c}^{1b,\mathrm{T}}\boldsymbol{\varepsilon}_{1b}^0\dot{\boldsymbol{\varphi}}_{1b}^0\right\rangle, \\ \mathbf{J}_{\mathbf{q}_1^{1c}}\left(\mathbf{B}\dot{\mathbf{q}}_1^{1c}\right)_{22} &= \mathbf{m}_1\boldsymbol{\gamma}_4 + \mathbf{m}_1\boldsymbol{\varepsilon}_1^{1c,\mathrm{T}}\left\langle\mathbf{c}_1^{1c,\mathrm{T}}\left\langle\mathbf{v}_1^{0,1c}\right\rangle\dot{\mathbf{r}}_1^{1c,1c}\right\rangle\boldsymbol{\varepsilon}_1^{1c} + \boldsymbol{\gamma}_5 \\ &\quad + \boldsymbol{\varepsilon}_1^{1c,\mathrm{T}}\mathbf{I}_1\boldsymbol{\gamma}_6 + \boldsymbol{\gamma}_7 + \boldsymbol{\varepsilon}_1^{1c,\mathrm{T}}\left\langle\boldsymbol{\omega}_1^{0,1}\right\rangle\mathbf{I}_1\boldsymbol{\gamma}_3 \\ &\quad -\boldsymbol{\varepsilon}_1^{1c,\mathrm{T}}\left\langle\mathbf{I}_1\boldsymbol{\varepsilon}_1^{1c}\dot{\boldsymbol{\varphi}}_1^{1c}\right\rangle\left\langle\mathbf{c}_1^{1c,\mathrm{T}}\mathbf{c}_{1c}^{1b,\mathrm{T}}\boldsymbol{\varepsilon}_{1b}^0\dot{\boldsymbol{\varphi}}_{1b}^0\right\rangle\boldsymbol{\varepsilon}_1^{1c} - \boldsymbol{\varepsilon}_1^{1c,\mathrm{T}}\left\langle\mathbf{I}_1\boldsymbol{\varepsilon}_1^{1c}\dot{\boldsymbol{\varphi}}_1^{1c}\right\rangle\boldsymbol{\gamma}_3.\end{aligned} \tag{33}$$

The Jacobian $\mathbf{J}_{\dot{\mathbf{q}}_1^{1c}}\left(\mathbf{B}\dot{\mathbf{q}}_1^{1c}\right)_{\mathbf{X}_{fix}}$ in (16) is calculated on a formula:

$$\begin{gathered}
\mathbf{J}_{\dot{\mathbf{q}}_1^{1c}}\left(\mathbf{B}\dot{\mathbf{q}}_1^{1c}\right)_{X_{fix}}=\begin{bmatrix}\mathbf{J}_{\dot{\mathbf{q}}_1^{1c}}\left(\mathbf{B}\dot{\mathbf{q}}_1^{1c}\right)_{11} & \mathbf{J}_{\dot{\mathbf{q}}_1^{1c}}\left(\mathbf{B}\dot{\mathbf{q}}_1^{1c}\right)_{12}\\ \mathbf{J}_{\dot{\mathbf{q}}_1^{1c}}\left(\mathbf{B}\dot{\mathbf{q}}_1^{1c}\right)_{21} & \mathbf{J}_{\dot{\mathbf{q}}_1^{1c}}\left(\mathbf{B}\dot{\mathbf{q}}_1^{1c}\right)_{22}\end{bmatrix},\\
\mathbf{J}_{\dot{\mathbf{q}}_1^{1c}}\left(\mathbf{B}\dot{\mathbf{q}}_1^{1c}\right)_{11}=\mathbf{m}_1\left\langle\boldsymbol{\omega}_{1b}^{0,1c}\right\rangle,\\
\mathbf{J}_{\dot{\mathbf{q}}_1^{1c}}\left(\mathbf{B}\dot{\mathbf{q}}_1^{1c}\right)_{12}=0,\\
\mathbf{J}_{\dot{\mathbf{q}}_1^{1c}}\left(\mathbf{B}\dot{\mathbf{q}}_1^{1c}\right)_{21}=\mathbf{m}_1\boldsymbol{\varepsilon}_1^{1c,\mathrm{T}}\mathbf{c}_1^{1c,\mathrm{T}}\left\langle\mathbf{v}_1^{0,1c}-\dot{\mathbf{r}}_1^{1c,1c}\right\rangle,\\
\mathbf{J}_{\dot{\mathbf{q}}_1^{1c}}\left(\mathbf{B}\dot{\mathbf{q}}_1^{1c}\right)_{22}=\boldsymbol{\varepsilon}_1^{1c,\mathrm{T}}\mathbf{I}_1\dot{\boldsymbol{\varepsilon}}_1^{1c}+\boldsymbol{\varepsilon}_1^{1c,\mathrm{T}}\left\langle\boldsymbol{\omega}_1^{0,1}\right\rangle\mathbf{I}_1\boldsymbol{\varepsilon}_1^{1c}+\boldsymbol{\varepsilon}_1^{1c,\mathrm{T}}\mathbf{I}_1\boldsymbol{\gamma}_3-\boldsymbol{\varepsilon}_1^{1c,\mathrm{T}}\langle\mathbf{I}_1\boldsymbol{\varepsilon}_1^{1c}\dot{\boldsymbol{\varphi}}_1^{1c}\rangle\boldsymbol{\varepsilon}_1^{1c}.
\end{gathered}\tag{34}$$

The Jacobian $\mathbf{J}_{\mathbf{q}_{1b}^0}\left(\mathbf{B}\dot{\mathbf{q}}_1^{1c}\right)_{\mathbf{X}_{fix}}$ in (16) is calculated on a formula:

$$\begin{gathered}
\mathbf{J}_{\mathbf{q}_{1b}^0}\left(\mathbf{B}\dot{\mathbf{q}}_1^{1c}\right)_{\mathbf{X}_{fix}}=\begin{bmatrix}\mathbf{J}_{\mathbf{q}_{1b}^0}\left(\mathbf{B}\dot{\mathbf{q}}_1^{1c}\right)_{11} & \mathbf{J}_{\mathbf{q}_{1b}^0}\left(\mathbf{B}\dot{\mathbf{q}}_1^{1c}\right)_{12}\\ \mathbf{J}_{\mathbf{q}_{1b}^0}\left(\mathbf{B}\dot{\mathbf{q}}_1^{1c}\right)_{21} & \mathbf{J}_{q_{1b}^0}\left(\mathbf{B}\dot{\mathbf{q}}_1^{1c}\right)_{22}\end{bmatrix},\\
\mathbf{J}_{\mathbf{q}_{1b}^0}\left(\mathbf{B}\dot{\mathbf{q}}_1^{1c}\right)_{11}=0,\ \mathbf{J}_{\mathbf{q}_{1b}^0}\left(\mathbf{B}\dot{\mathbf{q}}_1^{1c}\right)_{12}=-\mathbf{m}_1\left\langle\dot{\mathbf{r}}_1^{1c,1c}\right\rangle\mathbf{c}_{1c}^{1b,\mathrm{T}}\boldsymbol{\gamma}_2,\ \mathbf{J}_{\mathbf{q}_{1b}^0}\left(\mathbf{B}\dot{\mathbf{q}}_1^{1c}\right)_{21}=0,\\
\mathbf{J}_{\mathbf{q}_{1b}^0}\left(\mathbf{B}\dot{\mathbf{q}}_1^{1c}\right)_{22}=-\mathbf{m}_1\boldsymbol{\varepsilon}_1^{1c,\mathrm{T}}\mathbf{c}_1^{1c,\mathrm{T}}\left\langle\dot{\mathbf{r}}_1^{1c,1c}\right\rangle\mathbf{c}_{1c}^{1b,\mathrm{T}}\left\langle\mathbf{c}_{1b}^{0,\mathrm{T}}\dot{\mathbf{r}}_{1b}^{0,0}\right\rangle\boldsymbol{\varepsilon}_{1b}^{0}-\\
-\mathbf{m}_1\boldsymbol{\varepsilon}_1^{1c,\mathrm{T}}\mathbf{c}_1^{1c,\mathrm{T}}\left\langle\dot{\mathbf{r}}_1^{1c,1c}\right\rangle\mathbf{c}_{1c}^{1b,\mathrm{T}}\left\langle\mathbf{r}_{1c}^{1b,1b}+\mathbf{c}_{1c}^{1b}\mathbf{r}_1^{1c,1c}\right\rangle^{\mathrm{T}}\boldsymbol{\gamma}_2-\boldsymbol{\varepsilon}_1^{1c,\mathrm{T}}\langle\mathbf{I}_1\boldsymbol{\varepsilon}_1^{1c}\dot{\boldsymbol{\varphi}}_1^{1c}\rangle\mathbf{c}_1^{1c,\mathrm{T}}\mathbf{c}_{1c}^{1b,\mathrm{T}}\boldsymbol{\gamma}_2.
\end{gathered}\tag{35}$$

The Jacobian $\mathbf{J}_{\dot{\mathbf{q}}_{1b}^0}\left(\mathbf{B}\dot{\mathbf{q}}_1^{1c}\right)_{\mathbf{X}_{fix}}$ in (16) is calculated on a formula:

$$\begin{gathered}
\mathbf{J}_{\dot{\mathbf{q}}_{1b}^0}\left(\mathbf{B}\dot{\mathbf{q}}_1^{1c}\right)_{\mathbf{X}_{fix}}=\begin{bmatrix}\mathbf{J}_{\dot{\mathbf{q}}_{1b}^0}\left(\mathbf{B}\dot{\mathbf{q}}_1^{1c}\right)_{11} & \mathbf{J}_{\dot{\mathbf{q}}_{1b}^0}\left(\mathbf{B}\dot{\mathbf{q}}_1^{1c}\right)_{12}\\ \mathbf{J}_{\dot{\mathbf{q}}_{1b}^0}\left(\mathbf{B}\dot{\mathbf{q}}_1^{1c}\right)_{21} & \mathbf{J}_{\dot{\mathbf{q}}_{1b}^0}\left(\mathbf{B}\dot{\mathbf{q}}_1^{1c}\right)_{22}\end{bmatrix},\\
\mathbf{J}_{\dot{\mathbf{q}}_{1b}^0}\left(\mathbf{B}\dot{\mathbf{q}}_1^{1c}\right)_{11}=0,\ \mathbf{J}_{\dot{\mathbf{q}}_{1b}^0}\left(\mathbf{B}\dot{\mathbf{q}}_1^{1c}\right)_{12}=-\mathbf{m}_1\left\langle\dot{\mathbf{r}}_1^{1c,1c}\right\rangle\mathbf{c}_{1c}^{1b,\mathrm{T}}\boldsymbol{\varepsilon}_{1b}^{0},\\
\mathbf{J}_{\dot{\mathbf{q}}_{1b}^0}\left(\mathbf{B}\dot{\mathbf{q}}_1^{1c}\right)_{21}=-\mathbf{m}_1\boldsymbol{\varepsilon}_1^{1c,\mathrm{T}}\mathbf{c}_1^{1c,\mathrm{T}}\left\langle\dot{\mathbf{r}}_1^{1c,1c}\right\rangle\mathbf{c}_{1c}^{1b,\mathrm{T}}\mathbf{c}_{1b}^{0,\mathrm{T}},\\
\mathbf{J}_{\dot{\mathbf{q}}_{1b}^0}\left(\mathbf{B}\dot{\mathbf{q}}_1^{1c}\right)_{22}=-\mathbf{m}_1\boldsymbol{\varepsilon}_1^{1c,\mathrm{T}}\mathbf{c}_1^{1c,\mathrm{T}}\left\langle\dot{\mathbf{r}}_1^{1c,1c}\right\rangle\mathbf{c}_{1c}^{1b,\mathrm{T}}\left\langle\mathbf{r}_{1c}^{1b,1b}+\mathbf{c}_{1c}^{1b}\mathbf{r}_1^{1c,1c}\right\rangle^{\mathrm{T}}\boldsymbol{\varepsilon}_{1b}^{0}\\
-\boldsymbol{\varepsilon}_1^{1c,\mathrm{T}}\langle\mathbf{I}_1\boldsymbol{\varepsilon}_1^{1c}\dot{\boldsymbol{\varphi}}_1^{1c}\rangle\mathbf{c}_1^{1c,\mathrm{T}}\mathbf{c}_{1c}^{1b,\mathrm{T}}\boldsymbol{\varepsilon}_{1b}^{0}.
\end{gathered}\tag{36}$$

The item $\mathbf{A}_0\left(\mathbf{q}_1^{1c},\mathbf{q}_{1b}^0\right)\ddot{\mathbf{q}}_{1b}^0$ can be got by formula:

$$\begin{aligned}
\mathbf{A}_0\left(\mathbf{q}_1^{1c},\mathbf{q}_{1b}^0\right)\ddot{\mathbf{q}}_{1b}^0&=\mathbf{M}_1^{1c,\mathrm{T}}\boldsymbol{\Theta}_1^1\mathbf{L}_1^{1c,\mathrm{T}}\mathbf{L}_{1c}^{1b,\mathrm{T}}\mathbf{M}_{1b}^0\ddot{\mathbf{q}}_{1b}^0\\
&=\begin{bmatrix}\mathbf{m}_1\mathbf{c}_{1c}^{1b,\mathrm{T}}\mathbf{c}_{1b}^{0,\mathrm{T}} & \mathbf{m}_1\mathbf{c}_{1c}^{1b,\mathrm{T}}\left\langle\mathbf{r}_{1c}^{1b,1b}\right\rangle^{\mathrm{T}}\boldsymbol{\varepsilon}_{1b}^{0}+\mathbf{m}_1\left\langle\mathbf{r}_1^{1c,1c}\right\rangle^{\mathrm{T}}\mathbf{c}_{1c}^{1b,\mathrm{T}}\boldsymbol{\varepsilon}_{1b}^{0}\\ 0 & \boldsymbol{\varepsilon}_1^{1c,\mathrm{T}}\mathbf{I}_1\mathbf{c}_1^{1c,\mathrm{T}}\mathbf{c}_{1c}^{1b,\mathrm{T}}\boldsymbol{\varepsilon}_{1b}^{0}\end{bmatrix}\ddot{\mathbf{q}}_{1b}^0.
\end{aligned}\tag{37}$$

We linearize (37), then:

$$\begin{aligned}\mathbf{A}_0\left(\mathbf{q}_1^{1c},\mathbf{q}_{1b}^0\right)\ddot{\mathbf{q}}_{1b}^0 \approx{}& \mathbf{A}_0\left(\mathbf{q}_{1,fix}^{1c},\mathbf{q}_{1b,fix}^0\right)\ddot{\mathbf{q}}_{1b,fix}^0+\mathbf{J}_{\mathbf{q}_1^{1c}}\left(\mathbf{A}_0\left(\mathbf{q}_1^{1c},\mathbf{q}_{1b}^0\right)\ddot{\mathbf{q}}_{1b}^0\right)_{\mathbf{X}_{fix}}\delta\mathbf{q}_1^{1c}\\&+\mathbf{J}_{\mathbf{q}_{1b}^0}\left(\mathbf{A}_0\left(\mathbf{q}_1^{1c},\mathbf{q}_{1b}^0\right)\ddot{\mathbf{q}}_{1b}^0\right)_{\mathbf{X}_{fix}}\delta\mathbf{q}_{1b}^0+\mathbf{J}_{\ddot{\mathbf{q}}_{1b}^0}\left(\mathbf{A}_0\left(\mathbf{q}_1^{1c},\mathbf{q}_{1b}^0\right)\ddot{\mathbf{q}}_{1b}^0\right)_{\mathbf{X}_{fix}}\delta\ddot{\mathbf{q}}_{1b}^0.\end{aligned}\tag{38}$$

The first variation from (37) is defined as follows:

$$\begin{aligned}\delta\mathbf{A}_0\left(\mathbf{q}_1^{1c},\mathbf{q}_{1b}^0\right)\ddot{\mathbf{q}}_{1b}^0 ={}& \begin{bmatrix}\delta\left(\mathbf{m}_1\mathbf{c}_{1c}^{1b,\mathrm{T}}\mathbf{c}_{1b}^{0,\mathrm{T}}\right) & \delta\left(\mathbf{m}_1\mathbf{c}_{1c}^{1b,\mathrm{T}}\left\langle\mathbf{r}_{1c}^{1b,1b}\right\rangle^{\mathrm{T}}\boldsymbol{\varepsilon}_{1b}^0+\mathbf{m}_1\left\langle\mathbf{r}_1^{1c,1c}\right\rangle^{\mathrm{T}}\mathbf{c}_{1c}^{1b,\mathrm{T}}\boldsymbol{\varepsilon}_{1b}^0\right)\\ 0 & \delta\left(\boldsymbol{\varepsilon}_1^{1c,\mathrm{T}}\mathbf{I}_1\mathbf{c}_1^{1c,\mathrm{T}}\mathbf{c}_{1c}^{1b,\mathrm{T}}\boldsymbol{\varepsilon}_{1b}^0\right)\end{bmatrix}\\&\times\begin{bmatrix}\ddot{\mathbf{r}}_{1b}^0\\ \ddot{\varphi}_{1b}^0\end{bmatrix}+\begin{bmatrix}\mathbf{m}_1\mathbf{c}_{1c}^{1b,\mathrm{T}}\mathbf{c}_{1b}^{0,\mathrm{T}} & \mathbf{m}_1\mathbf{c}_{1c}^{1b,\mathrm{T}}\left\langle\mathbf{r}_{1c}^{1b,1b}\right\rangle^{\mathrm{T}}\boldsymbol{\varepsilon}_{1b}^0+\mathbf{m}_1\left\langle\mathbf{r}_1^{1c,1c}\right\rangle^{\mathrm{T}}\mathbf{c}_{1c}^{1b,\mathrm{T}}\boldsymbol{\varepsilon}_{1b}^0\\ 0 & \boldsymbol{\varepsilon}_1^{1c,\mathrm{T}}\mathbf{I}_1\mathbf{c}_1^{1c,\mathrm{T}}\mathbf{c}_{1c}^{1b,\mathrm{T}}\boldsymbol{\varepsilon}_{1b}^0\end{bmatrix}\begin{bmatrix}\delta\ddot{\mathbf{r}}_{1b}^0\\ \delta\ddot{\varphi}_{1b}^0\end{bmatrix},\end{aligned}\tag{39}$$

where $\delta\left(\mathbf{m}_1\mathbf{c}_{1c}^{1b,\mathrm{T}}\mathbf{c}_{1b}^{0,\mathrm{T}}\right)\ddot{\mathbf{r}}_{1b}^0$ can be got by formula:

$$\delta\left(\mathbf{m}_1\mathbf{c}_{1c}^{1b,\mathrm{T}}\mathbf{c}_{1b}^{0,\mathrm{T}}\right)\ddot{\mathbf{r}}_{1b}^0=\mathbf{m}_1\mathbf{c}_{1c}^{1b,\mathrm{T}}\left\langle\boldsymbol{\varepsilon}_{1b}^0\delta\varphi_{1b}^0\right\rangle^{\mathrm{T}}\mathbf{c}_{1b}^{0,\mathrm{T}}\ddot{\mathbf{r}}_{1b}^0=\mathbf{m}_1\mathbf{c}_{1c}^{1b,\mathrm{T}}\left\langle\mathbf{c}_{1b}^{0,\mathrm{T}}\ddot{\mathbf{r}}_{1b}^0\right\rangle\boldsymbol{\varepsilon}_{1b}^0\delta\varphi_{1b}^0.\tag{40}$$

The item $\delta\left(\mathbf{m}_1\mathbf{c}_{1c}^{1b,\mathrm{T}}\left\langle\mathbf{r}_{1c}^{1b,1b}\right\rangle^{\mathrm{T}}\boldsymbol{\varepsilon}_{1b}^0+\mathbf{m}_1\left\langle\mathbf{r}_1^{1c,1c}\right\rangle^{\mathrm{T}}\mathbf{c}_{1c}^{1b,\mathrm{T}}\boldsymbol{\varepsilon}_{1b}^0\right)\ddot{\varphi}_{1b}^0$ can be got by formula:

$$\begin{aligned}&\delta\left(\mathbf{m}_1\mathbf{c}_{1c}^{1b,\mathrm{T}}\left\langle\mathbf{r}_{1c}^{1b,1b}\right\rangle^{\mathrm{T}}\boldsymbol{\varepsilon}_{1b}^0+\mathbf{m}_1\left\langle\mathbf{r}_1^{1c,1c}\right\rangle^{\mathrm{T}}\mathbf{c}_{1c}^{1b,\mathrm{T}}\boldsymbol{\varepsilon}_{1b}^0\right)\ddot{\varphi}_{1b}^0\\&=\mathbf{m}_1\left\langle\mathbf{c}_{1c}^{1b,\mathrm{T}}\boldsymbol{\varepsilon}_{1b}^0\ddot{\varphi}_{1b}^0\right\rangle\delta\mathbf{r}_1^{1c,1c}+\left[\mathbf{m}_1\mathbf{c}_{1c}^{1b,\mathrm{T}}\left\langle\mathbf{r}_{1c}^{1b,1b}\right\rangle^{\mathrm{T}}+\mathbf{m}_1\left\langle\mathbf{r}_1^{1c,1c}\right\rangle^{\mathrm{T}}\mathbf{c}_{1c}^{1b,\mathrm{T}}\right]\delta\boldsymbol{\varepsilon}_{1b}^0\ddot{\varphi}_{1b}^0\\&=\mathbf{m}_1\left\langle\mathbf{c}_{1c}^{1b,\mathrm{T}}\boldsymbol{\varepsilon}_{1b}^0\ddot{\varphi}_{1b}^0\right\rangle\delta\mathbf{r}_1^{1c,1c}+\left[\mathbf{m}_1\mathbf{c}_{1c}^{1b,\mathrm{T}}\left\langle\mathbf{r}_{1c}^{1b,1b}\right\rangle^{\mathrm{T}}+\mathbf{m}_1\left\langle\mathbf{r}_1^{1c,1c}\right\rangle^{\mathrm{T}}\mathbf{c}_{1c}^{1b,\mathrm{T}}\right]\boldsymbol{\gamma}_8\delta\varphi_{1b}^0,\end{aligned}\tag{41}$$

where $\boldsymbol{\gamma}_8=\left[\boldsymbol{\lambda}_{1b,1}^0\ddot{\varphi}_{1b}^0|\boldsymbol{\lambda}_{1b,2}^{0,\mathrm{T}}\ddot{\varphi}_{1b}^0|\boldsymbol{\lambda}_{1b,3}^{0,\mathrm{T}}\ddot{\varphi}_{1b}^0\right]$. The item $\delta\left(\boldsymbol{\varepsilon}_1^{1c,\mathrm{T}}\mathbf{I}_1\mathbf{c}_1^{1c,\mathrm{T}}\mathbf{c}_{1c}^{1b,\mathrm{T}}\boldsymbol{\varepsilon}_{1b}^0\right)\ddot{\varphi}_{1b}^0$ can be got by formula:

$$\begin{aligned}&\delta\left(\boldsymbol{\varepsilon}_1^{1c,\mathrm{T}}\mathbf{I}_1\mathbf{c}_1^{1c,\mathrm{T}}\mathbf{c}_{1c}^{1b,\mathrm{T}}\boldsymbol{\varepsilon}_{1b}^0\right)\ddot{\varphi}_{1b}^0=\delta\boldsymbol{\varepsilon}_1^{1c,\mathrm{T}}\mathbf{I}_1\mathbf{c}_1^{1c,\mathrm{T}}\mathbf{c}_{1c}^{1b,\mathrm{T}}\boldsymbol{\varepsilon}_{1b}^0\ddot{\varphi}_{1b}^0+\boldsymbol{\varepsilon}_1^{1c,\mathrm{T}}\mathbf{I}_1\delta\mathbf{c}_1^{1c,\mathrm{T}}\mathbf{c}_{1c}^{1b,\mathrm{T}}\boldsymbol{\varepsilon}_{1b}^0\ddot{\varphi}_{1b}^0\\&+\boldsymbol{\varepsilon}_1^{1c,\mathrm{T}}\mathbf{I}_1\mathbf{c}_1^{1c,\mathrm{T}}\mathbf{c}_{1c}^{1b,\mathrm{T}}\delta\boldsymbol{\varepsilon}_{1b}^0\ddot{\varphi}_{1b}^0=\left[\boldsymbol{\gamma}_9+\boldsymbol{\varepsilon}_1^{1c,\mathrm{T}}\mathbf{I}_1\left\langle\mathbf{c}_1^{1c,\mathrm{T}}\mathbf{c}_{1c}^{1b,\mathrm{T}}\boldsymbol{\varepsilon}_{1b}^0\ddot{\varphi}_{1b}^0\right\rangle\boldsymbol{\varepsilon}_1^{1c}\right]\delta\varphi_1^{1c}\\&+\boldsymbol{\varepsilon}_1^{1c,\mathrm{T}}\mathbf{I}_1\mathbf{c}_1^{1c,\mathrm{T}}\mathbf{c}_{1c}^{1b,\mathrm{T}}\boldsymbol{\gamma}_8\delta\varphi_{1b}^0,\end{aligned}\tag{42}$$

where $\boldsymbol{\gamma}_9 = \left[\boldsymbol{\lambda}_{1,1}^{1c,\mathrm{T}}\mathbf{I}_1\mathbf{c}_1^{1c,\mathrm{T}}\mathbf{c}_{1c}^{1b,\mathrm{T}}\boldsymbol{\varepsilon}_{1b}^0\ddot{\varphi}_{1b}^0 | \boldsymbol{\lambda}_{1,2}^{1c,\mathrm{T}}\mathbf{I}_1\mathbf{c}_1^{1c,\mathrm{T}}\mathbf{c}_{1c}^{1b,\mathrm{T}}\boldsymbol{\varepsilon}_{1b}^0\ddot{\varphi}_{1b}^0 | \boldsymbol{\lambda}_{1,3}^{1c,\mathrm{T}}\mathbf{I}_1\mathbf{c}_1^{1c,\mathrm{T}}\mathbf{c}_{1c}^{1b,\mathrm{T}}\boldsymbol{\varepsilon}_{1b}^0\ddot{\varphi}_{1b}^0\right]$.

The Jacobian $\mathbf{J}_{\mathbf{q}_1^{1c}}\left(\mathbf{A}_0\left(\mathbf{q}_1^{1c},\mathbf{q}_{1b}^0\right)\ddot{\mathbf{q}}_{1b}^0\right)$ can be got by formula:

$$\begin{aligned}
&\mathbf{J}_{\mathbf{q}_1^{1c}}\left(\mathbf{A}_0\left(\mathbf{q}_1^{1c},\mathbf{q}_{1b}^0\right)\ddot{\mathbf{q}}_{1b}^0\right)_{\mathbf{X}_{fix}} = \begin{bmatrix} \mathbf{J}_{\mathbf{q}_1^{1c}}\left(\mathbf{A}_0\left(\mathbf{q}_1^{1c},\mathbf{q}_{1b}^0\right)\ddot{\mathbf{q}}_{1b}^0\right)_{11} & \mathbf{J}_{\mathbf{q}_1^{1c}}\left(\mathbf{A}_0\left(\mathbf{q}_1^{1c},\mathbf{q}_{1b}^0\right)\ddot{\mathbf{q}}_{1b}^0\right)_{12} \\ \mathbf{J}_{\mathbf{q}_1^{1c}}\left(\mathbf{A}_0\left(\mathbf{q}_1^{1c},\mathbf{q}_{1b}^0\right)\ddot{\mathbf{q}}_{1b}^0\right)_{21} & \mathbf{J}_{\mathbf{q}_1^{1c}}\left(\mathbf{A}_0\left(\mathbf{q}_1^{1c},\mathbf{q}_{1b}^0\right)\ddot{\mathbf{q}}_{1b}^0\right)_{22} \end{bmatrix}, \\
&\mathbf{J}_{\mathbf{q}_1^{1c}}\left(\mathbf{A}_0\left(\mathbf{q}_1^{1c},\mathbf{q}_{1b}^0\right)\ddot{\mathbf{q}}_{1b}^0\right)_{11} = \mathbf{m}_1\left\langle \mathbf{c}_{1c}^{1b,\mathrm{T}}\boldsymbol{\varepsilon}_{1b}^0\ddot{\varphi}_{1b}^0\right\rangle,\ \mathbf{J}_{\mathbf{q}_1^{1c}}\left(\mathbf{A}_0\left(\mathbf{q}_1^{1c},\mathbf{q}_{1b}^0\right)\ddot{\mathbf{q}}_{1b}^0\right)_{12} = 0, \\
&\mathbf{J}_{\mathbf{q}_1^{1c}}\left(\mathbf{A}_0\left(\mathbf{q}_1^{1c},\mathbf{q}_{1b}^0\right)\ddot{\mathbf{q}}_{1b}^0\right)_{21} = 0,\ \mathbf{J}_{\mathbf{q}_1^{1c}}\left(\mathbf{A}_0\left(\mathbf{q}_1^{1c},\mathbf{q}_{1b}^0\right)\ddot{\mathbf{q}}_{1b}^0\right)_{22} = \boldsymbol{\gamma}_9 + \boldsymbol{\varepsilon}_1^{1c,\mathrm{T}}\mathbf{I}_1\left\langle \mathbf{c}_1^{1c,\mathrm{T}}\mathbf{c}_{1c}^{1b,\mathrm{T}}\boldsymbol{\varepsilon}_{1b}^0\ddot{\varphi}_{1b}^0\right\rangle\boldsymbol{\varepsilon}_1^{1c}.
\end{aligned} \tag{43}$$

The Jacobian $\mathbf{J}_{\mathbf{q}_{1b}^0}\left(\mathbf{A}_0\left(\mathbf{q}_1^{1c},\mathbf{q}_{1b}^0\right)\ddot{\mathbf{q}}_{1b}^0\right)$ can be got by formula:

$$\begin{aligned}
&\mathbf{J}_{\mathbf{q}_{1b}^0}\left(\mathbf{A}_0\left(\mathbf{q}_1^{1c},\mathbf{q}_{1b}^0\right)\ddot{\mathbf{q}}_{1b}^0\right)_{\mathbf{X}_{fix}} = \begin{bmatrix} \mathbf{J}_{\mathbf{q}_{1b}^0}\left(\mathbf{A}_0\left(\mathbf{q}_1^{1c},\mathbf{q}_{1b}^0\right)\ddot{\mathbf{q}}_{1b}^0\right)_{11} & \mathbf{J}_{\mathbf{q}_{1b}^0}\left(\mathbf{A}_0\left(\mathbf{q}_1^{1c},\mathbf{q}_{1b}^0\right)\ddot{\mathbf{q}}_{1b}^0\right)_{12} \\ \mathbf{J}_{\mathbf{q}_{1b}^0}\left(\mathbf{A}_0\left(\mathbf{q}_1^{1c},\mathbf{q}_{1b}^0\right)\ddot{\mathbf{q}}_{1b}^0\right)_{21} & \mathbf{J}_{\mathbf{q}_{1b}^0}\left(\mathbf{A}_0\left(\mathbf{q}_1^{1c},\mathbf{q}_{1b}^0\right)\ddot{\mathbf{q}}_{1b}^0\right)_{22} \end{bmatrix}, \\
&\mathbf{J}_{\mathbf{q}_{1b}^0}\left(\mathbf{A}_0\left(\mathbf{q}_1^{1c},\mathbf{q}_{1b}^0\right)\ddot{\mathbf{q}}_{1b}^0\right)_{11} = 0, \\
&\mathbf{J}_{\mathbf{q}_{1b}^0}\left(\mathbf{A}_0\left(\mathbf{q}_1^{1c},\mathbf{q}_{1b}^0\right)\ddot{\mathbf{q}}_{1b}^0\right)_{12} = \mathbf{m}_1\mathbf{c}_{1c}^{1b,\mathrm{T}}\left\langle \mathbf{c}_{1b}^{0,\mathrm{T}}\ddot{\mathbf{r}}_{1b}^0\right\rangle\boldsymbol{\varepsilon}_{1b}^0 + \mathbf{m}_1\left[\mathbf{c}_{1c}^{1b,\mathrm{T}}\left\langle \mathbf{r}_{1c}^{1b,1b}\right\rangle^{\mathrm{T}} + \left\langle \mathbf{r}_1^{1c,1c}\right\rangle^{\mathrm{T}}\mathbf{c}_{1c}^{1b,\mathrm{T}}\right]\boldsymbol{\gamma}_8, \\
&\mathbf{J}_{\mathbf{q}_{1b}^0}\left(\mathbf{A}_0\left(\mathbf{q}_1^{1c},\mathbf{q}_{1b}^0\right)\ddot{\mathbf{q}}_{1b}^0\right)_{21} = 0, \\
&\mathbf{J}_{\mathbf{q}_{1b}^0}\left(\mathbf{A}_0\left(\mathbf{q}_1^{1c},\mathbf{q}_{1b}^0\right)\ddot{\mathbf{q}}_{1b}^0\right)_{22} = \boldsymbol{\varepsilon}_1^{1c,\mathrm{T}}\mathbf{I}_1\mathbf{c}_1^{1c,\mathrm{T}}\mathbf{c}_{1c}^{1b,\mathrm{T}}\boldsymbol{\gamma}_8.
\end{aligned} \tag{44}$$

The Jacobian $\mathbf{J}_{\ddot{\mathbf{q}}_{1b}^0}\left(\mathbf{A}_0\left(\mathbf{q}_1^{1c},\mathbf{q}_{1b}^0\right)\ddot{\mathbf{q}}_{1b}^0\right)$ can be got by formula:

$$\mathbf{J}_{\ddot{\mathbf{q}}_{1b}^0}\left(\mathbf{A}_0\left(\mathbf{q}_1^{1c},\mathbf{q}_{1b}^0\right)\ddot{\mathbf{q}}_{1b}^0\right) = \begin{bmatrix} \mathbf{m}_1\mathbf{c}_{1c}^{1b,\mathrm{T}}\mathbf{c}_{1b}^{0,\mathrm{T}} & \mathbf{m}_1\mathbf{c}_{1c}^{1b,\mathrm{T}}\left\langle \mathbf{r}_{1c}^{1b,1b}\right\rangle^{\mathrm{T}}\boldsymbol{\varepsilon}_{1b}^0 + \mathbf{m}_1\left\langle \mathbf{r}_1^{1c,1c}\right\rangle^{\mathrm{T}}\mathbf{c}_{1c}^{1b,\mathrm{T}}\boldsymbol{\varepsilon}_{1b}^0 \\ 0 & \boldsymbol{\varepsilon}_1^{1c,\mathrm{T}}\mathbf{I}_1\mathbf{c}_1^{1c,\mathrm{T}}\mathbf{c}_{1c}^{1b,\mathrm{T}}\boldsymbol{\varepsilon}_{1b}^0 \end{bmatrix}.$$

The item $\mathbf{B}_0\left(\mathbf{q}_1^{1c},\dot{\mathbf{q}}_1^{1c},\mathbf{q}_{1b}^0,\dot{\mathbf{q}}_{1b}^0\right)\dot{\mathbf{q}}_{1b}^0$ can be got by formula:

$$\begin{aligned}
&\mathbf{B}_0\left(\mathbf{q}_1^{1c},\dot{\mathbf{q}}_1^{1c},\mathbf{q}_{1b}^0,\dot{\mathbf{q}}_{1b}^0\right)\dot{\mathbf{q}}_{1b}^0 = \mathbf{b}_{0,1} + \mathbf{b}_{0,2}, \\
&\mathbf{b}_{0,1} = \mathbf{M}_1^{1c,\mathrm{T}}\boldsymbol{\Theta}_1^1\mathbf{L}_1^{1c,\mathrm{T}}\mathbf{L}_{1c}^{1b,\mathrm{T}}\dot{\mathbf{M}}_{1b}^0\dot{\mathbf{q}}_{1b}^0,\ \mathbf{b}_{0,2} = \mathbf{M}_1^{1c,\mathrm{T}}\left[\boldsymbol{\Theta}_1^1\boldsymbol{\Phi}_1^{1c,1,\mathrm{T}} + \boldsymbol{\Phi}_1^{0,1}\boldsymbol{\Theta}_1^1\right]\mathbf{L}_1^{1c,\mathrm{T}}\mathbf{L}_{1c}^{1b,\mathrm{T}}\mathbf{M}_{1b}^0\dot{\mathbf{q}}_{1b}^0,
\end{aligned} \tag{45}$$

where $\mathbf{b}_{0,1}$ will be:

$$\mathbf{b}_{0,1} = \begin{bmatrix} \mathbf{m}_1\mathbf{c}_{1c}^{1b,\mathrm{T}}\left\langle \boldsymbol{\varepsilon}_{1b}^0\dot{\boldsymbol{\varphi}}_{1b}^0\right\rangle^{\mathrm{T}}\mathbf{c}_{1b}^{0,\mathrm{T}}\dot{\mathbf{r}}_{1b}^{0,0} + \mathbf{m}_1\mathbf{c}_{1c}^{1b,\mathrm{T}}\left\langle \mathbf{r}_{1c}^{1b,1b}\right\rangle^{\mathrm{T}}\dot{\boldsymbol{\varepsilon}}_{1b}^0\dot{\boldsymbol{\varphi}}_{1b}^0 + \mathbf{m}_1\left\langle \mathbf{r}_1^{1c,1c}\right\rangle^{\mathrm{T}}\mathbf{c}_{1c}^{1b,\mathrm{T}}\dot{\boldsymbol{\varepsilon}}_{1b}^0\dot{\boldsymbol{\varphi}}_{1b}^0 \\ \boldsymbol{\varepsilon}_1^{1c,\mathrm{T}}\mathbf{I}_1\mathbf{c}_1^{1c,\mathrm{T}}\mathbf{c}_{1c}^{1b,\mathrm{T}}\dot{\boldsymbol{\varepsilon}}_{1b}^0\dot{\boldsymbol{\varphi}}_{1b}^0 \end{bmatrix}, \tag{46}$$

and $\mathbf{b}_{0,2}$ will be:

$$\begin{aligned}
\mathbf{b}_{0,2} &= \mathbf{M}_1^{1c,\mathrm{T}}\left[\boldsymbol{\Theta}_1^1\boldsymbol{\Phi}_1^{1c,1,\mathrm{T}} + \boldsymbol{\Phi}_1^{0,1}\boldsymbol{\Theta}_1^1\right]\mathbf{L}_1^{1c,\mathrm{T}}\mathbf{L}_{1c}^{1b,\mathrm{T}}\mathbf{M}_{1b}^0\dot{\mathbf{q}}_{1b}^0 = \begin{bmatrix}\mathbf{b}_{0,2,1}\\ \mathbf{b}_{0,2,2}\end{bmatrix},\\
\mathbf{b}_{0,2,1} &= \mathbf{m}_1\mathbf{c}_{1c}^{1b,\mathrm{T}}\langle\boldsymbol{\varepsilon}_{1b}^0\dot{\boldsymbol{\varphi}}_{1b}^0\rangle\mathbf{c}_{1b}^{0,\mathrm{T}}\dot{\mathbf{r}}_{1b}^{0,0} + \mathbf{m}_1\mathbf{c}_{1c}^{1b,\mathrm{T}}\langle\boldsymbol{\varepsilon}_{1b}^0\dot{\boldsymbol{\varphi}}_{1b}^0\rangle\left\langle\mathbf{r}_{1c}^{1b,1b}\right\rangle^{\mathrm{T}}\boldsymbol{\varepsilon}_{1b}^0\dot{\boldsymbol{\varphi}}_{1b}^0\\
&\quad + \mathbf{m}_1\mathbf{c}_{1c}^{1b,\mathrm{T}}\langle\boldsymbol{\varepsilon}_{1b}^0\dot{\boldsymbol{\varphi}}_{1b}^0\rangle\mathbf{c}_{1c}^{1b}\left\langle\mathbf{r}_1^{1c,1c}\right\rangle^{\mathrm{T}}\mathbf{c}_{1c}^{1b,\mathrm{T}}\boldsymbol{\varepsilon}_{1b}^0\dot{\boldsymbol{\varphi}}_{1b}^0 + \mathbf{m}_1\left\langle\dot{\mathbf{r}}_1^{1c,1c}\right\rangle^{\mathrm{T}}\mathbf{c}_{1c}^{1b,\mathrm{T}}\boldsymbol{\varepsilon}_{1b}^0\dot{\boldsymbol{\varphi}}_{1b}^0,\\
\mathbf{b}_{0,2,2} &= \mathbf{m}_1\boldsymbol{\varepsilon}_1^{1c,\mathrm{T}}\left\langle\mathbf{v}_1^{0,1}\right\rangle\mathbf{c}_1^{1c,\mathrm{T}}\mathbf{c}_{1c}^{1b,\mathrm{T}}\mathbf{c}_{1b}^{0,\mathrm{T}}\dot{\mathbf{r}}_{1b}^{0,0}\\
&\quad + \mathbf{m}_1\boldsymbol{\varepsilon}_1^{1c,\mathrm{T}}\left\langle\mathbf{v}_1^{0,1}\right\rangle\mathbf{c}_1^{1c,\mathrm{T}}\mathbf{c}_{1c}^{1b,\mathrm{T}}\left\langle\mathbf{r}_{1c}^{1b,1b}\right\rangle^{\mathrm{T}}\boldsymbol{\varepsilon}_{1b}^0\dot{\boldsymbol{\varphi}}_{1b}^0 + \mathbf{m}_1\boldsymbol{\varepsilon}_1^{1c,\mathrm{T}}\left\langle\mathbf{v}_1^{0,1}\right\rangle\mathbf{c}_1^{1c,\mathrm{T}}\left\langle\mathbf{r}_1^{1c,1c}\right\rangle^{\mathrm{T}}\mathbf{c}_{1c}^{1b,\mathrm{T}}\boldsymbol{\varepsilon}_{1b}^0\dot{\boldsymbol{\varphi}}_{1b}^0.
\end{aligned} \tag{47}$$

We linearize (46), then:

$$\mathbf{b}_{0,1} \approx \mathbf{b}_{0,1,fix} + \mathbf{J}_{\mathbf{q}_1^{1c}}\left(\mathbf{b}_{0,1}\right)_{\mathbf{X}_{fix}}\delta\mathbf{q}_1^{1c} + \mathbf{J}_{\mathbf{q}_{1b}^0}\left(\mathbf{b}_{0,1}\right)_{\mathbf{X}_{fix}}\delta\mathbf{q}_{1b}^0 + \mathbf{J}_{\dot{\mathbf{q}}_{1b}^0}\left(\mathbf{b}_{0,1}\right)_{\mathbf{X}_{fix}}\delta\dot{\mathbf{q}}_{1b}^0. \tag{48}$$

The first variation from (46) is defined as follows:

$$\begin{aligned}
\delta\mathbf{b}_{0,1} &= \begin{bmatrix}\delta\mathbf{b}_{0,1,1}\\ \delta\mathbf{b}_{0,1,2}\end{bmatrix},\ \delta\mathbf{b}_{0,1,1} = \delta\left(\mathbf{m}_1\mathbf{c}_{1c}^{1b,\mathrm{T}}\langle\boldsymbol{\varepsilon}_{1b}^0\dot{\boldsymbol{\varphi}}_{1b}^0\rangle^{\mathrm{T}}\mathbf{c}_{1b}^{0,\mathrm{T}}\dot{\mathbf{r}}_{1b}^{0,0}\right) + \delta\left(\mathbf{m}_1\mathbf{c}_{1c}^{1b,\mathrm{T}}\left\langle\mathbf{r}_{1c}^{1b,1b}\right\rangle^{\mathrm{T}}\dot{\boldsymbol{\varepsilon}}_{1b}^0\dot{\boldsymbol{\varphi}}_{1b}^0\right) +\\
&\quad + \delta\left(\mathbf{m}_1\left\langle\mathbf{r}_1^{1c,1c}\right\rangle^{\mathrm{T}}\mathbf{c}_{1c}^{1b,\mathrm{T}}\dot{\boldsymbol{\varepsilon}}_{1b}^0\dot{\boldsymbol{\varphi}}_{1b}^0\right),\ \delta\mathbf{b}_{0,1,2} = \delta\left(\boldsymbol{\varepsilon}_1^{1c,\mathrm{T}}\mathbf{I}_1\mathbf{c}_1^{1c,\mathrm{T}}\mathbf{c}_{1c}^{1b,\mathrm{T}}\dot{\boldsymbol{\varepsilon}}_{1b}^0\dot{\boldsymbol{\varphi}}_{1b}^0\right),
\end{aligned} \tag{49}$$

where the item $\delta\left(\mathbf{m}_1\mathbf{c}_{1c}^{1b,\mathrm{T}}\langle\boldsymbol{\varepsilon}_{1b}^0\dot{\boldsymbol{\varphi}}_{1b}^0\rangle^{\mathrm{T}}\mathbf{c}_{1b}^{0,\mathrm{T}}\dot{\mathbf{r}}_{1b}^{0,0}\right)$ equals to:

$$\begin{aligned}
&\delta\left(\mathbf{m}_1\mathbf{c}_{1c}^{1b,\mathrm{T}}\langle\boldsymbol{\varepsilon}_{1b}^0\dot{\boldsymbol{\varphi}}_{1b}^0\rangle^{\mathrm{T}}\mathbf{c}_{1b}^{0,\mathrm{T}}\dot{\mathbf{r}}_{1b}^{0,0}\right)\\
&\quad = \left[\mathbf{m}_1\mathbf{c}_{1c}^{1b,\mathrm{T}}\left\langle\mathbf{c}_{1b}^{0,\mathrm{T}}\dot{\mathbf{r}}_{1b}^{0,0}\right\rangle\boldsymbol{\gamma}_2 + \mathbf{m}_1\mathbf{c}_{1c}^{1b,\mathrm{T}}\langle\boldsymbol{\varepsilon}_{1b}^0\dot{\boldsymbol{\varphi}}_{1b}^0\rangle\left\langle\mathbf{c}_{1b}^{0,\mathrm{T}}\dot{\mathbf{r}}_{1b}^{0,0}\right\rangle^{\mathrm{T}}\boldsymbol{\varepsilon}_{1b}^0\right]\delta\varphi_{1b}^0\\
&\quad + \mathbf{m}_1\mathbf{c}_{1c}^{1b,\mathrm{T}}\langle\boldsymbol{\varepsilon}_{1b}^0\dot{\boldsymbol{\varphi}}_{1b}^0\rangle^{\mathrm{T}}\mathbf{c}_{1b}^{0,\mathrm{T}}\delta\dot{\mathbf{r}}_{1b}^{0,0} + \mathbf{m}_1\mathbf{c}_{1c}^{1b,\mathrm{T}}\left\langle\mathbf{c}_{1b}^{0,\mathrm{T}}\dot{\mathbf{r}}_{1b}^{0,0}\right\rangle\boldsymbol{\varepsilon}_{1b}^0\delta\dot{\boldsymbol{\varphi}}_{1b}^0,
\end{aligned} \tag{50}$$

the item $\delta\left(\mathbf{m}_1\mathbf{c}_{1c}^{1b,\mathrm{T}}\left\langle\mathbf{r}_{1c}^{1b,1b}\right\rangle^{\mathrm{T}}\dot{\boldsymbol{\varepsilon}}_{1b}^0\dot{\boldsymbol{\varphi}}_{1b}^0\right)$ equals to:

$$\begin{aligned}
&\delta\left(\mathbf{m}_1\mathbf{c}_{1c}^{1b,\mathrm{T}}\left\langle\mathbf{r}_{1c}^{1b,1b}\right\rangle^{\mathrm{T}}\dot{\boldsymbol{\varepsilon}}_{1b}^0\dot{\boldsymbol{\varphi}}_{1b}^0\right) = \mathbf{m}_1\mathbf{c}_{1c}^{1b,\mathrm{T}}\left\langle\mathbf{r}_{1c}^{1b,1b}\right\rangle^{\mathrm{T}}\boldsymbol{\gamma}_{10}\delta\varphi_{1b}^0\\
&+ \left[\mathbf{m}_1\mathbf{c}_{1c}^{1b,\mathrm{T}}\left\langle\mathbf{r}_{1c}^{1b,1b}\right\rangle^{\mathrm{T}}\boldsymbol{\gamma}_2 + \mathbf{m}_1\mathbf{c}_{1c}^{1b,\mathrm{T}}\left\langle\mathbf{r}_{1c}^{1b,1b}\right\rangle^{\mathrm{T}}\dot{\boldsymbol{\varepsilon}}_{1b}^0\right]\delta\dot{\boldsymbol{\varphi}}_{1b}^0,\ \boldsymbol{\gamma}_{10} = \left[\boldsymbol{\phi}_{1b,1}^0\dot{\boldsymbol{\varphi}}_{1b}^0|\boldsymbol{\phi}_{1b,2}^0\dot{\boldsymbol{\varphi}}_{1b}^0|\boldsymbol{\phi}_{1b,3}^0\dot{\boldsymbol{\varphi}}_{1b}^0\right],
\end{aligned} \tag{51}$$

the item $\delta\left(\mathbf{m}_1\left\langle\mathbf{r}_1^{1c,1c}\right\rangle^{\mathrm{T}}\mathbf{c}_{1c}^{1b,\mathrm{T}}\dot{\boldsymbol{\varepsilon}}_{1b}^{0}\dot{\boldsymbol{\varphi}}_{1b}^{0}\right)$ equals to:

$$\begin{gathered}\delta\left(\mathbf{m}_1\left\langle\mathbf{r}_1^{1c,1c}\right\rangle^{\mathrm{T}}\mathbf{c}_{1c}^{1b,\mathrm{T}}\dot{\boldsymbol{\varepsilon}}_{1b}^{0}\dot{\boldsymbol{\varphi}}_{1b}^{0}\right)=\mathbf{m}_1\left\langle\mathbf{c}_{1c}^{1b,\mathrm{T}}\dot{\boldsymbol{\varepsilon}}_{1b}^{0}\dot{\boldsymbol{\varphi}}_{1b}^{0}\right\rangle\delta\mathbf{r}_1^{1c,1c}\\+\mathbf{m}_1\left\langle\mathbf{r}_1^{1c,1c}\right\rangle^{\mathrm{T}}\mathbf{c}_{1c}^{1b,\mathrm{T}}\boldsymbol{\gamma}_{10}\delta\varphi_{1b}^{0}+\left[\mathbf{m}_1\left\langle\mathbf{r}_1^{1c,1c}\right\rangle^{\mathrm{T}}\mathbf{c}_{1c}^{1b,\mathrm{T}}\boldsymbol{\gamma}_2+\mathbf{m}_1\left\langle\mathbf{r}_1^{1c,1c}\right\rangle^{\mathrm{T}}\mathbf{c}_{1c}^{1b,\mathrm{T}}\dot{\boldsymbol{\varepsilon}}_{1b}^{0}\right]\delta\dot{\boldsymbol{\varphi}}_{1b}^{0},\end{gathered}\tag{52}$$

the item $\delta\left(\boldsymbol{\varepsilon}_1^{1c,\mathrm{T}}\mathbf{I}_1\mathbf{c}_1^{1c,\mathrm{T}}\mathbf{c}_{1c}^{1b,\mathrm{T}}\dot{\boldsymbol{\varepsilon}}_{1b}^{0}\dot{\boldsymbol{\varphi}}_{1b}^{0}\right)$ equals to:

$$\begin{gathered}\delta\left(\boldsymbol{\varepsilon}_1^{1c,\mathrm{T}}\mathbf{I}_1\mathbf{c}_1^{1c,\mathrm{T}}\mathbf{c}_{1c}^{1b,\mathrm{T}}\dot{\boldsymbol{\varepsilon}}_{1b}^{0}\dot{\boldsymbol{\varphi}}_{1b}^{0}\right)=\left[\boldsymbol{\gamma}_{11}+\boldsymbol{\varepsilon}_1^{1c,\mathrm{T}}\mathbf{I}_1\left\langle\mathbf{c}_1^{1c,\mathrm{T}}\mathbf{c}_{1c}^{1b,\mathrm{T}}\dot{\boldsymbol{\varepsilon}}_{1b}^{0}\dot{\boldsymbol{\varphi}}_{1b}^{0}\right\rangle\boldsymbol{\varepsilon}_1^{1c}\right]\delta\varphi_1^{1c}\\+\boldsymbol{\varepsilon}_1^{1c,\mathrm{T}}\mathbf{I}_1\mathbf{c}_1^{1c,\mathrm{T}}\mathbf{c}_{1c}^{1b,\mathrm{T}}\boldsymbol{\gamma}_{10}\delta\varphi_{1b}^{0}+\left[\boldsymbol{\varepsilon}_1^{1c,\mathrm{T}}\mathbf{I}_1\mathbf{c}_1^{1c,\mathrm{T}}\mathbf{c}_{1c}^{1b,\mathrm{T}}\boldsymbol{\gamma}_2+\boldsymbol{\varepsilon}_1^{1c,\mathrm{T}}\mathbf{I}_1\mathbf{c}_1^{1c,\mathrm{T}}\mathbf{c}_{1c}^{1b,\mathrm{T}}\dot{\boldsymbol{\varepsilon}}_{1b}^{0}\right]\delta\dot{\boldsymbol{\varphi}}_{1b}^{0},\\\boldsymbol{\gamma}_{11}=\left[\boldsymbol{\lambda}_{1,1}^{1c,\mathrm{T}}\mathbf{I}_1\mathbf{c}_1^{1c,\mathrm{T}}\mathbf{c}_{1c}^{1b,\mathrm{T}}\dot{\boldsymbol{\varepsilon}}_{1b}^{0}\dot{\boldsymbol{\varphi}}_{1b}^{0}|\boldsymbol{\lambda}_{1,2}^{1c,\mathrm{T}}\mathbf{I}_1\mathbf{c}_1^{1c,\mathrm{T}}\mathbf{c}_{1c}^{1b,\mathrm{T}}\dot{\boldsymbol{\varepsilon}}_{1b}^{0}\dot{\boldsymbol{\varphi}}_{1b}^{0}|\boldsymbol{\lambda}_{1,3}^{1c,\mathrm{T}}\mathbf{I}_1\mathbf{c}_1^{1c,\mathrm{T}}\mathbf{c}_{1c}^{1b,\mathrm{T}}\dot{\boldsymbol{\varepsilon}}_{1b}^{0}\dot{\boldsymbol{\varphi}}_{1b}^{0}\right].\end{gathered}\tag{53}$$

The Jacobian $\mathbf{J}_{\mathbf{q}_1^{1c}}(\mathbf{b}_{0,1})$ can be got by formula:

$$\begin{gathered}\mathbf{J}_{\mathbf{q}_1^{1c}}(\mathbf{b}_{0,1})=\begin{bmatrix}\mathbf{J}_{\mathbf{q}_1^{1c}}(\mathbf{b}_{0,1})_{11} & \mathbf{J}_{\mathbf{q}_1^{1c}}(\mathbf{b}_{0,1})_{12}\\ \mathbf{J}_{\mathbf{q}_1^{1c}}(\mathbf{b}_{0,1})_{21} & \mathbf{J}_{\mathbf{q}_1^{1c}}(\mathbf{b}_{0,1})_{22}\end{bmatrix},\\\mathbf{J}_{\mathbf{q}_1^{1c}}(\mathbf{b}_{0,1})_{11}=\mathbf{m}_1\left\langle\mathbf{c}_{1c}^{1b,\mathrm{T}}\dot{\boldsymbol{\varepsilon}}_{1b}^{0}\dot{\boldsymbol{\varphi}}_{1b}^{0}\right\rangle,\ \mathbf{J}_{\mathbf{q}_1^{1c}}(\mathbf{b}_{0,1})_{12}=0,\\\mathbf{J}_{\mathbf{q}_1^{1c}}(\mathbf{b}_{0,1})_{21}=0,\ \mathbf{J}_{\mathbf{q}_1^{1c}}(\mathbf{b}_{0,1})_{22}=\boldsymbol{\gamma}_{11}+\boldsymbol{\varepsilon}_1^{1c,\mathrm{T}}\mathbf{I}_1\left\langle\mathbf{c}_1^{1c,\mathrm{T}}\mathbf{c}_{1c}^{1b,\mathrm{T}}\dot{\boldsymbol{\varepsilon}}_{1b}^{0}\dot{\boldsymbol{\varphi}}_{1b}^{0}\right\rangle\boldsymbol{\varepsilon}_1^{1c}.\end{gathered}\tag{54}$$

The Jacobian $\mathbf{J}_{\mathbf{q}_{1b}^{0}}(\mathbf{b}_{0,1})$ can be got by formula:

$$\begin{gathered}\mathbf{J}_{\mathbf{q}_{1b}^{0}}(\mathbf{b}_{0,1})=\begin{bmatrix}\mathbf{J}_{\mathbf{q}_{1b}^{0}}(\mathbf{b}_{0,1})_{11} & \mathbf{J}_{\mathbf{q}_{1b}^{0}}(\mathbf{b}_{0,1})_{12}\\ \mathbf{J}_{\mathbf{q}_{1b}^{0}}(\mathbf{b}_{0,1})_{21} & \mathbf{J}_{\mathbf{q}_{1b}^{0}}(\mathbf{b}_{0,1})_{22}\end{bmatrix},\\\mathbf{J}_{\mathbf{q}_{1b}^{0}}(\mathbf{b}_{0,1})_{11}=0,\\\mathbf{J}_{\mathbf{q}_{1b}^{0}}(\mathbf{b}_{0,1})_{12}=\mathbf{m}_1\mathbf{c}_{1c}^{1b,\mathrm{T}}\left\langle\mathbf{c}_{1b}^{0,\mathrm{T}}\dot{\mathbf{r}}_{1b}^{0,0}\right\rangle\boldsymbol{\gamma}_2+\mathbf{m}_1\mathbf{c}_{1c}^{1b,\mathrm{T}}\langle\boldsymbol{\varepsilon}_{1b}^{0}\dot{\boldsymbol{\varphi}}_{1b}^{0}\rangle\left\langle\mathbf{c}_{1b}^{0,\mathrm{T}}\dot{\mathbf{r}}_{1b}^{0,0}\right\rangle^{\mathrm{T}}\boldsymbol{\varepsilon}_{1b}^{0}+\\+\mathbf{m}_1\mathbf{c}_{1c}^{1b,\mathrm{T}}\left\langle\mathbf{r}_{1c}^{1b,1b}\right\rangle^{\mathrm{T}}\boldsymbol{\gamma}_{10}+\mathbf{m}_1\left\langle\mathbf{r}_1^{1c,1c}\right\rangle^{\mathrm{T}}\mathbf{c}_{1c}^{1b,\mathrm{T}}\boldsymbol{\gamma}_{10},\\\mathbf{J}_{\mathbf{q}_{1b}^{0}}(\mathbf{b}_{0,1})_{21}=0,\ \mathbf{J}_{\mathbf{q}_{1b}^{0}}(\mathbf{b}_{0,1})_{22}=\boldsymbol{\varepsilon}_1^{1c,\mathrm{T}}\mathbf{I}_1\mathbf{c}_1^{1c,\mathrm{T}}\mathbf{c}_{1c}^{1b,\mathrm{T}}\boldsymbol{\gamma}_{10}.\end{gathered}\tag{55}$$

The Jacobian $\mathbf{J}_{\dot{\mathbf{q}}^0_{1b}}\left(\mathbf{b}_{0,1}\right)$ can be got by formula:

$$\begin{gathered}\mathbf{J}_{\dot{\mathbf{q}}^0_{1b}}\left(\mathbf{b}_{0,1}\right)=\begin{bmatrix}\mathbf{J}_{\dot{\mathbf{q}}^0_{1b}}\left(\mathbf{b}_{0,1}\right)_{11} & \mathbf{J}_{\dot{\mathbf{q}}^0_{1b}}\left(\mathbf{b}_{0,1}\right)_{12}\\ \mathbf{J}_{\dot{\mathbf{q}}^0_{1b}}\left(\mathbf{b}_{0,1}\right)_{21} & \mathbf{J}_{\dot{\mathbf{q}}^0_{1b}}\left(\mathbf{b}_{0,1}\right)_{22}\end{bmatrix},\\ \mathbf{J}_{\dot{\mathbf{q}}^0_{1b}}\left(\mathbf{b}_{0,1}\right)_{11}=\mathbf{m}_1\mathbf{c}_{1c}^{1b,\mathrm{T}}\left\langle\boldsymbol{\varepsilon}^0_{1b}\dot{\boldsymbol{\varphi}}^0_{1b}\right\rangle^{\mathrm{T}}\mathbf{c}_{1b}^{0,\mathrm{T}},\\ \mathbf{J}_{\dot{\mathbf{q}}^0_{1b}}\left(\mathbf{b}_{0,1}\right)_{12}=\mathbf{m}_1\mathbf{c}_{1c}^{1b,\mathrm{T}}\left\langle\mathbf{c}_{1b}^{0,\mathrm{T}}\dot{\mathbf{r}}_{1b}^{0,0}\right\rangle\boldsymbol{\varepsilon}^0_{1b}+\mathbf{m}_1\mathbf{c}_{1c}^{1b,\mathrm{T}}\left\langle\mathbf{r}_{1c}^{1b,1b}\right\rangle^{\mathrm{T}}\boldsymbol{\gamma}_2+\mathbf{m}_1\mathbf{c}_{1c}^{1b,\mathrm{T}}\left\langle\mathbf{r}_{1c}^{1b,1b}\right\rangle^{\mathrm{T}}\dot{\boldsymbol{\varepsilon}}^0_{1b}+\\ +\mathbf{m}_1\left\langle\mathbf{r}_1^{1c,1c}\right\rangle^{\mathrm{T}}\mathbf{c}_{1c}^{1b,\mathrm{T}}\boldsymbol{\gamma}_2+\mathbf{m}_1\left\langle\mathbf{r}_1^{1c,1c}\right\rangle^{\mathrm{T}}\mathbf{c}_{1c}^{1b,\mathrm{T}}\dot{\boldsymbol{\varepsilon}}^0_{1b},\\ \mathbf{J}_{\dot{\mathbf{q}}^0_{1b}}\left(\mathbf{b}_{0,1}\right)_{21}=0,\ \mathbf{J}_{\dot{\mathbf{q}}^0_{1b}}\left(\mathbf{b}_{0,1}\right)_{22}=\boldsymbol{\varepsilon}_1^{1c,\mathrm{T}}\mathbf{I}_1\mathbf{c}_1^{1c,\mathrm{T}}\mathbf{c}_{1c}^{1b,\mathrm{T}}\boldsymbol{\gamma}_2+\boldsymbol{\varepsilon}_1^{1c,\mathrm{T}}\mathbf{I}_1\mathbf{c}_1^{1c,\mathrm{T}}\mathbf{c}_{1c}^{1b,\mathrm{T}}\dot{\boldsymbol{\varepsilon}}^0_{1b}.\end{gathered}\tag{56}$$

We linearize (47), then:

$$\begin{gathered}\mathbf{b}_{0,2}\approx\mathbf{b}_{0,2,fix}+\mathbf{J}_{\mathbf{q}_1^{1c}}\left(\mathbf{b}_{0,2}\right)_{\mathbf{X}_{fix}}\delta\mathbf{q}_1^{1c}+\mathbf{J}_{\dot{\mathbf{q}}_1^{1c}}\left(\mathbf{b}_{0,2}\right)_{\mathbf{X}_{fix}}\delta\dot{\mathbf{q}}_1^{1c}+\\ +\mathbf{J}_{\mathbf{q}^0_{1b}}\left(\mathbf{b}_{0,2}\right)_{\mathbf{X}_{fix}}\delta\mathbf{q}^0_{1b}+\mathbf{J}_{\dot{\mathbf{q}}^0_{1b}}\left(\mathbf{b}_{0,2}\right)_{\mathbf{X}_{fix}}\delta\dot{\mathbf{q}}^0_{1b}.\end{gathered}\tag{57}$$

The first variation from (47) is defined as follows:

$$\begin{gathered}\delta\mathbf{b}_{0,2}=\begin{bmatrix}\delta\mathbf{b}_{0,2,1}\\ \delta\mathbf{b}_{0,2,2}\end{bmatrix},\\ \delta\mathbf{b}_{0,2,1}=\delta\left(\mathbf{m}_1\mathbf{c}_{1c}^{1b,\mathrm{T}}\left\langle\boldsymbol{\varepsilon}^0_{1b}\dot{\boldsymbol{\varphi}}^0_{1b}\right\rangle\mathbf{c}_{1b}^{0,\mathrm{T}}\dot{\mathbf{r}}_{1b}^{0,0}\right)+\delta\left(\mathbf{m}_1\mathbf{c}_{1c}^{1b,\mathrm{T}}\left\langle\boldsymbol{\varepsilon}^0_{1b}\dot{\boldsymbol{\varphi}}^0_{1b}\right\rangle\left\langle\mathbf{r}_{1c}^{1b,1b}\right\rangle^{\mathrm{T}}\boldsymbol{\varepsilon}^0_{1b}\dot{\boldsymbol{\varphi}}^0_{1b}\right)+\\ +\delta\left(\mathbf{m}_1\mathbf{c}_{1c}^{1b,\mathrm{T}}\left\langle\boldsymbol{\varepsilon}^0_{1b}\dot{\boldsymbol{\varphi}}^0_{1b}\right\rangle\mathbf{c}_{1c}^{1b}\left\langle\mathbf{r}_1^{1c,1c}\right\rangle^{\mathrm{T}}\mathbf{c}_{1c}^{1b,\mathrm{T}}\varepsilon^0_{1b}\dot{\boldsymbol{\varphi}}^0_{1b}\right)+\delta\left(\mathbf{m}_1\left\langle\dot{\mathbf{r}}_1^{1c,1c}\right\rangle^{\mathrm{T}}\mathbf{c}_{1c}^{1b,\mathrm{T}}\boldsymbol{\varepsilon}^0_{1b}\dot{\boldsymbol{\varphi}}^0_{1b}\right),\\ \delta\mathbf{b}_{0,2,2}=\delta\left(\mathbf{m}_1\boldsymbol{\varepsilon}_1^{1c,\mathrm{T}}\left\langle\mathbf{v}_1^{0,1}\right\rangle\mathbf{c}_1^{1c,\mathrm{T}}\mathbf{c}_{1c}^{1b,\mathrm{T}}\mathbf{c}_{1b}^{0,\mathrm{T}}\dot{\mathbf{r}}_{1b}^{0,0}\right)+\\ +\delta\left(\mathbf{m}_1\boldsymbol{\varepsilon}_1^{1c,\mathrm{T}}\left\langle\mathbf{v}_1^{0,1}\right\rangle\mathbf{c}_1^{1c,\mathrm{T}}\mathbf{c}_{1c}^{1b,\mathrm{T}}\left\langle\mathbf{r}_{1c}^{1b,1b}\right\rangle^{\mathrm{T}}\boldsymbol{\varepsilon}^0_{1b}\dot{\boldsymbol{\varphi}}^0_{1b}\right)+\delta\left(\mathbf{m}_1\boldsymbol{\varepsilon}_1^{1c,\mathrm{T}}\left\langle\mathbf{v}_1^{0,1}\right\rangle\mathbf{c}_1^{1c,\mathrm{T}}\left\langle\mathbf{r}_1^{1c,1c}\right\rangle^{\mathrm{T}}\mathbf{c}_{1c}^{1b,\mathrm{T}}\boldsymbol{\varepsilon}^0_{1b}\dot{\boldsymbol{\varphi}}^0_{1b}\right),\end{gathered}\tag{58}$$

where the item $\delta\left(\mathbf{m}_1\mathbf{c}_{1c}^{1b,\mathrm{T}}\left\langle\boldsymbol{\varepsilon}^0_{1b}\dot{\boldsymbol{\varphi}}^0_{1b}\right\rangle\mathbf{c}_{1b}^{0,\mathrm{T}}\dot{\mathbf{r}}_{1b}^{0,0}\right)$ equals to:

$$\begin{gathered}\delta\left(\mathbf{m}_1\mathbf{c}_{1c}^{1b,\mathrm{T}}\left\langle\boldsymbol{\varepsilon}^0_{1b}\dot{\boldsymbol{\varphi}}^0_{1b}\right\rangle\mathbf{c}_{1b}^{0,\mathrm{T}}\dot{\mathbf{r}}_{1b}^{0,0}\right)=\mathbf{m}_1\mathbf{c}_{1c}^{1b,\mathrm{T}}\left\langle\mathbf{c}_{1b}^{0,\mathrm{T}}\dot{\mathbf{r}}_{1b}^{0,0}\right\rangle^{\mathrm{T}}\boldsymbol{\gamma}_2\delta\varphi^0_{1b}\\ +\mathbf{m}_1\mathbf{c}_{1c}^{1b,\mathrm{T}}\left\langle\boldsymbol{\varepsilon}^0_{1b}\dot{\boldsymbol{\varphi}}^0_{1b}\right\rangle\mathbf{c}_{1b}^{0,\mathrm{T}}\delta\dot{\mathbf{r}}_{1b}^{0,0}+\mathbf{m}_1\mathbf{c}_{1c}^{1b,\mathrm{T}}\left[\mathbf{I}-\left\langle\boldsymbol{\varepsilon}^0_{1b}\dot{\boldsymbol{\varphi}}^0_{1b}\right\rangle\right]\left\langle\mathbf{c}_{1b}^{0,\mathrm{T}}\dot{\mathbf{r}}_{1b}^{0,0}\right\rangle^{\mathrm{T}}\boldsymbol{\varepsilon}^0_{1b}\delta\dot{\boldsymbol{\varphi}}^0_{1b},\end{gathered}\tag{59}$$

where $\mathbf{I}$—identity matrix.

The item $\delta\left(\mathbf{m}_1\mathbf{c}_{1c}^{1b,\mathrm{T}}\left\langle\boldsymbol{\varepsilon}_{1b}^0\dot{\boldsymbol{\varphi}}_{1b}^0\right\rangle\left\langle\mathbf{r}_{1c}^{1b,1b}\right\rangle^{\mathrm{T}}\boldsymbol{\varepsilon}_{1b}^0\dot{\boldsymbol{\varphi}}_{1b}^0\right)$ equals to:

$$\begin{aligned}&\delta\left(\mathbf{m}_1\mathbf{c}_{1c}^{1b,\mathrm{T}}\left\langle\boldsymbol{\varepsilon}_{1b}^0\dot{\boldsymbol{\varphi}}_{1b}^0\right\rangle\left\langle\mathbf{r}_{1c}^{1b,1b}\right\rangle^{\mathrm{T}}\boldsymbol{\varepsilon}_{1b}^0\dot{\boldsymbol{\varphi}}_{1b}^0\right)\\&=\mathbf{m}_1\mathbf{c}_{1c}^{1b,\mathrm{T}}\left[\left\langle\left\langle\mathbf{r}_{1c}^{1b,1b}\right\rangle\boldsymbol{\varepsilon}_{1b}^0\dot{\boldsymbol{\varphi}}_{1b}^0\right\rangle+\left\langle\boldsymbol{\varepsilon}_{1b}^0\dot{\boldsymbol{\varphi}}_{1b}^0\right\rangle\left\langle\mathbf{r}_{1c}^{1b,1b}\right\rangle^{\mathrm{T}}\right]\boldsymbol{\gamma}_2\delta\varphi_{1b}^0\\&+\mathbf{m}_1\mathbf{c}_{1c}^{1b,\mathrm{T}}\left[\left\langle\left\langle\mathbf{r}_{1c}^{1b,1b}\right\rangle\boldsymbol{\varepsilon}_{1b}^0\dot{\boldsymbol{\varphi}}_{1b}^0\right\rangle+\left\langle\boldsymbol{\varepsilon}_{1b}^0\dot{\boldsymbol{\varphi}}_{1b}^0\right\rangle\left\langle\mathbf{r}_{1c}^{1b,1b}\right\rangle^{\mathrm{T}}\right]\boldsymbol{\varepsilon}_{1b}^0\delta\dot{\boldsymbol{\varphi}}_{1b}^0.\end{aligned}\tag{60}$$

The item $\delta\left(\mathbf{m}_1\mathbf{c}_{1c}^{1b,\mathrm{T}}\left\langle\boldsymbol{\varepsilon}_{1b}^0\dot{\boldsymbol{\varphi}}_{1b}^0\right\rangle\mathbf{c}_{1c}^{1b}\left\langle\mathbf{r}_1^{1c,1c}\right\rangle^{\mathrm{T}}\mathbf{c}_{1c}^{1b,\mathrm{T}}\boldsymbol{\varepsilon}_{1b}^0\dot{\boldsymbol{\varphi}}_{1b}^0\right)$ equals to:

$$\begin{aligned}\delta\left(\mathbf{m}_1\mathbf{c}_{1c}^{1b,\mathrm{T}}\left\langle\boldsymbol{\varepsilon}_{1b}^0\dot{\boldsymbol{\varphi}}_{1b}^0\right\rangle\mathbf{c}_{1c}^{1b}\left\langle\mathbf{r}_1^{1c,1c}\right\rangle^{\mathrm{T}}\mathbf{c}_{1c}^{1b,\mathrm{T}}\boldsymbol{\varepsilon}_{1b}^0\dot{\boldsymbol{\varphi}}_{1b}^0\right)&=\mathbf{m}_1\mathbf{c}_{1c}^{1b,\mathrm{T}}\left\langle\boldsymbol{\varepsilon}_{1b}^0\dot{\boldsymbol{\varphi}}_{1b}^0\right\rangle\mathbf{c}_{1c}^{1b}\left\langle\mathbf{c}_{1c}^{1b,\mathrm{T}}\boldsymbol{\varepsilon}_{1b}^0\dot{\boldsymbol{\varphi}}_{1b}^0\right\rangle\delta\mathbf{r}_1^{1c,1c}\\&+\mathbf{m}_1\mathbf{c}_{1c}^{1b,\mathrm{T}}\left[\left\langle\mathbf{c}_{1c}^{1b}\left\langle\mathbf{r}_1^{1c,1c}\right\rangle\mathbf{c}_{1c}^{1b,\mathrm{T}}\boldsymbol{\varepsilon}_{1b}^0\dot{\boldsymbol{\varphi}}_{1b}^0\right\rangle+\left\langle\boldsymbol{\varepsilon}_{1b}^0\dot{\boldsymbol{\varphi}}_{1b}^0\right\rangle\mathbf{c}_{1c}^{1b}\left\langle\mathbf{r}_1^{1c,1c}\right\rangle^{\mathrm{T}}\mathbf{c}_{1c}^{1b,\mathrm{T}}\right]\boldsymbol{\gamma}_2\delta\varphi_{1b}^0\\&+\mathbf{m}_1\mathbf{c}_{1c}^{1b,\mathrm{T}}\left[\left\langle\mathbf{c}_{1c}^{1b}\left\langle\mathbf{r}_1^{1c,1c}\right\rangle\mathbf{c}_{1c}^{1b,\mathrm{T}}\boldsymbol{\varepsilon}_{1b}^0\dot{\boldsymbol{\varphi}}_{1b}^0\right\rangle+\left\langle\boldsymbol{\varepsilon}_{1b}^0\dot{\boldsymbol{\varphi}}_{1b}^0\right\rangle\mathbf{c}_{1c}^{1b}\left\langle\mathbf{r}_1^{1c,1c}\right\rangle^{\mathrm{T}}\mathbf{c}_{1c}^{1b,\mathrm{T}}\right]\boldsymbol{\varepsilon}_{1b}^0\delta\dot{\boldsymbol{\varphi}}_{1b}^0.\end{aligned}\tag{61}$$

The item $\delta\left(\mathbf{m}_1\left\langle\dot{\mathbf{r}}_1^{1c,1c}\right\rangle^{\mathrm{T}}\mathbf{c}_{1c}^{1b,\mathrm{T}}\boldsymbol{\varepsilon}_{1b}^0\dot{\boldsymbol{\varphi}}_{1b}^0\right)$ equals to:

$$\begin{aligned}\delta\left(\mathbf{m}_1\left\langle\dot{\mathbf{r}}_1^{1c,1c}\right\rangle^{\mathrm{T}}\mathbf{c}_{1c}^{1b,\mathrm{T}}\boldsymbol{\varepsilon}_{1b}^0\dot{\boldsymbol{\varphi}}_{1b}^0\right)&=\mathbf{m}_1\left\langle\mathbf{c}_{1c}^{1b,\mathrm{T}}\boldsymbol{\varepsilon}_{1b}^0\dot{\boldsymbol{\varphi}}_{1b}^0\right\rangle\delta\dot{\mathbf{r}}_1^{1c,1c}\\&+\mathbf{m}_1\left\langle\dot{\mathbf{r}}_1^{1c,1c}\right\rangle^{\mathrm{T}}\mathbf{c}_{1c}^{1b,\mathrm{T}}\boldsymbol{\gamma}_2\delta\varphi_{1b}^0+\mathbf{m}_1\left\langle\dot{\mathbf{r}}_1^{1c,1c}\right\rangle^{\mathrm{T}}\mathbf{c}_{1c}^{1b,\mathrm{T}}\boldsymbol{\varepsilon}_{1b}^0\delta\dot{\boldsymbol{\varphi}}_{1b}^0.\end{aligned}\tag{62}$$

The item $\delta\left(\mathbf{m}_1\boldsymbol{\varepsilon}_1^{1c,\mathrm{T}}\left\langle\mathbf{v}_1^{0,1}\right\rangle\mathbf{c}_1^{1c,\mathrm{T}}\mathbf{c}_{1c}^{1b,\mathrm{T}}\mathbf{c}_{1b}^{0,\mathrm{T}}\dot{\mathbf{r}}_{1b}^{0,0}\right)$ equals to:

$$\begin{aligned}\delta\left(\mathbf{m}_1\boldsymbol{\varepsilon}_1^{1c,\mathrm{T}}\left\langle\mathbf{v}_1^{0,1}\right\rangle\mathbf{c}_1^{1c,\mathrm{T}}\mathbf{c}_{1c}^{1b,\mathrm{T}}\mathbf{c}_{1b}^{0,\mathrm{T}}\dot{\mathbf{r}}_{1b}^{0,0}\right)&=\mathbf{m}_1\boldsymbol{\varepsilon}_1^{1c,\mathrm{T}}\mathbf{c}_1^{1c,\mathrm{T}}\mathbf{c}_{1c}^{1b,\mathrm{T}}\left\langle\mathbf{c}_{1b}^{0,\mathrm{T}}\dot{\mathbf{r}}_{1b}^{0,0}\right\rangle\left\langle\boldsymbol{\varepsilon}_{1b}^0\dot{\boldsymbol{\varphi}}_{1b}^0\right\rangle^{\mathrm{T}}\mathbf{c}_{1c}^{1b}\delta\mathbf{r}_1^{1c,1c}\\&+\mathbf{m}_1\left[\boldsymbol{\gamma}_{12}+\boldsymbol{\varepsilon}_1^{1c,\mathrm{T}}\left\langle\mathbf{c}_1^{1c,\mathrm{T}}\left\langle\mathbf{v}_1^{0,1c}\right\rangle\mathbf{c}_{1c}^{1b,\mathrm{T}}\mathbf{c}_{1b}^{0,\mathrm{T}}\dot{\mathbf{r}}_{1b}^{0,0}\right\rangle\boldsymbol{\varepsilon}_1^{1c}\right]\delta\varphi_1^{1c}\\&+\mathbf{m}_1\boldsymbol{\varepsilon}_1^{1c,\mathrm{T}}\mathbf{c}_1^{1c,\mathrm{T}}\left\langle\mathbf{c}_{1c}^{1b,\mathrm{T}}\mathbf{c}_{1b}^{0,\mathrm{T}}\dot{\mathbf{r}}_{1b}^{0,0}\right\rangle^{\mathrm{T}}\delta\dot{\mathbf{r}}_1^{1c,1c}\\&+\mathbf{m}_1\boldsymbol{\varepsilon}_1^{1c,\mathrm{T}}\mathbf{c}_1^{1c,\mathrm{T}}\left\langle\mathbf{v}_1^{0,1c}\right\rangle\mathbf{c}_{1c}^{1b,\mathrm{T}}\left\langle\mathbf{c}_{1b}^{0,\mathrm{T}}\dot{\mathbf{r}}_{1b}^{0,0}\right\rangle\boldsymbol{\varepsilon}_{1b}^0\delta\varphi_{1b}^0\\&+\mathbf{m}_1\boldsymbol{\varepsilon}_1^{1c,\mathrm{T}}\mathbf{c}_1^{1c,\mathrm{T}}\mathbf{c}_{1c}^{1b,\mathrm{T}}\left\langle\mathbf{c}_{1b}^{0,\mathrm{T}}\dot{\mathbf{r}}_{1b}^{0,0}\right\rangle^{\mathrm{T}}\left[\left\langle\mathbf{c}_{1b}^{0,\mathrm{T}}\dot{\mathbf{r}}_{1b}^{0,0}\right\rangle\boldsymbol{\varepsilon}_{1b}^0+\left\langle\mathbf{r}_{1c}^{1b,1b}+\mathbf{c}_{1c}^{1b}\mathbf{r}_1^{1c,1c}\right\rangle^{\mathrm{T}}\boldsymbol{\gamma}_2\right]\delta\varphi_{1b}^0\\&+\mathbf{m}_1\boldsymbol{\varepsilon}_1^{1c,\mathrm{T}}\mathbf{c}_1^{1c,\mathrm{T}}\left[\left\langle\mathbf{v}_1^{0,1c}\right\rangle\mathbf{c}_{1c}^{1b,\mathrm{T}}\mathbf{c}_{1b}^{0,\mathrm{T}}+\mathbf{c}_{1c}^{1b,\mathrm{T}}\mathbf{c}_{1b}^{0,\mathrm{T}}\left\langle\dot{\mathbf{r}}_{1b}^{0,0}\right\rangle^{\mathrm{T}}\right]\delta\dot{\mathbf{r}}_{1b}^{0,0}\\&+\mathbf{m}_1\boldsymbol{\varepsilon}_1^{1c,\mathrm{T}}\mathbf{c}_1^{1c,\mathrm{T}}\mathbf{c}_{1c}^{1b,\mathrm{T}}\left\langle\mathbf{c}_{1b}^{0,\mathrm{T}}\dot{\mathbf{r}}_{1b}^{0,0}\right\rangle\left\langle\mathbf{r}_{1c}^{1b,1b}+\mathbf{c}_{1c}^{1b}\mathbf{r}_1^{1c,1c}\right\rangle\boldsymbol{\varepsilon}_{1b}^0\delta\dot{\boldsymbol{\varphi}}_{1b}^0,\\\boldsymbol{\gamma}_{12}&=\left[0|\boldsymbol{\lambda}_{1,2}^{1c,\mathrm{T}}\mathbf{c}_1^{1c,\mathrm{T}}\left\langle\mathbf{v}_1^{0,1c}\right\rangle\mathbf{c}_{1c}^{1b,\mathrm{T}}\mathbf{c}_{1b}^{0,\mathrm{T}}\dot{\mathbf{r}}_{1b}^{0,0}|\boldsymbol{\lambda}_{1,3}^{1c,\mathrm{T}}\mathbf{c}_1^{1c,\mathrm{T}}\left\langle\mathbf{v}_1^{0,1c}\right\rangle\mathbf{c}_{1c}^{1b,\mathrm{T}}\mathbf{c}_{1b}^{0,\mathrm{T}}\dot{\mathbf{r}}_{1b}^{0,0}\right].\end{aligned}\tag{63}$$

The item $\delta\left(\mathbf{m}_1\boldsymbol{\varepsilon}_1^{1c,\mathrm{T}}\left\langle\mathbf{v}_1^{0,1}\right\rangle\mathbf{c}_1^{1c,\mathrm{T}}\mathbf{c}_{1c}^{1b,\mathrm{T}}\left\langle\mathbf{r}_{1c}^{1b,1b}\right\rangle^{\mathrm{T}}\boldsymbol{\varepsilon}_{1b}^{0}\dot{\boldsymbol{\varphi}}_{1b}^{0}\right)$ equals to:

$$
\begin{aligned}
&\delta\left(\mathbf{m}_1\boldsymbol{\varepsilon}_1^{1c,\mathrm{T}}\left\langle\mathbf{v}_1^{0,1}\right\rangle\mathbf{c}_1^{1c,\mathrm{T}}\mathbf{c}_{1c}^{1b,\mathrm{T}}\left\langle\mathbf{r}_{1c}^{1b,1b}\right\rangle^{\mathrm{T}}\boldsymbol{\varepsilon}_{1b}^{0}\dot{\boldsymbol{\varphi}}_{1b}^{0}\right)\\
&=\mathbf{m}_1\boldsymbol{\varepsilon}_1^{1c,\mathrm{T}}\mathbf{c}_1^{1c,\mathrm{T}}\left\langle\mathbf{c}_{1c}^{1b,\mathrm{T}}\left\langle\mathbf{r}_{1c}^{1b,1b}\right\rangle\boldsymbol{\varepsilon}_{1b}^{0}\dot{\boldsymbol{\varphi}}_{1b}^{0}\right\rangle\left\langle\mathbf{c}_{1c}^{1b,\mathrm{T}}\boldsymbol{\varepsilon}_{1b}^{0}\dot{\boldsymbol{\varphi}}_{1b}^{0}\right\rangle\delta\mathbf{r}_1^{1c,1c}\\
&\quad+\mathbf{m}_1\left[\boldsymbol{\gamma}_{13}+\boldsymbol{\varepsilon}_1^{1c,\mathrm{T}}\left\langle\mathbf{c}_1^{1c,\mathrm{T}}\left\langle\mathbf{v}_1^{0,1c}\right\rangle\mathbf{c}_{1c}^{1b,\mathrm{T}}\left\langle\mathbf{r}_{1c}^{1b,1b}\right\rangle^{\mathrm{T}}\boldsymbol{\varepsilon}_{1b}^{0}\dot{\boldsymbol{\varphi}}_{1b}^{0}\right\rangle\boldsymbol{\varepsilon}_1^{1c}\right]\delta\varphi_1^{1c}\\
&\quad+\mathbf{m}_1\boldsymbol{\varepsilon}_1^{1c,\mathrm{T}}\mathbf{c}_1^{1c,\mathrm{T}}\left\langle\mathbf{c}_{1c}^{1b,\mathrm{T}}\left\langle\mathbf{r}_{1c}^{1b,1b}\right\rangle\boldsymbol{\varepsilon}_{1b}^{0}\dot{\boldsymbol{\varphi}}_{1b}^{0}\right\rangle\delta\dot{\mathbf{r}}_1^{1c,1c}+\mathbf{m}_1\boldsymbol{\varepsilon}_1^{1c,\mathrm{T}}\mathbf{c}_1^{1c,\mathrm{T}}\left\langle\mathbf{v}_1^{0,1c}\right\rangle\mathbf{c}_{1c}^{1b,\mathrm{T}}\left\langle\mathbf{r}_{1c}^{1b,1b}\right\rangle^{\mathrm{T}}\boldsymbol{\gamma}_2\delta\varphi_{1b}^{0}\\
&\quad+\mathbf{m}_1\boldsymbol{\varepsilon}_1^{1c,\mathrm{T}}\mathbf{c}_1^{1c,\mathrm{T}}\mathbf{c}_{1c}^{1b,\mathrm{T}}\left\langle\left\langle\mathbf{r}_{1c}^{1b,1b}\right\rangle\boldsymbol{\varepsilon}_{1b}^{0}\dot{\boldsymbol{\varphi}}_{1b}^{0}\right\rangle\left[\left\langle\mathbf{c}_{1b}^{0,\mathrm{T}}\dot{\mathbf{r}}_{1b}^{0,0}\right\rangle\boldsymbol{\varepsilon}_{1b}^{0}+\left\langle\mathbf{r}_{1c}^{1b,1b}+\mathbf{c}_{1c}^{1b}\mathbf{r}_1^{1c,1c}\right\rangle^{\mathrm{T}}\boldsymbol{\gamma}_2\right]\delta\varphi_{1b}^{0}\\
&\quad+\mathbf{m}_1\boldsymbol{\varepsilon}_1^{1c,\mathrm{T}}\mathbf{c}_1^{1c,\mathrm{T}}\mathbf{c}_{1c}^{1b,\mathrm{T}}\left\langle\left\langle\mathbf{r}_{1c}^{1b,1b}\right\rangle\boldsymbol{\varepsilon}_{1b}^{0}\dot{\boldsymbol{\varphi}}_{1b}^{0}\right\rangle\mathbf{c}_{1b}^{0,\mathrm{T}}\delta\dot{\mathbf{r}}_{1b}^{0,0}\\
&\quad+\mathbf{m}_1\boldsymbol{\varepsilon}_1^{1c,\mathrm{T}}\mathbf{c}_1^{1c,\mathrm{T}}\left[\left\langle\mathbf{v}_1^{0,1c}\right\rangle\mathbf{c}_{1c}^{1b,\mathrm{T}}\left\langle\mathbf{r}_{1c}^{1b,1b}\right\rangle^{\mathrm{T}}+\mathbf{c}_{1c}^{1b,\mathrm{T}}\left\langle\left\langle\mathbf{r}_{1c}^{1b,1b}\right\rangle\boldsymbol{\varepsilon}_{1b}^{0}\dot{\boldsymbol{\varphi}}_{1b}^{0}\right\rangle\left\langle\mathbf{r}_{1c}^{1b,1b}+\mathbf{c}_{1c}^{1b}\mathbf{r}_1^{1c,1c}\right\rangle^{\mathrm{T}}\right]\boldsymbol{\varepsilon}_{1b}^{0}\delta\dot{\boldsymbol{\varphi}}_{1b}^{0},\\
&\boldsymbol{\gamma}_{13}=\left[0\middle|\boldsymbol{\lambda}_{1,2}^{1c,\mathrm{T}}\mathbf{c}_1^{1c,\mathrm{T}}\left\langle\mathbf{v}_1^{0,1c}\right\rangle\mathbf{c}_{1c}^{1b,\mathrm{T}}\left\langle\mathbf{r}_{1c}^{1b,1b}\right\rangle^{\mathrm{T}}\boldsymbol{\varepsilon}_{1b}^{0}\dot{\boldsymbol{\varphi}}_{1b}^{0}\middle|\boldsymbol{\lambda}_{1,3}^{1c,\mathrm{T}}\mathbf{c}_1^{1c,\mathrm{T}}\left\langle\mathbf{v}_1^{0,1c}\right\rangle\mathbf{c}_{1c}^{1b,\mathrm{T}}\left\langle\mathbf{r}_{1c}^{1b,1b}\right\rangle^{\mathrm{T}}\boldsymbol{\varepsilon}_{1b}^{0}\dot{\boldsymbol{\varphi}}_{1b}^{0}\right].
\end{aligned}
\tag{64}
$$

The item $\delta\left(\mathbf{m}_1\boldsymbol{\varepsilon}_1^{1c,\mathrm{T}}\left\langle\mathbf{v}_1^{0,1}\right\rangle\mathbf{c}_1^{1c,\mathrm{T}}\left\langle\mathbf{r}_1^{1c,1c}\right\rangle^{\mathrm{T}}\mathbf{c}_{1c}^{1b,\mathrm{T}}\boldsymbol{\varepsilon}_{1b}^{0}\dot{\boldsymbol{\varphi}}_{1b}^{0}\right)$ equals to:

$$
\begin{aligned}
&\delta\left(\mathbf{m}_1\boldsymbol{\varepsilon}_1^{1c,\mathrm{T}}\left\langle\mathbf{v}_1^{0,1}\right\rangle\mathbf{c}_1^{1c,\mathrm{T}}\left\langle\mathbf{r}_1^{1c,1c}\right\rangle^{\mathrm{T}}\mathbf{c}_{1c}^{1b,\mathrm{T}}\boldsymbol{\varepsilon}_{1b}^{0}\dot{\boldsymbol{\varphi}}_{1b}^{0}\right)\\
&\quad=\mathbf{m}_1\boldsymbol{\varepsilon}_1^{1c,\mathrm{T}}\mathbf{c}_1^{1c,\mathrm{T}}\left[\left\langle\mathbf{v}_1^{0,1c}\right\rangle+\left\langle\left\langle\mathbf{r}_1^{1c,1c}\right\rangle\mathbf{c}_{1c}^{1b,\mathrm{T}}\boldsymbol{\varepsilon}_{1b}^{0}\dot{\boldsymbol{\varphi}}_{1b}^{0}\right\rangle\right]\left\langle\mathbf{c}_{1c}^{1b,\mathrm{T}}\boldsymbol{\varepsilon}_{1b}^{0}\dot{\boldsymbol{\varphi}}_{1b}^{0}\right\rangle\delta\mathbf{r}_1^{1c,1c}\\
&\quad+\mathbf{m}_1\left[\boldsymbol{\gamma}_{14}+\boldsymbol{\varepsilon}_1^{1c,\mathrm{T}}\left\langle\mathbf{c}_1^{1c,\mathrm{T}}\left\langle\mathbf{v}_1^{0,1c}\right\rangle\left\langle\mathbf{r}_1^{1c,1c}\right\rangle^{\mathrm{T}}\mathbf{c}_{1c}^{1b,\mathrm{T}}\boldsymbol{\varepsilon}_{1b}^{0}\dot{\boldsymbol{\varphi}}_{1b}^{0}\right\rangle\boldsymbol{\varepsilon}_1^{1c}\right]\delta\varphi_1^{1c}\\
&\quad+\mathbf{m}_1\boldsymbol{\varepsilon}_1^{1c,\mathrm{T}}\mathbf{c}_1^{1c,\mathrm{T}}\left\langle\left\langle\mathbf{r}_1^{1c,1c}\right\rangle\mathbf{c}_{1c}^{1b,\mathrm{T}}\boldsymbol{\varepsilon}_{1b}^{0}\dot{\boldsymbol{\varphi}}_{1b}^{0}\right\rangle\delta\dot{\mathbf{r}}_1^{1c,1c}+\mathbf{m}_1\boldsymbol{\varepsilon}_1^{1c,\mathrm{T}}\mathbf{c}_1^{1c,\mathrm{T}}\left\langle\mathbf{v}_1^{0,1c}\right\rangle\left\langle\mathbf{r}_1^{1c,1c}\right\rangle^{\mathrm{T}}\mathbf{c}_{1c}^{1b,\mathrm{T}}\boldsymbol{\gamma}_2\delta\varphi_{1b}^{0}\\
&\quad+\mathbf{m}_1\boldsymbol{\varepsilon}_1^{1c,\mathrm{T}}\mathbf{c}_1^{1c,\mathrm{T}}\left\langle\left\langle\mathbf{r}_1^{1c,1c}\right\rangle\mathbf{c}_{1c}^{1b,\mathrm{T}}\boldsymbol{\varepsilon}_{1b}^{0}\dot{\boldsymbol{\varphi}}_{1b}^{0}\right\rangle\mathbf{c}_{1c}^{1b,\mathrm{T}}\left[\left\langle\mathbf{c}_{1b}^{0,\mathrm{T}}\dot{\mathbf{r}}_{1b}^{0,0}\right\rangle\boldsymbol{\varepsilon}_{1b}^{0}+\left\langle\mathbf{r}_{1c}^{1b,1b}+\mathbf{c}_{1c}^{1b}\mathbf{r}_1^{1c,1c}\right\rangle^{\mathrm{T}}\boldsymbol{\gamma}_2\right]\delta\varphi_{1b}^{0}\\
&\quad+\mathbf{m}_1\boldsymbol{\varepsilon}_1^{1c,\mathrm{T}}\mathbf{c}_1^{1c,\mathrm{T}}\left\langle\left\langle\mathbf{r}_1^{1c,1c}\right\rangle\mathbf{c}_{1c}^{1b,\mathrm{T}}\boldsymbol{\varepsilon}_{1b}^{0}\dot{\boldsymbol{\varphi}}_{1b}^{0}\right\rangle\mathbf{c}_{1c}^{1b,\mathrm{T}}\mathbf{c}_{1b}^{0,\mathrm{T}}\delta\dot{\mathbf{r}}_{1b}^{0,0}\\
&\quad+\mathbf{m}_1\boldsymbol{\varepsilon}_1^{1c,\mathrm{T}}\mathbf{c}_1^{1c,\mathrm{T}}\left\langle\mathbf{v}_1^{0,1c}\right\rangle\left\langle\mathbf{r}_1^{1c,1c}\right\rangle^{\mathrm{T}}\mathbf{c}_{1c}^{1b,\mathrm{T}}\boldsymbol{\varepsilon}_{1b}^{0}\delta\dot{\boldsymbol{\varphi}}_{1b}^{0}\\
&\quad+\mathbf{m}_1\boldsymbol{\varepsilon}_1^{1c,\mathrm{T}}\mathbf{c}_1^{1c,\mathrm{T}}\left\langle\left\langle\mathbf{r}_1^{1c,1c}\right\rangle\mathbf{c}_{1c}^{1b,\mathrm{T}}\boldsymbol{\varepsilon}_{1b}^{0}\dot{\boldsymbol{\varphi}}_{1b}^{0}\right\rangle\mathbf{c}_{1c}^{1b,\mathrm{T}}\left\langle\mathbf{r}_{1c}^{1b,1b}+\mathbf{c}_{1c}^{1b}\mathbf{r}_1^{1c,1c}\right\rangle^{\mathrm{T}}\boldsymbol{\varepsilon}_{1b}^{0}\delta\dot{\boldsymbol{\varphi}}_{1b}^{0},
\end{aligned}
\tag{65}
$$

where

$$
\boldsymbol{\gamma}_{14}=\left[0\middle|\boldsymbol{\lambda}_{1,2}^{1c,\mathrm{T}}\mathbf{c}_1^{1c,\mathrm{T}}\left\langle\mathbf{v}_1^{0,1c}\right\rangle\left\langle\mathbf{r}_1^{1c,1c}\right\rangle^{\mathrm{T}}\mathbf{c}_{1c}^{1b,\mathrm{T}}\boldsymbol{\varepsilon}_{1b}^{0}\dot{\boldsymbol{\varphi}}_{1b}^{0}\middle|\boldsymbol{\lambda}_{1,3}^{1c,\mathrm{T}}\mathbf{c}_1^{1c,\mathrm{T}}\left\langle\mathbf{v}_1^{0,1c}\right\rangle\left\langle\mathbf{r}_1^{1c,1c}\right\rangle^{\mathrm{T}}\mathbf{c}_{1c}^{1b,\mathrm{T}}\boldsymbol{\varepsilon}_{1b}^{0}\dot{\boldsymbol{\varphi}}_{1b}^{0}\right].
$$

The Jacobian $\mathbf{J}_{\mathbf{q}_1^{1c}}\left(\mathbf{b}_{0,2}\right)$ can be got by formula:

$$\mathbf{J}_{\mathbf{q}_1^{1c}}(\mathbf{b}_{0,2}) = \begin{bmatrix} \mathbf{J}_{\mathbf{q}_1^{1c}}(\mathbf{b}_{0,2})_{11} & \mathbf{J}_{\mathbf{q}_1^{1c}}(\mathbf{b}_{0,2})_{12} \\ \mathbf{J}_{\mathbf{q}_1^{1c}}(\mathbf{b}_{0,2})_{21} & \mathbf{J}_{\mathbf{q}_1^{1c}}(\mathbf{b}_{0,2})_{22} \end{bmatrix},$$

$$\mathbf{J}_{\mathbf{q}_1^{1c}}(\mathbf{b}_{0,2})_{11} = \mathbf{m}_1 \mathbf{c}_{1c}^{1b,\mathrm{T}} \left\langle \boldsymbol{\varepsilon}_{1b}^0 \dot{\boldsymbol{\varphi}}_{1b}^0 \right\rangle \mathbf{c}_{1c}^{1b} \left\langle \mathbf{c}_{1c}^{1b,\mathrm{T}} \boldsymbol{\varepsilon}_{1b}^0 \dot{\boldsymbol{\varphi}}_{1b}^0 \right\rangle,$$

$$\mathbf{J}_{\mathbf{q}_1^{1c}}(\mathbf{b}_{0,2})_{12} = 0,$$

$$\begin{aligned}
\mathbf{J}_{\mathbf{q}_1^{1c}}(\mathbf{b}_{0,2})_{21} &= \mathbf{m}_1 \boldsymbol{\varepsilon}_1^{1c,\mathrm{T}} \mathbf{c}_1^{1c,\mathrm{T}} \mathbf{c}_{1c}^{1b,\mathrm{T}} \left\langle \mathbf{c}_{1b}^{0,\mathrm{T}} \dot{\mathbf{r}}_{1b}^{0,0} \right\rangle \left\langle \boldsymbol{\varepsilon}_{1b}^0 \dot{\boldsymbol{\varphi}}_{1b}^0 \right\rangle^{\mathrm{T}} \mathbf{c}_{1c}^{1b} \\
&+ \mathbf{m}_1 \boldsymbol{\varepsilon}_1^{1c,\mathrm{T}} \mathbf{c}_1^{1c,\mathrm{T}} \left\langle \mathbf{c}_{1c}^{1b,\mathrm{T}} \left\langle \mathbf{r}_{1c}^{1b,1b} \right\rangle \boldsymbol{\varepsilon}_{1b}^0 \dot{\boldsymbol{\varphi}}_{1b}^0 \right\rangle \left\langle \mathbf{c}_{1c}^{1b,\mathrm{T}} \boldsymbol{\varepsilon}_{1b}^0 \dot{\boldsymbol{\varphi}}_{1b}^0 \right\rangle \\
&+ \mathbf{m}_1 \boldsymbol{\varepsilon}_1^{1c,\mathrm{T}} \mathbf{c}_1^{1c,\mathrm{T}} \left[\left\langle \mathbf{v}_1^{0,1c} \right\rangle + \left\langle \left\langle \mathbf{r}_1^{1c,1c} \right\rangle \mathbf{c}_{1c}^{1b,\mathrm{T}} \boldsymbol{\varepsilon}_{1b}^0 \dot{\boldsymbol{\varphi}}_{1b}^0 \right\rangle \right] \left\langle \mathbf{c}_{1c}^{1b,\mathrm{T}} \boldsymbol{\varepsilon}_{1b}^0 \dot{\boldsymbol{\varphi}}_{1b}^0 \right\rangle, \\
\mathbf{J}_{\mathbf{q}_1^{1c}}(\mathbf{b}_{0,2})_{22} &= \mathbf{m}_1 \left[\boldsymbol{\gamma}_{12} + \boldsymbol{\varepsilon}_1^{1c,\mathrm{T}} \left\langle \mathbf{c}_1^{1c,\mathrm{T}} \left\langle \mathbf{v}_1^{0,1c} \right\rangle \mathbf{c}_{1c}^{1b,\mathrm{T}} \mathbf{c}_{1b}^{0,\mathrm{T}} \dot{\mathbf{r}}_{1b}^{0,0} \right\rangle \boldsymbol{\varepsilon}_1^{1c} \right] \\
&+ \mathbf{m}_1 \left[\boldsymbol{\gamma}_{13} + \boldsymbol{\varepsilon}_1^{1c,\mathrm{T}} \left\langle \mathbf{c}_1^{1c,\mathrm{T}} \left\langle \mathbf{v}_1^{0,1c} \right\rangle \mathbf{c}_{1c}^{1b,\mathrm{T}} \left\langle \mathbf{r}_{1c}^{1b,1b} \right\rangle^{\mathrm{T}} \boldsymbol{\varepsilon}_{1b}^0 \dot{\boldsymbol{\varphi}}_{1b}^0 \right\rangle \boldsymbol{\varepsilon}_1^{1c} \right] \\
&+ \mathbf{m}_1 \left[\boldsymbol{\gamma}_{14} + \boldsymbol{\varepsilon}_1^{1c,\mathrm{T}} \left\langle \mathbf{c}_1^{1c,\mathrm{T}} \left\langle \mathbf{v}_1^{0,1c} \right\rangle \left\langle \mathbf{r}_1^{1c,1c} \right\rangle^{\mathrm{T}} \mathbf{c}_{1c}^{1b,\mathrm{T}} \boldsymbol{\varepsilon}_{1b}^0 \dot{\boldsymbol{\varphi}}_{1b}^0 \right\rangle \boldsymbol{\varepsilon}_1^{1c} \right].
\end{aligned} \tag{66}$$

The Jacobian $\mathbf{J}_{\dot{\mathbf{q}}_1^{1c}}(\mathbf{b}_{0,2})$ can be got by formula:

$$\begin{aligned}
&\mathbf{J}_{\dot{\mathbf{q}}_1^{1c}}(\mathbf{b}_{0,2}) = \begin{bmatrix} \mathbf{J}_{\dot{\mathbf{q}}_1^{1c}}(\mathbf{b}_{0,2})_{11} & \mathbf{J}_{\dot{\mathbf{q}}_1^{1c}}(\mathbf{b}_{0,2})_{12} \\ \mathbf{J}_{\dot{\mathbf{q}}_1^{1c}}(\mathbf{b}_{0,2})_{21} & \mathbf{J}_{\dot{\mathbf{q}}_1^{1c}}(\mathbf{b}_{0,2})_{22} \end{bmatrix}, \mathbf{J}_{\dot{\mathbf{q}}_1^{1c}}(\mathbf{b}_{0,2})_{11} = \mathbf{m}_1 \left\langle \mathbf{c}_{1c}^{1b,\mathrm{T}} \boldsymbol{\varepsilon}_{1b}^0 \dot{\boldsymbol{\varphi}}_{1b}^0 \right\rangle, \\
&\mathbf{J}_{\dot{\mathbf{q}}_1^{1c}}(\mathbf{b}_{0,2})_{12} = 0, \\
&\mathbf{J}_{\dot{\mathbf{q}}_1^{1c}}(\mathbf{b}_{0,2})_{21} = \mathbf{m}_1 \boldsymbol{\varepsilon}_1^{1c,\mathrm{T}} \mathbf{c}_1^{1c,\mathrm{T}} \left\langle \mathbf{c}_{1c}^{1b,\mathrm{T}} \mathbf{c}_{1b}^{0,\mathrm{T}} \dot{\mathbf{r}}_{1b}^{0,0} \right\rangle^{\mathrm{T}} + \mathbf{m}_1 \boldsymbol{\varepsilon}_1^{1c,\mathrm{T}} \mathbf{c}_1^{1c,\mathrm{T}} \left\langle \left\langle \mathbf{r}_1^{1c,1c} \right\rangle \mathbf{c}_{1c}^{1b,\mathrm{T}} \boldsymbol{\varepsilon}_{1b}^0 \dot{\boldsymbol{\varphi}}_{1b}^0 \right\rangle, \\
&\mathbf{J}_{\dot{\mathbf{q}}_1^{1c}}(\mathbf{b}_{0,2})_{22} = 0.
\end{aligned} \tag{67}$$

The Jacobian $\mathbf{J}_{\mathbf{q}_{1b}^0}(\mathbf{b}_{0,2})$ can be got by formula:

$$\mathbf{J}_{\mathbf{q}_{1b}^0}(\mathbf{b}_{0,2}) = \begin{bmatrix} \mathbf{J}_{\mathbf{q}_{1b}^0}(\mathbf{b}_{0,2})_{11} & \mathbf{J}_{\mathbf{q}_{1b}^0}(\mathbf{b}_{0,2})_{12} \\ \mathbf{J}_{\mathbf{q}_{1b}^0}(\mathbf{b}_{0,2})_{21} & \mathbf{J}_{\mathbf{q}_{1b}^0}(\mathbf{b}_{0,2})_{22} \end{bmatrix},$$

$$\mathbf{J}_{\mathbf{q}_{1b}^0}(\mathbf{b}_{0,2})_{11} = 0,$$

$$\begin{aligned}
\mathbf{J}_{\mathbf{q}_{1b}^0}(\mathbf{b}_{0,2})_{12} &= \mathbf{m}_1 \mathbf{c}_{1c}^{1b,\mathrm{T}} \left\langle \mathbf{c}_{1b}^{0,\mathrm{T}} \dot{\mathbf{r}}_{1b}^{0,0} \right\rangle^{\mathrm{T}} \boldsymbol{\gamma}_2 \\
&+ \mathbf{m}_1 \mathbf{c}_{1c}^{1b,\mathrm{T}} \left[\left\langle \left\langle \mathbf{r}_{1c}^{1b,1b} \right\rangle \boldsymbol{\varepsilon}_{1b}^0 \dot{\boldsymbol{\varphi}}_{1b}^0 \right\rangle + \left\langle \boldsymbol{\varepsilon}_{1b}^0 \dot{\boldsymbol{\varphi}}_{1b}^0 \right\rangle \left\langle \mathbf{r}_{1c}^{1b,1b} \right\rangle^{\mathrm{T}} \right] \boldsymbol{\gamma}_2 + \\
&+ \mathbf{m}_1 \mathbf{c}_{1c}^{1b,\mathrm{T}} \left[\left\langle \mathbf{c}_{1c}^{1b} \left\langle \mathbf{r}_1^{1c,1c} \right\rangle \mathbf{c}_{1c}^{1b,\mathrm{T}} \boldsymbol{\varepsilon}_{1b}^0 \dot{\boldsymbol{\varphi}}_{1b}^0 \right\rangle + \left\langle \boldsymbol{\varepsilon}_{1b}^0 \dot{\boldsymbol{\varphi}}_{1b}^0 \right\rangle \mathbf{c}_{1c}^{1b} \left\langle \mathbf{r}_1^{1c,1c} \right\rangle^{\mathrm{T}} \mathbf{c}_{1c}^{1b,\mathrm{T}} \right] \boldsymbol{\gamma}_2 \\
&+ \mathbf{m}_1 \left\langle \dot{\mathbf{r}}_1^{1c,1c} \right\rangle^{\mathrm{T}} \mathbf{c}_{1c}^{1b,\mathrm{T}} \boldsymbol{\gamma}_2,
\end{aligned}$$

$$\mathbf{J}_{\mathbf{q}_{1b}^0}\left(\mathbf{b}_{0,2}\right)_{21}=0, \tag{68}$$

$$\begin{aligned}
\mathbf{J}_{\mathbf{q}_{1b}^0}\left(\mathbf{b}_{0,2}\right)_{22} &= \mathbf{m}_1\boldsymbol{\varepsilon}_1^{1c,\mathrm{T}}\mathbf{c}_1^{1c,\mathrm{T}}\left\langle\mathbf{v}_1^{0,1c}\right\rangle\mathbf{c}_{1c}^{1b,\mathrm{T}}\left\langle\mathbf{c}_{1b}^{0,\mathrm{T}}\dot{\mathbf{r}}_{1b}^{0,0}\right\rangle\boldsymbol{\varepsilon}_{1b}^0\\
&+\mathbf{m}_1\boldsymbol{\varepsilon}_1^{1c,\mathrm{T}}\mathbf{c}_1^{1c,\mathrm{T}}\mathbf{c}_{1c}^{1b,\mathrm{T}}\left\langle\mathbf{c}_{1b}^{0,\mathrm{T}}\dot{\mathbf{r}}_{1b}^{0,0}\right\rangle^{\mathrm{T}}\left[\left\langle\mathbf{c}_{1b}^{0,\mathrm{T}}\dot{\mathbf{r}}_{1b}^{0,0}\right\rangle\boldsymbol{\varepsilon}_{1b}^0+\left\langle\mathbf{r}_{1c}^{1b,1b}+\mathbf{c}_{1c}^{1b}\mathbf{r}_1^{1c,1c}\right\rangle^{\mathrm{T}}\boldsymbol{\gamma}_2\right]\\
&+\mathbf{m}_1\boldsymbol{\varepsilon}_1^{1c,\mathrm{T}}\mathbf{c}_1^{1c,\mathrm{T}}\left\langle\mathbf{c}_{1c}^{1b,\mathrm{T}}\left\langle\mathbf{r}_{1c}^{1b,1b}\right\rangle\boldsymbol{\varepsilon}_{1b}^0\dot{\boldsymbol{\varphi}}_{1b}^0\right\rangle\delta\dot{\mathbf{r}}_1^{1c,1c}+\mathbf{m}_1\boldsymbol{\varepsilon}_1^{1c,\mathrm{T}}\mathbf{c}_1^{1c,\mathrm{T}}\left\langle\mathbf{v}_1^{0,1c}\right\rangle\mathbf{c}_{1c}^{1b,\mathrm{T}}\left\langle\mathbf{r}_{1c}^{1b,1b}\right\rangle^{\mathrm{T}}\boldsymbol{\gamma}_2\\
&+\mathbf{m}_1\boldsymbol{\varepsilon}_1^{1c,\mathrm{T}}\mathbf{c}_1^{1c,\mathrm{T}}\mathbf{c}_{1c}^{1b,\mathrm{T}}\left\langle\left\langle\mathbf{r}_{1c}^{1b,1b}\right\rangle\boldsymbol{\varepsilon}_{1b}^0\dot{\boldsymbol{\varphi}}_{1b}^0\right\rangle\left[\left\langle\mathbf{c}_{1b}^{0,\mathrm{T}}\dot{\mathbf{r}}_{1b}^{0,0}\right\rangle\boldsymbol{\varepsilon}_{1b}^0+\left\langle\mathbf{r}_{1c}^{1b,1b}+\mathbf{c}_{1c}^{1b}\mathbf{r}_1^{1c,1c}\right\rangle^{\mathrm{T}}\boldsymbol{\gamma}_2\right]\\
&+\mathbf{m}_1\boldsymbol{\varepsilon}_1^{1c,\mathrm{T}}\mathbf{c}_1^{1c,\mathrm{T}}\left\langle\mathbf{v}_1^{0,1c}\right\rangle\left\langle\mathbf{r}_1^{1c,1c}\right\rangle^{\mathrm{T}}\mathbf{c}_{1c}^{1b,\mathrm{T}}\boldsymbol{\gamma}_2\\
&+\mathbf{m}_1\boldsymbol{\varepsilon}_1^{1c,\mathrm{T}}\mathbf{c}_1^{1c,\mathrm{T}}\left\langle\left\langle\mathbf{r}_1^{1c,1c}\right\rangle\mathbf{c}_{1c}^{1b,\mathrm{T}}\boldsymbol{\varepsilon}_{1b}^0\dot{\boldsymbol{\varphi}}_{1b}^0\right\rangle\mathbf{c}_{1c}^{1b,\mathrm{T}}\left[\left\langle\mathbf{c}_{1b}^{0,\mathrm{T}}\dot{\mathbf{r}}_{1b}^{0,0}\right\rangle\boldsymbol{\varepsilon}_{1b}^0+\left\langle\mathbf{r}_{1c}^{1b,1b}+\mathbf{c}_{1c}^{1b}\mathbf{r}_1^{1c,1c}\right\rangle^{\mathrm{T}}\boldsymbol{\gamma}_2\right].
\end{aligned}$$

The Jacobian $\mathbf{J}_{\dot{\mathbf{q}}_{1b}^0}\left(\mathbf{b}_{0,2}\right)$ can be got by formula:

$$\begin{aligned}
\mathbf{J}_{\dot{\mathbf{q}}_{1b}^0}\left(b_{0,2}\right) &= \begin{bmatrix}\mathbf{J}_{\dot{\mathbf{q}}_{1b}^0}\left(\mathbf{b}_{0,2}\right)_{11} & \mathbf{J}_{\dot{\mathbf{q}}_{1b}^0}\left(\mathbf{b}_{0,2}\right)_{12}\\ \mathbf{J}_{\dot{\mathbf{q}}_{1b}^0}\left(\mathbf{b}_{0,2}\right)_{21} & \mathbf{J}_{\dot{\mathbf{q}}_{1b}^0}\left(\mathbf{b}_{0,2}\right)_{22}\end{bmatrix},\\
\mathbf{J}_{\dot{\mathbf{q}}_{1b}^0}\left(\mathbf{b}_{0,2}\right)_{11} &= \mathbf{m}_1\mathbf{c}_{1c}^{1b,\mathrm{T}}\langle\boldsymbol{\varepsilon}_{1b}^0\dot{\boldsymbol{\varphi}}_{1b}^0\rangle\mathbf{c}_{1b}^{0,\mathrm{T}},\\
\mathbf{J}_{\dot{\mathbf{q}}_{1b}^0}\left(\mathbf{b}_{0,2}\right)_{12} &= \mathbf{m}_1\mathbf{c}_{1c}^{1b,\mathrm{T}}\left[\mathbf{I}-\langle\boldsymbol{\varepsilon}_{1b}^0\dot{\boldsymbol{\varphi}}_{1b}^0\rangle\right]\left\langle\mathbf{c}_{1b}^{0,\mathrm{T}}\dot{\mathbf{r}}_{1b}^{0,0}\right\rangle^{\mathrm{T}}\boldsymbol{\varepsilon}_{1b}^0\\
&+\mathbf{m}_1\mathbf{c}_{1c}^{1b,\mathrm{T}}\left[\left\langle\left\langle\mathbf{r}_{1c}^{1b,1b}\right\rangle\boldsymbol{\varepsilon}_{1b}^0\dot{\boldsymbol{\varphi}}_{1b}^0\right\rangle+\langle\boldsymbol{\varepsilon}_{1b}^0\dot{\boldsymbol{\varphi}}_{1b}^0\rangle\left\langle\mathbf{r}_{1c}^{1b,1b}\right\rangle^{\mathrm{T}}\right]\boldsymbol{\varepsilon}_{1b}^0\\
&+\mathbf{m}_1\mathbf{c}_{1c}^{1b,\mathrm{T}}\left[\left\langle\mathbf{c}_{1c}^{1b}\left\langle\mathbf{r}_1^{1c,1c}\right\rangle\mathbf{c}_{1c}^{1b,\mathrm{T}}\boldsymbol{\varepsilon}_{1b}^0\dot{\boldsymbol{\varphi}}_{1b}^0\right\rangle+\langle\boldsymbol{\varepsilon}_{1b}^0\dot{\boldsymbol{\varphi}}_{1b}^0\rangle\mathbf{c}_{1c}^{1b}\left\langle\mathbf{r}_1^{1c,1c}\right\rangle^{\mathrm{T}}\mathbf{c}_{1c}^{1b,\mathrm{T}}\right]\boldsymbol{\varepsilon}_{1b}^0\\
&+\mathbf{m}_1\left\langle\dot{\mathbf{r}}_1^{1c,1c}\right\rangle^{\mathrm{T}}\mathbf{c}_{1c}^{1b,\mathrm{T}}\boldsymbol{\varepsilon}_{1b}^0,
\end{aligned} \tag{69}$$

$$\begin{aligned}
\mathbf{J}_{\dot{\mathbf{q}}_{1b}^0}\left(\mathbf{b}_{0,2}\right)_{22} &= \mathbf{m}_1\boldsymbol{\varepsilon}_1^{1c,\mathrm{T}}\mathbf{c}_1^{1c,\mathrm{T}}\mathbf{c}_{1c}^{1b,\mathrm{T}}\left\langle\mathbf{c}_{1b}^{0,\mathrm{T}}\dot{\mathbf{r}}_{1b}^{0,0}\right\rangle\left\langle\mathbf{r}_{1c}^{1b,1b}+\mathbf{c}_{1c}^{1b}\mathbf{r}_1^{1c,1c}\right\rangle\boldsymbol{\varepsilon}_{1b}^0\\
&+\mathbf{m}_1\boldsymbol{\varepsilon}_1^{1c,\mathrm{T}}\mathbf{c}_1^{1c,\mathrm{T}}\left[\left\langle\mathbf{v}_1^{0,1c}\right\rangle\mathbf{c}_{1c}^{1b,\mathrm{T}}\left\langle\mathbf{r}_{1c}^{1b,1b}\right\rangle^{\mathrm{T}}+\mathbf{c}_{1c}^{1b,\mathrm{T}}\left\langle\left\langle\mathbf{r}_{1c}^{1b,1b}\right\rangle\boldsymbol{\varepsilon}_{1b}^0\dot{\boldsymbol{\varphi}}_{1b}^0\right\rangle\left\langle\mathbf{r}_{1c}^{1b,1b}+\mathbf{c}_{1c}^{1b}\mathbf{r}_1^{1c,1c}\right\rangle^{\mathrm{T}}\right]\boldsymbol{\varepsilon}_{1b}^0\\
&+\mathbf{m}_1\boldsymbol{\varepsilon}_1^{1c,\mathrm{T}}\mathbf{c}_1^{1c,\mathrm{T}}\left\langle\mathbf{v}_1^{0,1c}\right\rangle\left\langle\mathbf{r}_1^{1c,1c}\right\rangle^{\mathrm{T}}\mathbf{c}_{1c}^{1b,\mathrm{T}}\boldsymbol{\varepsilon}_{1b}^0\\
&+\mathbf{m}_1\boldsymbol{\varepsilon}_1^{1c,\mathrm{T}}\mathbf{c}_1^{1c,\mathrm{T}}\left\langle\left\langle\mathbf{r}_1^{1c,1c}\right\rangle\mathbf{c}_{1c}^{1b,\mathrm{T}}\boldsymbol{\varepsilon}_{1b}^0\dot{\boldsymbol{\varphi}}_{1b}^0\right\rangle\mathbf{c}_{1c}^{1b,\mathrm{T}}\left\langle\mathbf{r}_{1c}^{1b,1b}+\mathbf{c}_{1c}^{1b}\mathbf{r}_1^{1c,1c}\right\rangle^{\mathrm{T}}\boldsymbol{\varepsilon}_{1b}^0.
\end{aligned}$$

Then the linearized equations of a platform without forces and torques will have a form:

$$\mathbf{A}_3\ddot{\mathbf{x}}+\mathbf{A}_2\dot{\mathbf{x}}+\mathbf{A}_1\mathbf{x}+\mathbf{A}_0=-\mathbf{B}_3\ddot{\mathbf{y}}-\mathbf{B}_2\dot{\mathbf{y}}-\mathbf{B}_1\mathbf{y}-\mathbf{B}_0, \tag{70}$$

where $\mathbf{x}$ and $\mathbf{y}$—the corresponding deviations from a basic trajectory: $\mathbf{x}=\Delta\mathbf{q}_1^{1c}=\mathbf{q}_1^{1c}-\mathbf{q}_{1,fix}^{1c}$, $\mathbf{y}=\Delta\mathbf{q}_{1b}^0=\mathbf{q}_{1b}^0-\mathbf{q}_{1b,fix}^0$, and matrixes of parameters of model (70) have a form:

$$\mathbf{A}_3 = \mathbf{J}_{\ddot{\mathbf{q}}_1^{1c}}\left(\mathbf{A}\left(\mathbf{q}_1^{1c}\right)\ddot{\mathbf{q}}_1^{1c}\right)_{\mathbf{X}_{fix}},\ \mathbf{A}_2 = \mathbf{J}_{\dot{\mathbf{q}}_1^{1c}}\left(\mathbf{B}\dot{\mathbf{q}}_1^{1c}\right)_{\mathbf{X}_{fix}} + \mathbf{J}_{\dot{\mathbf{q}}_1^{1c}}\left(\mathbf{b}_{0,2}\right)_{X_{fix}},$$
$$\mathbf{A}_1 = \mathbf{J}_{\mathbf{q}_1^{1c}}\left(\mathbf{A}\left(\mathbf{q}_1^{1c}\right)\ddot{\mathbf{q}}_1^{1c}\right)_{\mathbf{X}_{fix}} + \mathbf{J}_{\mathbf{q}_1^{1c}}\left(\mathbf{B}\dot{\mathbf{q}}_1^{1c}\right)_{X_{fix}}$$
$$+ \mathbf{J}_{\mathbf{q}_1^{1c}}\left(\mathbf{A}_0\left(\mathbf{q}_1^{1c}, \mathbf{q}_{1b}^0\right)\ddot{\mathbf{q}}_{1b}^0\right)_{\mathbf{X}_{fix}} + \mathbf{J}_{\mathbf{q}_1^{1c}}\left(\mathbf{b}_{0,1}\right)_{\mathbf{X}_{fix}} + \mathbf{J}_{\mathbf{q}_1^{1c}}\left(\mathbf{b}_{0,2}\right)_{X_{fix}},$$
$$\mathbf{A}_0 = \mathbf{A}\left(\mathbf{q}_{1,fix}^{1c}\right)\ddot{\mathbf{q}}_{1,fix}^{1c},$$

$$\mathbf{B}_3 = \mathbf{J}_{\ddot{\mathbf{q}}_{1b}^0}\left(\mathbf{A}_0\left(\mathbf{q}_1^{1c}, \mathbf{q}_{1b}^0\right)\ddot{\mathbf{q}}_{1b}^0\right)_{\mathbf{X}_{fix}},\ \mathbf{B}_2 = \mathbf{J}_{\dot{\mathbf{q}}_{1b}^0}\left(\mathbf{B}\dot{\mathbf{q}}_1^{1c}\right)_{\mathbf{X}_{fix}} + \mathbf{J}_{\dot{\mathbf{q}}_{1b}^0}\left(\mathbf{b}_{0,1}\right)_{\mathbf{X}_{fix}} + \mathbf{J}_{\dot{\mathbf{q}}_{1b}^0}\left(\mathbf{b}_{0,2}\right)_{\mathbf{X}_{fix}},$$
$$\mathbf{B}_1 = \mathbf{J}_{\mathbf{q}_{1b}^0}\left(\mathbf{B}\dot{\mathbf{q}}_1^{1c}\right)_{\mathbf{X}_{fix}} + \mathbf{J}_{\mathbf{q}_{1b}^0}\left(\mathbf{A}_0\left(\mathbf{q}_1^{1c}, \mathbf{q}_{1b}^0\right)\ddot{\mathbf{q}}_{1b}^0\right)_{\mathbf{X}_{fix}}\delta\mathbf{q}_{1b}^0 + \mathbf{J}_{\mathbf{q}_{1b}^0}\left(\mathbf{b}_{0,1}\right)_{\mathbf{X}_{fix}} + \mathbf{J}_{\mathbf{q}_{1b}^0}\left(\mathbf{b}_{0,2}\right)_{\mathbf{X}_{fix}},$$
$$\mathbf{B}_0 = \mathbf{B}\left(\mathbf{q}_{1,fix}^{1c}, \dot{\mathbf{q}}_{1,fix}^{1c}, \mathbf{q}_{1b,fix}^0, \dot{\mathbf{q}}_{1b,fix}^0\right)\dot{\mathbf{q}}_{1,fix}^{1c}$$
$$+ \mathbf{A}_0\left(\mathbf{q}_{1,fix}^{1c}, \mathbf{q}_{1b,fix}^0\right)\ddot{\mathbf{q}}_{1b,fix}^0 + \mathbf{A}\left(\mathbf{q}_{1,fix}^{1c}\right)\ddot{\mathbf{q}}_{1,fix}^{1c} + \mathbf{b}_{0,1,fix} + \mathbf{b}_{0,2,fix}.$$

The model (70) needs to be added with the equations describing forces and torques operating on the AP. Creation of model of forces and the torques is carried out by a similar technique by an expansion in a series with deduction of the linear item.

3 The Linearized Equations of Vectors of Forces and the Torques of SEMS Block with n Actuators

Forces and torques operating on an adaptive platform in details are considered in [1, 2, 5].

We linearize expressions for the item $\mathbf{Q}_\xi\left(\mathbf{q}_1^{1c}, \dot{\mathbf{q}}_1^{1c}, \mathbf{q}_{1b}^0, \mathbf{u}, \mathbf{p}\right)$ from (9):

$$\begin{gathered}\mathbf{Q}_\xi\left(\mathbf{q}_1^{1c}, \dot{\mathbf{q}}_1^{1c}, \mathbf{q}_{1b}^0, \mathbf{u}, \mathbf{p}\right) \\ \approx \mathbf{Q}_\xi\left(\mathbf{q}_{1,fix}^{1c}, \dot{\mathbf{q}}_{1,fix}^{1c}, \mathbf{q}_{1b,fix}^0, \mathbf{u}_{fix}, \mathbf{p}_{fix}\right) + \mathbf{J}_{\mathbf{q}_1^{1c}}\left(\mathbf{Q}_\xi\right)_{\mathbf{X}_{fix}}\delta\mathbf{q}_1^{1c} + \mathbf{J}_{\dot{\mathbf{q}}_1^{1c}}\left(\mathbf{Q}_\xi\right)_{\mathbf{X}_{fix}}\delta\dot{\mathbf{q}}_1^{1c} \\ + \mathbf{J}_{\mathbf{q}_{1b}^0}\left(\mathbf{Q}_\xi\right)_{\mathbf{X}_{fix}}\delta\mathbf{q}_{1b}^0 + \mathbf{J}_{\mathbf{u}}\left(\mathbf{Q}_\xi\right)_{\mathbf{X}_{fix}}\delta\mathbf{u} + \mathbf{J}_{\mathbf{p}}\left(\mathbf{Q}_\xi\right)_{\mathbf{X}_{fix}}\delta\mathbf{p},\end{gathered} \tag{71}$$

The generalized forces can be found through projections of forces and the torques in CS AP:

$$\mathbf{Q}_\xi\left(\mathbf{q}_1^{1c}, \dot{\mathbf{q}}_1^{1c}, \mathbf{u}, \mathbf{p}\right) = \mathbf{M}_1^{1c,\mathrm{T}}\boldsymbol{\Xi}_1^1, \tag{72}$$

where forces $\mathbf{F}_1$ and torques $\mathbf{M}_1$ operating on an adaptive platform in CS AP have a form:

$$\mathbf{F}_1 = \sum_{i=1}^{n}\mathbf{F}_{1,i}^1 + \mathbf{G}_1^1 + \mathbf{P}_1^1,\ \mathbf{M}_1 = \sum_{i=1}^{6}\left\langle\mathbf{r}_{1ji}^{1,1}\right\rangle\mathbf{F}_{1,i}^1 + \sum_{i=1}^{6}\mathbf{N}_{1,i}^1 + \mathbf{K}_1^1, \tag{73}$$

where $\mathbf{F}^1_{1,i}$—the elastic forces and damping forces operating on AP from ith actuator in CS AP, $\mathbf{N}^1_{1,i}$—torques of friction in ith hinge of AP in CS AP, $\mathbf{P}^1_1$—the external forces operating on AP, $\mathbf{K}^1_1$—the external torques operating on AP, $\mathbf{G}^1_1$—the gravity force operating on AP. The forces $\mathbf{F}^1_{1,i}$ operate along the actuator and it is collinear to the vector $\mathbf{r}^{1bji}_{1ji}$. The torques $\mathbf{N}^1_{1,i}$ operate against motion in the hinge.

Let's find expressions for forces and the torques $\mathbf{G}^1_1, \mathbf{P}^1_1$ and $\mathbf{K}^1_1$ into CS AP:

$$\begin{gathered}\mathbf{G}^1_1 = \mathbf{c}^{1c,\mathrm{T}}_1 \mathbf{c}^{1b,\mathrm{T}}_{1c} \mathbf{c}^{0,\mathrm{T}}_{1b} \mathbf{m}_1 \mathbf{g},\ \mathbf{g} = [\,0 \quad 0 \quad -g\,]^{\mathrm{T}},\\ \mathbf{P}^1_1 = \mathbf{c}^{1c,\mathrm{T}}_1 \mathbf{c}^{1b,\mathrm{T}}_{1c} \mathbf{c}^{0,\mathrm{T}}_{1b} \mathbf{p}_F,\ \mathbf{K}^1_1 = \mathbf{c}^{1c,\mathrm{T}}_1 \mathbf{c}^{1b,\mathrm{T}}_{1c} \mathbf{c}^{0,\mathrm{T}}_{1b} \mathbf{p}_M,\end{gathered} \tag{74}$$

where $\mathbf{p}_F$ and $\mathbf{p}_M$—the components external forces and toques in $\mathbf{p}$, g—the acceleration of gravity.

Let's pass from (74) to the generalized forces according to (72):

$$\mathbf{Q}_g = \mathbf{c}^{1b,\mathrm{T}}_{1c} \mathbf{c}^{0,\mathrm{T}}_{1b} \mathbf{m}_1 \mathbf{g},\ \mathbf{Q}_P = \mathbf{c}^{1b,\mathrm{T}}_{1c} \mathbf{c}^{0,\mathrm{T}}_{1b} \mathbf{p}_F,\ \mathbf{Q}_K = \boldsymbol{\varepsilon}^{1c,\mathrm{T}}_1 \mathbf{c}^{1c,\mathrm{T}}_1 \mathbf{c}^{1b,\mathrm{T}}_{1c} \mathbf{c}^{0,\mathrm{T}}_{1b} \mathbf{p}_M. \tag{75}$$

We linearize (75) by expansion in a series of Taylor in the $\mathbf{X}_{fix}$:

$$\begin{gathered}\mathbf{Q}_g \approx \mathbf{Q}_g\left(\mathbf{q}^0_{1b,fix}, \mathbf{p}_{fix}\right) + \mathbf{J}_{\mathbf{q}^0_{1b}}(\mathbf{Q}_g)_{\mathbf{X}_{fix}} \delta\mathbf{q}^0_{1b},\ \mathbf{J}_{\mathbf{q}^0_{1b}}(\mathbf{Q}_g) = \mathbf{c}^{1b,\mathrm{T}}_{1c} \left\langle \mathbf{c}^{0,\mathrm{T}}_{1b} \mathbf{m}_1 \mathbf{g} \right\rangle \boldsymbol{\varepsilon}^0_{1b},\\ \mathbf{Q}_P \approx \mathbf{Q}_P\left(\mathbf{q}^0_{1b,fix}, \mathbf{p}_{fix}\right) + \mathbf{J}_{\mathbf{q}^0_{1b}}(\mathbf{Q}_P)_{\mathbf{X}_{fix}} \delta\mathbf{q}^0_{1b} + \mathbf{J}_{\mathbf{p}_F}(\mathbf{Q}_P)_{\mathbf{X}_{fix}} \delta\mathbf{p}_F,\\ \mathbf{J}_{\mathbf{q}^0_{1b}}(\mathbf{Q}_P) = \mathbf{c}^{1b,\mathrm{T}}_{1c} \left\langle \mathbf{c}^{0,\mathrm{T}}_{1b} \mathbf{p}_F \right\rangle \boldsymbol{\varepsilon}^0_{1b},\ \mathbf{J}_{\mathbf{p}_F}(\mathbf{Q}_P) = \mathbf{c}^{1b,\mathrm{T}}_{1c} \mathbf{c}^{0,\mathrm{T}}_{1b},\\ \mathbf{Q}_K \approx \mathbf{Q}_K\left(\mathbf{q}^{1c}_{1,fix}, \mathbf{q}^0_{1b,fix}, \mathbf{p}_{fix}\right) + \mathbf{J}_{\mathbf{q}^{1c}_1}(\mathbf{Q}_K)_{\mathbf{X}_{fix}} \delta\mathbf{q}^{1c}_1 +\\ + \mathbf{J}_{\mathbf{q}^0_{1b}}(\mathbf{Q}_K)_{\mathbf{X}_{fix}} \delta\mathbf{q}^0_{1b} + \mathbf{J}_{\mathbf{p}_M}(\mathbf{Q}_K)_{\mathbf{X}_{fix}} \delta\mathbf{p}_M,\\ \mathbf{J}_{\mathbf{q}^{1c}_1}(\mathbf{Q}_K) = \boldsymbol{\gamma}_{15} + \boldsymbol{\varepsilon}^{1c,\mathrm{T}}_1 \left\langle \mathbf{c}^{1c,\mathrm{T}}_1 \mathbf{c}^{1b,\mathrm{T}}_{1c} \mathbf{c}^{0,\mathrm{T}}_{1b} \mathbf{p}_M \right\rangle \boldsymbol{\varepsilon}^{1c}_1,\\ \mathbf{J}_{\mathbf{q}^0_{1b}}(\mathbf{Q}_K) = \boldsymbol{\varepsilon}^{1c,\mathrm{T}}_1 \mathbf{c}^{1c,\mathrm{T}}_1 \mathbf{c}^{1b,\mathrm{T}}_{1c} \left\langle \mathbf{c}^{0,\mathrm{T}}_{1b} \mathbf{p}_M \right\rangle \boldsymbol{\varepsilon}^0_{1b},\ \mathbf{J}_{\mathbf{p}_M}(\mathbf{Q}_K) = \boldsymbol{\varepsilon}^{1c,\mathrm{T}}_1 \mathbf{c}^{1c,\mathrm{T}}_1 \mathbf{c}^{1b,\mathrm{T}}_{1c} \mathbf{c}^{0,\mathrm{T}}_{1b},\\ \boldsymbol{\gamma}_{15} = \left[\boldsymbol{\lambda}^{1c,\mathrm{T}}_{1,1} \mathbf{c}^{1c,\mathrm{T}}_1 \mathbf{c}^{1b,\mathrm{T}}_{1c} \mathbf{c}^{0,\mathrm{T}}_{1b} \mathbf{p}_M | \boldsymbol{\lambda}^{1c,\mathrm{T}}_{1,2} \mathbf{c}^{1c,\mathrm{T}}_1 \mathbf{c}^{1b,\mathrm{T}}_{1c} \mathbf{c}^{0,\mathrm{T}}_{1b} \mathbf{p}_M | \boldsymbol{\lambda}^{1c,\mathrm{T}}_{1,3} \mathbf{c}^{1c,\mathrm{T}}_1 \mathbf{c}^{1b,\mathrm{T}}_{1c} \mathbf{c}^{0,\mathrm{T}}_{1b} \mathbf{p}_M\right].\end{gathered} \tag{76}$$

We linearize elastic forces and damping forces. This question in details was considered in [5]. The generalized elastic forces operating on AP are described by expression:

$$\mathbf{Q}_C = \begin{bmatrix} -\mathbf{c}^{1b,\mathrm{T}}_{1c} \sum\limits_{i=1}^{n} \frac{\mathbf{r}^{1bji,1b}_{1ji}}{l^{1bji}_{1ji}} C_i \left[l^{1bji}_{1ji} - \frac{\psi_i}{I_i} - l_{0i} \right] \\ -\boldsymbol{\varepsilon}^{1c,\mathrm{T}}_1 \sum\limits_{i=1}^{n} \left\langle \mathbf{r}^{1,1}_{1ji} \right\rangle \mathbf{c}^{1c,\mathrm{T}}_1 \mathbf{c}^{1b,\mathrm{T}}_{1c} \frac{\mathbf{r}^{1bji,1b}_{1ji}}{l^{1bji}_{1ji}} C_i \left[l^{1bji}_{1ji} - \frac{\psi_i}{I_i} - l_{0i} \right] \end{bmatrix}, \tag{77}$$

where C_i—stiffness of actuator.

We linearize (78) by an expansion in a series of Taylor:

$$\mathbf{Q}_c \cong \mathbf{Q}_c\left(\mathbf{X}_{fix}\right) + \mathbf{J}_{\mathbf{q}_1^{1c}}(\mathbf{Q}_c)_{\mathbf{X}_{fix}}\delta\mathbf{x} + \mathbf{J}_{\mathbf{u}}(\mathbf{Q}_c)_{\mathbf{X}_{fix}}\delta\mathbf{u}, \tag{78}$$

where $\mathbf{J}_{\mathbf{u}}$—the matrix of Jacobi from $\mathbf{Q}_C$ on coordinates $\mathbf{u}$; $\delta\mathbf{u}$—the variations of the corresponding coordinates.

Let's find linearized expressions for the generalized forces $\mathbf{Q}_{fc}$:

$$\mathbf{Q}_{fc} = -\mathbf{c}_{1c}^{1b,\mathrm{T}} \sum_{i=1}^{n} \frac{\mathbf{r}_{1ji}^{1bji,1b}}{l_{1ji}^{1bji}} C_i \left[l_{1ji}^{1bji} - \frac{\psi_i + I_i l_{0i}}{I_i} \right], \tag{79}$$

proceeding from definition (78) and having considered results in [5]:

$$\begin{aligned}
\mathbf{J}_{\mathbf{q}_1^{1c}}\left(\mathbf{Q}_{fc}\right) &= \left[\mathbf{J}_{\mathbf{r}_1^{1c,1c}}\left(\mathbf{Q}_{fc}\right) \quad \mathbf{J}_{\varphi_1^{1c}}\left(\mathbf{Q}_{fc}\right) \right], \\
\mathbf{J}_{\mathbf{r}_1^{1c,1c}}\left(\mathbf{Q}_{fc}\right) &= \sum_{i=1}^{n} C_i \left[\mathbf{I} - \frac{\psi_i + I_i l_{0i}}{l_{1ji}^{1bji}}\mathbf{I} + \frac{\psi_i + I_i l_{0i}}{I_i} \frac{\mathbf{c}_{1c}^{1b,\mathrm{T}} \mathbf{r}_{1ji}^{1bji,1b} \mathbf{r}_{1ji}^{1bji,1b,\mathrm{T}} \mathbf{c}_{1c}^{1b}}{\left(l_{1ji}^{1bji}\right)^3} \right] = \sum_{i=1}^{n} \bar{\mathbf{C}}_i, \\
\mathbf{J}_{\varphi_1^{1c}}\left(\mathbf{Q}_{fc}\right) &= \sum_{i=1}^{n} \bar{\mathbf{C}}_i \mathbf{c}_1^{1c} \left\langle \mathbf{r}_{1ji}^{1,1} \right\rangle^{\mathrm{T}} \boldsymbol{\varepsilon}_1^{1c}, \; \mathbf{J}_{\psi}\left(\mathbf{Q}_f\right) = \boldsymbol{\gamma}_{16}, \\
\boldsymbol{\gamma}_{16} &= \left[\mathbf{c}_{1c}^{1b,\mathrm{T}} \mathbf{r}_{1j1}^{1bj1,1b} \frac{C_1}{I_1 l_{1j1}^{1bj1}} | \ldots | \mathbf{c}_{1c}^{1b,\mathrm{T}} \mathbf{r}_{1jn}^{1bjn,1b} \frac{C_n}{I_n l_{1jn}^{1bjn}} \right],
\end{aligned} \tag{80}$$

where $\mathbf{I}$—identity matrix 3 × 3; $\bar{\mathbf{C}}_i$—the unit stiffness of ith of the actuator, it is determined by a formula

$$\bar{\mathbf{C}}_i = C_i \left[\mathbf{I} - \frac{\psi_i + I_i l_{0i}}{l_{1ji}^{1bji}}\mathbf{I} + \frac{\psi_i + I_i l_{0i}}{I_i} \frac{\mathbf{c}_{1c}^{1b,\mathrm{T}} \mathbf{r}_{1ji}^{1bji,1b} \mathbf{r}_{1ji}^{1bji,1b,\mathrm{T}} \mathbf{c}_{1c}^{1b}}{\left(l_{1ji}^{1bji}\right)^3} \right]. \tag{81}$$

Let's find linearized expressions for the generalized torques of Q_M using results in [5]:

$$\mathbf{Q}_{Mc} = -\sum_{i=1}^{n} \boldsymbol{\varepsilon}_1^{1c,\mathrm{T}} \left\langle \mathbf{r}_{1ji}^{1,1} \right\rangle \mathbf{c}_1^{1c,\mathrm{T}} \mathbf{c}_{1c}^{1b,\mathrm{T}} \frac{\mathbf{r}_{1ji}^{1bji,1b}}{l_{1ji}^{1bji}} C_i \left[l_{1ji}^{1bji} - \frac{\psi_i + I_i l_{0i}}{I_i} \right], \tag{82}$$

proceeding from definition (78):

$$\begin{aligned}
\mathbf{J}_{\mathbf{q}_1^{1c}}(\mathbf{Q}_{Mc}) &= \left[\mathbf{J}_{\mathbf{r}_1^{1c}}(\mathbf{Q}_{Mc}) \quad \mathbf{J}_{\varphi_1^{1c}}(\mathbf{Q}_{Mc})\right],\\
\mathbf{J}_{\mathbf{r}_1^{1c,1c}}(\mathbf{Q}_{Mc}) &= \sum_{i=1}^{n} \boldsymbol{\varepsilon}_1^{1c,\mathrm{T}} \left\langle \mathbf{r}_{1ji}^{1,1} \right\rangle \mathbf{c}_1^{1c,\mathrm{T}} \bar{\mathbf{C}}_i,\\
\mathbf{J}_{\varphi_1^{1c}}(\mathbf{Q}_{Mc}) &= \sum_{i=1}^{n} \boldsymbol{\varepsilon}_1^{1c,\mathrm{T}} \left\langle \mathbf{r}_{1ji}^{1,1} \right\rangle \mathbf{c}_1^{1c,\mathrm{T}} \bar{\mathbf{C}}_i \mathbf{c}_1^{1c} \left\langle \mathbf{r}_{1ji}^{1,1} \right\rangle^{\mathrm{T}} \boldsymbol{\varepsilon}_1^{1c}\\
&\quad + \sum_{i=1}^{n} \left[\left\langle \mathbf{r}_{1ji}^{1bji,1} \right\rangle^{\mathrm{T}} \boldsymbol{\chi}_i + \left\langle \mathbf{r}_{1ji}^{1,1} \right\rangle^{\mathrm{T}} \boldsymbol{\eta}_i - \boldsymbol{\varepsilon}_1^{1c,\mathrm{T}} \left\langle \mathbf{r}_{1ji}^{1,1} \right\rangle \left\langle \mathbf{r}_{1ji}^{1bji,1} \right\rangle^{\mathrm{T}} \boldsymbol{\varepsilon}_1^{1c} \right] C_i \left[1 - \frac{\psi_i + I_i l_{0i}}{I_i l_{1ji}^{1bji}} \right],\\
\mathbf{J}_{\psi}(\mathbf{Q}_{Mc}) &= \boldsymbol{\gamma}_{17},\\
\boldsymbol{\gamma}_{17} &= \left[\boldsymbol{\varepsilon}_1^{1c,\mathrm{T}} \left\langle \mathbf{r}_{1j1}^{1,1} \right\rangle \mathbf{c}_1^{1c,\mathrm{T}} \mathbf{c}_{1c}^{1b,\mathrm{T}} \mathbf{r}_{1j1}^{1bj1,1b} \frac{C_1}{I_1 l_{1j1}^{1bj1}} | \ldots | \boldsymbol{\varepsilon}_1^{1c,\mathrm{T}} \left\langle \mathbf{r}_{1jn}^{1,1} \right\rangle \mathbf{c}_1^{1c,\mathrm{T}} \mathbf{c}_{1c}^{1b,\mathrm{T}} \mathbf{r}_{1jn}^{1bjn,1b} \frac{C_n}{I_n l_{1jn}^{1bjn}} \right],
\end{aligned} \tag{83}$$

where $\mathbf{r}_{1ji}^{1bji,1} = \mathbf{c}_1^{1c,\mathrm{T}} \mathbf{c}_{1c}^{1b,\mathrm{T}} \mathbf{r}_{1ji}^{1bji,1b}$, $\boldsymbol{\chi}_i\left(\mathbf{r}_{1ji}^{1,1}, \varphi_1^{1c}\right)$ and $\boldsymbol{\eta}_i\left(\mathbf{r}_{1ji}^{1bji,1}, \varphi_1^{1c}\right)$ have got from expressions:

$$\boldsymbol{\chi}_i = \begin{bmatrix} 0 & 0 & -\cos(\alpha_1^{1c}) y_{1ji}^{1,1} - \sin(\alpha_1^{1c}) x_{1ji}^{1,1} \\ 0 & -\cos(\alpha_1^{1c}) \sin(\theta_1^{1c}) y_{1ji}^{1,1} - \sin(\alpha_1^{1c}) \sin(\theta_1^{1c}) x_{1ji}^{1,1} & -\sin(\alpha_1^{1c}) \cos(\theta_1^{1c}) y_{1ji}^{1,1} + \cos(\alpha_1^{1c}) \cos(\theta_1^{1c}) x_{1ji}^{1,1} \\ 0 & -\cos(\alpha_1^{1c}) \sin(\theta_1^{1c}) z_{1ji}^{1,1} - \cos(\theta_1^{1c}) x_{1ji}^{1,1} & -\sin(\alpha_1^{1c}) z_{1ji}^{1,1} - \sin(\alpha_1^{1c}) \cos(\theta_1^{1c}) z_{1ji}^{1,1} \end{bmatrix}; \tag{84}$$

$$\boldsymbol{\eta}_i = \begin{bmatrix} 0 & -\cos(\alpha_1^{1c}) \sin(\theta_1^{1c}) x_{1ji}^{1bji,1} & -\sin(\alpha_1^{1c}) \cos(\theta_1^{1c}) x_{1ji}^{1bji,1} + \cos(\alpha_1^{1c}) y_{1ji}^{1bji,1} \\ 0 & \sin(\alpha_1^{1c}) \sin(\theta_1^{1c}) x_{1ji}^{1bji,1} & -\cos(\alpha_1^{1c}) \cos(\theta_1^{1c}) x_{1ji}^{1bji,1} - \sin(\alpha_1^{1c}) y_{1ji}^{1bji,1} \\ 0 & \cos(\theta_1^{1c}) x_{1ji}^{1bji,1} & 0 \end{bmatrix}.$$

The generalized forces of damping operating on AP are described by expression:

$$\mathbf{Q}_D = \begin{bmatrix} -\mathbf{c}_{1c}^{1b,\mathrm{T}} \sum_{i=1}^{n} \frac{\mathbf{r}_{1ji}^{1bji,1b}}{l_{1ji}^{1bji}} D_i \left[\dot{l}_{1ji}^{1bji} - \frac{\dot{\psi}_i}{I_i} \right] \\ -\boldsymbol{\varepsilon}_1^{1c,\mathrm{T}} \sum_{i=1}^{n} \left\langle \mathbf{r}_{1ji}^{1,1} \right\rangle \mathbf{c}_1^{1c,\mathrm{T}} \mathbf{c}_{1c}^{1b,\mathrm{T}} \frac{\mathbf{r}_{1ji}^{1bji,1b}}{l_{1ji}^{1bji}} D_i \left[\dot{l}_{1ji}^{1bji} - \frac{\dot{\psi}_i}{I_i} \right] \end{bmatrix}, \tag{85}$$

where D_i—the actuator damping coefficients.

We linearize (85) by an expansion in a series of Taylor:

$$\mathbf{Q}_D \cong \mathbf{Q}_D(\mathbf{X}_{fix}) + \mathbf{J}_{\mathbf{q}_1^{1c}}(\mathbf{Q}_D)_{\mathbf{X}_{fix}} \delta\mathbf{x} + \mathbf{J}_{\dot{\mathbf{q}}_1^{1c}}(\mathbf{Q}_D)_{\mathbf{X}_{fix}} \delta\dot{\mathbf{x}} + \mathbf{J}_{\mathbf{u}}(\mathbf{Q}_D)_{\mathbf{X}_{fix}} \delta\mathbf{u},$$

where $\mathbf{J}_{\mathbf{u}}$—the matrix of Jacobi from $\mathbf{Q}_D$ on coordinates $\mathbf{u}$; $\delta\mathbf{u}$—the variations of the corresponding coordinates.

Let's find linearized expressions for the generalized forces $\mathbf{Q}_{fd}$. The variation of velocity of displacement of the actuator is equal:

$$\delta \dot{l}_{1ji}^{1bji} = \mathbf{v}_{1ji}^{1bji,1b,\mathrm{T}} \delta \left(\frac{\mathbf{r}_{1ji}^{1bji,1bji}}{l_{1ji}^{1bji}} \right) + \frac{\mathbf{r}_{1ji}^{1bji,1b,\mathrm{T}}}{l_{1ji}^{1bji}} \delta \mathbf{v}_{1ji}^{1bji,1b}, \tag{86}$$

where the corresponding variations are calculated on formulas (87):

$$\begin{aligned}
\delta \left(\frac{\mathbf{r}_{1ji}^{1bji,1b}}{l_{1ji}^{1bji}} \right) &= \left(\frac{\mathbf{c}_{1c}^{1b}}{l_{1ji}^{1bji}} - \frac{\mathbf{r}_{1ji}^{1bji,1b} \mathbf{r}_{1ji}^{1bji,1b,\mathrm{T}} \mathbf{c}_{1c}^{1b}}{\left(l_{1ji}^{1bji} \right)^3} \right) \delta \mathbf{r}_1^{1c,1c} + \left(\frac{\mathbf{c}_{1c}^{1b}}{l_{1ji}^{1bji}} - \frac{\mathbf{r}_{1ji}^{1bji,1b} \mathbf{r}_{1ji}^{1bji,1b,\mathrm{T}} \mathbf{c}_{1c}^{1b}}{\left(l_{1ji}^{1bji} \right)^3} \right) \mathbf{c}_1^{1c} \left\langle \mathbf{r}_{1ji}^{1,1} \right\rangle^{\mathrm{T}} \boldsymbol{\varepsilon}_1^{1c} \delta \varphi_1^{1c}, \\
\delta \mathbf{v}_{1ji}^{1bji,1b} &= \mathbf{c}_{1c}^{1b} \delta \dot{\mathbf{r}}_1^{1c,1c} + \mathbf{c}_{1c}^{1b} \delta \mathbf{c}_1^{1c} \left\langle \mathbf{r}_{1ji}^{1,1} \right\rangle^{\mathrm{T}} \boldsymbol{\varepsilon}_1^{1c} \dot{\varphi}_1^{1c} + \mathbf{c}_{1c}^{1b} \mathbf{c}_1^{1c} \left\langle \mathbf{r}_{1ji}^{1,1} \right\rangle^{\mathrm{T}} \delta \boldsymbol{\varepsilon}_1^{1c} \dot{\varphi}_1^{1c} + \mathbf{c}_{1c}^{1b} \mathbf{c}_1^{1c} \left\langle \mathbf{r}_{1ji}^{1,1} \right\rangle^{\mathrm{T}} \boldsymbol{\varepsilon}_1^{1c} \delta \dot{\varphi}_1^{1c} \\
&= \mathbf{c}_{1c}^{1b} \left[\mathbf{c}_1^{1c} \left\langle \left\langle \mathbf{r}_{1ji}^{1,1} \right\rangle \boldsymbol{\varepsilon}_1^{1c} \dot{\varphi}_1^{1c} \right\rangle \boldsymbol{\varepsilon}_1^{1c} + \mathbf{c}_1^{1c} \left\langle \mathbf{r}_{1ji}^{1,1} \right\rangle^{\mathrm{T}} \boldsymbol{\gamma}_3 \right] \delta \varphi_1^{1c} + \mathbf{c}_{1c}^{1b} \delta \dot{\mathbf{r}}_1^{1c,1c} + \mathbf{c}_{1c}^{1b} \mathbf{c}_1^{1c} \left\langle \mathbf{r}_{1ji}^{1,1} \right\rangle^{\mathrm{T}} \boldsymbol{\varepsilon}_1^{1c} \delta \dot{\varphi}_1^{1c}.
\end{aligned} \tag{87}$$

Having substituted (87) in (86), we will get:

$$\begin{aligned}
\delta \dot{l}_{1ji}^{1bji} &= \mathbf{v}_{1ji}^{1bji,1b,\mathrm{T}} \mathbf{c}_{1c}^{1b} \left(\frac{\mathbf{I}}{l_{1ji}^{1bji}} - \frac{\mathbf{c}_{1c}^{1b,\mathrm{T}} \mathbf{r}_{1ji}^{1bji,1b} \mathbf{r}_{1ji}^{1bji,1b,\mathrm{T}} \mathbf{c}_{1c}^{1b}}{\left(l_{1ji}^{1bji} \right)^3} \right) \delta \mathbf{r}_1^{1c,1c} \\
&\quad + \mathbf{v}_{1ji}^{1bji,1b,\mathrm{T}} \mathbf{c}_{1c}^{1b} \left(\frac{\mathbf{I}}{l_{1ji}^{1bji}} - \frac{\mathbf{c}_{1c}^{1b,\mathrm{T}} \mathbf{r}_{1ji}^{1bji,1b} \mathbf{r}_{1ji}^{1bji,1b,\mathrm{T}} \mathbf{c}_{1c}^{1b}}{\left(l_{1ji}^{1bji} \right)^3} \right) \mathbf{c}_1^{1c} \left\langle \mathbf{r}_{1ji}^{1,1} \right\rangle^{\mathrm{T}} \boldsymbol{\varepsilon}_1^{1c} \delta \varphi_1^{1c} \\
&\quad + \frac{\mathbf{r}_{1ji}^{1bji,1b,\mathrm{T}} \mathbf{c}_{1c}^{1b}}{l_{1ji}^{1bji}} \left[\mathbf{c}_1^{1c} \left\langle \left\langle \mathbf{r}_{1ji}^{1,1} \right\rangle \boldsymbol{\varepsilon}_1^{1c} \dot{\varphi}_1^{1c} \right\rangle \boldsymbol{\varepsilon}_1^{1c} + \mathbf{c}_1^{1c} \left\langle \mathbf{r}_{1ji}^{1,1} \right\rangle^{\mathrm{T}} \boldsymbol{\gamma}_3 \right] \delta \varphi_1^{1c} \\
&\quad + \frac{\mathbf{r}_{1ji}^{1bji,1b,\mathrm{T}} \mathbf{c}_{1c}^{1b}}{l_{1ji}^{1bji}} \delta \dot{\mathbf{r}}_1^{1c,1c} + \frac{\mathbf{r}_{1ji}^{1bji,1b,\mathrm{T}} \mathbf{c}_{1c}^{1b}}{l_{1ji}^{1bji}} \mathbf{c}_1^{1c} \left\langle \mathbf{r}_{1ji}^{1,1} \right\rangle^{\mathrm{T}} \boldsymbol{\varepsilon}_1^{1c} \delta \dot{\varphi}_1^{1c}.
\end{aligned} \tag{88}$$

The first variation at forces of damping in (85) will be:

$$\begin{aligned}
\delta \mathbf{Q}_{fd} &= -\sum_{i=1}^{n} \mathbf{c}_{1c}^{1b,\mathrm{T}} \delta \left(\frac{\mathbf{r}_{1ji}^{1bji,1b}}{l_{1ji}^{1bji}} \right) D_i \left[\dot{l}_{1ji}^{1bji} - \frac{\dot{\psi}_i}{I_i} \right] - \sum_{i=1}^{n} \frac{\mathbf{c}_{1c}^{1b,\mathrm{T}} \mathbf{r}_{1ji}^{1bji,1b}}{l_{1ji}^{1bji}} D_i \delta \dot{l}_{1ji}^{1bji} \\
&\quad + \sum_{i=1}^{n} \frac{\mathbf{c}_{1c}^{1b,\mathrm{T}} \mathbf{r}_{1ji}^{1bji,1b}}{l_{1ji}^{1bji}} \frac{D_i}{I_i} \delta \dot{\psi}_i.
\end{aligned} \tag{89}$$

Having substituted (87) and (88) in (89) we will get:

$$\begin{aligned}
\delta\mathbf{Q}_{fd} = &-\sum_{i=1}^{n}\left[\dot{l}_{1ji}^{1bji}-\frac{\dot{\psi}_i}{I_i}\right]D_i\left(\frac{\mathbf{I}}{l_{1ji}^{1bji}}-\frac{\mathbf{c}_{1c}^{1b,\mathrm{T}}\mathbf{r}_{1ji}^{1bji,1b}\mathbf{r}_{1ji}^{1bji,1b,\mathrm{T}}\mathbf{c}_{1c}^{1b}}{\left(l_{1ji}^{1bji}\right)^3}\right)\delta\mathbf{r}_1^{1c,1c}\\
&-\sum_{i=1}^{n}\frac{\mathbf{c}_{1c}^{1b,\mathrm{T}}\mathbf{r}_{1ji}^{1bji,1b}\mathbf{v}_{1ji}^{1bji,1b,\mathrm{T}}\mathbf{c}_{1c}^{1b}}{l_{1ji}^{1bji}}D_i\left(\frac{\mathbf{I}}{l_{1ji}^{1bji}}-\frac{\mathbf{c}_{1c}^{1b,\mathrm{T}}\mathbf{r}_{1ji}^{1bji,1b}\mathbf{r}_{1ji}^{1bji,1b,\mathrm{T}}\mathbf{c}_{1c}^{1b}}{\left(l_{1ji}^{1bji}\right)^3}\right)\delta\mathbf{r}_1^{1c,1c}\\
&-\sum_{i=1}^{n}\left[\dot{l}_{1ji}^{1bji}-\frac{\dot{\psi}_i}{I_i}\right]D_i\left(\frac{\mathbf{I}}{l_{1ji}^{1bji}}-\frac{\mathbf{c}_{1c}^{1b,\mathrm{T}}\mathbf{r}_{1ji}^{1bji,1b}\mathbf{r}_{1ji}^{1bji,1b,\mathrm{T}}\mathbf{c}_{1c}^{1b}}{\left(l_{1ji}^{1bji}\right)^3}\right)\mathbf{c}_1^{1c}\left\langle\mathbf{r}_{1ji}^{1,1}\right\rangle^{\mathrm{T}}\boldsymbol{\varepsilon}_1^{1c}\delta\varphi_1^{1c}\\
&-\sum_{i=1}^{n}\frac{\mathbf{c}_{1c}^{1b,\mathrm{T}}\mathbf{r}_{1ji}^{1bji,1b}\mathbf{v}_{1ji}^{1bji,1b,\mathrm{T}}\mathbf{c}_{1c}^{1b}}{l_{1ji}^{1bji}}D_i\left(\frac{\mathbf{I}}{l_{1ji}^{1bji}}-\frac{\mathbf{c}_{1c}^{1b,\mathrm{T}}\mathbf{r}_{1ji}^{1bji,1b}\mathbf{r}_{1ji}^{1bji,1b,\mathrm{T}}\mathbf{c}_{1c}^{1b}}{\left(l_{1ji}^{1bji}\right)^3}\right)\mathbf{c}_1^{1c}\left\langle\mathbf{r}_{1ji}^{1,1}\right\rangle^{\mathrm{T}}\boldsymbol{\varepsilon}_1^{1c}\delta\varphi_1^{1c}\\
&-\sum_{i=1}^{n}\frac{\mathbf{c}_{1c}^{1b,\mathrm{T}}\mathbf{r}_{1ji}^{1bji,1b}\mathbf{r}_{1ji}^{1bji,1b,\mathrm{T}}\mathbf{c}_{1c}^{1b}}{\left(l_{1ji}^{1bji}\right)^2}D_i\left[\mathbf{c}_1^{1c}\left\langle\left\langle\mathbf{r}_{1ji}^{1,1}\right\rangle\boldsymbol{\varepsilon}_1^{1c}\dot{\varphi}_1^{1c}\right\rangle\boldsymbol{\varepsilon}_1^{1c}+\mathbf{c}_1^{1c}\left\langle\mathbf{r}_{1ji}^{1,1}\right\rangle^{\mathrm{T}}\boldsymbol{\gamma}_3\right]\delta\varphi_1^{1c}\\
&-\sum_{i=1}^{n}\frac{\mathbf{c}_{1c}^{1b,\mathrm{T}}\mathbf{r}_{1ji}^{1bji,1b}\mathbf{r}_{1ji}^{1bji,1b,\mathrm{T}}\mathbf{c}_{1c}^{1b}}{\left(l_{1ji}^{1bji}\right)^2}D_i\delta\dot{\mathbf{r}}_1^{1c,1c}-\sum_{i=1}^{n}\frac{\mathbf{c}_{1c}^{1b,\mathrm{T}}\mathbf{r}_{1ji}^{1bji,1b}\mathbf{r}_{1ji}^{1bji,1b,\mathrm{T}}\mathbf{c}_{1c}^{1b}}{\left(l_{1ji}^{1bji}\right)^2}D_i\mathbf{c}_1^{1c}\left\langle\mathbf{r}_{1ji}^{1,1}\right\rangle^{\mathrm{T}}\boldsymbol{\varepsilon}_1^{1c}\delta\dot{\varphi}_1^{1c}\\
&+\sum_{i=1}^{n}\frac{\mathbf{c}_{1c}^{1b,\mathrm{T}}\mathbf{r}_{1ji}^{1bji,1b}}{l_{1ji}^{1bji}}\frac{D_i}{I_i}\delta\dot{\psi}_i.
\end{aligned}\tag{90}$$

The equivalent matrix of damping $\mathbf{D}$ has a form:

$$\begin{aligned}
&\mathbf{D}=\begin{bmatrix}\mathbf{d}_{11} & \mathbf{d}_{12}\\ \mathbf{d}_{21} & \mathbf{d}_{22}\end{bmatrix},\mathbf{d}_{11}=\sum_{i=1}^{n}\frac{\mathbf{c}_{1c}^{1b,\mathrm{T}}\mathbf{r}_{1ji}^{1bji,1b}\mathbf{r}_{1ji}^{1bji,1b,\mathrm{T}}\mathbf{c}_{1c}^{1b}}{\left(l_{1ji}^{1bji}\right)^2}=\sum_{i=1}^{n}\bar{\mathbf{D}}_i,\\
&\mathbf{d}_{12}=\sum_{i=1}^{n}\frac{\mathbf{c}_{1c}^{1b,\mathrm{T}}\mathbf{r}_{1ji}^{1bji,1b}\mathbf{r}_{1ji}^{1bji,1b,\mathrm{T}}\mathbf{c}_{1c}^{1b}}{\left(l_{1ji}^{1bji}\right)^2}D_i\mathbf{c}_1^{1c}\left\langle\mathbf{r}_{1ji}^{1,1}\right\rangle^{\mathrm{T}}\boldsymbol{\varepsilon}_1^{1c}=\sum_{i=1}^{n}\bar{\mathbf{D}}_i\mathbf{c}_1^{1c}\left\langle\mathbf{r}_{1ji}^{1,1}\right\rangle^{\mathrm{T}}\boldsymbol{\varepsilon}_1^{1c},
\end{aligned}\tag{91}$$

where $\bar{\mathbf{D}}_i$—the unit matrix of damping of ith actuator, it is determined by a formula:

$$\bar{\mathbf{D}}_i=D_i\frac{\mathbf{c}_{1c}^{1b,\mathrm{T}}\mathbf{r}_{1ji}^{1bji,1b}\mathbf{r}_{1ji}^{1bji,1b,\mathrm{T}}\mathbf{c}_{1c}^{1b}}{\left(l_{1ji}^{1bji}\right)^2}.\tag{92}$$

Expression (90) besides variations on the generalized velocities contains items with $\delta\dot{\psi}_i$, matrix $\boldsymbol{\gamma}_{18}$ at these items in (90) will have a form:

$$\boldsymbol{\gamma}_{18} = \left[\frac{\mathbf{c}_{1c}^{1b,\mathrm{T}}\mathbf{r}_{1j1}^{1bj1,1b}}{l_{1j1}^{1bj1}}\frac{D_1}{I_1}|\ldots|\frac{\mathbf{c}_{1c}^{1b,\mathrm{T}}\mathbf{r}_{1jn}^{1bjn,1b}}{l_{1jn}^{1bjn}}\frac{D_n}{I_n}\right]. \tag{93}$$

Also in (90) there are variations from the generalized coordinates $\delta\mathbf{r}_1^{1c,1c}$ and $\delta\varphi_1^{1c}$, the components of a matrix $\mathbf{O}$ corresponding to them will have a form:

$$\mathbf{O} = \begin{bmatrix}\mathbf{o}_{11} & \mathbf{o}_{12}\\ \mathbf{o}_{21} & \mathbf{o}_{22}\end{bmatrix},$$

$$\mathbf{o}_{11} = \sum_{i=1}^{n}\left[\dot{l}_{1ji}^{1bji}\mathbf{I} - \frac{\dot{\psi}_i}{I_i}\mathbf{I} + \frac{\mathbf{c}_{1c}^{1b,\mathrm{T}}\mathbf{r}_{1ji}^{1bji,1b}\mathbf{v}_{1ji}^{1bji,1b,\mathrm{T}}\mathbf{c}_{1c}^{1b}}{l_{1ji}^{1bji}}\right]D_i\left(\frac{\mathbf{I}}{l_{1ji}^{1bji}} - \frac{\mathbf{c}_{1c}^{1b,\mathrm{T}}\mathbf{r}_{1ji}^{1bji,1b}\mathbf{r}_{1ji}^{1bji,1b,\mathrm{T}}\mathbf{c}_{1c}^{1b}}{\left(l_{1ji}^{1bji}\right)^3}\right), \tag{94}$$

$$\mathbf{o}_{12} = -\sum_{i=1}^{n}\left[\dot{l}_{1ji}^{1bji}\mathbf{I} - \frac{\dot{\psi}_i}{I_i}\mathbf{I} + \frac{\mathbf{c}_{1c}^{1b,\mathrm{T}}\mathbf{r}_{1ji}^{1bji,1b}\mathbf{v}_{1ji}^{1bji,1b,\mathrm{T}}\mathbf{c}_{1c}^{1b}}{l_{1ji}^{1bji}}\right]D_i\left(\frac{\mathbf{I}}{l_{1ji}^{1bji}} - \frac{\mathbf{c}_{1c}^{1b,\mathrm{T}}\mathbf{r}_{1ji}^{1bji,1b}\mathbf{r}_{1ji}^{1bji,1b,\mathrm{T}}\mathbf{c}_{1c}^{1b}}{\left(l_{1ji}^{1bji}\right)^3}\right)\mathbf{c}_1^{1c}\left\langle\mathbf{r}_{1ji}^{1,1}\right\rangle^{\mathrm{T}}\boldsymbol{\varepsilon}_1^{1c}$$
$$-\sum_{i=1}^{n}\frac{\mathbf{c}_{1c}^{1b,\mathrm{T}}\mathbf{r}_{1ji}^{1bji,1b}\mathbf{r}_{1ji}^{1bji,1b,\mathrm{T}}\mathbf{c}_{1c}^{1b}}{\left(l_{1ji}^{1bji}\right)^2}D_i\left[\mathbf{c}_1^{1c}\left\langle\left\langle\mathbf{r}_{1ji}^{1,1}\right\rangle\boldsymbol{\varepsilon}_1^{1c}\dot{\varphi}_1^{1c}\right\rangle\boldsymbol{\varepsilon}_1^{1c} + \mathbf{c}_1^{1c}\left\langle\mathbf{r}_{1ji}^{1,1}\right\rangle^{\mathrm{T}}\boldsymbol{\gamma}_3\right]\delta\varphi_1^{1c}.$$

Let's find expression for the first variation of the generalized forces $\mathbf{Q}_{Md}$:

$$\delta\mathbf{Q}_{Md} = -\sum_{i=1}^{n}\delta\left(\boldsymbol{\varepsilon}_1^{1c,\mathrm{T}}\left\langle\mathbf{r}_{1ji}^{1,1}\right\rangle\mathbf{c}_1^{1c,\mathrm{T}}\mathbf{c}_{1c}^{1b,\mathrm{T}}\mathbf{r}_{1ji}^{1bji,1b}\right)\frac{1}{l_{1ji}^{1bji}}D_i\left[\dot{l}_{1ji}^{1bji} - \frac{\dot{\psi}_i}{I_i}\right]$$
$$-\sum_{i=1}^{n}\boldsymbol{\varepsilon}_1^{1c,\mathrm{T}}\left\langle\mathbf{r}_{1ji}^{1,1}\right\rangle\mathbf{c}_1^{1c,\mathrm{T}}\mathbf{c}_{1c}^{1b,\mathrm{T}}\mathbf{r}_{1ji}^{1bji,1b}\delta\left(\frac{1}{l_{1ji}^{1bji}}\right)D_i\left[\dot{l}_{1ji}^{1bji} - \frac{\dot{\psi}_i}{I_i}\right]$$
$$-\sum_{i=1}^{n}\boldsymbol{\varepsilon}_1^{1c,\mathrm{T}}\left\langle\mathbf{r}_{1ji}^{1,1}\right\rangle\mathbf{c}_1^{1c,\mathrm{T}}\mathbf{c}_{1c}^{1b,\mathrm{T}}\frac{\mathbf{r}_{1ji}^{1bji,1b}}{l_{1ji}^{1bji}}D_i\delta\dot{l}_{1ji}^{1bji} - \sum_{i=1}^{n}\boldsymbol{\varepsilon}_1^{1c,\mathrm{T}}\left\langle\mathbf{r}_{1ji}^{1,1}\right\rangle\mathbf{c}_1^{1c,\mathrm{T}}\mathbf{c}_{1c}^{1b,\mathrm{T}}\frac{\mathbf{r}_{1ji}^{1bji,1b}}{l_{1ji}^{1bji}}\frac{D_i}{I_i}\delta\dot{\psi}_i. \tag{95}$$

Let's find expression for variations $\delta\left(\frac{1}{l_{1ji}^{1bji}}\right)$ and $\delta\left(\boldsymbol{\varepsilon}_1^{1c,\mathrm{T}}\left\langle\mathbf{r}_{1ji}^{1,1}\right\rangle\mathbf{c}_1^{1c,\mathrm{T}}\mathbf{c}_{1c}^{1b,\mathrm{T}}\mathbf{r}_{1ji}^{1bji,1b}\right)$:

$$\delta\left(\frac{1}{l_{1ji}^{1bji}}\right)=-\frac{\mathbf{r}_{1ji}^{1bji,1b,\mathrm{T}}\mathbf{c}_{1c}^{1b}}{\left(l_{1ji}^{1bji}\right)^3}\delta\mathbf{r}_1^{1c,1c}-\frac{\mathbf{r}_{1ji}^{1bji,1b,\mathrm{T}}\mathbf{c}_{1c}^{1b}}{\left(l_{1ji}^{1bji}\right)^3}\mathbf{c}_1^{1c}\left\langle\mathbf{r}_{1ji}^{1,1}\right\rangle^{\mathrm{T}}\boldsymbol{\varepsilon}_1^{1c}\delta\varphi_1^{1c},$$

$$\delta\left(\boldsymbol{\varepsilon}_1^{1c,\mathrm{T}}\left\langle\mathbf{r}_{1ji}^{1,1}\right\rangle\mathbf{c}_1^{1c,\mathrm{T}}\mathbf{c}_{1c}^{1b,\mathrm{T}}\mathbf{r}_{1ji}^{1bji,1b}\right)=\delta\left(\boldsymbol{\varepsilon}_1^{1c,\mathrm{T}}\left\langle\mathbf{r}_{1ji}^{1,1}\right\rangle\mathbf{r}_{1ji}^{1bji,1}\right)=\boldsymbol{\varepsilon}_1^{1c,\mathrm{T}}\left\langle\mathbf{r}_{1ji}^{1,1}\right\rangle\mathbf{c}_1^{1c,\mathrm{T}}\delta\mathbf{r}_1^{1c,1c}$$
$$+\left[\left\langle\mathbf{r}_{1ji}^{1bji,1}\right\rangle^{\mathrm{T}}\boldsymbol{\chi}_i+\left\langle\mathbf{r}_{1ji}^{1,1}\right\rangle^{\mathrm{T}}\boldsymbol{\eta}_i-\boldsymbol{\varepsilon}_1^{1c,\mathrm{T}}\left\langle\mathbf{r}_{1ji}^{1,1}\right\rangle\left\langle\mathbf{r}_{1ji}^{1bji,1}\right\rangle^{\mathrm{T}}\boldsymbol{\varepsilon}_1^{1c}+\boldsymbol{\varepsilon}_1^{1c,\mathrm{T}}\left\langle\mathbf{r}_{1ji}^{1,1}\right\rangle\left\langle\mathbf{r}_{1ji}^{1,1}\right\rangle^{\mathrm{T}}\boldsymbol{\varepsilon}_1^{1c}\right]\delta\varphi_1^{1c}. \tag{96}$$

Having substituted (88) and (96) in (95) we will get:

$$\delta\mathbf{Q}_{Md}=-\sum_{i=1}^{n}\boldsymbol{\varepsilon}_1^{1c,\mathrm{T}}\left\langle\mathbf{r}_{1ji}^{1,1}\right\rangle\mathbf{c}_1^{1c,\mathrm{T}}\left[\dot{l}_{1ji}^{1bji}\mathbf{I}-\frac{\dot{\psi}_i}{I_i}\mathbf{I}-\frac{\mathbf{c}_{1c}^{1b,\mathrm{T}}\mathbf{r}_{1ji}^{1bji,1b}\mathbf{v}_{1ji}^{1bji,1b,\mathrm{T}}\mathbf{c}_{1c}^{1b}}{l_{1ji}^{1bji}}\right]D_i\left(\frac{\mathbf{I}}{l_{1ji}^{1bji}}-\frac{\mathbf{c}_{1c}^{1b,\mathrm{T}}\mathbf{r}_{1ji}^{1bji,1b}\mathbf{r}_{1ji}^{1bji,1b,\mathrm{T}}\mathbf{c}_{1c}^{1b}}{\left(l_{1ji}^{1bji}\right)^3}\right)\delta\mathbf{r}_1^{1c,1c}$$
$$-\sum_{i=1}^{n}\frac{D_i}{l_{1ji}^{1bji}}\left[\dot{l}_{1ji}^{1bji}-\frac{\dot{\psi}_i}{I_i}\right]\left[\left\langle\mathbf{r}_{1ji}^{1bji,1}\right\rangle^{\mathrm{T}}\boldsymbol{\chi}_i+\left\langle\mathbf{r}_{1ji}^{1,1}\right\rangle^{\mathrm{T}}\boldsymbol{\eta}_i-\boldsymbol{\varepsilon}_1^{1c,\mathrm{T}}\left\langle\mathbf{r}_{1ji}^{1,1}\right\rangle\left\langle\mathbf{r}_{1ji}^{1bji,1}\right\rangle^{\mathrm{T}}\boldsymbol{\varepsilon}_1^{1c}+\boldsymbol{\varepsilon}_1^{1c,\mathrm{T}}\left\langle\mathbf{r}_{1ji}^{1,1}\right\rangle\left\langle\mathbf{r}_{1ji}^{1,1}\right\rangle^{\mathrm{T}}\boldsymbol{\varepsilon}_1^{1c}\right]\delta\varphi_1^{1c}$$
$$+\sum_{i=1}^{n}\boldsymbol{\varepsilon}_1^{1c,\mathrm{T}}\left\langle\mathbf{r}_{1ji}^{1,1}\right\rangle\mathbf{c}_1^{1c,\mathrm{T}}\left[\dot{l}_{1ji}^{1bji}-\frac{\dot{\psi}_i}{I_i}\right]D_i\frac{\mathbf{c}_{1c}^{1b,\mathrm{T}}\mathbf{r}_{1ji}^{1bji,1b}\mathbf{r}_{1ji}^{1bji,1b,\mathrm{T}}\mathbf{c}_{1c}^{1b}}{\left(l_{1ji}^{1bji}\right)^3}\mathbf{c}_1^{1c}\left\langle\mathbf{r}_{1ji}^{1,1}\right\rangle^{\mathrm{T}}\boldsymbol{\varepsilon}_1^{1c}\delta\varphi_1^{1c}$$
$$-\sum_{i=1}^{n}\boldsymbol{\varepsilon}_1^{1c,\mathrm{T}}\left\langle\mathbf{r}_{1ji}^{1,1}\right\rangle\mathbf{c}_1^{1c,\mathrm{T}}\frac{\mathbf{c}_{1c}^{1b,\mathrm{T}}\mathbf{r}_{1ji}^{1bji,1b}\mathbf{v}_{1ji}^{1bji,1b,\mathrm{T}}\mathbf{c}_{1c}^{1b}}{l_{1ji}^{1bji}}D_i\left(\frac{\mathbf{I}}{l_{1ji}^{1bji}}-\frac{\mathbf{c}_{1c}^{1b,\mathrm{T}}\mathbf{r}_{1ji}^{1bji,1b}\mathbf{r}_{1ji}^{1bji,1b,\mathrm{T}}\mathbf{c}_{1c}^{1b}}{\left(l_{1ji}^{1bji}\right)^3}\right)\mathbf{c}_1^{1c}\left\langle\mathbf{r}_{1ji}^{1,1}\right\rangle^{\mathrm{T}}\boldsymbol{\varepsilon}_1^{1c}\delta\varphi_1^{1c} \tag{97}$$

$$-\sum_{i=1}^{n}\boldsymbol{\varepsilon}_1^{1c,\mathrm{T}}\left\langle\mathbf{r}_{1ji}^{1,1}\right\rangle\mathbf{c}_1^{1c,\mathrm{T}}\frac{\mathbf{c}_{1c}^{1b,\mathrm{T}}\mathbf{r}_{1ji}^{1bji,1b}\mathbf{r}_{1ji}^{1bji,1b,\mathrm{T}}\mathbf{c}_{1c}^{1b}}{\left(l_{1ji}^{1bji}\right)^2}D_i\left[\mathbf{c}_1^{1c}\left\langle\left\langle\mathbf{r}_{1ji}^{1,1}\right\rangle\boldsymbol{\varepsilon}_1^{1c}\dot{\varphi}_1^{1c}\right\rangle\boldsymbol{\varepsilon}_1^{1c}+\mathbf{c}_1^{1c}\left\langle\mathbf{r}_{1ji}^{1,1}\right\rangle^{\mathrm{T}}\boldsymbol{\gamma}_3\right]\delta\varphi_1^{1c}$$
$$-\sum_{i=1}^{n}\boldsymbol{\varepsilon}_1^{1c,\mathrm{T}}\left\langle\mathbf{r}_{1ji}^{1,1}\right\rangle\mathbf{c}_1^{1c,\mathrm{T}}D_i\frac{\mathbf{c}_{1c}^{1b,\mathrm{T}}\mathbf{r}_{1ji}^{1bji,1b}\mathbf{r}_{1ji}^{1bji,1b,\mathrm{T}}\mathbf{c}_{1c}^{1b}}{\left(l_{1ji}^{1bji}\right)^2}\delta\dot{\mathbf{r}}_1^{1c,1c}$$
$$-\sum_{i=1}^{n}\boldsymbol{\varepsilon}_1^{1c,\mathrm{T}}\left\langle\mathbf{r}_{1ji}^{1,1}\right\rangle\mathbf{c}_1^{1c,\mathrm{T}}D_i\frac{\mathbf{c}_{1c}^{1b,\mathrm{T}}\mathbf{r}_{1ji}^{1bji,1b}\mathbf{r}_{1ji}^{1bji,1b,\mathrm{T}}\mathbf{c}_{1c}^{1b}}{\left(l_{1ji}^{1bji}\right)^2}\mathbf{c}_1^{1c}\left\langle\mathbf{r}_{1ji}^{1,1}\right\rangle^{\mathrm{T}}\boldsymbol{\varepsilon}_1^{1c}\delta\dot{\varphi}_1^{1c}$$
$$-\sum_{i=1}^{n}\boldsymbol{\varepsilon}_1^{1c,\mathrm{T}}\left\langle\mathbf{r}_{1ji}^{1,1}\right\rangle\mathbf{c}_1^{1c,\mathrm{T}}\frac{\mathbf{c}_{1c}^{1b,\mathrm{T}}\mathbf{r}_{1ji}^{1bji,1b}}{l_{1ji}^{1bji}}\frac{D_i}{I_i}\delta\dot{\psi}_i.$$

From (97) we will find matrix components of $\mathbf{D}$:

$$\mathbf{d}_{21}=\sum_{i=1}^{n}\boldsymbol{\varepsilon}_1^{1c,\mathrm{T}}\left\langle\mathbf{r}_{1ji}^{1,1}\right\rangle\mathbf{c}_1^{1c,\mathrm{T}}\bar{\mathbf{D}}_i,\ \mathbf{d}_{22}=\sum_{i=1}^{n}\boldsymbol{\varepsilon}_1^{1c,\mathrm{T}}\left\langle\mathbf{r}_{1ji}^{1,1}\right\rangle\mathbf{c}_1^{1c,\mathrm{T}}\bar{\mathbf{D}}_i\mathbf{c}_1^{1c}\left\langle\mathbf{r}_{1ji}^{1,1}\right\rangle^{\mathrm{T}}\boldsymbol{\varepsilon}_1^{1c}. \tag{98}$$

From (97) we will find matrix components of **O**:

$$\mathbf{o}_{21} = \sum_{i=1}^{n} \boldsymbol{\varepsilon}_1^{1c,\mathrm{T}} \left\langle \mathbf{r}_{1ji}^{1,1} \right\rangle \mathbf{c}_1^{1c,\mathrm{T}} \left[\dot{l}_{1ji}^{1bji} \mathbf{I} - \frac{\dot{\psi}_i}{I_i} \mathbf{I} - \frac{\mathbf{c}_{1c}^{1b,\mathrm{T}} \mathbf{r}_{1ji}^{1bji,1b} \mathbf{v}_{1ji}^{1bji,1b,\mathrm{T}} \mathbf{c}_{1c}^{1b}}{l_{1ji}^{1bji}} \right] D_i \left(\frac{\mathbf{I}}{l_{1ji}^{1bji}} - \frac{\mathbf{c}_{1c}^{1b,\mathrm{T}} \mathbf{r}_{1ji}^{1bji,1b} \mathbf{r}_{1ji}^{1bji,1b,\mathrm{T}} \mathbf{c}_{1c}^{1b}}{\left(l_{1ji}^{1bji} \right)^3} \right),$$

$$\begin{aligned}
\mathbf{o}_{22} = & \sum_{i=1}^{n} \frac{D_i}{l_{1ji}^{1bji}} \left[\dot{l}_{1ji}^{1bji} - \frac{\dot{\psi}_i}{I_i} \right] \left[\left\langle \mathbf{r}_{1ji}^{1bji,1} \right\rangle^{\mathrm{T}} \boldsymbol{\chi}_i + \left\langle \mathbf{r}_{1ji}^{1,1} \right\rangle^{\mathrm{T}} \boldsymbol{\eta}_i - \boldsymbol{\varepsilon}_1^{1c,\mathrm{T}} \left\langle \mathbf{r}_{1ji}^{1,1} \right\rangle \left\langle \mathbf{r}_{1ji}^{1bji,1} \right\rangle^{\mathrm{T}} \boldsymbol{\varepsilon}_1^{1c} + \boldsymbol{\varepsilon}_1^{1c,\mathrm{T}} \left\langle \mathbf{r}_{1ji}^{1,1} \right\rangle \left\langle \mathbf{r}_{1ji}^{1,1} \right\rangle^{\mathrm{T}} \boldsymbol{\varepsilon}_1^{1c} \right] \\
& - \sum_{i=1}^{n} \boldsymbol{\varepsilon}_1^{1c,\mathrm{T}} \left\langle \mathbf{r}_{1ji}^{1,1} \right\rangle \mathbf{c}_1^{1c,\mathrm{T}} \left[\dot{l}_{1ji}^{1bji} - \frac{\dot{\psi}_i}{I_i} \right] D_i \frac{\mathbf{c}_{1c}^{1b,\mathrm{T}} \mathbf{r}_{1ji}^{1bji,1b} \mathbf{r}_{1ji}^{1bji,1b,\mathrm{T}} \mathbf{c}_{1c}^{1b}}{\left(l_{1ji}^{1bji} \right)^3} \mathbf{c}_1^{1c} \left\langle \mathbf{r}_{1ji}^{1,1} \right\rangle^{\mathrm{T}} \boldsymbol{\varepsilon}_1^{1c} \\
& + \sum_{i=1}^{n} \boldsymbol{\varepsilon}_1^{1c,\mathrm{T}} \left\langle \mathbf{r}_{1ji}^{1,1} \right\rangle \mathbf{c}_1^{1c,\mathrm{T}} \frac{\mathbf{c}_{1c}^{1b,\mathrm{T}} \mathbf{r}_{1ji}^{1bji,1b} \mathbf{v}_{1ji}^{1bji,1b,\mathrm{T}} \mathbf{c}_{1c}^{1b}}{l_{1ji}^{1bji}} D_i \left(\frac{\mathbf{I}}{l_{1ji}^{1bji}} - \frac{\mathbf{c}_{1c}^{1b,\mathrm{T}} \mathbf{r}_{1ji}^{1bji,1b} \mathbf{r}_{1ji}^{1bji,1b,\mathrm{T}} \mathbf{c}_{1c}^{1b}}{\left(l_{1ji}^{1bji} \right)^3} \right) \mathbf{c}_1^{1c} \left\langle \mathbf{r}_{1ji}^{1,1} \right\rangle^{\mathrm{T}} \boldsymbol{\varepsilon}_1^{1c} \\
& + \sum_{i=1}^{n} \boldsymbol{\varepsilon}_1^{1c,\mathrm{T}} \left\langle \mathbf{r}_{1ji}^{1,1} \right\rangle \mathbf{c}_1^{1c,\mathrm{T}} \frac{\mathbf{c}_{1c}^{1b,\mathrm{T}} \mathbf{r}_{1ji}^{1bji,1b} \mathbf{r}_{1ji}^{1bji,1b,\mathrm{T}} \mathbf{c}_{1c}^{1b}}{\left(l_{1ji}^{1bji} \right)^2} D_i \left[\mathbf{c}_1^{1c} \left\langle \left\langle \mathbf{r}_{1ji}^{1,1} \right\rangle \boldsymbol{\varepsilon}_1^{1c} \varphi_1^{1c} \right\rangle \boldsymbol{\varepsilon}_1^{1c} + \mathbf{c}_1^{1c} \left\langle \mathbf{r}_{1ji}^{1,1} \right\rangle^{\mathrm{T}} \boldsymbol{\gamma}_3 \right].
\end{aligned} \tag{99}$$

Expression (97) besides variations on the generalized velocities contains items with $\delta\dot{\psi}_i$, matrix $\boldsymbol{\gamma}_{19}$ at these items in (97) will have a form:

$$\boldsymbol{\gamma}_{19} = \left[\boldsymbol{\varepsilon}_1^{1c,\mathrm{T}} \left\langle \mathbf{r}_{1j1}^{1,1} \right\rangle \mathbf{c}_1^{1c,\mathrm{T}} \frac{\mathbf{c}_{1c}^{1b,\mathrm{T}} \mathbf{r}_{1j1}^{1bj1,1b}}{l_{1j1}^{1bj1}} \frac{D_1}{I_1} | \ldots | \boldsymbol{\varepsilon}_1^{1c,\mathrm{T}} \left\langle \mathbf{r}_{1jn}^{1,1} \right\rangle \mathbf{c}_1^{1c,\mathrm{T}} \frac{\mathbf{c}_{1c}^{1b,\mathrm{T}} \mathbf{r}_{1jn}^{1bjn,1b}}{l_{1jn}^{1bjn}} \frac{D_n}{I_n} \right]. \tag{100}$$

There are the friction torques $\mathbf{N}_{1,i}^1$ in hinges of actuators. The generalized friction torques will have a form:

$$\mathbf{Q}_N = \begin{bmatrix} 0 \\ \sum_{i=1}^{n} \boldsymbol{\varepsilon}_1^{1c,\mathrm{T}} \mathbf{N}_{1,i}^1 \end{bmatrix}. \tag{101}$$

It should be noted that creation of model of friction forces is one of the most complex challenges in similar mechanisms. Therefore we will be limited to the generalized model in which parameters need to be determined experimentally:

$$\mathbf{Q}_N \approx \mathbf{Q}_N \left(\mathbf{X}_{fix} \right) - \boldsymbol{\mu}_1 \left(\mathbf{X}_{fix} \right) \delta \mathbf{q}_1^{1c} - \boldsymbol{\mu}_2 \left(\mathbf{X}_{fix} \right) \delta \dot{\mathbf{q}}_1^{1c} - \boldsymbol{\mu}_3 \left(\mathbf{X}_{fix} \right) \delta \mathbf{u}, \tag{102}$$

where $\boldsymbol{\mu}_i$—the matrixes of parameters deciding as a result of experiments on an adaptive platform.

4 The Linearized Dynamics Equations Taking into Account Forces and the Torques

Let's substitute in (70) the linearized expressions for forces and the torques from (71) to (102):

$$\begin{aligned}\mathbf{A}_3\ddot{\mathbf{x}} + [\mathbf{A}_2 + \mathbf{D}_2 + \boldsymbol{\mu}_2]\dot{\mathbf{x}} + [\mathbf{A}_1 + \mathbf{C}_1 + \mathbf{D}_1 + \boldsymbol{\Pi}_1 + \boldsymbol{\mu}_1]\mathbf{x} = \boldsymbol{\Pi}_3\mathbf{z} + [\mathbf{H}_1 + \mathbf{H}_2 + \mathbf{H}_3]\mathbf{w} \\ - \mathbf{B}_3\ddot{\mathbf{y}} - \mathbf{B}_2\dot{\mathbf{y}} + [\mathbf{G}_1 - \mathbf{B}_1 + \boldsymbol{\Pi}_2]\mathbf{y} + [\mathbf{A}_0 - \mathbf{B}_0 + \mathbf{G}_0 + \mathbf{C}_0 + \mathbf{D}_0 + \boldsymbol{\mu}_0 + \boldsymbol{\Pi}_0],\end{aligned} \tag{103}$$

where $\mathbf{x}$ and $\mathbf{y}$—the corresponding deviations from a basic trajectory: $\mathbf{x} = \Delta\mathbf{q}_1^{1c} = \mathbf{q}_1^{1c} - \mathbf{q}_{1,fix}^{1c}, \mathbf{y} = \Delta\mathbf{q}_{1b}^0 = \mathbf{q}_{1b}^0 - \mathbf{q}_{1b,fix}^0$, and $\mathbf{z}$—the deviations of loadings from values in a stationary point: $\mathbf{z} = \Delta\mathbf{p} = \mathbf{p} - \mathbf{p}_{fix}$, $\mathbf{w}$—the deviations of the operating influences from the corresponding values in a stationary point: $\mathbf{w} = \Delta\mathbf{u} = \mathbf{u} - \mathbf{u}_{fix}$, and the matrixes of parameters of model (103) have a form:

$$\begin{aligned}
&\mathbf{G}_0 = \begin{bmatrix} \mathbf{Q}_g\left(\mathbf{q}_{1b,fix}^0, \mathbf{p}_{fix}\right) & 0 \\ 0 & 0 \end{bmatrix}, \mathbf{G}_1 = \begin{bmatrix} \mathbf{J}_{\mathbf{q}_{1b}^0}(\mathbf{Q}_g)_{\mathbf{X}_{fix}} & 0 \\ 0 & 0 \end{bmatrix}, \\
&\boldsymbol{\Pi}_0 = \begin{bmatrix} \mathbf{Q}_P\left(\mathbf{q}_{1b,fix}^0, \mathbf{p}_{fix}\right) & 0 \\ 0 & \mathbf{Q}_K\left(\mathbf{q}_{1,fix}^{1c}, \mathbf{q}_{1b,fix}^0, \mathbf{p}_{fix}\right) \end{bmatrix} \\
&\boldsymbol{\Pi}_2 = \begin{bmatrix} \mathbf{J}_{\mathbf{q}_{1b}^0}(\mathbf{Q}_P)_{\mathbf{X}_{fix}} & 0 \\ 0 & \mathbf{J}_{\mathbf{q}_{1b}^0}(\mathbf{Q}_K)_{\mathbf{X}_{fix}} \end{bmatrix}, \boldsymbol{\Pi}_1 = \begin{bmatrix} 0 & 0 \\ 0 & \mathbf{J}_{\mathbf{q}_1^{1c}}(\mathbf{Q}_K)_{\mathbf{X}_{fix}} \end{bmatrix}, \\
&\boldsymbol{\Pi}_3 = \begin{bmatrix} \mathbf{J}_{\mathbf{p}_F}(\mathbf{Q}_P)_{\mathbf{X}_{fix}} & 0 \\ 0 & \mathbf{J}_{\mathbf{p}_M}(\mathbf{Q}_K)_{\mathbf{X}_{fix}} \end{bmatrix}, \mathbf{C}_0 = \mathbf{Q}_c\left(\mathbf{X}_{fix}\right), \mathbf{C}_1 = \mathbf{J}_{\mathbf{q}_1^{1c}}(\mathbf{Q}_c)_{\mathbf{X}_{fix}}, \\
&\mathbf{H}_1 = \mathbf{J}_{\mathbf{u}}(\mathbf{Q}_c)_{\mathbf{X}_{fix}}, \mathbf{D}_0 = \mathbf{Q}_D\left(\mathbf{X}_{fix}\right), \mathbf{D}_1 = \mathbf{J}_{\mathbf{q}_1^{1c}}(\mathbf{Q}_D)_{\mathbf{X}_{fix}}, \mathbf{D}_2 = \mathbf{J}_{\dot{\mathbf{q}}_1^{1c}}(\mathbf{Q}_D)_{\mathbf{X}_{fix}} \\
&\mathbf{H}_2 = \mathbf{J}_{\mathbf{u}}(\mathbf{Q}_D)_{\mathbf{X}_{fix}}, \boldsymbol{\mu}_0 = \mathbf{Q}_N\left(\mathbf{X}_{fix}\right).
\end{aligned} \tag{104}$$

5 Conclusion

Formulas of calculation of matrixes of parameters of the linearized model of dynamics of mechanisms on the basis of the adaptive platforms moved with packages of actuators are given in article. This model can be used for the solution of problems of synthesis of a control system in the modes of stabilization and tracking. This model can be used as the state identifier for estimation of the similar plants which aren't measured a component of a vector of a state.

References

1. Gorodetskiy, A.E.: Smart Electromechanical Systems. Springer, Berlin (2016). doi:10.1007/978-3-319-27547-5, 277 p
2. Artemenko, Yu. N., Agapov V.A., Dubarenko V.V., Kuchmin A.Yu.: Co-operative control of subdish actuators of radio-telescope. *Informatsionno-upravliaiushchie sistemy*. vol. 59, no. 4. pp. 2–9 (2012) (in Russian)
3. Artemenko Yu. N., Gorodetskiy, A.E., Dubarenko, V.V., Kuchmin, A.Yu., Agapov V.A.: Analysis of dynamics of automatic control system of space radio-telescope subdish actuators. *Informatsionno-upravliaiushchie sistemy*. vol. 55, no. 6. pp. 2–6 (2011) (in Russian)
4. Artemenko, Yu. N., Gorodetskiy, A.E., Doroshenko, M.S., Dubarenko, V.V., Konovalov, A. S., Kuchmin, A.Yu., Tarasova I.L.: Problems of the choice of electric drives of space radio-telescope system dish system. Mechatronics, automation, control, no. 1. pp. 26–31 (2012) (in Russian)
5. Kuchmin A. Yu.: Modeling of equivalent stiffness of adaptive platforms with the parallel structure executive mechanism. *Informatsionno-upravliaiushchie sistemy*. vol. 70, no. 3. pp. 30–39 (2014) (in Russian)

Part V
Automatic Control Systems

Multiagent Approach to Control a Multisection Trunk-Type Manipulator

Yu.T. Kaganov and A.P. Karpenko

Abstract *Purpose* We consider a multisection trunk type manipulator built on the basis of parallel structure mechanisms, for example, on the basis of tripods or hexapods. Control of such a manipulator is a serious problem, as, in addition to control of each section of the manipulator, it is necessary to control the entire structure. To resolve this problem we suggest using a multiagent approach, neural networks and neuro-fuzzy technologies. We introduce an automatic control system for the trunk type manipulator, as well as the functions implemented by the coordinator and agents of this system. *Results* We investigate the efficiency of the adaptive agent built on the basis of a neural network inverse model of the control object, as well as on the basis of the reference model of the object in the form of another multilayer neural network. *Practical value* The presented in the article the automatic control system for the trunk type manipulator can be used to create intelligent robotic system capable to react to changing uncertain conditions in real time.

Keywords Intelligent robotics-based SEMS · Parallel mechanism · Multiple-arm · Multi-agent system · Neural networks Neuro-fuzzy

1 Introduction

A serious drawback of classical multilink lever manipulators is their lack of rigidity that complicates control of these manipulators, makes it difficult to use the high-energy process tool and to achieve high-precision processing. To a large extent these drawbacks can be overcome by trunk-type manipulators built on the basis of multi-section parallel mechanisms [1–6].

Yu.T. Kaganov · A.P. Karpenko (✉)
The Bauman Moscow State Technical University, Moscow, Russia
e-mail: apkarpenk@mail.ru

Yu.T. Kaganov
e-mail: yurijkaganov@gmail.com

A.E. Gorodetskiy and V.G. Kurbanov (eds.), *Smart Electromechanical Systems: The Central Nervous System*, Studies in Systems, Decision and Control 95,
DOI 10.1007/978-3-319-53327-8_14

Controlling a multi-section trunk-type manipulator (MTTM) is a complex task that consists of strategic, tactical and executive levels [7–10]. Manipulator target configuration is performed at the strategic level; synthesis of the transition path from the current state of the manipulator to the target state is performed at the tactical level; drives of the manipulator's sections are controlled at the executive level. In this paper we consider the executive level of controlling the MTTM.

Operation of multiagent control systems is based on the following principle: decomposition of the general control task to a number of local tasks; distribution of these tasks among agent control systems; planning of agent collective behavior; coordination of agents' interaction on the basis of cooperation.

The agent receives information from the external environment, as well as from the neighboring agents. In addition, it receives information from a higher level agent (coordinator). During operation, the agent affects the environment and learns. On the basis of the interaction among the agents, each agent develops trade-off decisions which are stored by both the agent and the coordinator.

We consider the multiagent approach to the MTTM control system synthesis that uses adaptive methods of neural network and neurofuzzy control.

A MTTM can be built on the basis of parallel-kinematics mechanisms with two, three, four and six degrees of freedom [5–7]. As an example, in this paper we consider a manipulator whose sections are tripods—parallel mechanisms with two rotational degrees of freedom [5, 6].

2 Structure of the Multiagent MTTM Control System

In the multiagent MTTM control system [11–13] we consider each agent consider as an intelligent mechatronic object which has its own knowledge base and is able to adapt to changing operating conditions in an environment with obstacles. The general schematic diagram of the multiagent MTTM control system is shown in Fig. 1 [8, 14].

We believe that control is performed by the position of the MTTM gripper. With minor changes, the presented model of the control system can be used to control other MTTM phase variables (speed, acceleration).

The agent i determines the position $r_{i-1}(t)$ of the base platform of the corresponding MTTM section, calculates the position $r_i(t)$ of the controlled platform, calculates the error $e_i(t) = r_i^0(t) - r_i(t)$ for this platform, generates control signals $F_{ij}(t)$ for the drives of the corresponding actuators. Herein, $r_i^0(t)$ is the vector of required positions of the i-platform [4, 5].

The structure of one of the lower-level agents is shown in Fig. 2 where, for simplicity sake, it is assumed that the MTTM is based on tripods: $L1$, $L2$, $L3$ are actuators of the MTTM section under review.

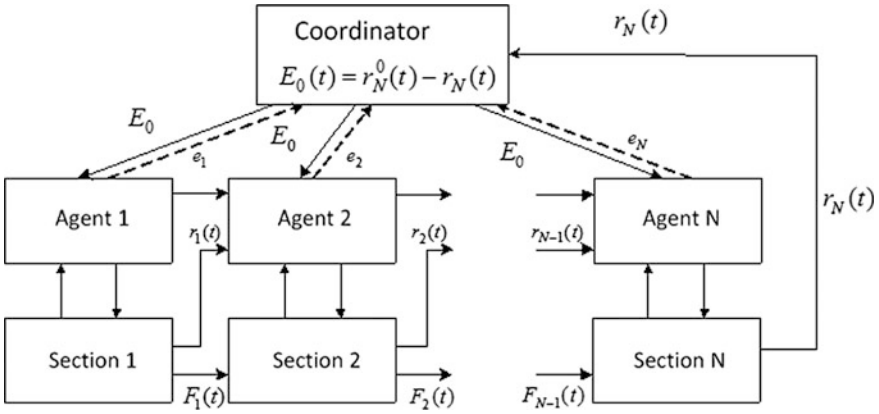

Fig. 1 Structure of multiagent control system for MTTM

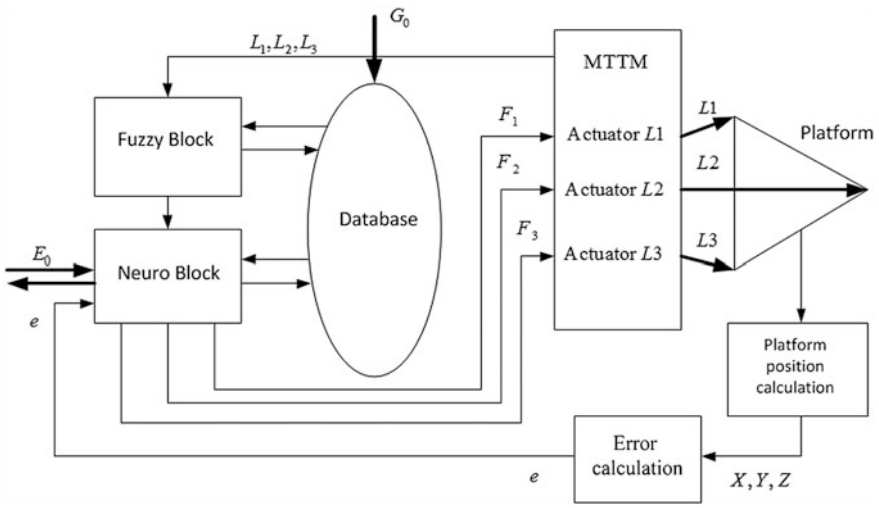

Fig. 2 Structure of the lower-level agent (tripod-based MTTM): X, Y, Z are geometric coordinates of the platform in the inertial coordinate system

The agent's fuzzy inference unit performs the following functions: converting displacements of actuators $L1$, $L2$, $L3$ of "their own" platform into fuzzy variables with corresponding values of membership functions (fuzzification); fuzzy *modus ponens* based on Mamdani-Larsen and Takagi-Sugeno fuzzy models (fuzzy inference); calculation of accurate values of variables by means of the centroid method (defuzzification) [14–17].

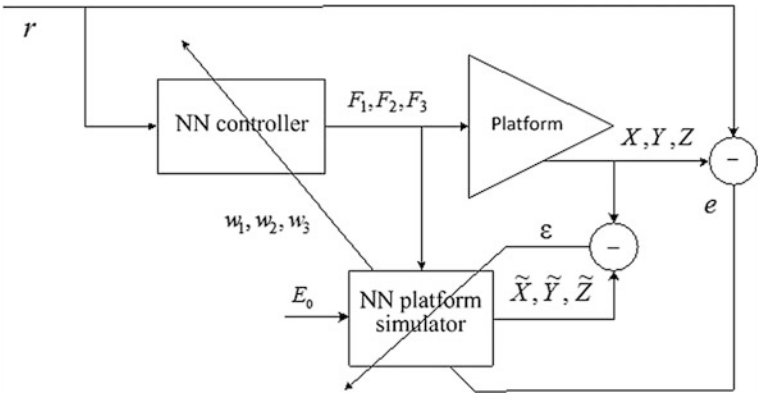

Fig. 3 Neural network structure

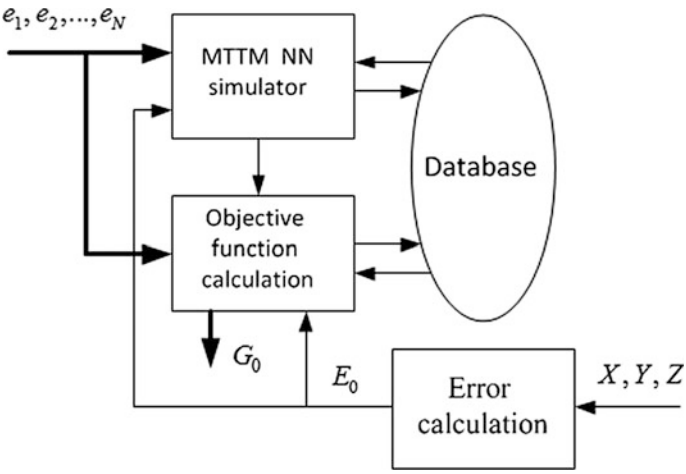

Fig. 4 Coordinator structure

Neural network agent unit (Fig. 3) teaches the emulator of "its own" platform, that is, it forms weight coefficients w_1, w_2, w_3; generates signals F_1, F_2, F_3 that control the corresponding actuator. At that, both the local error e and the global error E_0 are taken into account.

The coordinator (Fig. 4) forms the error vector $E_0(t) = r_N^0(t) - r_N(t)$, and on this basis it solves the problem of multipurpose optimal control of the MMTT with the vector-valued global objective functional $G_0(E_0(t)) = G_0(t)$ (time of processing of the reference trajectory, energy cost, etc.).

The learning process of the multiagent system is based on the SARSA strategy of reinforcement learning [18].

3 Lower-Level Neural Network Adaptive Agent

The tripod's actuator (actuating link) is considered as a direct current (DC) motor in combination with a screw gear which converts rotational motion of the electric motor shaft into linear motion of the tripod rod.

The block diagram of the neural network adaptive automatic control system (ACS) of one of the tripod's rods is shown in Fig. 5. The controller is based on the neural network inverse model of the control object, and another multilayer neural network is used as a reference model. In essence, learning objectives of both neural networks are neural network identification problems of corresponding dynamic systems.

We use multilayer NARX neural networks as reference and inverse models [15, 17].

The inverse model is a reverse model of the control object together with the actuating link [14, 15, 19]. The model was obtained at step input actions of various amplitudes and has the form shown in Fig. 6. The corresponding neural network inverse model obtained using the *Neural Network Toolbox* module is shown in the same Figure. Figure 6 shows high accuracy of the inverse model's neural network approximation—the approximation error does not exceed 0.5%.

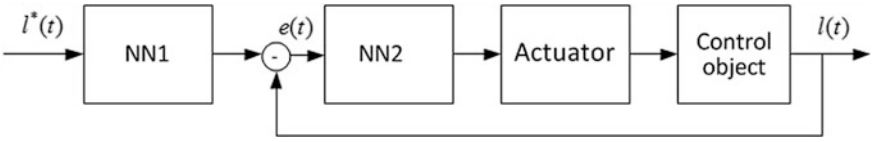

Fig. 5 Structure of the neural network adaptive ACS: NN1, NN2 are the neural networks of the reference and inverse models, respectively

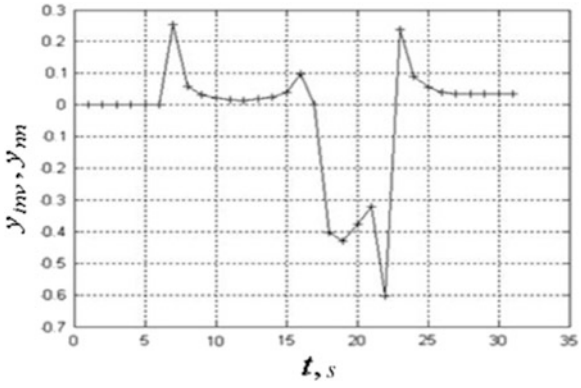

Fig. 6 Inverse characteristic of the control object and the actuating link $y_{inv}(t)$ (*solid line*) and its neural network approximation $y_{nn}(t)$ (*crosses*)

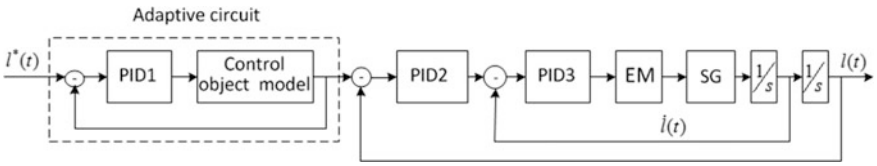

Fig. 7 Structure of the classical adaptive ACS: *EM* electric motor; *SG* screw gear

Alongside with this, we consider the adaptive ACS based on classic controllers (Fig. 7). The system has three loops—an adaptive loop, a displacement loop and velocity loop. The adaptive loop is based on the linearized mathematical model of the tripod (reference model), and the PID controller. The output of the adaptive loop is the reference, which eliminates identification of the control object in real time.

By $K_i = (k_{i,P}, k_{i,I}, k_{i,D})$, we indicate the coefficient vector of the PID controller which controls the length of the rod l_i; $i = 1, 3$, where $k_{i,P}$, $k_{i,I}$, $k_{i,D}$ are coefficients of the proportional, integral and differential components of the controller, respectively. The value $e(t)$ is used as the control error—the output deviation of the control object $l_i(t)$ from the output of the reference model $l_i^M(t)$ is as follows:

$$e_i(t) = \left| l_i(t) - l_i^M(t) \right|; \quad i = 1, 3$$

The problem of adaptive control of the length of the rod l_i is selection, in the process of operation of the control system, of such values of the coefficients $K_i = K_i(t)$ that provide the minimum value of the error $e_i(t)$.

4 Computing Experiment

Transients in the adaptive ACS received via its *Simulink*-model are shown in Fig. 8 [19].

The moment $T_{вн} = 5$ Нм applied at the time $t = 0.5$ s to the motor shaft is considered as the disturbance torque. Comparison of these transients with corresponding processes in the non-adaptive classical ACS shows that high-frequency oscillations are not present in the adaptive ACS. When the same transition time, the overshoot magnitude in the adaptive ACS is significantly smaller (about 1%). On the whole, our research suggests that the classical adaptive ACS is less sensitive to changes in the parameters of the control object compared to a similar non-adaptive ACS.

Transients in the adaptive neural network ACS received via its *Simulink*-model are presented in Fig. 9. Similar processes in this ACS in a situation where the centrally-axial symmetry of the platform is disturbed is shown in Fig. 10. It is understood that the platform's inertia tensor is set by the asymmetric matrix

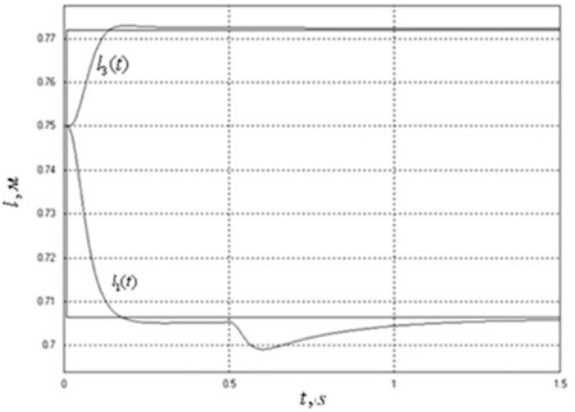

Fig. 8 Transients in classical adaptive ACS: at the time $t = 0.5$ s external disturbance torque is applied

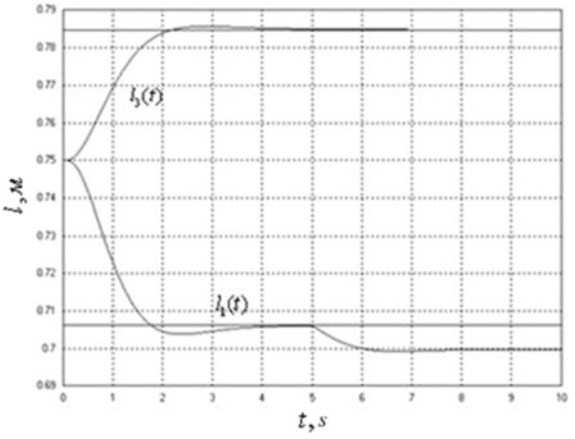

Fig. 9 Transients in the adaptive neural network ACS: external disturbance torque is applied at the time $t = 0.5$ s

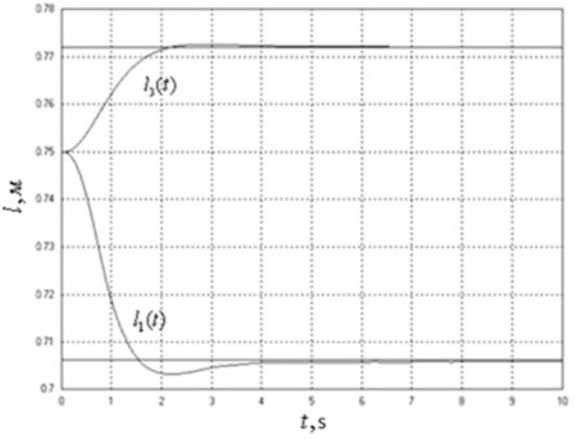

Fig. 10 Transients in the adaptive neural network ACS: disturbance of the centrally-axial symmetry of the platform occurs

$$\begin{matrix} 1.8 & 0 & 0.8 \\ 0 & 1.8 & 0 \\ 0.6 & 0 & 3.6 \end{matrix}$$

We also performed similar studies for the classical non-adaptive ACS. It is important that in the adaptive neural network ACS, as opposed to the classical non-adaptive system, static control errors do not occur.

5 Conclusion

In this paper a multiagent approach to control the multi-section trunk-type manipulator (MTTM) is considered. We propose a general structure of the multi-agent control system for the MTTM, which includes mathematical models of the manipulator sections, agents that control movements of each of the sections, as well as a coordinator that forms a global objective function for multicriteria optimization of the manipulator's evolutions.

Lower-level agents, each of which controls its "own" MTTM section, include a fuzzy inference unit, a neural network controller unit and an emulator unit.

The coordinator (the upper-level agent) generates control actions for lower level agents so as to provide multipurpose optimal control of the MTTM as a whole. The coordinator uses the MTTM neural network emulator.

We consider an example of implementation of the elements of the proposed multiagent system of controlling MTTM whose sections are parallel tripod-type mechanisms.

The results of the computing experiment presented in this work show that using the adaptive neural network automatic control system (ACS) as a lower-level agent is very promising.

In development of the work it is expected to consider the possibility of increasing control quality through the use of neuro-fuzzy ACS, to investigate ACS effectiveness when taking into account stochastic errors in measurement channels, as well as when taking into account stochastic external actions on MTTM platforms.

References

1. Merlet, J.P.: Parallel Robots (Solid Mechanics and Its Applications), 2nd edn., 416 p. Springer, Berlin (2006)
2. Kong, X., Gosselin, C.: Type Synthesis of Parallel Mechanisms, 274 p. Springer, Berlin (2007)
3. Glazunov, V.A., Koliskor, A.Sh., Krainev, A.F.: Spatial parallel structure mechanisms, 95 p. M.: Nauka, Moscow (1991)

4. Kheilo, S.V., Glazunov V.A., Palochkin, S.V.: Manipulation Mechanisms of Parallel Structure. Structural Synthesis. Kinematic and Force Analysis, 153 p. M.: FGOUVPO "MSTU by name A. N. Kosygina" (2011)
5. Kaganov, Yu.T. Mathematical Modeling of Kinematics and Dynamics of Robot Manipulator of Type "Trunk". Kaganov, Yu.T, Karpenko, A.P.: 1. Mathematical Models of the Manipulator Section as a Mechanism of Parallel Kinematics of the "Tripod". Science and education: electronic scientific and technical journal (2009), no. 10. [Electronic resource] (http://technomag.edu.ru/doc/133262.html)
6. Kaganov, Yu.T.: Mathematical Modeling of Kinematics and Dynamics of Robot Manipulator of Type "Trunk". Kaganov, Yu.T., Karpenko, A.P.: 2. Mathematical Models of the Manipulator Section as a Mechanism of Parallel Kinematics Type "Hexapod". Science and education: electronic scientific and technical journal (2009), no. 11. [Electronic resource] (http://technomag.edu.ru/doc/133731.html)
7. Karpenko, A.P.: Modeling and Optimization of Some Parallel Mechanisms. Karpenko, A.P., Kaganov, Yu.T., Volkomorov S.V.: Information Technology. App, vol. 5, pp. 1–32 (2010)
8. Mesarović, M., Mako, D., Takahara, Y.: Theory of Hierarchical Multilevel Systems, 294 p. Academic, New York (1970)
9. Ferguson, I.A.: Integrated Control and Coordinated Behavior: A case for Agent Models. Ferguson, I.A.: Proceedings of the ECAI-94 Workshop on Agent Theories, Architecture and Languages, pp. 203–218. Springer, Amsterdam, The Netherlands, 8–9 Aug 1994
10. Zenkevich, S.L., Yushchenko, A.S.: Foundation of Control of Manipulation Robots, 480 p. M.: MSTU by name N. E. Bauman (2004)
11. Shoham, Y., Leyton-Brown, K.: Multiagent Systems: Algorithmic, Game-Theoretic, and Logical Foundations, 532 p. Cambridge University Press, Cambridge (2008)
12. Wooldridge, M.: An Introduction to Multiagent Systems, 2nd edn., 365 p. Wiley, New York (2009)
13. Karl, T, Weiss, G.: Multiagent Learning: Basics, Challenges, and Prospects. Association for the Advancement of Artificial Intelligence, pp. 41–53 (2012)
14. Pupkov, K.A., Egupov, N.D.: Methods of robust, neuro and adaptive control, 744 p. M.: Publishing House: MSTU by name N. E. Bauman (2002)
15. Omatu, S., Khalid, M., Yusof, R.: Neuro-Control and Its Applications, 256 p. Springer-Verlag London Limited, London (1996)
16. Piegat, A.: Fuzzy Modeling and Control, 728 p. Physica-Verlag, Heidelberg (2001)
17. Shtovba, S.D.: Design of fuzzy systems by means of MATLAB, 288 p. M.: Hot line, Telecom (2007)
18. Satton, R.S., Barto, A.G.: Reinforcement Learning: An Introduction, 2nd edn., 334 p., in progress. The MIT Press, Cambridge (2012)
19. Buyankin, V.M.: Fuzzy control of neurocontroller for current and speed contours of the electric device. Buyankin, V.M., Pantjuhin, D.V.: Neurocomputers: Development and Application, No. 7, pp. 50–54 (2009)

Self-learning Neural Network Control System for Physical Model with One Degree of Freedom of System of Active Vibration Isolation and Pointing of Payload Spacecraft

S.N. Sayapin, Yu.N. Artemenko and S.V. Panteleev

Abstract *Purpose* The area of biomimetic robots is successfully developing in intelligent robotics using SEMS and Neurotechnology. These robots are based on the borrowing its core elements from nature and able to adapt to the environment of the real world and to be truly intelligent autonomous robotic devices. For example, the neural network control system are used in intelligent robots, capable of self-learning like brain. Overall, the self-learning neural network control system have a structure similar central and peripheral nervous systems of vertebrates and man. The aim of the publication is the description of the developed model of the self-learning neural network control of a single-stage physical model of intelligence system of active vibration protection and very precise pointing of large precision space antennas. *Results* Model of the self-learning neural network control system of a single-stage physical model of intelligence system of active vibration protection and very precise pointing of the payload of the spacecraft is developed and tested. The advantages of application of neural PID controller are shown compared with conventional PID controller. *Practical value* The presented in the article the self-learning neural network control system of a single-stage physical model can be used to create autonomous intelligent robotic system capable to react to changing uncertain conditions in real time outside the operator's actions, for example in deep space.

S.N. Sayapin (✉)
The Blagonravov Institute for Machine Science of the Russian Academy of Sciences, The Bauman Moscow State Technical University, Moscow, Russia
e-mail: S.Sayapin@rambler.ru

Yu.N. Artemenko
The Astro Space Center of P. N., Lebedev Physical Institute, Russian Academy of Sciences, Moscow, Russia
e-mail: Artemenko.AKC@yandex.ru

S.V. Panteleev
The Vyksa Branch, N. E., Alekseev Nizhny Novgorod State Technical University, Moscow, Russia
e-mail: ser-panteleev@yandex.ru

A.E. Gorodetskiy and V.G. Kurbanov (eds.), *Smart Electromechanical Systems: The Central Nervous System*, Studies in Systems, Decision and Control 95,
DOI 10.1007/978-3-319-53327-8_15

Keywords Intelligent robotics-based SEMS · Biomimetic robots · The nervous system of a human and a robot · The active vibration isolation · Precision pointing payload · An active intelligent structure · Artificial neural networks · The self-learning neural network control system · Neural PID controller

1 Introduction

Currently work is underway in Russia with the participation of some other countries to create the orbital space Observatory Millimetron precision space telescope (ST) with a diameter of 10 m in the vicinity of the Lagrange point L2. As a result ST in conjunction with the largest radio telescopes in the world forms an interferometer with superlong basis. It is planned to create multi-element interferometer space-based, including a group ST (Fig. 1). Moreover, ST will exchange information with not only the Earth but also each other. To ensure the precision of large elastic structures of ST at orbit it will be necessary to create systems of vibration protection from external and internal microdynamics effects and high-precision pointing on the studied objects in real time. Given the enormous distance from the Earth, such systems should be intelligent and capable of long-term and autonomous to function in extreme conditions [1, 2].

The area of biomimetic robots using neurotechnology is successfully developing in intelligent robotics. These robots are based on the borrowing own core elements from nature and able to adapt to the environment of the real world and to be truly autonomous robotic devices [3, 4]. In this regard, the functional and organizational

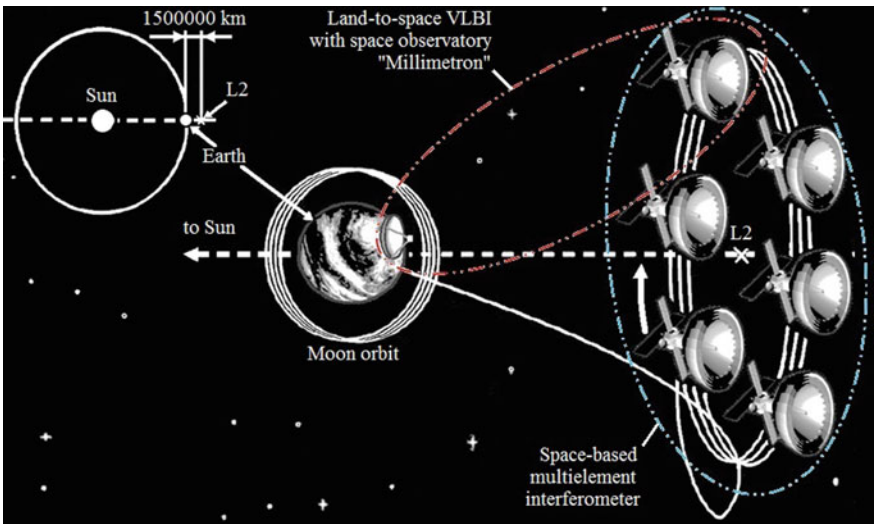

Fig. 1 Multi-element interferometer

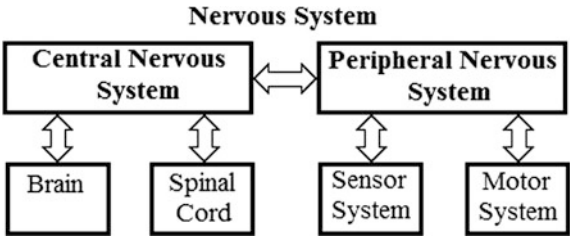

Fig. 2 Nervous system

principles of biological systems are actively used at construction of self-learning intelligent control systems for autonomous robots based on the nervous system of vertebrates and man [4–6]. A high-level functional diagram of the nervous system of vertebrates that consists of the central and peripheral nervous systems is shown in Fig. 2 [7].

Central nervous system (CNS) includes brain and spinal cord and serves as a link between the sensors (sensory receptors) and motor (effectors, muscles, etc.) of peripheral nervous system (PNS). The CNS performs the following basic functions: sensory, integration and the solution (computation), and motor (action). The human brain is responsible for the following main functions of the functioning of the body: the regulation of homeostasis and coordination; reception, integration and processing of sensory information; the neural processing and integration of information; image processing; short-term and long-term memory; learning ability; making decision and development of motor commands [7]. The main function of the spinal cord—reflex and conductive. Through the reflex activities are carried out in simple motor reflexes (flexion, extension, etc.). Conductive feature is impulses which transmitted from receptors of skin, muscles and internal organs and from the brain to the spinal cord, then to the periphery to the organs by the conducting pathways of the spinal cord to the brain. The activities of the spinal cord is under the control of the brain that regulates spinal reflexes.

The PNS consists of sensory and motor systems (Fig. 2). In the sensory system sensory neurons transmit information from internal and external environment to the CNS, and motor neurons carry information from brain or spinal cord to nerve endings. Motor system feeds signals (commands) from the CNS to muscles (effectors) and glands.

As indicated above, one of the functional features of the brain is its ability to self-education. The use of this ability in intelligent robotic systems will allow them to function in a changing uncertain conditions outside the operator's actions, for example in deep space. Thus, the development of self-learning control systems, capable of providing autonomous operation of intelligent robotic systems in real time is an urgent task. Below it is a description of self-learning neural network control (SLNNC) for physical model with one degree of freedom of intelligence system of active vibration isolation and pointing (ISAVIP) of precision payload spacecraft (PPS) in real time.

2 Overview of Intelligent Management

The modern period of development of control theory is characterized by the formulation and solution of tasks, taking into account the imprecision of our knowledge about the object or external disturbances acting on them. The developed algorithms should be robust under any perturbation. The notion of uncertainty in the system plays an essential role in the formulation and solution of such problems. Traditional control methods are mainly based on the theory of linear systems, while real objects of control is inherently nonlinear. Ordinary computers have to be pre-programmed to be able to process the data; they cannot operate outside of solutions specified by the program. Thus, knowledge of engineering can not be fully implemented on conventional computers since they are unable to make decisions in new environments. Therefore, the optimal control under conditions of uncertainty and limited observability, which should function ISAVIP PPS requires introduction to management elements of artificial intelligence. Moreover, the requirement in terms of processing spatial information in real-time necessitates a parallel data processing on the basis of neuroprocessor and modern means of formation and use of knowledge base [1]. Intelligent control systems (ICS) have the ability for understanding and learning in relation to the object of control, disturbances, external environment, work conditions. The learner is the most important property of ISU. The basis of the current IMS are neural network technology. Characteristic property of the neural network (NN) is a self—organization learning ability. This means that NN can autonomously "learn" the statistical and dynamic properties of the controlled object on the basis of the results of measurements made in the past, and then to act in such a way as to make the best decision for the unknown state of the environment. According to [8] there are four approaches to the study NN:

1. **The psychological approach**, when psychological paradigm was modeled, which is constructed and studied some of the NN structure.
2. **Neurophysiological approach** is constructed and studied NN based on the knowledge about the structure of some section of the brain, simulating the features of this section of the brain. Examples include models of neurons McCulloch and Pitts (1943) that implement the operations AND, OR, NOT and MEMORY (Fig. 3) [9]. These model neurons are strikingly repeat the scheme of the mechanism of formation of conditioned reflex, proposed by Pavlov (1908–1909) [10] (Fig. 4) and are widely used at present [8, 9].

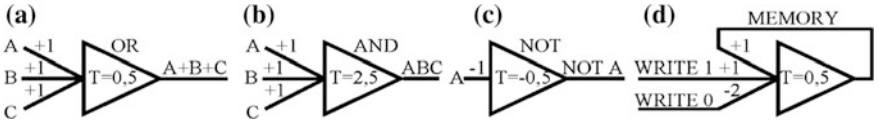

Fig. 3 OR, AND, NOT, and MEMORY operations using networks with McCullon-Pitts neuron model

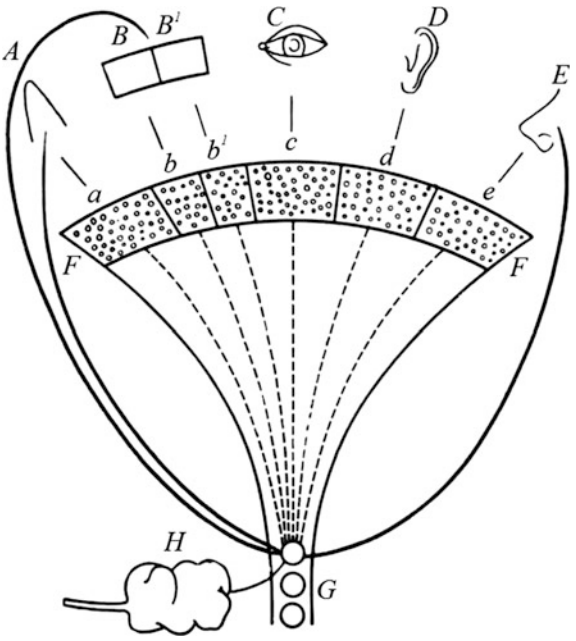

Fig. 4 Scheme of the mechanism of formation of conditioned reflex, proposed by I.P. Pavlov (1908–1909). *A*—tongue; *B*—the skin (tactile stimulation); B^1—skin (primary irritation); *C*—eye; *D*—ear; *E*—nose; *FF*—cortex; *G*—medulla oblongata; *H*—the salivary gland. Cortical receptive language centres (*a*), skin (tactile irritation, *b*), skin (thermal irritation, b^1), eye (*c*) ear (*d*) nose (*e*)

3. **An algorithmic approach**, when a math problem is done and an adequate NS and its algorithms settings for this task were constructed, based on this statement.
4. **A systematic approach** that combines these approaches.

The problem of identification of transfer function of object of management to ensure more effective compensation raises in the development of active vibration isolation systems using neural network technologies. In this case, NN can be implemented according to the scheme with training in real time (neuroadaptive), and the pre-trained NN.

NN is a network with a finite number of layers of homogeneous elements—analogues of neurons with different types of connections between layers. The main advantages of NN are the invariance of methods of synthesis of the NN to the dimension of the feature space and the size of the NN, the adequacy of modern technologies and fault tolerance.

The main advantages of neural computers (NC) are associated with massively parallel processing. The result is high speed, low requirements for stability and accuracy of the parameters of the elementary nodes, resistance to interference and destruction. Due to its advantages NC are an effective means of implementing the systems of active vibration protection. Objects of the synthesis of such systems are not only neural control, but the method of placement of sensors and actuators on the subject of active vibration protection.

3 Description SLNNC for Physical Model with One Degree of Freedom of ISAVIP of PPS

In [11] introduced the concept of ISAVIP of PPS, capable of functioning autonomously in real-time. In Fig. 5 shows a block diagram of ISAVIP of PPS. The PPS, for example the ST, including the deployable primary mirror 1 with heat shields 2, the support system 3, the secondary mirror 4 and star trackers 5. The ST is mounted on the module of service systems (MSS) 6 with the solar panels 7 and the high-quality radio complex 8 using active transient farm (ATF) 9, made in the form of a spatial parallel structure mechanisms [12]. The platform 10 is pivotally connected with the base 11 by means of suspension with 6-DOF, in the form of a spatial manipulator (ATF 9) including at least six identical unit individual active vibration isolation modules (IAVIM) 12. IAVIM 12 provide the ATF 9 6-DOF in working condition and a geometric resistance in the off state [1, 2, 11, 13–17].

Each of IAVIM 12 is provided with a linear actuator, sensors of the spatial position and accelerations 13 and 14, respectively, and relative displacement and velocity sensors 25. In ISAVIP of PPS also received information from star trackers 5 and outside the APF 9 combined sensors positions and accelerations 15, 16 and 17 mounted on the extended elastic elements of ST and MSS 6 (heat shields 2, the heat sinks 30 of the cooling system of ST, solar panel 7). This allows you to forward information about microdynamics perturbations and organize the advanced management of ISAVIP of PPS [1]. While ATF 9 in advance translates to a position most advantageous for the parry occurs microdynamics disturbances.

Structure ISAVIP of PPS built like the nervous system of vertebrates, shown in Fig. 2. Here CNS of ISAVIP made in the form of On-board High-Performance Information Measuring and Control System (OBHPIMCS) 18. OBHPIMCS 18 includes a neurocomputer 19 with the corresponding means of software 20 and digital/analog converters (DAC) 21. PNC of ISAVIP includes sensors 5, 13–17, 25 with the respective analog-to-digital converters 22–24, power amplifiers 26 and executive elements (IAVIM 12 and the slewing drives 27 of the solar panels 7). The structure of the PNC of ISAVIP also includes a system ensuring functioning ISAVIP, such as power system, thermal control, etc. (in Fig. 3 not shown). In the process of operation of ST is a continuous processing of vector information from the sensors. Based on the analysis of this information in OBHPIMCS 18 are formed in real-time control commands, which are served on executive elements. Through the high-quality radio complex 8 and radio link 28 neurocomputer 19 may exchange information with the other ST (Fig. 1) or with ground-based radio system 29.

For testing of SLNNC of ISAVIP of PPS a single-stage physical model was used, depicted in Fig. 6 [1]. The design of the physical model made in the form of a rigid rocker arm with cylindrical hinges at the ends and in the middle part. One end of the lever is directly connected to the rigid base. The other end of the lever is connected with a rigid Foundation through perturbing the hydraulic cylinder. To the middle part of rocker arm via a compensating hydraulic cylinder articulated

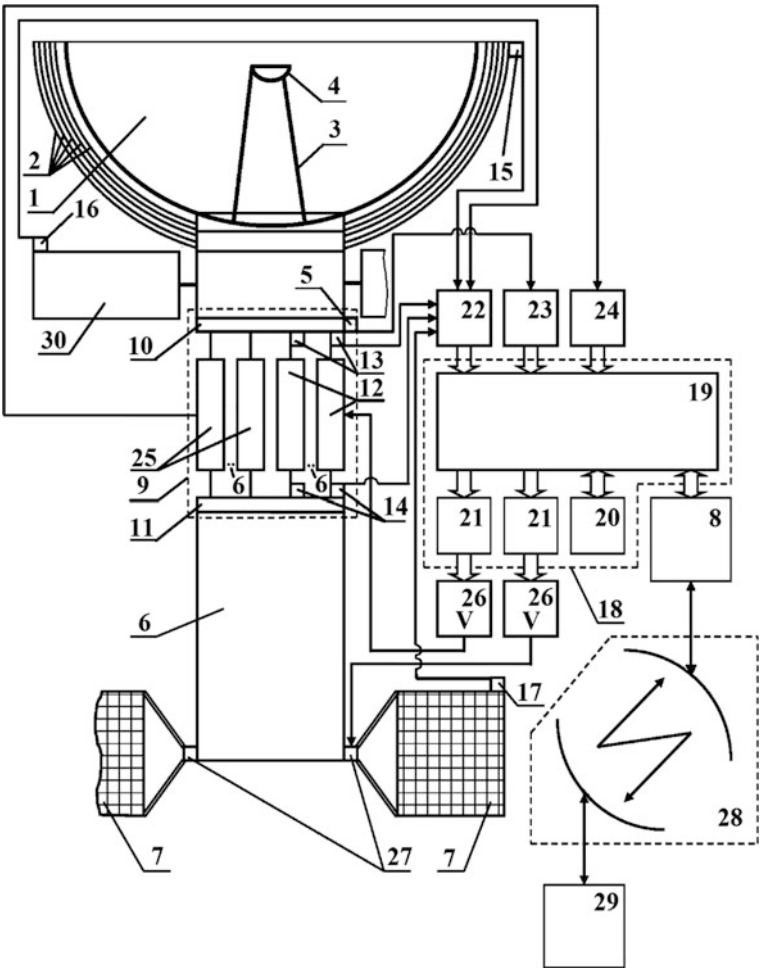

Fig. 5 Block diagram of ISAVIP of PPS

suspended cargo variable (0–50 kg). The control unit is implemented on a PC with the Board I/o signals of the firm LCARD. In the form of half-rings the load cells are shown, measuring the forces in the hydraulic cylinders. The hydraulic cylinders are equipped with electromechanical displacement sensors of the rod. The bench is equipped with a recording system efforts in the cylinders. Control of hydraulic cylinders was conducted on the frequency (up to f = 5 Hz) and the amplitude.

To obtain the mathematical model of the shake table will take the following assumptions:

- the extent of the deformation dependence of the reaction forces of rocker arm from the amount of deformation is linear;

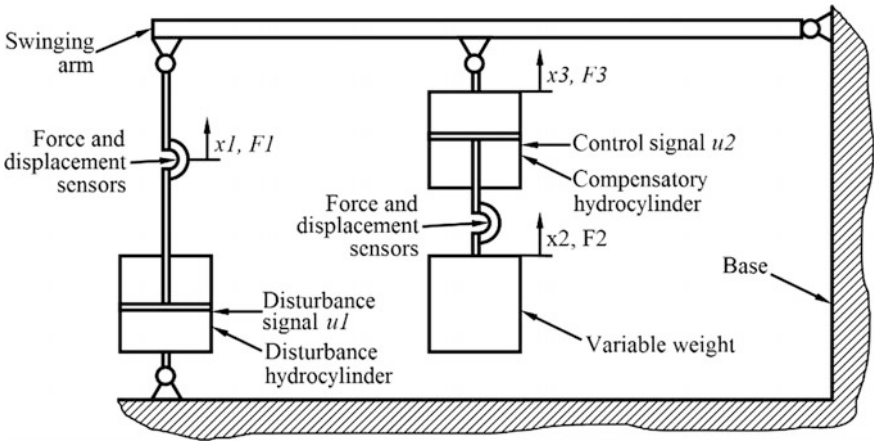

Fig. 6 Testing of SLNNC of ISAVIP of PPS a single-stage physical model

- zero position is taken position of the system without perturbation and control actions;
- losses from friction are not taken into account.

Denote the input, output and intermediate variables:

u_1 the stress applied to the input perturbation of the hydraulic cylinder;
u_2 the stress applied to the compensating cylinder;
x_1 the vertical offset of the left edge of the rocker arm;
x_2 vertical displacement of the load;
x_3 vertical displacement of the point of suspension of the compensating cylinder with a load;
F_1 the force acting on the oscillating arm from the perturbation of the hydraulic cylinder;
F_2 the force acting on the load;
F_3 the force acting on the oscillating arm from the compensating hydraulic cylinder with a load.

Weekend (observed) parameters:

$$y_1 = x_1;\ y_2 = F_1,\ y_3 = x_2,\ y_4 = F_2,\ y_5 = u_1,\ y_6 = u_2$$

We set up a system of differential equations in system of active vibration protection in operator form.

$$\begin{cases} F_2 = M \cdot x_2 \cdot s^2 \\ F_3 = F_2 + M_c \cdot x_3 \cdot s^2 \\ F_3 = c\left(\frac{x_1}{2} - x_3\right) \\ F_1 = 2 \cdot F_3 \\ x_1 = \frac{1}{k_1 \cdot s + k_2} u_1 \\ x_3 - x_2 = \frac{1}{k_1 \cdot s + k_2} u_2 \end{cases} \quad (1)$$

As received, the system (1) is not convenient for modeling, because it contains unobservable parameters and as well as there is no explicit dependency between input and output variables.

We transform the system (1) so that all control parameters were subject to input and have already received parameters:

$$\begin{cases} y_1 = x_1 = \frac{1}{k_1 \cdot s + k_2} u_1 \\ y_3 = x_2 = \frac{c}{2((M + M_c)s^2 + c)} x_1 - \frac{M_c \cdot s^2 + c}{(M + M_c)s^2 + c} \cdot \frac{1}{k_1 \cdot s + k_2} u_2 \\ y_4 = F_2 = M \cdot x_2 \cdot s^2 \\ y_2 = F_1 = 2 \cdot \left(F_2 + M_c \cdot s^2 \cdot (x_2 + \frac{1}{k_1 \cdot s + k_2} u_2)\right) \\ y_5 = u_1 \\ y_6 = u_2 \end{cases} \quad (2)$$

To verify the obtained model and simplification of the program experiments will build in the Matlab model according to the system of Eq. (2). The model has a hierarchical structure.

The appearance of the model at the top level is presented in Fig. 7.

At this level, the model consists of vibrostend model with two inputs (u1, u2) and six outputs (y1–y6) according to the system of Eq. (2), and six units of observation (y1–y6) connected to its outputs. Input action in the process of conducting experiments will vary according to the plan of experiments. To signal disturbances at the input of the model used unit asked source, the output of which is fed with an arbitrary function specified by the user.

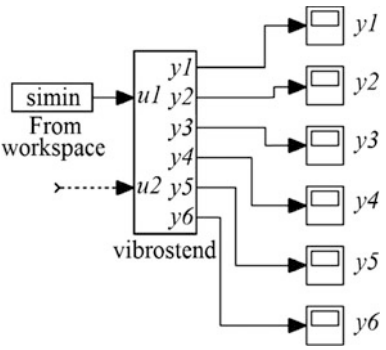

Fig. 7 Top level model of shaker

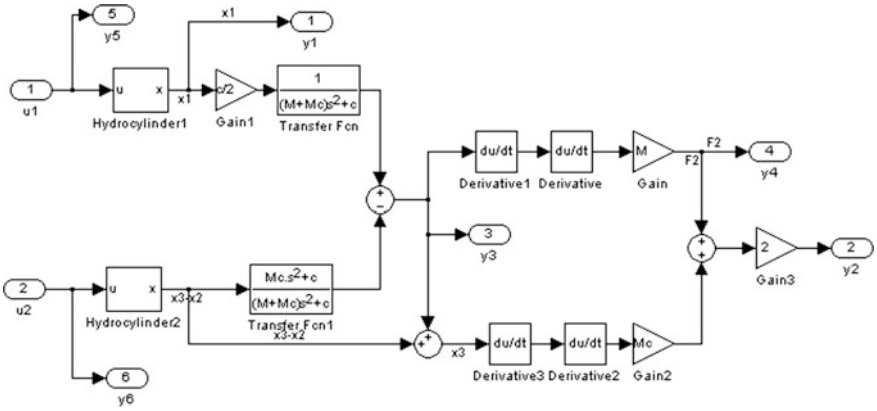

Fig. 8 The scheme of the shake table

The internal structure of the block vibrostend shown in Fig. 8. The block has two inputs (u1, u2) and six outputs (y1–y6). Since the inputs signals are the block model of the hydraulic cylinder (Hydrocylinder 1 and Hydrocylinder 2), the structure of which is described below, the received signals are converted using blocks with a given transfer function (Transfer Fcn) differentiating units (Derivative) proportional units (Gain).

In order to avoid complications (extended period simulation and error due to proliferation calculations) related to the cyclic connections, the unit has a unidirectional structure, i.e. it lacks feedback.

The structure of the block Hydrocylinder shown in Fig. 9. The block has one input (u), one output (x) and implements the transfer function: $x = [1/(k_1 \cdot s + k_2)]u$.

As a generator of disturbances in the model, we use the block set generator. The generated signal is specified by the "simin", which is a two-dimensional array with two columns, the first of which measured time and the second value of the signal generator at these points in time.

Network training hold for all perturbations according to the plan of the experiment, changing the value of the load mass of the object. In terms of experiments has a specified input signal as moving the left end of the beam (or cylinder rod of indignation). When it is implemented on the model, you must set the form and parameters of the control signal of the cylinder perturbations (voltage supplied to its input), as it is set directly in the experiment. So you need to get the disturbance in control signal. To solve the problem of control of a dynamic object is large the use of adaptive linear network, ADALINE. The task of the national Assembly is to form a model that in the process of learning determines the parameters of the object, and then uses them for simulation with arbitrary values of the entrance.

Settings of this network is performed offline using the method of group learning using data obtained when testing the real object.

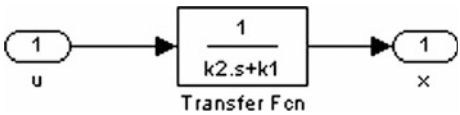

Fig. 9 Diagram of hydraulic cylinder

For nonlinear systems this approach for sufficiently small amplitudes, the input signal provides the linearization with minimal RMS error. If the nonlinear system moves to a different operating point, change the parameters of the neural network. To get the linearized model for a short time, the frequency of measurements should be high enough and the input of the nonlinear system must submit a test signal in the form of a random process of small amplitude. This will accelerate the adaptation of the network, as will be presented a larger number of measurements characterizing the dynamics of the system, for a short time interval. Accounting for non-linear systems of a larger number of delayed inputs allows to minimize the error in modeling nonlinear systems.

Thus, to solve this problem we choose two-layer NN. NN will train on the basis of the disturbing signal according to the experiment plan. NN is implemented in the software package MATLAB in the following way.

Input 1 NN signal move the load: P(1,:) = yout(:, 3).
Input 2 is connected to NN output NN network-emulator:

net.inputconnect = net1.Yout;

$$P(2,:) = Yout.net1.$$

Set the desired value signal of the load move: P(3,:) = 0.
Given the vectors of objectives: T(1,:) = q1; T(2,:) = q2; T(3,:) = q3.
The deviation of the input variable P(1,:) from the desired P(3,:) - e(:,1:Q) we define based on the current and previous two input values P:

$$Q = \text{size}(P);$$
$$e(1,1:Q) = \text{abs}[P(3,1:Q) - P(1,1:Q)];$$
$$e(2,1:Q) = \text{abs}[P(3,1:(Q - 1)) - P(1,1:(Q - 1))];$$
$$e(3,1:Q) = \text{abs}[P(3,1:(Q - 2)) - P(1,1:(Q - 2))].$$

Write the algorithm of functioning of PID controller:

$$P(1,1:Q) = P(1,1:(Q - 1)) + q1 * e(1,1:Q) + q2 * e(2,1:Q) + q3 * e(3,1:Q).$$

Form NN direct signal transmission with two layers, three neurons in the input layer with a tansig activation function, and three neurons at the output of the activation function purelin. The entrance of NN takes values from −5 to 5. As a training function trainrp use:

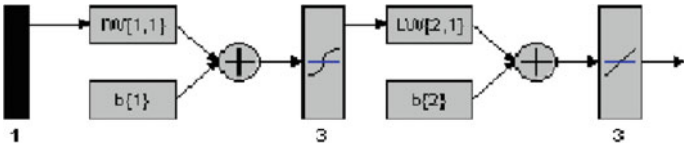

Fig. 10 Flow of NN

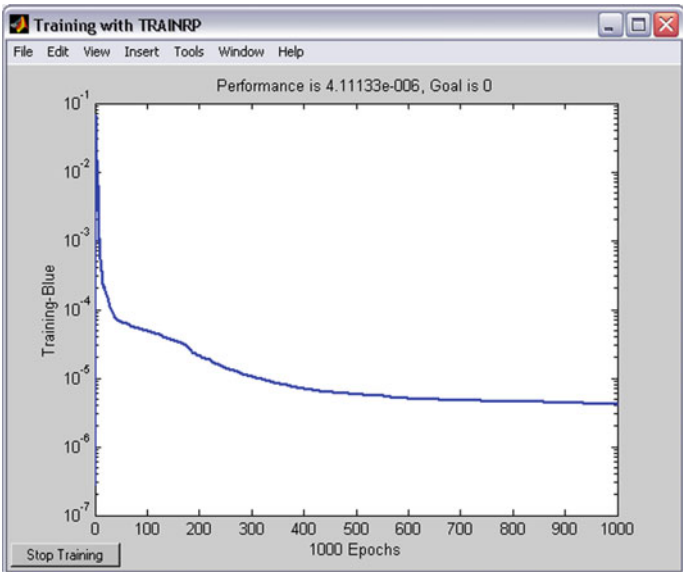

Fig. 11 Characteristic of the accuracy of learning of NN

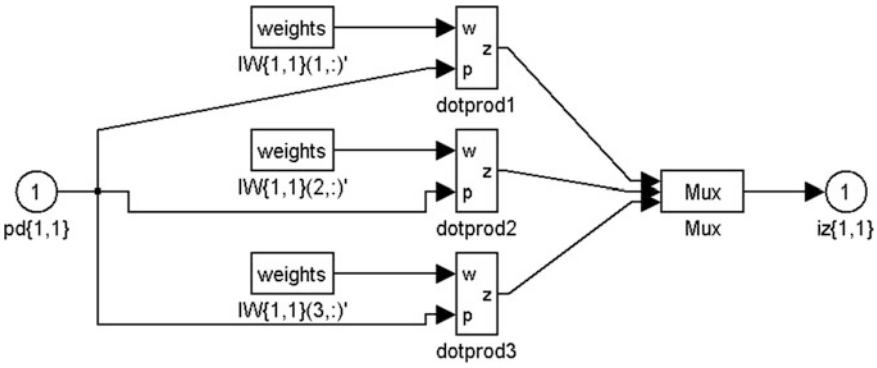

Fig. 12 Structure of the 1st layer of NN

net = newff([-5 5], [3 3],{'tansig','purelin'},'trainrp').
Produce a trained NN. The number of cycles – 1000:
net.trainParam.epochs = 1000;
net = train(net,P,T).

Figure 10 shows the NN and in Fig. 11 the characteristic precision of her studies. NN is trained for 1000 cycles, the learning error is $4.11133 * 10^{-6}$.

In Fig. 12 shows the structure of the 1st layer of NN, consisting of three neurons.

4 Analysis of Experimental Results

Consider one of the experiments the system response to the impact in the form of harmonic oscillations with a constant frequency. In the remaining experiments, the overall picture is the same.

In Fig. 13a blue color shows the displacement of the left edge of rocker arm (Fig. 6) and green—load depending on time. As can be seen from the graphs, the movement of goods is a proportional to the repetition move the left edge of the rocker arm with superimposed oscillation. The amplitude of displacements in the natural vibrations of relatively small amplitude displacements, forced vibration (forced oscillation of about 6 cm, own less than 1 cm).

However, the picture changes dramatically if we consider the acceleration of the load (Fig. 13b). On the chart acceleration, we can see two components of fluctuations of the cargo: a necessary (dotted line). The amplitude of the forced oscillations is 2 m/s^2, self −50 m/s^2.

Thus, the amplitude of oscillation to accelerate up to 25 times higher than the amplitude of forced vibration on acceleration. In the remaining experiments, the overall picture is the same: the main contribution to the acceleration of bring your own vibrations of the system the "swinging lever—a hydraulic cylinder with load".

Therefore, in the foreground in the regulation system on the criterion of minimizing the acceleration of the load is damping the natural oscillations of the system "swinging lever—a hydraulic cylinder with load".

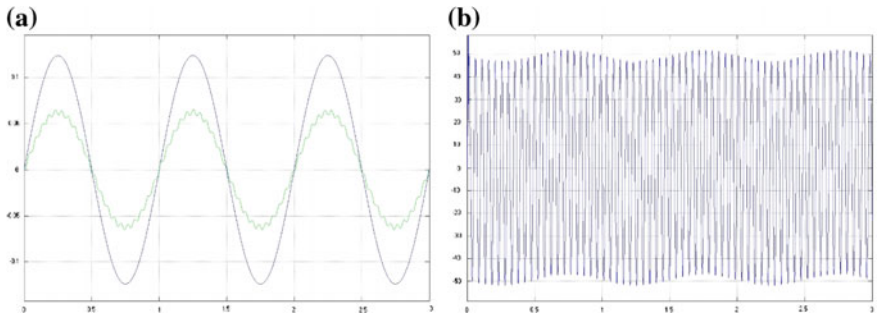

Fig. 13 **a** Moves and **b** the acceleration

5 The Operation of the System with PID Controller

Adding to the model of PID controller. To optimize system response to the disturbance in the system is the PID controller. The PID controller implements a transfer function $\frac{Ki + Kp \cdot s + Kd \cdot s^2}{s}$. Ki, Kp, and Kd (integral, proportional and differential coefficients, respectively) are the parameters of PID controller.

The scheme of inclusion of PID controller shown in Fig. 14.

The switching circuit also added two differentiating unit, a multiplexer to form vector signal, and two units of observation y7 and y8 to display the acceleration of the load and simultaneous display movement of the point of suspension and the left edge of the rocker arm.

The system uses a discrete PID controller discrete-time with small (1 mks) sampling period. The main advantages of this type of controller: the ability to work in conditions of sharp and significant changes, no need for initialization when switching from manual mode to automatic.

The choice of coefficients of PID controller. For a successful control system using PID-controller you need to set its coefficients. In classical control theory, the choice of coefficients is done by peer selection based on the evaluation of errors. In our case, the criterion of quality of operation of the control system is to minimize the acceleration of the load. Thus, it is necessary to select such coefficients of PID controller in which the maximum acceleration of the load during the occurrence of the transition process will be minimal.

For selection coefficients of PID controller will simulate the system behavior when a step input with zero impact factors. The control action in this case is shown in Fig. 15a. Here is shown the control signal for a given step impact.

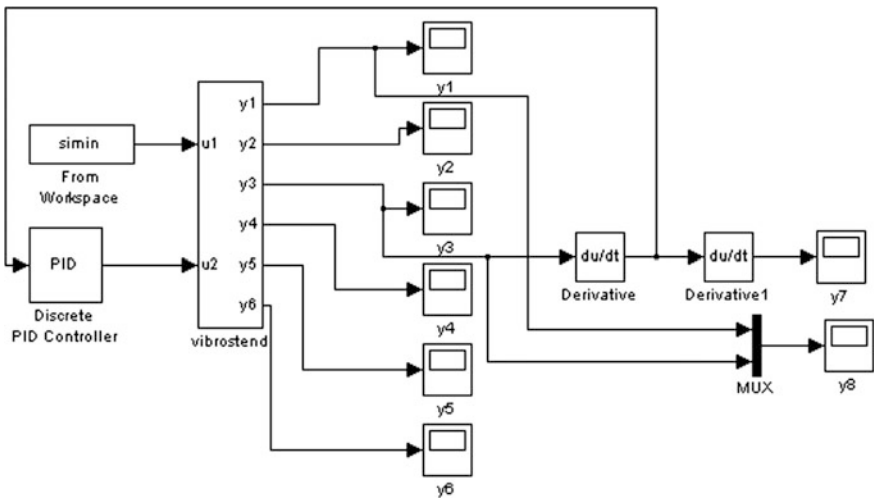

Fig. 14 The scheme of inclusion of PID controller

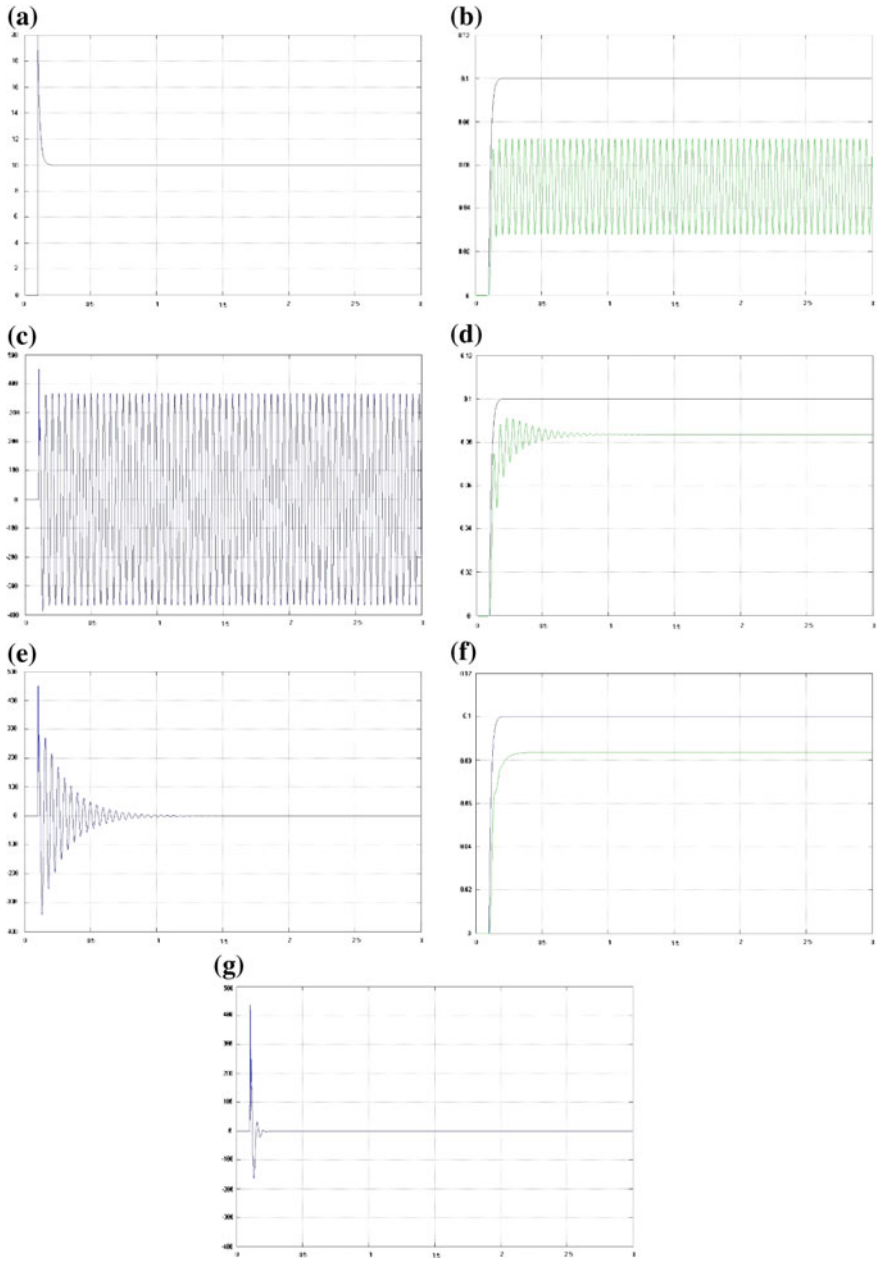

Fig. 15 Control signal for a given step impact

Moving the left cylinder rod of disturbance and load is shown in Fig. 15b. It depicts move with a step-perturbation and zero regulation. In Fig. 15b and further

in the graphs of the displacements in blue shows the movement of the left end of the rocker arm, green is the movement of cargo. As can be seen from Fig. 15b, the load rises under the influence of indignation and begins to vibrate at the natural frequency (about 22 Hz) with a rather large amplitude (about 1 cm). Due to the lack of a table of the elements, damping, damping is virtually nonexistent.

The acceleration of the load shown in Fig. 15c. This shows the acceleration of the load with a step-forcing and zero regulation. As can be seen from Fig. 15c, the load is experiencing a pretty significant acceleration (up to 50 g).

Change the coefficient Ki for reducing the acceleration. The optimal reaction gives a value of Ki = −40. Displacement and acceleration are shown in Fig. 15d, f. In Fig. 15d shows the displacement for a given step impact (Ki = −40). In Fig. 15f shows the acceleration of the load with a step-like effect (Ki = −40). As can be seen from Fig. 15d, f, if such regulation appears attenuation (in e times over a period of about 0.5 s.). However, the ejection of the acceleration remains large.

Change the coefficient Kd on the best −0.015. The response of the system shown in Fig. 15g, h. Here in Fig. 15g shows the displacement, while Fig. 15h to accelerate, with a step-like effect (Ki = −40, Kd = 0.015).

As can be seen from the drawings, the damping is increased even more (time of vibration is approximately equal to the time of the establishment of the position of the left edge of the rocker arm). However, the ejection acceleration remains.

Any change of the coefficient Kp leads to system instability. So leave it to 0.

6 Experiments with Neural Network PID Controller

The structure of neuropil control. As shown above, the choice of coefficients of PID controller is a typical task and very subjective, depending on the experience and qualifications of the developer. Application NS for the regulation of ratios allows virtually nullify subjective factors in real time to make the appropriate adjustments.

Analysis of the results of experiments with neural network PID controller. Let us consider one of the most typical cases—the harmonic impact of constant frequency with added noise of low intensity. As the regulator was used that was developed, neural network PID controller.

Figure 16a presents a graph of the displacement of the left edge of the rocker arm (blue line) and load (green graph) from time to time. Figure 16b presents the graph of the acceleration of the load from time to time.

From Fig. 16a shows that after the introduction of the controller the movement of goods in proportion repeats moving the left edge of the rocker arm. Self-oscillations on the graph are missing.

If we consider the acceleration of the load, then from the graph in Fig. 16b shows that after a short transient process, established forced oscillations with the amplitude of the acceleration around 4 m/s^2. This is 12.5 times less than the amplitude of the vibrations that occur when managing a stand of conventional PID

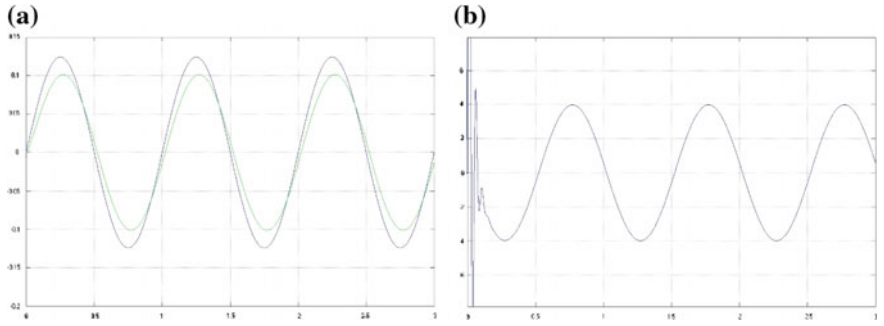

Fig. 16 Displacement of the left edge of the rocker arm

controller with experimentally selected fixed odds. Thus, the introduction of neural network PID controller reduced the amplitude of the accelerations of the cargo in 15–20 times.

7 Conclusion

The choice of coefficients of PID controller is very atypical and subjective task and depends on the experience and qualifications of the developer. Application NN for adjusting the coefficients allows to eliminate the subjective factors in real time to make the appropriate adjustments.

Strong nonlinearity of the system confirms the rationale of applying self-learning neural network control.

The introduction of neural network PID controller reduced the amplitude of the accelerations of the cargo in 15–20 times.

References

1. Sayapin, S.N.: Analysis and synthesis of flexible spaceborne precision large mechanisms and designs of space radio telescopes of the petal type. Doctor Technical Science Dissertation, M.: IMash RAN, Moscow (2003) (in Russian)
2. Sayapin, S.N., Artemenko, Y.N., Myshonkova, N.V.: High precision problems of observatory "MILLIMETRON" cryogenic space telescope. Nat. Sci. **2**(53), 50–76 (2014) (Vestnik MGTU, in Russian)
3. Ayers, J., Davis, J., Rudolph, A.J.: Neurotechnology for Biomimetic Robots. MIT Press, Cambridge (2002)
4. Westphal, A., Rulkov, N.F., Ayers, J., Brady, D., Hunt, M.: Controlling a lamprey-based robot with an electronic nervous system. Smart Struct. Sys. **8**(1), 39–52 (2011)
5. Berna-Martinez, J.V., Macia-Perez, F.: Robotic control based on the human nervous system. Int. J. Artif. Intell. Appl. (IJAIA) **2**(4), 107–121 (2011)

6. Bar-Cohen Y. (ed.): Biomimetics: Nature-Based Innovation, pp. 477–523. Taylor & Francis Group, London (2012)
7. Lyshevski S.E.: Nano-and micro-electromechanical systems: fundamentals of nano-and microengineering, 2nd ed., pp. 61–63. CRC Press, New York (2005)
8. Galushkin, A.I.: Theory of Neural Networks. IPRZHR, Moscow (2000) (in Russian)
9. Wilamowski, B.M.: Neural networks and fuzzy systems, chapter 32 of section iv "systems and control. In: Bishop, R.H(ed.) The Mechatronics Handbook, 2nd edn pp. 948-973. CRC Press, Boca Raton (2002)
10. Anochin, P.K.: Biology and Neurophysiology of Acquired reflex. p. 112. Meditcina, Moscow (1968) (in Russian)
11. Sayapin, S.N., Artemenko, Y.N: Intelligence System for Active Vibration Isolation and Pointing of Ultrahigh-Precision Large Space Structures in Real Time". In: Gorodetskiy, A.E (ed.) Smart Electromechanical Systems. Series Studies in Systems, Decision and Control", Series Vol. 49, Chapter 10, Synthesis of Automatic Control Systems, pp. 103–115. Springer, Switzerland, (2016)
12. Glazunov, V.A., Koliskor, A.S., Krainev, A.F.: Spatial parallel structure mechanisms. Nauka, Moscow (1991) (in Russian)
13. Sayapin, S.N., Sineov, A.V., Trubnikov, A.G.: Russian Patent 2161109, Byull. Izobret., no. 36 (2000)
14. Sayapin, S.N.: Prospects and possible use of three-dimensional mechanisms of parallel structure in space engineering. J. Mach. Manuf. Reliab. No. 1, pp. 13–22 (2001)
15. Sayapin, S.N.: Application of parallel kinematics machines for active vibration isolation and pointing of high-precision large deployable space structure (HLDSS). In 3rd Chemnitzer Parallelkinematik Seminar, pages 957–962, Chemnitz, April, 23–25, 2002
16. Sayapin, S.N., Kokushkin, V.V.: Russian Patent 2323136, Byull. Izobret., No. 12 (2008)
17. Panteleev S.V.: Development, Research and Using of Neural Network Algorithms of Identification and Control of Dinamical Systems, Doctor Dissertation, MSIEM, Moscow (2005) (in Russian)

Synthesis of Control of Hinged Bodies Relative Motion Ensuring Move of Orientable Body to Necessary Absolute Position

Yu.N. Artemenko, A.P. Karpenko and P.P. Belonozhko

Abstract *Purpose*: Taking into account evolution trends of space-system engineering, on solution of tasks concerned with control systems elaboration, making of Robot Central Nervous System (RCNS) for perspective space-purpose robotic systems, we can talk about urgency of problems of brake-release mode analysis, which specificity is determined by functionality of systems under consideration and orbital external environment. The paper considers characteristic features of controlled motion of space system "movable platform-manipulator—payload", which moves in inertial space under the action of the hinged control in conditions free of external forces. *Results*: Using mathematical model obtained in Artemenko et al. (Smart electromechanical systems. Springer International Publishing, Switzerland, pp. 177–190, 2016, [1]) the paper examines an example of task solution of control synthesis of relative movement of orientable and lifting body, providing setting of orientable body in desired absolute position. *Practical importance*: There are perspective space systems, for which the considered type of controlled motion is possible as normal mode of operation being of applied interest.

Keywords Manipulator · Movable basis · Massive payload · Research of dynamic conditions · Model task

Yu.N. Artemenko
The Astrospace Center of P.N. Lebedev Physical Institute of the Russian Academy of Sciences, Moscow, Russia
e-mail: artemenko.akc@yandex.ru

A.P. Karpenko · P.P. Belonozhko (✉)
The Bauman Moscow State Technical University, Moscow, Russia
e-mail: byelonozhko@mail.ru

A.P. Karpenko
e-mail: apkarpenko@mail.ru

A.E. Gorodetskiy and V.G. Kurbanov (eds.), *Smart Electromechanical Systems: The Central Nervous System*, Studies in Systems, Decision and Control 95,
DOI 10.1007/978-3-319-53327-8_16

1 Introduction

Perspective class of robotized space system equipped with manipulators installed on movable foundation, relative to which payload is moved, generally sufficiently massive.

Possibility of realization of external forces-free modes is characteristic of given class of systems, where system moves under the influence of control forces and moments produced by manipulator degrees of freedom drives. According to terminology existing in literature on space robotics term "free-floating" is used for this mode, unlike "free-flying" mode marked by off-system forces and moments also occuring, for example, applied to foundation.

Generally possibility of realization of "free-floating" mode exists for any space systems equipped with manipulators. Case of comparable mass and lag characteristics of movable foundation and payload is of particular interest.

Intelligent system of active vibration protection and high-precision guidance of on-orbit uncovered space telescope may make an example of perspective system "movable foundation—manipulation mechanism—payload", where it is based on use manipulator of parallel structure, able to ensure vibration protection of space telescope with its simultaneous guidance on prototype systems in real-time mode; concept of such system is presented in [2–6]. Possibility of substantially different dynamic conditions is apparent for mentioned system. Also notice that mathematical formulation of system dynamics for definite version of its technical implementation is quite cumbersome. In connection with stated we consider as very urgent examination of model problems, whose outstanding feature is effective simplification of mechanical design diagram with conservation of being of most interest qualitative dynamic features inherent to investigated mode.

Implying as significant guidance mode, i.e. assurance of required angular position of orientable body and supposing expedient its implementation at the expense of mutual displacement of orientable (telescope) and carrying (spacecraft) bodies by means of manipulator, let us consider model problem formulated in [1].

2 Problem Statement

Let us consider plane system of two solid bodies (Fig. 1) with mass m_1 and m_2, connected by ideal one-degree of freedom rotary hinge, moving in inertial space under the action of moment M, generated by hinge drive. J_1, J_2 are bodies moments of inertia relative to axes passing through their centers of mass perpendicular to plane of motion (plane of a figure). Distance from center of mass of body 1 to axe of hinge is equal to l_1, distance from center of mass of body 2 to axe of hinge is equal to l_2. Let us determine body 1 as orientable (telescope) and body 2 as carrying (movable foundation—spacecraft). Let us describe absolute position of orientable body by angle φ_1, relative position of orientable body about carrying—by angle ψ.

Fig. 1 System initial position

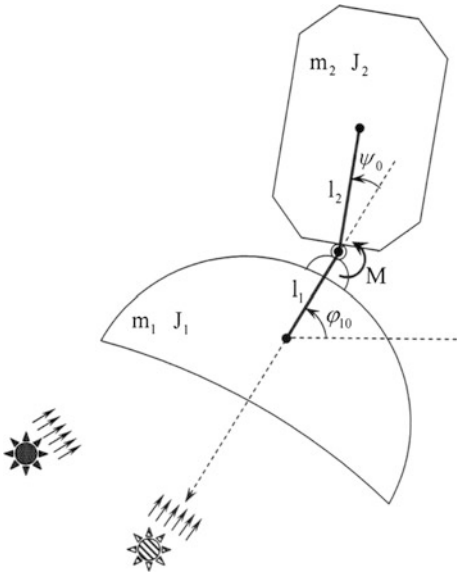

Positive directions of angle reading are given at the figure. Let's take control moment directed at side of augmentation of ψ (reduction of φ_1) as positive. Then we examine problem of program control synthesis $M(t)$, ensuring required changing $\varphi_1(t)$ of absolute angular position of orientable body. At the same time it is suggested that any external forces don't influence the system and control moment in hinge $M(t)$ is unique active internal force.

As shown in [1], it is necessary to distinguish cases of presence and lack of system initial angular momentum.

Then let us consider following case: system ($\dot{\psi}_0 = 0$ и $\dot{\varphi}_{10} = 0$) at rest in initial instant $t_0 = 0$, with some reference configuration ψ_0, when orientable body holds some absolute angular position φ_{10} (Fig. 1), should be placed to position assuring $\varphi_1(t_k) = \varphi_{1k}$ and $\dot{\varphi}_1(t_k) = 0$ in a time t_k by means of desired control action $M(t)$, i.e. it is necessary to realize telescope guidance on desired direction (Fig. 2).

In [1] independent dynamic equation of relative motion (motion of orientable body 1 relative to carrying body 2) is obtained

$$\ddot{\psi}\frac{\alpha_1\alpha_2 - \beta^2\cos^2\psi}{\alpha_1+\alpha_2+2\beta\cos\psi} + \dot{\psi}^2\frac{\beta\sin\psi(\alpha_1+\beta\cos\psi)(\alpha_2+\beta\cos\psi)}{(\alpha_1+\alpha_2+2\beta\cos\psi)^2} + \frac{L^2\beta\sin\psi}{(\alpha_1+\alpha_2+2\beta\cos\psi)^2} = M, \tag{1}$$

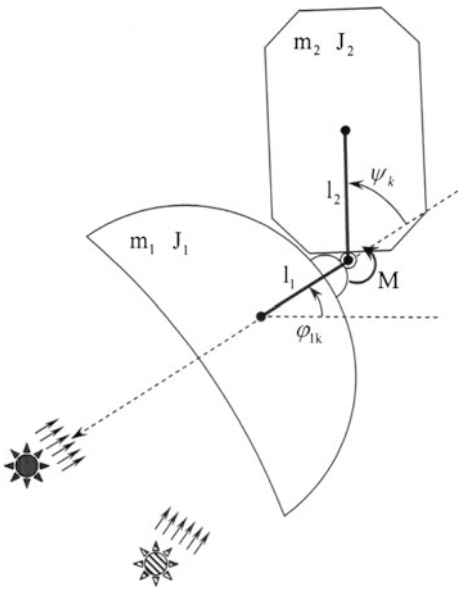

Fig. 2 Desired system position

where $\alpha_1 = J_1 + \tilde{m}l_1^2$, $\alpha_2 = J_2 + \tilde{m}l_2^2$, $\beta = \tilde{m}l_1 l_2$, $\tilde{m} = \frac{m_1 m_2}{m_1 + m_2}$, L—is system angular momentum conserved permanent in process of motion and determined by expression.

$$\dot{\varphi}_1\left(J_1 + J_2 + \tilde{m}l_1^2 + \tilde{m}l_2^2 + 2\tilde{m}l_1 l_2 \cos\psi\right) + \dot{\psi}\left(J_2 + \tilde{m}l_2^2 + \tilde{m}l_1 l_2 \cos\psi\right) = L. \quad (2)$$

In case at issue angular momentum of system at rest in initial instant is evidently equal to zero

$$L = 0. \quad (3)$$

Then as it is shown in [1], in view of load known relative motion $\psi(t)$, we deduce absolute angular motion $\varphi_1(t)$ of foundation using integration of Eq. (2) taking into account (3)

$$\begin{aligned} \varphi_1(t) &= -\frac{1}{2}\psi(t) - \frac{b}{a} arctg\left(\frac{tg\frac{\psi(t)}{2}}{a}\right) + C_{\varphi_1\psi}, \\ a &= \sqrt{\frac{\alpha_1 + \alpha_2 + 2\beta}{\alpha_1 + \alpha_2 - 2\beta}} = \sqrt{\frac{J_1 + J_2 + \tilde{m}(l_1 + l_2)^2}{J_1 + J_2 + \tilde{m}(l_1 - l_2)^2}}, \\ b &= \frac{\alpha_2 - \alpha_1}{\alpha_1 + \alpha_2 - 2\beta} = \frac{J_2 + \tilde{m}l_2^2 - J_1 - \tilde{m}l_1^2}{J_1 + J_2 + \tilde{m}(l_1 - l_2)^2}. \end{aligned} \quad (4)$$

In (4) constant of integration is determined by system initial position and configuration

$$C_{\varphi_1\psi} = \varphi_1^{(0)} + \frac{1}{2}\psi^{(0)} + \frac{b}{a} arctg\left(\frac{tg\frac{\psi^{(0)}}{2}}{a}\right). \tag{5}$$

3 Algorithm of Control Synthesis

Let's set oneself law of variation $\psi(t)$ in form

$$\psi(t) = \psi_0 + (\psi_k - \psi_0)\left(10 - 15\frac{t}{t_k} + 6\frac{t^2}{t_k^2}\right)\frac{t^3}{t_k^3}. \tag{6}$$

It is easy to see that in this case

$$\begin{aligned} &\psi(t_0) = \psi(0) = \psi_0, \\ &\psi(t_k) = \psi_k, \\ &\dot{\psi}(t_0) = \dot{\psi}(0) = 0, \\ &\dot{\psi}(t_k) = 0, \\ &\ddot{\psi}(t_0) = \ddot{\psi}(0) = 0, \\ &\ddot{\psi}(t_k) = 0. \end{aligned} \tag{7}$$

At the same time taking into account (2)–(5) we have

$$\begin{aligned} &\varphi_1(t_0) = \varphi_1(0) = \varphi_{10}, \\ &\varphi_1(t_k) = \varphi_{1k}, \\ &\dot{\varphi}_1(t_0) = \dot{\varphi}_1(0) = 0, \\ &\dot{\varphi}_1(t_k) = 0, \\ &\ddot{\varphi}_1(t_0) = \ddot{\varphi}_1(0) = 0, \\ &\ddot{\varphi}_1(t_k) = 0. \end{aligned} \tag{8}$$

At the same time ψ_k and φ_{1k} are linked by relation (4) written for point of time t_k, where constant of integration $C_{\varphi_1\psi}$ is determined by relation (5) at predetermined ψ_0 and φ_{10}.

In such a way described below algorithm of solution of problem of control moment synthesis in hinge, assuring move of orientable body from prearranged position to desired, may be realized for the case (3) of lack of initial angular momentum and selected law of variation of bodies relative position (6).

Let's suppose following characteristics to be predetermined:

- system mass and lag characteristics and geometry features m_1, m_2, J_1, J_2, l_1 and l_2;
- initial position of orientable body φ_{10} and system reference configuration ψ_0;

– necessary position of orientable body φ_{1k} and time t_k, body should be moved within it.

Substituting φ_{10} and ψ_0 to (5) we define $C_{\varphi_1\psi}$. We define ψ_k from relation (4) written for point of time t_k. Substituting ψ_0, ψ_k and t_k to (6) and received result to (1) we obtain desired control low $M(t)$.

4 Example of Control Synthesis

Digressing from possible system engineering realization within the framework of simplified model problem under consideration let's preset some arbitrary parameter values, meaning to confirm operability of proposed algorithm in workmanlike manner.

Let $m_1 = 10$ [kg], $m_2 = 10$ [kg], $J_1 = 1$ [kg m^2], $J_2 = 1$ [kg m^2], $l_1 = 1$ [m] and $l_2 = 1$ [m]. Let's set initial system position $\varphi_{10} = \frac{\pi}{8}$ [rad] and initial configuration $\psi_0 = \frac{\pi}{4}$ [rad]. It is necessary to move system at position $\varphi_{1k} = 0$ [rad] in a time $t_k = 10$ [s].

According to algorithm described above we define finite configuration

$$\psi_k = 1.57 \text{ [rad]}. \tag{9}$$

Relative motion of orientable and lifting bodies

$$\psi(t) = 0.785 + 0.000785\ t^3\left(10 - 1.5\,t + 0.06\,t^2\right) \text{ [rad]}. \tag{10}$$

Absolute motion of orientable body

$$\varphi_1(t) = 0.393 + 0.000393\ t^3\left(10 - 1.5\ t + 0.06\ t^2\right) \text{ [rad]} \tag{11}$$

Graphic presentation $\psi(t)$ and $\varphi_1(t)$ is shown at Fig. 3.

Desired hinged control $M(t)$ assuring necessary absolute motion of orientable body (11)

$$\begin{aligned} M(t) &= \sin(4.71 \cdot 10^{-5} \cdot t^5 - 1.18 \cdot 10^{-3} \cdot t^4 + 7.85 \cdot 10^{-3} \cdot t^3 + 0.785) \\ &\times (6.94 \cdot 10^{-8} \cdot t^8 - 2.78 \cdot 10^{-6} \cdot t^7 + 4.16 \cdot 10^{-5} \cdot t^6 - 2.78 \cdot 10^{-4} \cdot t^5 + 6.94 \cdot 10^{-4} \cdot t^4) \\ &+ \cos(4.71 \cdot 10^{-5} \cdot t^5 - 1.18 \cdot 10^{-3} \cdot t^4 + 7.85 \cdot 10^{-3} \cdot t^3 + 0.785) \\ &\times (-2.36 \cdot 10^{-3} \cdot t^3 + 3.53 \cdot 10^{-2} \cdot t^2 - 0.118 \cdot t) \\ &+ (2.83 \cdot 10^{-3} \cdot t^3 - 4.24 \cdot 10^{-2} \cdot t^2 + 0.141 \cdot t) \text{ [N m]}. \end{aligned} \tag{12}$$

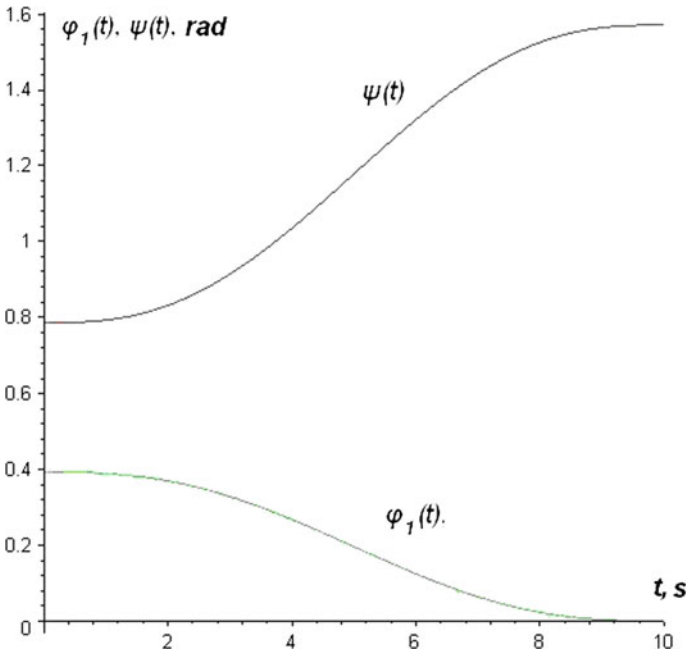

Fig. 3 Relative motion of bodies $\psi(t)$ assuring necessary absolute motion of orientable body $\varphi_1(t)$

It is significant to point out that control moment doesn't equal to zero only on interval $[t_0, t_k]$, i.e.

$$M(t) = \begin{cases} 0, \ t < t_0, \\ M(t), \ t_0 \le t \le t_k, \\ 0, \ t_k < t. \end{cases} \tag{13}$$

Diagram of control law (12) on interval $[t_0, t_k]$ is shown at Fig. 4.

It is profitable to do test of validity of received results using direct modeling of motion under consideration by means of physical simulation package. Software tools of present class are meant for automation of investigation of mechanical objects that may be represented by system of perfectly rigid bodies interconnected with the aid of kinematical and force-summing elements. Preparation of object model consists in description by dint of mechanical analytical model package. Derivation of dynamic equation is realized automatically. Consequently physical simulation packages may provide an effective means of operative validation of received analytic relationships.

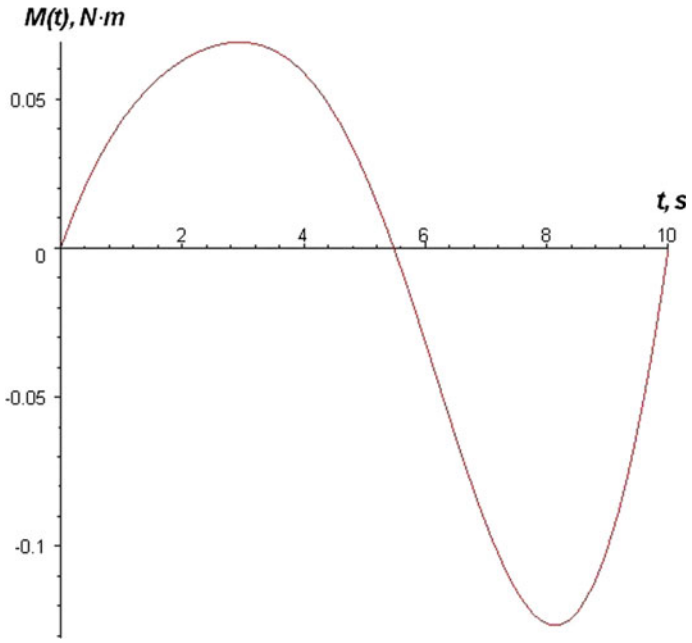

Fig. 4 Control law—hinged moment assuring necessary absolute motion of orientable body (11)

5 Conclusion

Example of problem solution of control synthesis of orientable and lifting bodies relative motion, ensuring move of orientable body to necessary absolute position is pursued using simulator received in [1]. Type of controlled movement under consideration is possible as normal behavior mode being of applied interest.

References

1. Artemenko, Yu.N., Karpenko, A.P., Belonozhko, P.P.: Features of manipulator dynamics modeling into account a movable platform. In: Gorodetskiy, A.E. (eds.) Smart electromechanical systems. Studies in Systems, Decision and Control, vol. 49, pp. 177–190. Springer International Publishing Switzerland (2016). doi:10.1007/978-3-319-27547-5_17
2. Artemenko, Yu.N.: Synthesis of orientation mechanisms for the space observatory " Millimetron". 1. Capabilities of parallel mechanisms for orientation of the space observatory "Millimetron". Science and Education of the Bauman MSTU (2013). No. 1. doi:10.7463/0113.0534292
3. Artemenko, Iu.N., Karpenko, A.P., Pashchenko, V.N., Martyniuk, V.A., Volkomorov, S.V., Temerev, K.A., Sharygin, A.V.: Synthesis of orientation mechanisms for the space observatory "Millimetron" . 2. Synthesis and optimization of a parallel multi-sectional

manipulator for orientation of the space observatory “Millimetron”. Science and Education of the Bauman MSTU (2013). No. 3. doi:10.7463/0413.0554360
4. Artemenko, Yu.N., Glazunov, V.A., Sil’vestrov, E.E., Korenovskiy, V.V., Demidov, S.M.: Synthesis of orientation mechanisms for the space observatory “Millimetron” . 3. Synthesis of parallel mechanisms for orientation of the antenna of space observatory. Science and Education of the Bauman MSTU (2013). No 5. doi:10.7463/0513.0571127
5. Artemenko, Yu.N., Sayapin, S.N.: Synthesis of orientation mechanisms for the space observatory “Millimetron”. 4. The concept of intelligence system of active vibration protection and very precise pointing of the space observatory “Millimetron”. Science and Education of the Bauman MSTU (2013). No 6. doi:10.7463/0613.0574243
6. Artemenko, Yu.N., Belonozhko, P.P., Karpenko, A.P., Saypin, S.N., Fokov, A.A.: Mechanisms of parallel structure for mutual positioning useful loading and space ship. Robot. Tech. Cybern. **1**(C), 65–71 (2013)

Automatic Control System of Adaptive Capture

Vugar G. Kurbanov, Andrey E. Gorodetskiy and I.L. Tarasova

Abstract *Purpose*: in solving modern problems of robotics, development of systems of automatic control for adaptive captures imitating work of human hands is getting more urgency. The purpose of this work is to develop a new structure of systems of automatic control for adaptive capture providing adjustment to the taken object by means of change of form and rigidity of fingers. *Results*: the systems of automatic control for adaptive capture imitating work of a hand and providing prompt and exact adaptation to the size and form of the taken object by means of control over rigidity and shape of phalanxes of fingers is suggested in the paper. The algorithm of work of such system of automatic control is also suggested here. *Practical importance*: the system of automatic control for adaptive capture with the controlled rigidity and form can be used in micro robots of different function. When developing dynamics and setup of parameters of the system of automatic control of adaptive capture with the controlled form and rigidity, the mathematical and computer model of automatic control of SEMS module can be employed.

Keywords System of automatic control · Adaptive capture · Biological systems · A hand · Fingers · Phalanxes · Tiny propeller · Control over rigidity and form

V.G. Kurbanov (✉) · A.E. Gorodetskiy · I.L. Tarasova
Institute of Problems of Mechanical Engineering,
Russian Academy of Sciences, Saint Petersburg, Russia
e-mail: vugar_borchali@yahoo.com

A.E. Gorodetskiy
e-mail: g27764@yandex.ru

I.L. Tarasova
e-mail: g17265@yandex.ru

A.E. Gorodetskiy and V.G. Kurbanov (eds.), *Smart Electromechanical Systems: The Central Nervous System*, Studies in Systems, Decision and Control 95,
DOI 10.1007/978-3-319-53327-8_17

1 Introduction

Research on the development of automatic control system of the mobile elements of robots with parallel structures, designed to operate in conditions of a priori uncertainty dynamically changing environment, actively carried in all the industrialized countries of the world [1, 2]. Using hexapod structures SEMS in the construction of the adaptive capture for these robots gives the opportunity to get their automatic control systems maximum precision actuators with minimal movement of the time due to the introduction of parallelism in the measurement processes, computing, travel and the use of high-precision piezo motor able to work in extreme conditions, including in outer space [3, 4]. However, such structures have complex kinematics. This requires improving the algorithms of automatic control systems (ACS). ACS must provide solutions to new, complex problems of adaptation to the parameters of the objects captured by optimal trajectories without jamming platforms SEMS modules, which are designed on the basis of palm and phalanges considered adaptive capture.

The structures of the automatic control system, as well as its mathematical and computer models of standard modules (SM) SEMS described in [3, 4]. These systems provide the dynamic on speed and accuracy of the control shifts and rotations of platform modules, as well as reconfiguration of this platform. However, a number questions related to adaptation captures considered taking into account the dynamics of the environment should be further improved automatic control systems of adaptive capture, simulating work hands. This adaptability of such mechanisms at the expense of controlling the shape ST5 SEMS module platforms, forming a phalanx capture fingers, as well as by controlling the rigidity the special hardness blocks [5], placed between the capture fingers phalanges. To ensure high speed of automatic control systems like captures advantageously in automatic control systems (ACS) use neuroprocessors providing parallelization process control computation [6, 7].

2 Architecture of the Automatic Control System

ACS adaptive capture (ACS AC) has an architecture of the “tree” (see Fig. 1). It has on the upper level the central control computer (CCC), vision system (VS) and the following modules:

- Neuroprocessor simulation module (NSM);
- Neuroprocessor optimization module (NOM);
- Neuroprocessor decision making module (NDMM);
- Neuroprocessor module control computation (NMCC);

The second level the ACS AC contains subsystems: automatic control of the capture coordinates (SAC CC), automatic control of the palm (SAC P), automatic

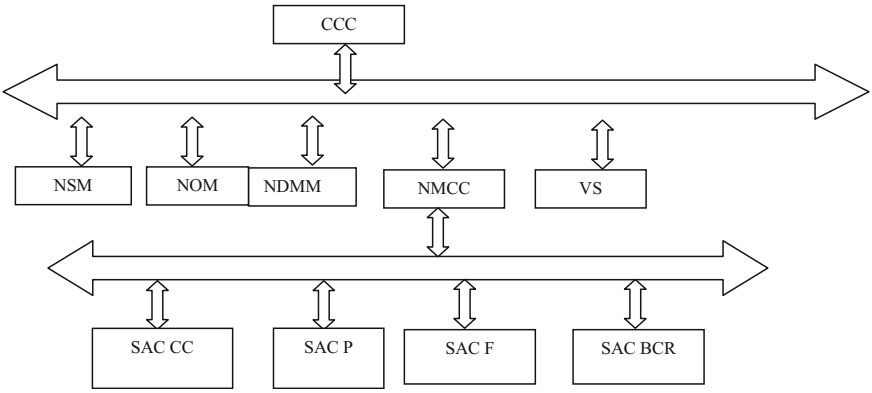

Fig. 1 Architecture ACS AC

control of the fingers (SAC F) and automatic control of the block with controlled rigidity (SAC BCR).

CCC provides a solution to problems of the choice of execution strategies required by the operator and/or systems of higher level jobs and the formation of a sequence of actions (algorithms), required for its implementation. In addition, it should ensure a prompt correction of behavior depending on the information about the change of the environment coming from the VS, and coordination of the subsystems. Operation CCC requires advanced skills to acquire knowledge of the laws governing the environment, to the interpretation, classification and identification of emerging situations, to analyze and memorize the consequences of their actions on the basis of experience (self-learning property).

Modules NSM, NOM, NDMM, NMCC together provide a solution to the tactical level control tasks. Its difficulty lies primarily in finding a solution to one of the key tasks associated with capturing adaptation is not completely in certain circumstances, taking into account the dynamics of the executive subsystems and current changes in the operational environment.

VS on command from CCC controls the parameters of CCD matrix, collects the information from them, and transmits it to the neuroprocessor recognition module (NRM). NRM makes identification of capture objects and the state of the operational environment and transmits this information to the CCC. Matrix CCD can be supplied pixels switches that can change the configuration and size of the matrix on commands from CCC. This ensures adaptation of the matrix CCD to the parameters of the identifiable capture objects [8, 9]. Usually VS capture is part of VS robot.

NOM, based on the input information from the VS about the state of the environment and in accordance with the algorithms of behavior formed CCC, performs the planning of optimal movement and reconfigurations SEMS module platform of the palm and fingers. At the same time the operational reorganization of the control laws within the constraints and dynamics of the executive subsystems must be ensured.

NSM provides a prediction of the dynamics of the executive subsystems for issuing corrections planned NOM optimal control laws and adaptation parameters computed control actions. This NDMM determines the conditions under which NOM and NMCC will be made corrections.

NMCC on the information received from the NOM, NSM and NDMM and in accordance with algorithms coming from CCC generates control exposure to second-level subsystems. SAC CC carries out the required travel the capture and the center of the palms in point of the object captured on the axes X, Y and Z. SAC P provides adaptation palm to the size and shape of the object captured. SAC F provides adaptation fingers to the size and shape of the object captured and capture of the object (shifts, rotations, compression and tension). SAC BCR controls change in rigidity of the BCR.

3 Subsystems Automatic Control Mobile Elements

SAC CC fault is usually part of an automatic control system of a robot arm and comprises three stepping motors for moving on the corresponding coordinates X, Y, Z. The algorithm of the SAC CC is described, for example, in [10], and SAC CC structure is shown in Fig. 2.

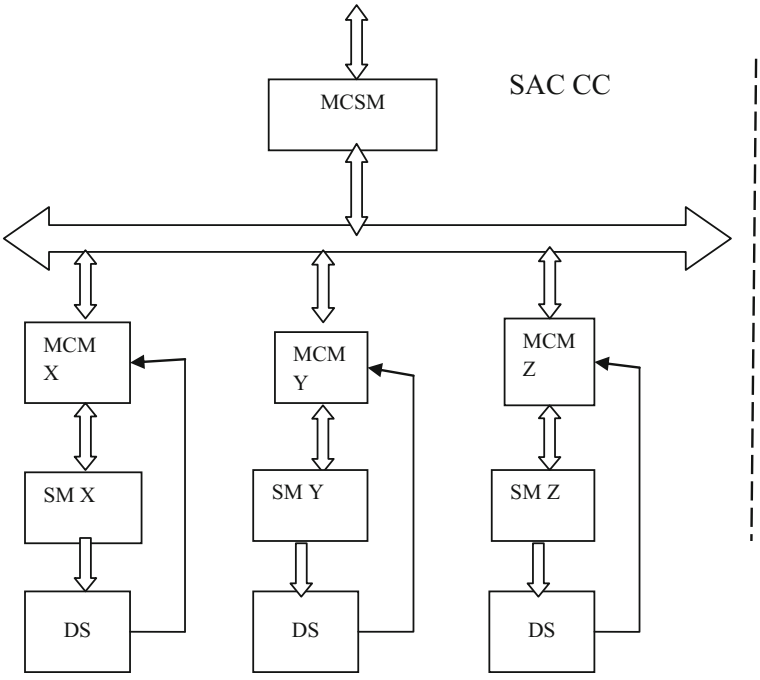

Fig. 2 SAC CC structure

The structure contains a module calculation steps move (MCSM) to the coordinates X, Y, Z;—motor controllers move (MCM X, MCM Y, MCM Z) to the coordinates X, Y, Z; stepper motors (SM X, SM Y, SM Z) to the coordinates X, Y, Z; displacement sensors (DS X, DS Y, DS Z) to the coordinates X, Y, Z.

SAC P constructed on the basis of SM5 SEMS module [11] and its structure and operation is similar to the automatic control system this module (ACS M) [12].

SAC F contains a module calculating the coordinates of the fingers (MCCF) and group controls the fingers (GCF1–GCF3), each of which outputs control signals to the ACS Ph. ACS Ph is a control system phalanges (Fig. 3).

GCF1–GCF3 (see Fig. 3) generates and applies control to the automatic control system modules phalanges (ACS Ph). Controllers legs (CL1)–(CL6) (see Fig. 4) ACS Ph using a feedback sensor signals [linear encoders (LE), angular displacement sensors (ADS), force sensors (FS) and tactile sensor (TS)] calculating the error signals and produce according to a predetermined control laws (e.g. laws PID) control inputs to the respective leg motors (LM1)–(LM6). Last carried out the required extension legs (L1)–(L6) (see Fig. 4).

In addition GCF1–GCF3 generates and outputs the control actions in automatic control systems rods reconfiguration (ACS RR). It as the previous system of control rods controllers reconfiguration (CRCR1)–(CRCR6) using a feedback sensor signals [linear encoders (LE), angular displacement sensors (ADS), force sensors

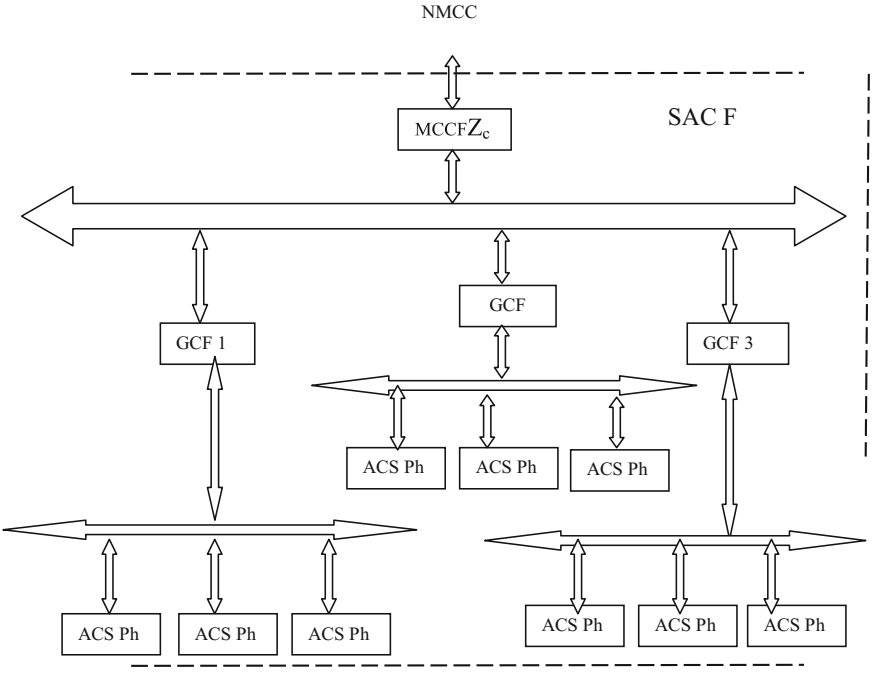

Fig. 3 Structure SAC F

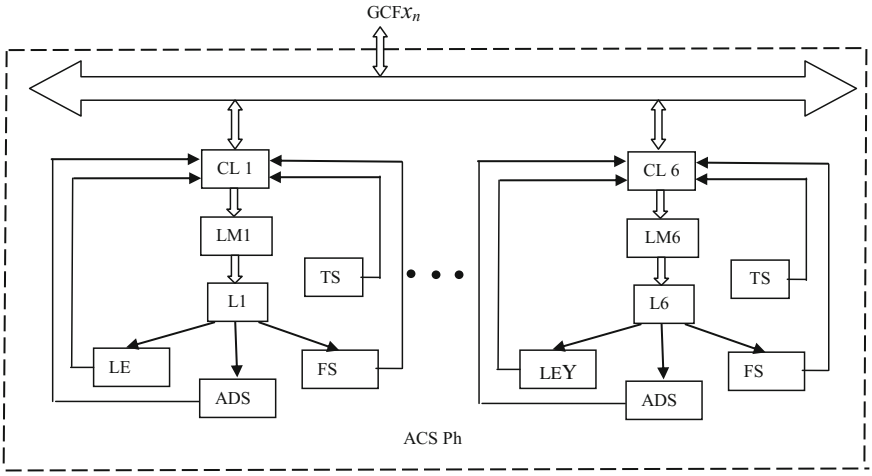

Fig. 4 Structure automatic control system legs (ACS L)

(FS) and tactile sensor (TS)] calculating error signals and produce according to a predetermined control laws (e.g. laws PID) control inputs to the respective motors rods reconfiguration (MRR1)–(MRR6). The last performed the required extension of the rod reconfiguration (RR 1)–(RR 6).

Tactile sensors and force sensors are typically used for the adaptation of automatic control systems. The sensors of linear and angular displacements provide feedback circuit of the automatic control systems during transients.

SAC BCR contains a module calculation finger rigidity of (MCFR) and group controls the drive current (GCDC) for blocks controlled rigidity. MCFR on the signals from the NMCC calculates the required rigidity of the fingers and GCDC calculates and outputs a corresponding current in the BCR.

4 Conclusion

ACS adaptive capture are constructed as multi-level system of the "tree" architecture. Its CCC provides a solution to problems of the choice of execution strategies required by the operator and/or systems of higher level jobs and the formation of a sequence of actions (algorithms), required for its implementation. In addition, it should ensure a prompt correction of behavior depending on the information about the change of the environment coming from the VS, and coordination of the subsystems.

Tactical level control solution of problems carry subsystems, which are usually used neuroprocessor modules to easily parallelize computing processes to improve speed and accuracy of calculations. At the same time they need to ensure not only

progress towards the goal of a priori given the trajectories, but also the necessary arbitrary changes to promote a given target object.

The vision systems it is advisable to use adaptive CCD. Its can change the shape and size of matrices on the commands from the controller, allowing them to adapt to the parameters of the identifiable objects. This makes it possible to improve the accuracy and speed of recognition due to the transfer of the recognition algorithm into hardware.

Subsystems automatic control moving elements have the same architecture "tree" type (see Fig. 3) and usually contain neuroprocessor module for calculating the optimal motion. This module calculates optimal elongation and turns without jams. Besides these subsystems contain group controls regulators of the same type, tactile sensors and force sensors, serving for the adaptation of automatic control systems, as well as sensors of linear and angular movements that provide a feedback circuit of automatic control systems to improve the quality of transients.

Acknowledgements The author would like to thank the Russian Foundation for Basic Researches (grants 14-07-00257, 15-07-04760, 15-07-02757, 16-29-04424, and 16-29-12901) for partial funding of this research.

References

1. Popov, E.P., Pismennov, G.V. (eds.): Fundamentals of Robotics. Vishaya Shkola, Moscou, 224 p. (1990) (in Russian)
2. Chernukhin, Y.V., Pisarenko, S.N.: Extrapolation structures in neural network-based control systems for intelligent mobile robots. Optical Mem. Neural Netw. **11**(2), 105–115 (2002)
3. Gorodetsky, A.E., Tarasova, I.L., Kurbanov, V.G., Agapov, V.A.: Mathematical model of automatic control system for SEMS module. Informatsionno-upravliaiushchie sistemy **3**(59), 40–45 (2015) (In Russian). doi:10.15217/issn1684-8853.2015.3.40
4. Gorodetsky, A.E.: Smart electromechanical systems architectures. In: Gorodetskiy, A.E. (ed.) Smart Electromechanical Systems, 277 p. Springer International Publishing (2016). doi:10.1007/978-3-319-27547-5
5. Gorodetsky, A.E., Tarasova, I.L., Kurbanov, V.G.: Controlled Ciliated Propulsion (in this volume)
6. Tarasova, I.L., Gorodetskiy, A.E., Kurbanov, V.G.: Neuroprocessor automatic control system of the module SEMS. In: Gorodetskiy, A.E. (ed.) Smart Electromechanical Systems, 277 p. Springer International Publishing (2016). doi:10.1007/978-3-319-27547-5
7. Ruchkin, V.N., Romanchuk, V.A.: Development of algorithms and software for neurocomputer systems of SEMS automatic control modules. In: Gorodetskiy, A.E. (ed.) Smart Electromechanical Systems, 277 p. Springer International Publishing (2016). doi:10.1007/978-3-319-27547-5
8. Gorodetskiy, A.E., Kurbanov, V.G., Tarasova, I.L., Agapov, V.A.: Problems of increase of efficiency of use of matrix receivers for radio images in astronomy. Radio Eng. **1**, 88–96 (2015)
9. Gorodetskiy, A.E., Tarasova, I.L.: Detection and identification of dangerous space objects using adaptive matrix receivers radio. Informatsionno-upravliaiushchie sistemy [Inf. Control Syst.] **5**, 18–23 (2014) (In Russian)

10. Kurbanov, V.G., Gorodetskiy, A.E., Tarasova, I.L.: Automatic control systems of SEMS. In: Gorodetskiy, A.E. (ed.) Smart Electromechanical Systems, 277 p. Springer International Publishing (2016). doi:10.1007/978-3-319-27547-5
11. Gorodetskiy, A.E.: Smart electromechanical systems modules. In: Gorodetskiy, A.E. (ed.) Smart Electromechanical Systems, 277 p. Springer International Publishing (2016). doi:10.1007/978-3-319-27547-5
12. Tarasova, I.L., Gorodetskiy, A.E., Kurbanov, V.G.: Mathematical models of the automatic control systems SEMS modules. In: Gorodetskiy, A.E. (ed.) Smart Electromechanical Systems, 277 p. Springer International Publishing (2016). doi:10.1007/978-3-319-27547-5

Computer Simulation of Automatic Control System Ciliated Propulsion

Vugar G. Kurbanov, Andrey E. Gorodetskiy and I.L. Tarasova

Abstract *Purpose*: in solving modern problems of automatic control of robots imitating complexity and adaptability of biological systems, computer modeling with its potential to develop dynamics and setting configuration of control systems gains more ground. It is particularly urgent for the medical micro robots equipped by controlled tiny and energy-efficient propellers. The purpose of this work is to develop computer models of control systems for new adaptive propellers imitating muscle work of animals and people. *Results*: the computer models of control systems for new types of tiny adaptive propellers imitating operation of ciliary apparatus of a human and allowing to adapt to the environment by means of control over rigidity and form of elements of the propeller are suggested in the article. With the use of computer modeling, suggested types of propellers allow to reach the dynamic characteristics required for medical micro robots. *Practical importance*: computer models of control systems for ciliary propellers allow to estimate their dynamics and to perform setting of parameters of the considered propellers in micro robots of different function. Development of dynamics and setup of parameters of ciliary propellers by means of computer modeling can be improved by inclusion of the model of SEMS module into the constructed model designed by authors earlier.

Keywords Biological systems · Ciliary apparatus · Adaptive propeller · System of automatic control · Computer modeling · Control over rigidity and form

V.G. Kurbanov (✉) · A.E. Gorodetskiy · I.L. Tarasova
Institute of Problems of Mechanical Engineering,
Russian Academy of Sciences, V.O., Bolshoy pr., 61, 199178
Saint Petersburg, Russia
e-mail: vugar_borchali@yahoo.com

A.E. Gorodetskiy
e-mail: g27764@yandex.ru

I.L. Tarasova
e-mail: g17265@yandex.ru

A.E. Gorodetskiy and V.G. Kurbanov (eds.), *Smart Electromechanical Systems: The Central Nervous System*, Studies in Systems, Decision and Control 95,
DOI 10.1007/978-3-319-53327-8_18

1 Introduction

Research on the development of mathematical models of elements of robots with parallel structures, designed to operate in conditions of a priori uncertainty dynamically changing environment, actively carried in all the industrialized countries of the world [1, 2]. Use in the construction of propulsion such robots hexapod structures SEMS provides an opportunity to get the maximum precision actuators with minimum travel time by introducing parallelism in processes measurement, calculation, and the use of high-precision displacement piezo motors able to work in extreme conditions, including in outer space [3, 4]. However, such structures have complex kinematics. This requires improvement of their control algorithms and corresponding mathematical models of automatic control systems (ACS), providing, including the solving new, complex optimization problems finding optimal trajectories of movement without jamming.

Mathematical and computer models of standard modules (SM) are described in [2, 5, 6]. They provide a study of the dynamics of automatic control systems of translation and rotation module platforms, as well as automatic control system reconfiguration such platforms. However, a number of questions of the dynamics of automatic control systems ciliated propulsion on the basis of serial communication modules SEMS, require further study using computer simulations.

2 Modeling Simple Ciliated Propulsion

The most simple computer model control ciliated propulsion is model comprised of N series-connected blocks of effective phase and the same return phase blocks. The signals from the outputs of the blocks effectively phase summed. As summed signals output from the return phases blocks. In this model, the sum of the output signals of the return phase is deducted from signal of the effective phase. To obtain the desired timing diagram, each block effective phase in response to the impact of an abrupt input produces a given delay τ output pulse $\alpha = \pi/N$, and return each block in response to the supplied delayed input $N * \tau$ abrupt impact produces a given delay 4τ output pulse of the same amplitude $\alpha = \pi/N$. In this phase of the output signals of the effective blocks are added and form an angle of stroke $\beta = \pi$. As output signals the return phase blocks are added and form a return angle $\alpha = \pi/N$. The proposed model is implemented in an environment Simulink MatLab, it is shown in Fig. 1. automatic control system model of each of the N—SEMS modules, which are built on the basis of the effective blocks and return phases ciliary propulsion vibrations is described in [2].

Figure 2 is a timing diagram, obtained at the output of the computer model. You can be seen three phases: stroke, return and recovery, which confirm the correct operation of ciliated propulsion.

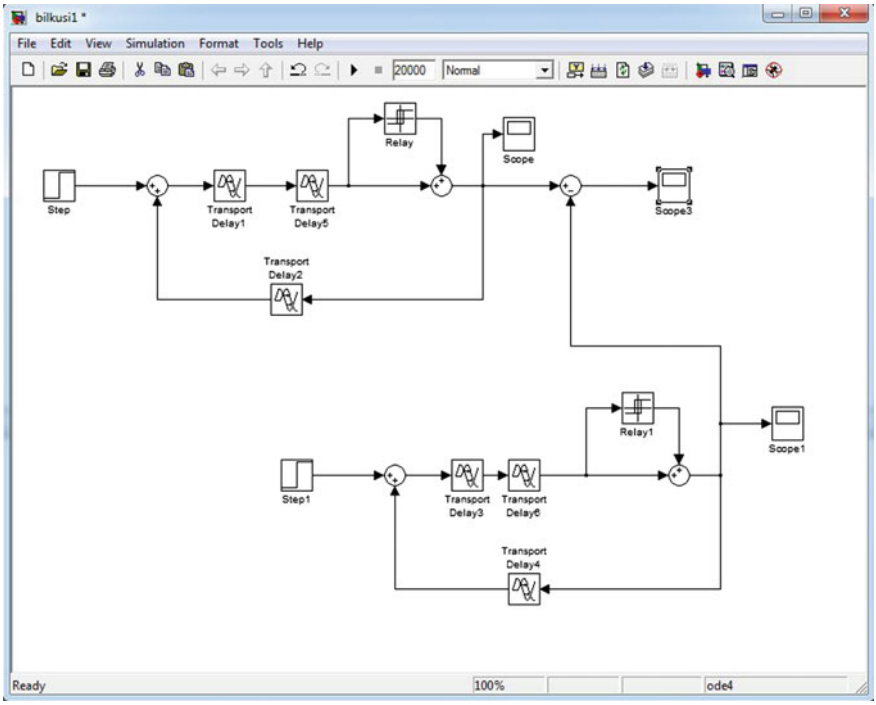

Fig. 1 Scheme of the model implemented in Simulink MatLab environment

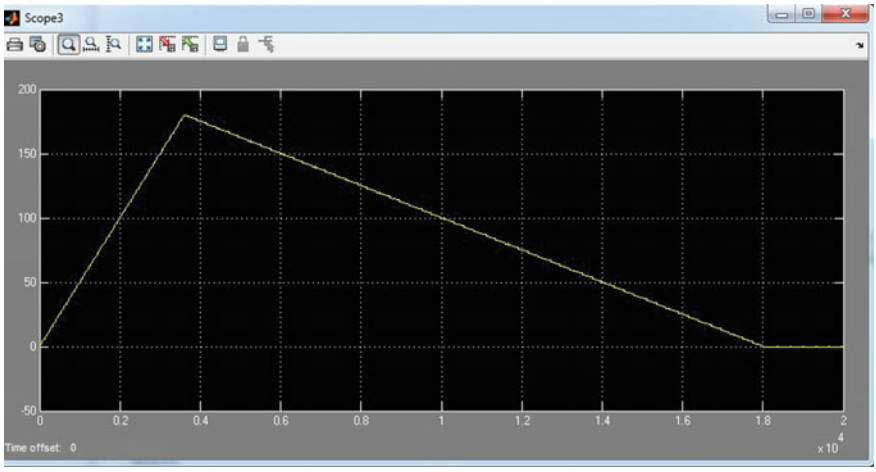

Fig. 2 Timing diagram obtained on the computer model

3 Simulation of the Automatic Control System of the Motor Control Rods

The structure of the linear mathematical model of the automatic control system (ACS) motor control rods (MCR) is shown in Fig. 3.

If the MCR to use miniature piezo motors, their linear mathematical model can be represented as follows [2]:

$$dF_e/dt = (K_0/C_0R_{in})e_c - (1/\ C_0R_{in})F_e - (K_0K_p/C_0)v \quad (1)$$

$$dv/dt = (1/m_\Sigma)F_e - ((K_e + K_s)/im_\Sigma x - (K_d/m_\Sigma)v \quad (2)$$

$$dx/dt = iv \quad (3)$$

where Fe—force developed pezo motor, K_0—inverse piezoelectric coefficient, C_0—the capacity of the piezoelectric element, R_{in}—internal resistance of the EMF source, e_c—EMF control, K_p—coefficient of the direct piezoelectric effect, m_Σ—mass to be moved, K_e—piezo coefficient of elasticity, K_s—stiffness coefficient, x—displacement, K_d—damping factor, v—velocity, i—reduction coefficient.

Applying the Eqs. (1)–(3) Laplace transform, one can obtain the following transfer function MCR:

$$W_{MCR} = \frac{K}{T^2p + 2\xi Tp + 1} \quad (4)$$

where K—gain, T—time constant, ξ—oscillation.

If used in the modeling Eq. (4) for the description of MCR, the regulator should be used as a PID controller with the transfer function:

$$W_p = a_1 + a_2/s + a_3s = \left(a_2\left(a_3s^2/a_2 + a_1s/a_2 + 1\right)\right)/s \quad (5)$$

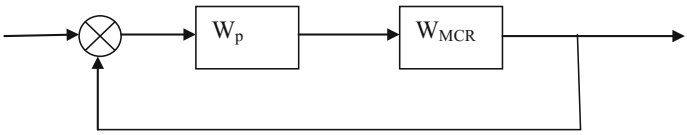

Fig. 3 Structure model ACS MCR. Wp and W_{MCR}—transfer functions PID control and MCR

At the same time, if we are given in relative terms the error δ when the input signal changes the frequency ω, then the coefficients a_1, a_2, a_3 controller settings is easy to calculate, based on the following relations:

$$\omega a_2 K = 1/\delta, \tag{6}$$

$$a_3/a_2 = T^2, \tag{7}$$

$$a_1/a_2 = 2\xi T \tag{8}$$

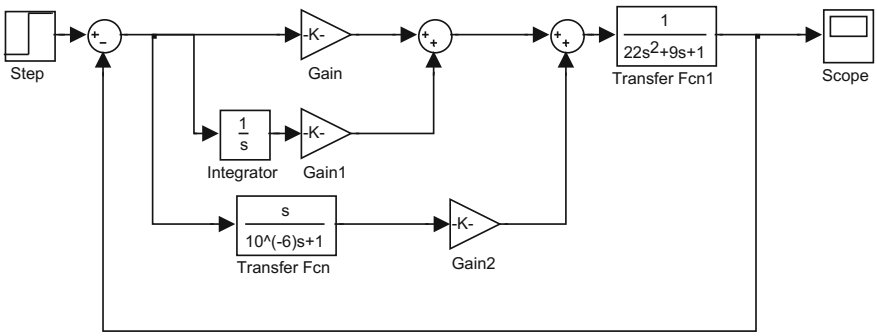

Fig. 4 The scheme model ACS MCR

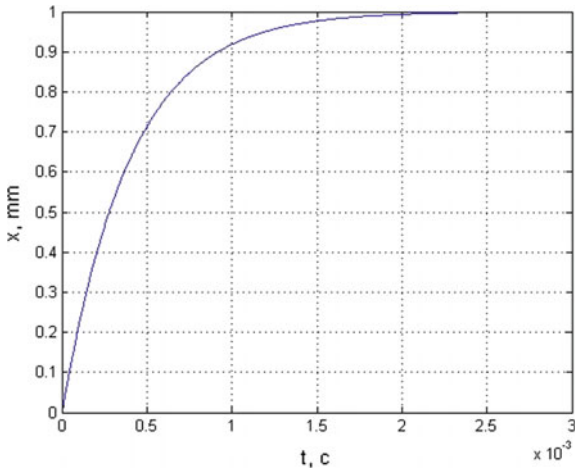

Fig. 5 The transition process of step increase impact

The scheme model ACS MCR implemented in the environment of Simulink MatLab, shown in Fig. 4, and the resulting transient response to a step impact—in Fig. 5.

From Fig. 5 shows that by setting the PID control can be obtained aperiodic transition process in ACS MCR with the required parameters.

4 Modeling of Automatic Control System of Block with Controllable Rigidity

The structure of the linear mathematical model of automatic control system of block with controllable rigidity (BCR) is shown in Fig. 6.

The linear mathematical model of BCR may be represented as follows:

$$Ri + Ldi/dt = u \tag{9}$$

$$k_c C + k_g dC/dt = i, \tag{10}$$

where R—input resistance, i—current control, L—inductance of the control circuit, t—time, u—control voltage, C—controlled rigidity, kc and kd—static and dynamic coefficients depending on the type of electrically insulating material BCR, impregnated electrorheological suspension, which typically are determined from experiments.

Introducing replace d/dt = s and substituting in (10) the value i from (9), we obtain:

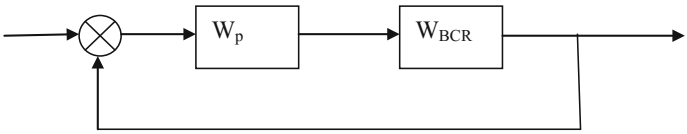

Fig. 6 Structure model ACS BCR

$$W_{BCR} = C/u = (1/R)(1/k_c)/(Ls/R+1)\left(k_g s/k_c + 1\right) = k_1 k_2/((T_1 s\ +1)(T_2 s\ +1)) = K_{BCR}/\left(T_1 T_2 s^2 + (T_1 + T_2)s + 1\right), \tag{11}$$

where $k_1 = 1/R$, $k_2 = 1/k_c$, $T_1 = L/R$, $T_2 = k_g/k_c$, $K_{BCR} = k_1 k_2$.

Usually set value

$$R \ll Lk_c/k_g \tag{12}$$

Then:

$$W_{BCR} \approx K_{BCR}/(\ T_1 s + 1) \tag{13}$$

When used to describe the modeling BCR Eq. (11), the regulator should be used as a PID controller with the transfer function:

$$W_p = a_1 + a_2/s + a_3 s = a_2\left(a_3 s^2/a_2 + a_1 s/a_2 + 1\right)/s \tag{14}$$

In this case, if the specified error delta, then the coefficients a_1, a_2, a_3 controller settings should be selected based on the following relations:

$$a_2\, K_{BCR} = 1/\delta, \tag{15}$$

$$a_3/a_2 = T_1 T_2, \tag{16}$$

$$a_1/a_2 = T_1 + T_2 \tag{17}$$

In computer simulation ACS BCR was taken:

$$L = 0.05\,\Gamma_H,\ R = 100\,O_M,\ T_2 = k_g/k_c = 5 \times 10^{-8}/10^{-3} = 5\,10^{-5}c$$

$$T_1 = L/R = 5 \times 10^{-4}c,\ K_{BCR} = (1/R)(text1/k_c) = (1/100)\left(1/10^{-3}\right) = 10$$

Then: $W_{BCR} = 10/(2.5 \times 10^{-8}\ s^2 + 5.5 \times 10^{-4}\ s + 1)$.

Therefore, for a given accuracy $\delta = 0.005$ tuning PID controller is as follows:

$$a_2 = 1/\ \delta K_{BCR} = 1/0.005 \times 10 = 20,$$
$$a_3 = a_2 T_1 T_2 = 20 \times 5 \times 10^{-5} \cdot 5 \times 10^{-4} = 5 \times 10^{-7},$$
$$a_1 = a_2(T_1 + T_2) = 20\left(5 \times 10^{-5} + 5 \times 10^{-4}\right) = 1.1 \times 10^{-2}$$

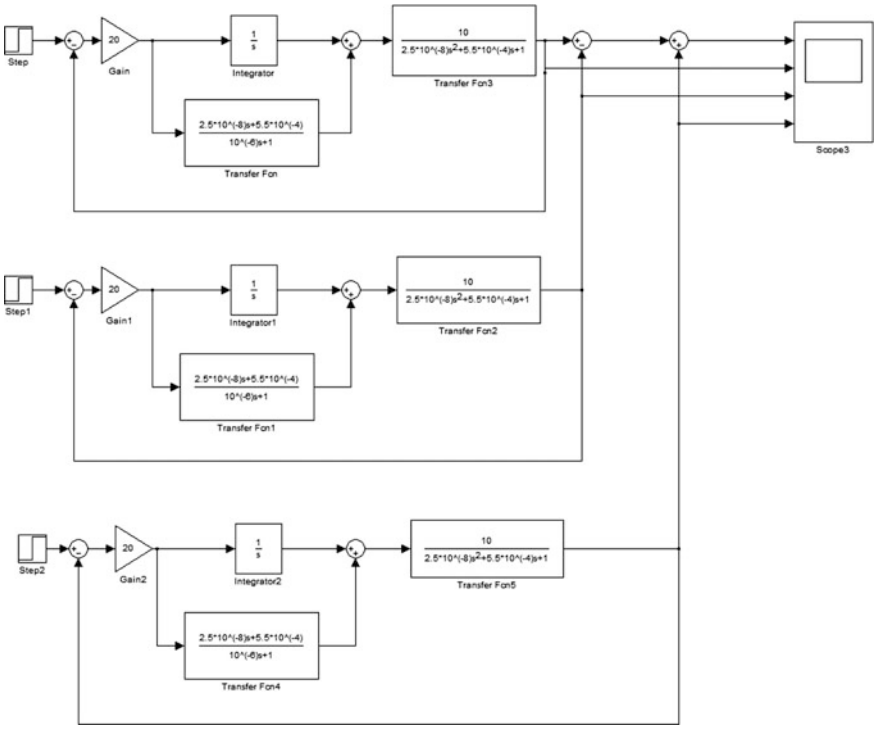

Fig. 7 The scheme model ACS BCR

In the simulation in Simulink MatLab environment, the transfer function of the PID controller can be represented in the following form: $W_p = W_1(W_2 + W_3)$.

when: $W_1 = a_2 = 20$

$$W_2 = 1/s,\ W_3 = (T_1T_2s + T_1 + T_2)/(T_ks + 1) = \left(2.5 \times 10^{-8}\ s + 5.5 \times 10^{-4}\right)/\left(10^{-6}\ s + 1\right),$$

Conditions $T_k \ll (T_1 + T_2)$ required to avoid large errors in the simulation.

The scheme model ACS BCR implemented in an environment Simulink MatLab, shown in Fig. 7. The transition process obtained for one BCR at step impact is shown in Fig. 8, and the process of changing rigidity of electromechanical cilia (EMC) in the fungus and return—Fig. 9. In the latter case, the computer model can be simplified scheme (see Fig. 10).

From Fig. 8 shows that by setting the PID control can be obtained aperiodic transition process in ACS BCR with the required parameters. Figure 9 shows a virtually abrupt change in rigidity of EMC in the transition from the phase of the stroke to the return phase.

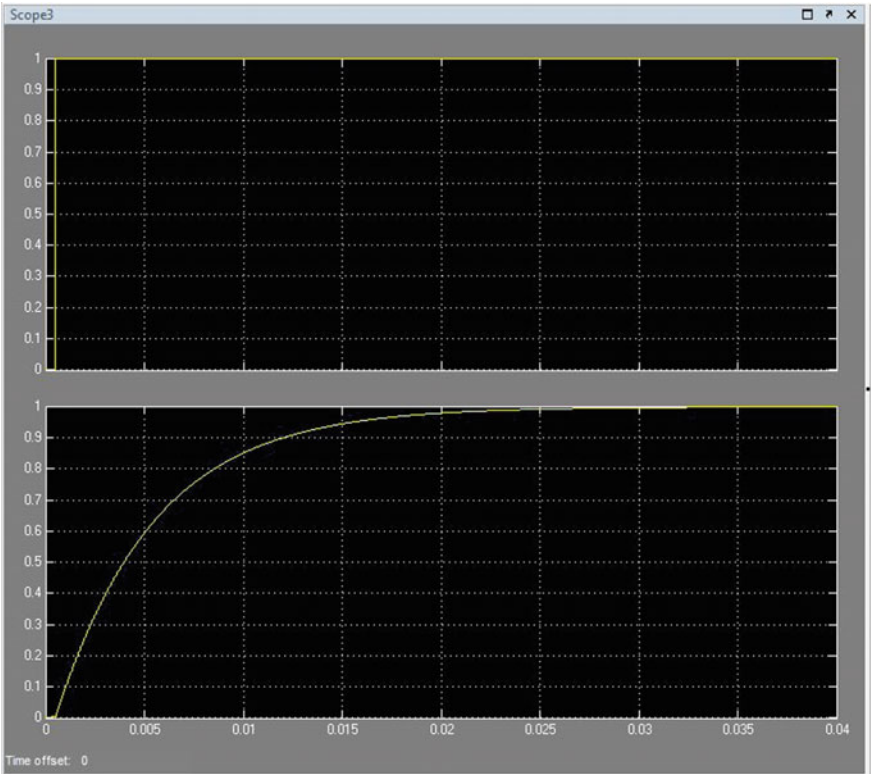

Fig. 8 The transition process in the BCR

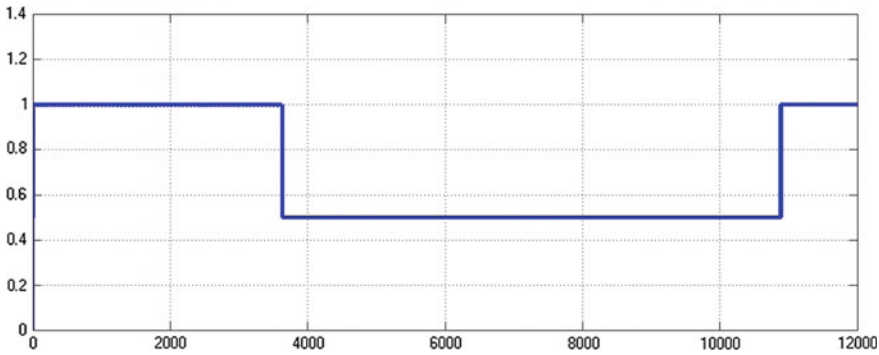

Fig. 9 The process of changing rigidity of EMC with fungus and return

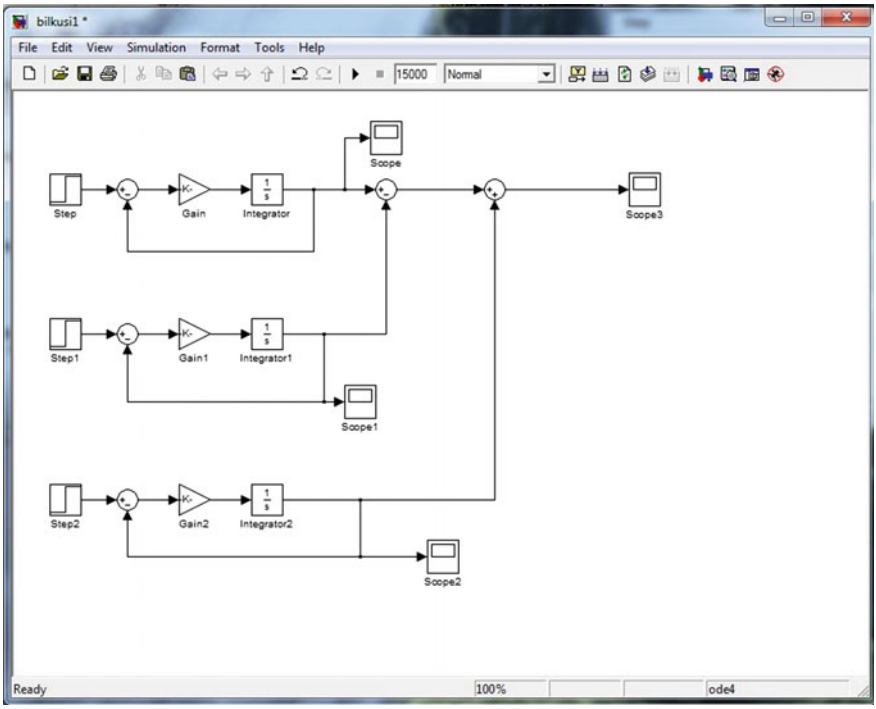

Fig. 10 Simplified computational model

5 Conclusion

The structure of the ACS controlled ciliated propulsion (CCP) similar to that of ACS SEMS. Therefore debugging of its dynamics and parameter setting can be carried out with the help of a simple computer model of the ACS CCP and known SEMS model.

Computer simulation of automatic control systems results confirmed the correctness of the functioning of ciliated propulsion. As the simulation results showed that with the right setting PID controllers in the ACS MCR and ACS BCR can obtain an aperiodic transition process in the past. Further simulations have shown that it is possible to obtain practically discontinuous change in rigidity of EMC during the transition stroke phase to a return phase. Consequently, the proposed ciliated type of propulsion can achieve required for medical micro robots of dynamic characteristics.

Acknowledgements The author would like to thank the Russian Foundation for Basic Researches (grants 14-07-00257, 15-07-04760, 15-07-02757, 16-29-04424, and 16-29-12901) for partial funding of this research.

References

1. Merlet, J.P.: Parallel Robots, p. 383. Sophia-Antipolis, France Springer, Inria (2006)
2. Gorodetskiy, A.E., Tarasova, I.L., Kurbanov, V.G.: Mathematical model of the automatic control systems SEMS modules. In: Gorodetskiy, A.E. (eds.) Smart Electromechanical Systems, 277 p. Springer International Publishing (2016). doi:10.1007/978-3-319-27547-5
3. Agapov, V.A. (RU), Gorodetskiy, A. E. (RU), Kuchmin, A.J. (RU), Selivanova, E.N. (RU): Medical microrobot. Patent RU, No. 2469752 (2011)
4. Artemenko, Iu.A., Gorodetskii, A.E., Dubarenko, V.V., Kuchmin, A.Iu., Agapov, V.A.: Analiz dinamiki sistem avtomaticheskogo upravleniia aktuatorami kontrreflektora kosmicheskogo radioteleskopa (Analysis of the dynamics of automatic control systems, actuators of kontrreflektora space radio telescope). Informatsionno—upravliaiushchie sistemy. [Information and Control Systems] (2011), No. 6, pp. 2–5
5. Tarasova, I.L., Gorodetskiy, A.E., Kurbanov, V.G.: Computer modeling ACS of SEMS actuator of space radio telescope subdish. In: Gorodetskiy, A.E. (eds.) Smart Electromechanical Systems, 277 p. Springer International Publishing (2016). doi:10.1007/978-3-319-27547-5
6. Artemenko, Y.N., Karpenko, A.P., Byelonozhko, P.P.: Features of manipulator dynamics modeling into account a movable platform. In: Gorodetskiy, A.E. (eds) Smart Electromechanical Systems, 277 p. Springer International Publishing (2016). doi:10.1007/978-3-319-27547-5

Methodical Features of Acquisition of Independent Dynamic Equation of Relative Movement of One-Degree of Freedom Manipulator on Movable Foundation as Control Object

P.P. Belonozhko

Abstract *Purpose* Model problems, where dynamic conditions permit an analytical treatment and it is possible to reveal qualitative movement pattern, to analyze influence of control object parameters to its execution behaviour, are of substantial interest in the view of features of synthesis of control and making a Robot Central Nervous System (RCNS) for perspective robot systems. *Results* During the stated problem formulated in [1] a procedure of acquisition of independent dynamic equation of a plain articulate two-element mechanism relative motion, based on separation of generalized coordinates on cyclic and positional, is considered. *Practical importance* Received results have a method value in the view of research of the case being of applied interest of spatial motion of system of two solids connected using spatial mechanism with purposive variable configuration (manipulator).

Keywords Manipulator · Movable basis · Research of dynamic conditions · Model task · Routhan equation

1 Introduction

Resulting trending of space robotics advancement a promising class of assembly and service self-contained robotic space modules is emphasized in [1] and [2], where a diversity of possible functioning modes is an important feature.

The following most common elements of construction of assembly and service self-contained robotic space modules are singled out [2]:

– availability of movable foundation—a space module possessing a sufficiently high level autonomy, able to move independently in space and adapted for

P.P. Belonozhko (✉)
The Bauman Moscow State Technical University, Moscow, Russia
e-mail: byelonozhko@mail.ru

A.E. Gorodetskiy and V.G. Kurbanov (eds.), *Smart Electromechanical Systems: The Central Nervous System*, Studies in Systems, Decision and Control 95,
DOI 10.1007/978-3-319-53327-8_19

contact interaction with other space objects, for example, manipulator stations or mountable (attended) objects;
– availability of one or several foundation-mounted manipulators, providing a possibility of controlled movement of trapped load, generally enough massive, relatively to foundation.

Within the limits of procedure of orbital assembly an analysis was realized of functioning modes in posse of such module, supposing different versions of combination of controlled movement of movable platform in inertial space with controlled movement of load relatively to platform by means of manipulator [2].

As mentioned in [3], problems of dynamics of transporting movements of multilink kinematics are highly complicated for qualitative analytical investigation. This makes the more important problems wherein dynamic conditions of manipulator movement admit analytical study. Such tasks are of model character and they permit to reveal qualitative movement picture, analyze an influence of manipulator characteristic on its dynamics and characteristics of trajectories of mechanical gripper movement.

We particularly mark out expediency of study of several purely inertial motions of manipulator device, analogous to natural mode shape of mechanical system, in the view of construction optimal in a certain sense active control actions. As an example we give collinear control wherein geometrical motion behavior proves identical to behavior of free inertial movements. We also point out important role of dynamic effects at acceleration-braking, expediency of examination of pulse (shock) modes of controlled movement, possibility of motion optimization through characteristic and starting conditions matching.

2 Problem Statement

Let us consider plane motion of assembly and service robotic space module with trapped slip-free load presented simplistically as system of two solids 1 and 2, connected with ideal one-link one-degree of freedom rotary joint. Masses of bodies are correspondingly m_1 and m_2, J_1 and J_2-moments of bodies inertia relatively their centers of mass, l_1 and l_2-distances from centers of mass to joint (Fig. 1).

Say lack of outside forces and moments influence on system. Then non-rotational co-ordinates XOY (doesn't shown at drawing) with origin in system center of mass will be inertial. We will determine position of system in respect of XOY by an angle ϕ_1 counted out counter-clockwise between abscissa and line, passing through center of mass of first body and rotary joint, and hinged angle q also counted out counter-clockwise between line, passing through joint and center of mass of second body, and line passing through center of first body and joint. System position meet zero valuations of co-ordinates φ_1 and q, where bodies centers of mass and joint are placed on abscissa, at the same time center of mass of

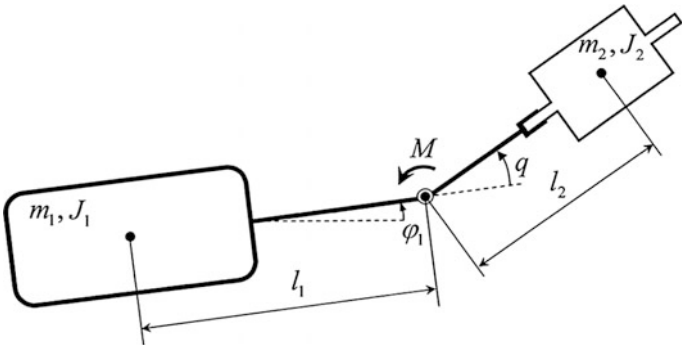

Fig. 1 Simplified representation assembly and service robotic space module with trapped slip-free load

first body has smaller abscissa, center of mass of second body has bigger abscissa, joint is placed between bodies center of mass.

By definition of bodies system center of mass co-ordinates of first body center of mass are connected with coordinates φ_1 and q by relations

$$x_1 = -\frac{m_2}{m_1 + m_2}(l_1 \cos\varphi_1 + l_2 \cos(\varphi_1 + q)), \tag{1}$$

$$y_1 = -\frac{m_2}{m_1 + m_2}(l_1 \sin\varphi_1 + l_2 \sin(\varphi_1 + q)). \tag{2}$$

Thus when given φ_1 and q a position of foundation (of body 1) in inertial coordinates XOY(generalized coordinates x_1, y_1 and φ_1) and position of load (of body 2) relatively to foundation (generalized coordinate q) are unambiguously determined.

3 System Positional and Cyclic Coordinates, Cyclic Integral

Expression for system kinetic energy as quadratic form of independent generalized coordinates φ_1 и q looks like

$$T = \frac{1}{2}\dot{\varphi}_1^2\left(J_1 + J_2 + \tilde{m}l_1^2 + \tilde{m}l_2^2 + 2\tilde{m}l_1 l_2 \cos q\right) + \dot{\varphi}_1\dot{q}\left(J_2 + \tilde{m}l_2^2 + \tilde{m}l_1 l_2 \cos q\right) + \frac{1}{2}\dot{q}^2\left(J_2 + \tilde{m}l_2^2\right), \tag{3}$$

where $\tilde{m} = \frac{m_1 m_2}{m_1 + m_2}$.

Let's introduce notations

$$\begin{aligned} a_{\dot{\varphi}_1} &= a_{\dot{\varphi}_1}(q) = J_1 + J_2 + \tilde{m}l_1^2 + \tilde{m}l_2^2 + 2\tilde{m}l_1 l_1 \cos q, \\ a_{\dot{\varphi}_1\dot{q}} &= a_{\dot{\varphi}_1\dot{q}}(q) = J_2 + \tilde{m}l_2^2 + \tilde{m}l_1 l_1 \cos q, \\ a_{\dot{q}} &= a_{\dot{q}}(q) = J_2 + \tilde{m}l_2^2. \end{aligned} \tag{4}$$

It is evident that

$$\dot{a}_{\dot{\varphi}_1} = \frac{d}{dt}a_{\dot{\varphi}_1} = \frac{\partial a_{\dot{\varphi}_1}}{\partial q}\dot{q}, \quad \dot{a}_{\dot{\varphi}_1\dot{q}} = \frac{d}{dt}a_{\dot{\varphi}_1\dot{q}} = \frac{\partial a_{\dot{\varphi}_1\dot{q}}}{\partial q}\dot{q}, \quad \dot{a}_{\dot{q}} = \frac{d}{dt}a_{\dot{q}} = \frac{\partial a_{\dot{q}}}{\partial q}\dot{q}, \tag{5}$$

$$\frac{\partial a_{\dot{\varphi}_1}}{\partial q} = -2\tilde{m}l_1 l_2 \sin q, \quad \frac{\partial a_{\dot{\varphi}_1\dot{q}}}{\partial q} = -\tilde{m}l_1 l_2 \sin q, \quad \frac{\partial a_{\dot{q}}}{\partial q} = 0. \tag{6}$$

By notations (4) expression for kinetic energy (3) will take on form

$$T = \frac{1}{2}a_{\dot{\varphi}_1}\dot{\varphi}_1^2 + a_{\dot{\varphi}_1\dot{q}}\dot{\varphi}_1\dot{q} + \frac{1}{2}a_{\dot{q}}\dot{q}^2. \tag{7}$$

Taking into consideration done supposition about lack of outside forces and moments it follows from (3) that coordinate q is positional and coordinate φ_1 is cyclic. This is the case of cyclic integral

$$\begin{aligned} \frac{\partial T}{\partial \dot{\varphi}_1} &= \dot{\varphi}_1\left(J_1 + J_2 + \tilde{m}l_1^2 + \tilde{m}l_2^2 + 2\tilde{m}l_1 l_2 \cos q\right) + \dot{q}\left(J_2 + \tilde{m}l_2^2 + \tilde{m}l_1 l_2 \cos q\right) \\ &= a_{\dot{\varphi}_1}\dot{\varphi}_1 + a_{\dot{\varphi}_1\dot{q}}\dot{q} = L = const, \end{aligned} \tag{8}$$

testifying to constancy of kinetic momentum of system L in the absence of outside moments.

Cyclic velocity $\dot{\varphi}_1$ may be expressed from (8)

$$\dot{\varphi}_1 = \dot{\varphi}_1(\dot{q}, q, L) = -\frac{a_{\dot{\varphi}_1\dot{q}}}{a_{\dot{\varphi}_1}}\dot{q} + \frac{1}{a_{\dot{\varphi}_1}}L. \tag{9}$$

4 Lagrange's Equations of the 2nd Kind

Let's write Lagrange's equations of the 2nd kind for coordinates φ_1 and q

$$\frac{d}{dt}\left(\frac{\partial T}{\partial \dot{\varphi}_1}\right) - \frac{\partial T}{\partial \varphi_1} = Q_{\varphi_1}, \quad \frac{d}{dt}\left(\frac{\partial T}{\partial \dot{q}}\right) - \frac{\partial T}{\partial q} = Q_q. \tag{10}$$

Considering the fact that in concordance with accepted assumption of lack of external forces $Q_{\dot{\phi}_1} = 0$, and $Q_{\dot{q}} = M$, after substitution (7) into (10) and transformations subject to (5) we receive system of dynamic equations of system under consideration in coordinates φ_1 and q

$$\ddot{\varphi}_1 a_{\dot{\phi}_1} + \ddot{q} a_{\dot{\phi}_1 \dot{q}} + \dot{\varphi}_1 \dot{q} \frac{\partial a_{\dot{\phi}_1}}{\partial q} + \dot{q}^2 \frac{\partial a_{\dot{\phi}_1 \dot{q}}}{\partial q} = 0, \tag{11}$$

$$\ddot{\varphi}_1 a_{\dot{\phi}_1 \dot{q}} + \ddot{q} a_{\dot{q}} - \frac{1}{2} \dot{\varphi}_1^2 \frac{\partial a_{\dot{\phi}_1}}{\partial q} + \frac{1}{2} \dot{q}^2 \frac{\partial a_{\dot{q}}}{\partial q} = M. \tag{12}$$

System (11) and (12) is written in the general form in the case of representation of kinetic energy in the form of (7). Substituting in (11) and (12) expressions (4) and (5) for quadratic form coefficients and their positional coordinate derivatives as positional coordinate functions, systems geometrical and mass and lag parameters, we obtain

$$\begin{aligned} &\ddot{\varphi}_1 (J_1 + J_2 + \tilde{m} l_1^2 + \tilde{m} l_2^2 + 2\tilde{m} l_1 l_1 \cos q) + \ddot{q} (J_2 + \tilde{m} l_2^2 + \tilde{m} l_1 l_1 \cos q) \\ &\quad - 2\dot{\varphi}_1 \dot{q} \tilde{m} l_1 l_1 \sin q - \dot{q}^2 \tilde{m} l_1 l_1 \sin q = 0, \end{aligned} \tag{13}$$

$$\ddot{\varphi}_1 (J_2 + \tilde{m} l_2^2 + \tilde{m} l_1 l_1 \cos q) + \ddot{q} (J_2 + \tilde{m} l_2^2) + \dot{\varphi}_1^2 \tilde{m} l_1 l_1 \sin q = M. \tag{14}$$

It is easily seen that Eq. (13) is expression (8) differentiated according to time.

5 Receiving of Independent Dynamic Equation of Relative Motion by Transformation of System of Lagrange's Equations of the 2nd Kind Using Cyclic Integral

Substituting (9) to (11) we obtain

$$\ddot{\varphi}_1 = -\ddot{q} \frac{a_{\dot{\phi}_1 \dot{q}}}{a_{\dot{\phi}_1}} - \dot{q}^2 \frac{1}{a_{\dot{\phi}_1}} \left(\frac{\partial a_{\dot{\phi}_1 \dot{q}}}{\partial q} - \frac{a_{\dot{\phi}_1 \dot{q}}}{a_{\dot{\phi}_1}} \frac{\partial a_{\dot{\phi}_1}}{\partial q} \right) - \dot{q} \frac{L}{a_{\dot{\phi}_1}} \frac{\partial a_{\dot{\phi}_1}}{\partial q}. \tag{15}$$

We have from (9)

$$\dot{\varphi}_1^2 = \frac{a_{\dot{\phi}_1 \dot{q}}^2}{a_{\dot{\phi}_1}^2} \dot{q}^2 - 2 \frac{a_{\dot{\phi}_1 \dot{q}}}{a_{\dot{\phi}_1}^2} \dot{q} L + \frac{1}{a_{\dot{\phi}_1}^2} L^2. \tag{16}$$

Substituting (15) and (16) to (12) we obtain after transformations

$$\ddot{q}\left(a_{\dot{q}}-\frac{a_{\dot{\varphi}_1\dot{q}}^2}{a_{\dot{\varphi}_1}}\right)+\dot{q}^2\left(\frac{1}{2}\frac{a_{\dot{\varphi}_1\dot{q}}^2}{a_{\dot{\varphi}_1}^2}\frac{\partial a_{\dot{\varphi}_1}}{\partial q}-\frac{a_{\dot{\varphi}_1\dot{q}}}{a_{\dot{\varphi}_1}}\frac{\partial a_{\dot{\varphi}_1\dot{q}}}{\partial q}+\frac{1}{2}\frac{\partial a_{\dot{q}}}{\partial q}\right)-L^2\frac{1}{2}\frac{1}{a_{\dot{\varphi}_1}^2}\frac{\partial a_{\dot{\varphi}_1}}{\partial q}=M. \quad (17)$$

Then substituting (4) and (6) to (17) we obtain after transformations

$$\begin{aligned}&\ddot{q}\frac{\left(J_1+\tilde{m}l_1^2\right)\left(J_2+\tilde{m}l_2^2\right)-\tilde{m}^2l_1^2l_2^2\cos^2 q}{\left(J_1+J_2+\tilde{m}l_1^2+\tilde{m}l_2^2+2\tilde{m}l_1l_2\cos q\right)}\\&+\dot{q}^2\frac{\tilde{m}l_1l_2\sin q\left(J_1+\tilde{m}l_1^2+\tilde{m}l_1l_2\cos q\right)\left(J_2+\tilde{m}l_2^2+\tilde{m}l_1l_2\cos q\right)}{\left(J_1+J_2+\tilde{m}l_1^2+\tilde{m}l_2^2+2\tilde{m}l_1l_2\cos q\right)^2}\\&+L^2\frac{\tilde{m}l_1l_2\sin q}{\left(J_1+J_2+\tilde{m}l_1^2+\tilde{m}l_2^2+2\tilde{m}l_1l_2\cos q\right)^2}=M.\end{aligned} \quad (18)$$

Equation (17) is also obtained in the general form in the case when kinetic energy looks like quadratic form (7), coordinate q is positional and coordinate φ_1 is cyclic, i.e. $Q_{\dot{\varphi}_1}=0$ and coefficients of quadratic form (7) vary depending on q and don't vary depending on φ_1. After substitution of expressions for quadratic form coefficients (4) and their positional coordinate derivatives (6) to (17) we obtained Eq. (18) concurrent with received equation at [1].

In such a way within the framework of model task under consideration independent dynamic equation of relative motion of movable foundation and payload relocatable by manipulator is written in the form (17), and Eq. (18) is obtained by formal substitution of (4) and (6) to (17), that is of interest, for example, from the point of view of possibility of symbolic mathematics use.

6 Receiving of Independent Dynamic Equation of Relative Motion by Transformation of Expressions for Derivatives

Equation (17) also may be obtained as follows

$$\frac{d}{dt}\left(\frac{\partial T}{\partial \dot{q}}\right)^*-\left(\frac{\partial T}{\partial q}\right)^*=M, \quad (19)$$

where

$$\left(\frac{\partial T}{\partial \dot{q}}\right)^{*} = \left.\frac{\partial T}{\partial \dot{q}}\right|_{\dot{\varphi}_1=\dot{\varphi}_1(\dot{q},q,L)}$$
$$\left(\frac{\partial T}{\partial q}\right)^{*} = \left.\frac{\partial T}{\partial q}\right|_{\dot{\varphi}_1=\dot{\varphi}_1(\dot{q},q,L)} \tag{20}$$

Equation (19) appears as independent Lagrange's equation of the 2nd kind where cyclic velocity $\dot{\varphi}_1$ is excluded from expressions for positional velocity $\dot{q}$ and positional coordinate q derivatives from kinetic energy (7) using cyclic integral (8).

We have

$$\left(\frac{\partial T}{\partial \dot{q}}\right)^{*} = \left(a_{\dot{\varphi}_1\dot{q}}\dot{\varphi}_1 + a_{\dot{q}}\dot{q}\right)\Big|_{\dot{\varphi}_1=-\frac{a_{\dot{\varphi}_1\dot{q}}}{a_{\dot{\varphi}_1}}\dot{q}+\frac{1}{a_{\dot{\varphi}_1}}L} = \dot{q}\left(a_{\dot{q}} - \frac{a_{\dot{\varphi}_1\dot{q}}^2}{a_{\dot{\varphi}_1}}\right) + \frac{a_{\dot{\varphi}_1\dot{q}}}{a_{\dot{\varphi}_1}}L, \tag{21}$$

$$\begin{aligned}\left(\frac{\partial T}{\partial q}\right)^{*} &= \left(\frac{1}{2}\dot{\varphi}_1^2\frac{\partial a_{\dot{\varphi}_1}}{\partial q} + \dot{\varphi}_1\dot{q}\frac{\partial a_{\dot{\varphi}_1\dot{q}}}{\partial q} + \frac{1}{2}\dot{q}^2\frac{\partial a_{\dot{q}}}{\partial q}\right)\Bigg|_{\dot{\varphi}_1=-\frac{a_{\dot{\varphi}_1\dot{q}}}{a_{\dot{\varphi}_1}}\dot{q}+\frac{1}{a_{\dot{\varphi}_1}}L} \\ &= \dot{q}^2\left(\frac{1}{2}\frac{a_{\dot{\varphi}_1\dot{q}}^2}{a_{\dot{\varphi}_1}^2}\frac{\partial a_{\dot{\varphi}_1}}{\partial q} - \frac{a_{\dot{\varphi}_1\dot{q}}}{a_{\dot{\varphi}_1}}\frac{\partial a_{\dot{\varphi}_1\dot{q}}}{\partial q} + \frac{1}{2}\frac{\partial a_{\dot{q}}}{\partial q}\right) \\ &\quad + \dot{q}L\left(\frac{1}{a_{\dot{\varphi}_1}}\frac{\partial a_{\dot{\varphi}_1\dot{q}}}{\partial q} - \frac{a_{\dot{\varphi}_1\dot{q}}}{a_{\dot{\varphi}_1}^2}\frac{\partial a_{\dot{\varphi}_1}}{\partial q}\right) + \frac{1}{2}\frac{L^2}{a_{\dot{\varphi}_1}^2}\frac{\partial a_{\dot{\varphi}_1}}{\partial q}.\end{aligned} \tag{22}$$

Substituting expressions (21) and (22) to (19) taking into account (5) we receive (17).

7 Receiving of Independent Dynamic Equation of Relative Motion as Routhan Equation

Let's exclude cyclic velocity $\dot{\varphi}_1$ from expression for kinetic energy (6) using cyclic integral (7)

$$\begin{aligned}T^{*} &= T^{*}(\dot{q},q,L) = T|_{\dot{\varphi}_1=\dot{\varphi}_1(\dot{q},q,L)} = \frac{1}{2}a_{\dot{\varphi}_1}\dot{\varphi}_1^2 + a_{\dot{\varphi}_1\dot{q}}\dot{\varphi}_1\dot{q} + \frac{1}{2}a_{\dot{q}}\dot{q}^2\Big|_{\dot{\varphi}_1=-\frac{a_{\dot{\varphi}_1\dot{q}}}{a_{\dot{\varphi}_1}}\dot{q}+\frac{1}{a_{\dot{\varphi}_1}}L} \\ &= \frac{1}{2}\left(a_{\dot{q}} - \frac{a_{\dot{\varphi}_1\dot{q}}^2}{a_{\dot{\varphi}_1}}\right)\dot{q}^2 + \frac{1}{2}\frac{1}{a_{\dot{\varphi}_1}}L^2.\end{aligned} \tag{23}$$

Let's form Routh function [4]

$$R = T^*(\dot{q}, q, L) - \dot{\varphi}_1(\dot{q}, q, L) \cdot L = \frac{1}{2}\left(a_{\dot{q}} - \frac{a_{\dot{\varphi}_1\dot{q}}^2}{a_{\dot{\varphi}_1}}\right)\dot{q}^2 - \frac{1}{2}\frac{1}{a_{\dot{\varphi}_1}}L^2 + \dot{q}L\frac{a_{\dot{\varphi}_1\dot{q}}}{a_{\dot{\varphi}_1}}. \quad (24)$$

Then Routhan equation taking the form of Lagrange's equation of the 2nd kind where Routh function (24) plays a part of kinetic energy may be written for positional coordinate

$$\frac{d}{dt}\left(\frac{\partial R}{\partial \dot{q}}\right) - \frac{\partial R}{\partial q} = M. \quad (25)$$

Substituting (24) to (25) we also receive (17).

Taking into account (4) and (6) expressions (23) and (24) will become

$$T^*(\dot{q}, q, L) = \frac{1}{2}\dot{q}^2\frac{\left(J_1 + \tilde{m}l_1^2\right)\left(J_2 + \tilde{m}l_2^2\right) - \tilde{m}^2 l_1^2 l_2^2 \cos^2 q}{\left(J_1 + J_2 + \tilde{m}l_1^2 + \tilde{m}l_2^2 + 2\tilde{m}l_1 l_2 \cos q\right)} + L^2\frac{1}{\left(J_1 + J_2 + \tilde{m}l_1^2 + \tilde{m}l_2^2 + 2\tilde{m}l_1 l_2 \cos q\right)}, \quad (26)$$

$$R = R(\dot{q}, q, L) = \frac{1}{2}\dot{q}^2\frac{\left(J_1 + \tilde{m}l_1^2\right)\left(J_2 + \tilde{m}l_2^2\right) - \tilde{m}^2 l_1^2 l_2^2 \cos^2 q}{\left(J_1 + J_2 + \tilde{m}l_1^2 + \tilde{m}l_2^2 + 2\tilde{m}l_1 l_2 \cos q\right)} + \dot{q}L\frac{\left(J_2 + \tilde{m}l_2^2 + \tilde{m}l_1 l_2 \cos q\right)}{\left(J_1 + J_2 + \tilde{m}l_1^2 + \tilde{m}l_2^2 + 2\tilde{m}l_1 l_2 \cos q\right)} - \frac{1}{2}L^2\frac{1}{\left(J_1 + J_2 + \tilde{m}l_1^2 + \tilde{m}l_2^2 + 2\tilde{m}l_1 l_2 \cos q\right)}. \quad (27)$$

Substituting (27) to (25) we obtain as evidently expression (18).

8 Physical Interpretation of Received Independent Equation of Relative Motion

As shown in [1], when linearized in the vicinity of position $q = 0$, Eq. (18) will take the form

$$\ddot{q}\frac{\left(J_1 + \tilde{m}l_1^2\right)\left(J_2 + \tilde{m}l_2^2\right) - \tilde{m}^2 l_1^2 l_2^2}{\left(J_1 + J_2 + \tilde{m}l_1^2 + \tilde{m}l_2^2 + 2\tilde{m}l_1 l_2\right)} + qL^2\frac{\tilde{m}l_1 l_2}{\left(J_1 + J_2 + \tilde{m}l_1^2 + \tilde{m}l_2^2 + 2\tilde{m}l_1 l_2\right)^2} = M. \quad (28)$$

In the absence of control moment in joint $M = 0$ Eq. (28) will take the form of equation of harmonic oscillator

$$\ddot{q} + \omega^2 q = 0, \tag{29}$$

where self-resonant frequency determines by relation

$$\omega = \sqrt{\frac{\tilde{m} l_1 l_2}{\left((J_1 + \tilde{m} l_1^2)(J_2 + \tilde{m} l_2^2) - \tilde{m}^2 l_1^2 l_2^2\right)\left(J_1 + J_2 + \tilde{m} l_1^2 + \tilde{m} l_2^2 + 2\tilde{m} l_1 l_2\right)}} L. \tag{30}$$

Equation (29) permits pictorial physical interpretation. Let system start to move with zero relative initial velocity $\dot{q}^{(0)} = 0$ and initial displacement in joint $q^{(0)}$ within the limits allowing linearization i.e. usage of Eq. (28). Then according to (8) constant kinetic moment of system determines by relation

$$L = \dot{\varphi}_1^{(0)} J_C, \tag{31}$$

where $J_C = \left(J_1 + J_2 + \tilde{m} l_1^2 + \tilde{m} l_2^2 + 2\tilde{m} l_1 l_2 \cos q^{(0)}\right)$ is moment of inertia relatively to center of mass of system «solidified» at configuration $q^{(0)}$.

In that way kinetic moment of system is in that case kinetic moment of solid body with moment of inertia J_C, turning around center of mass with constant velocity $\dot{\varphi}_1^{(0)}$. Given motion will occur in case if we fix joint degree of freedom in position $q^{(0)}$ and give initial angular velocity $\dot{\varphi}_1^{(0)}$ to lifting body. With reasonable conventionality for preliminary estimate we may interpret given movement as displacement of robot module with load in manipulator hand. If now we take off fixation of joint degree of freedom then in the absence of control moment in joint $M = 0$ system will execute free harmonic vibrations in accordance with Eq. (29) with frequency determinate by correlation following from (29) and (31)

$$\omega = \dot{\varphi}_1^{(0)} \sqrt{\frac{\tilde{m} l_1 l_2 \left(J_1 + J_2 + \tilde{m} l_1^2 + \tilde{m} l_2^2 + 2\tilde{m} l_1 l_2 \cos q^{(0)}\right)^2}{\left((J_1 + \tilde{m} l_1^2)(J_2 + \tilde{m} l_2^2) - \tilde{m}^2 l_1^2 l_2^2\right)\left(J_1 + J_2 + \tilde{m} l_1^2 + \tilde{m} l_2^2 + 2\tilde{m} l_1 l_2\right)}} \tag{32}$$

Thus frequency of system own joint vibrations appearing at initial nonzero kinetic moment L, zero relative initial velocity $\dot{q}^{(0)} = 0$ and nonzero initial displacement $q^{(0)}$ from position of relative equilibrium $q = 0$ is linear function of initial angular velocity $\dot{\varphi}_1^{(0)}$ «solidified» at system position $q^{(0)}$.

9 Conclusion

In the absence of external forces and moments motion regarding non-driving co-ordinates with the beginning at the system center of mass is examined. In that case the generalized coordinate describing an absolute angular position of the

foundation will be cyclic and generalized coordinate describing a relative angular position of the foundation will be positional. At the same time the first integral expressing angular momentum conservation law of system in the absence of external moments may be received as cyclic and the independent dynamic equation of a relative movement may be written in the form of a Routhan equation. This equation, to which some reduced system may correspond, allows visual physical interpretation.

References

1. Artemenko, Y.N., Karpenko, A.P., Belonozhko, P.P.: Features of manipulator dynamics modeling into account a movable platform In: Gorodetskiy A.E (ed.) Smart Electromechanical Systems. Studies in Systems, Decision and Control 49, pp. 177–190. Springer International Publishing Switzerland, Berlin (2016). DOI 10.1007/978-3-319-27547-5_17
2. Belonozhko, P.P.: Prospective installation-service robotic space modules. Robot. Tech. Cybern. **2**(7), 18–23 (2015) (in Russian)
3. Smol'nikov B.A.: Problemy Mekhaniki I Optimizatsii Robotov (Problems of mechanics and optimization of robots), p. 232 Nauka Publications, Moscow (1991) (in Russian)
4. Lurie A.I.: Analitycheskaya Mekhanika (Analytical Mechanics), p. 824 Fizmatgiz Publications, Moscow (1961) (in Russian)